ANDRA BGR CHEVRON CRIEPI ENRESA ENSI GRS IRSN
JAEA NAGRA NWMO OBAYASHI SCK•CEN SWISSTOPO

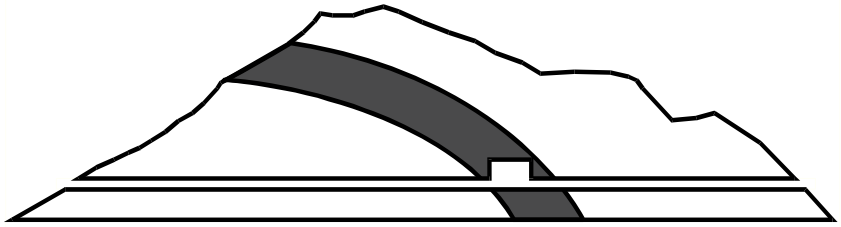

Mont Terri Project

TECHNICAL REPORT 2009-06
February 2012

PC (Porewater chemistry) Experiment: synthesis report

[1] O. Leupin, [1] [3] P. Wersin, [1] [4] S. Mettler, [2] U. Mäder,
[5] E.C. Gaucher, [6] A. Vinsot, [7] P. De Cannière, [8] H.E. Gäbler,
[9] L. Eichinger, [10] T. Kunimaro, [11] K. Kiho,

[1] NAGRA, [2] University of Berne,
[3] Gruner Ldt., [4] Solexperts Ldt., Switzerland
[5] BRGM, [6] ANDRA, France
[7] SCK-CEN, Belgium
[8] BGR, [9] Hydroisotop, Germany
[10] JAEA, [11] CRIEPI, Japan

Distribution:

Standard distribution:

ANDRA (S. Dewonck)

BGR (K. Schuster)

CHEVRON (P. Connolly)

CRIEPI (K. Kiho)

ENRESA (J.C. Mayor)

ENSI (E. Frank)

GRS (T. Rothfuchs)

IRSN (J.-M. Matray)

JAEA (K. Aoki)

NAGRA (T. Vietor)

NWMO (M. Jensen)

OBAYASHI (H. Kawamura, T. Kikuchi)

SCK•CEN (G. Volckaert)

SWISSTOPO (P. Bossart, A. Möri and Ch. Nussbaum)

Additional distribution:

Every organisation & contractor takes care of their own distribution.

Applied Geochemistry 26 (2011) 929–930

Contents lists available at ScienceDirect

Applied Geochemistry

journal homepage: www.elsevier.com/locate/apgeochem

Editorial

Foreword

For decades, the geochemical study of clay rocks has been relatively neglected by our scientific community at large. This is understandable as such rocks are indeed generally poor in economic mineralisation and their low permeability prevents any great production of oil, gas, or drinking water. However, over the last 15 years, knowledge concerning these rocks has improved considerably, due in particular to investigations carried out in relation to the issue of nuclear waste confinement, and a corpus of coherent measurements, modelling and concepts is now available.

The safe disposal of nuclear waste in deep underground repositories is indeed a key issue for the development of the nuclear industry in most countries. After decades of research and sociopolitical debates, the solution to the long-term management of nuclear waste remains largely consensual amongst the scientific and technological communities although discussion is ongoing and other strategies are sometimes promoted. Diverse geological formations, having extremely different characteristics in terms of mineralogy, geochemistry, permeability, mechanics and structure, have been investigated as possible hosts for nuclear waste repositories: crystalline rocks, salt domes, volcanic rocks, argillaceous rocks, etc. The multibarrier concept, whatever the specific designs and technologies involved which may vary from one country to another, has been developed to prevent the dispersion of radionuclides to the biosphere, where they could possibly impact human beings and the ecosystem, and, therefore, to fully guaranty the safety of repositories. This guaranty is also based on the modelling of solid/liquid interaction and transport phenomena, a science which has benefited from major progress in recent years, notably for coupled thermo-hydro-geochemical processes. However, the modelling of migration of radionuclides through complex geological systems remains a technically difficult task, in particular, when predictions over very long periods of time are necessary, which requires a thorough understanding of all fundamental mechanisms and processes involved, particularly within the geological barrier. This is exactly why research work carried out in underground laboratories is invaluable, not only because it is the only way to collect a wide range of data and information from *in situ* exploration and/or experimentation but also because it allows the development and testing of investigation methodologies. These underground laboratories also provide a unique opportunity to make major scientific and technological progress within the framework of large international projects and collaborations where the consensus of experts can be progressively built. For many years, Switzerland has been at the forefront of scientific research dedicated to the development of a safe nuclear wastes repository in a deep-seated geological formation and, notably, by means of experimentation in underground laboratories. The Mont Terri Rock Laboratory, situated in an Opalinus clay formation of the Jura District (Switzerland), is a reputed laboratory where high quality research recognized worldwide is carried out through strong international cooperation.

The present special issue of Applied Geochemistry reports the results of a programme of research conducted at Mont Terri for a period of five years. It essentially deals with the investigation of biogeochemical processes which are affecting the porewater chemistry in this low permeability Opalinus clay formation, particularly pH and pCO_2 parameters, due to microbiologically-induced redox reactions which were initially unexpected. These results are of great interest for the (bio)geochemists involved in studying such geological formations in relation to the disposal of nuclear wastes because little attention has been given to date to this interaction between microbiology and geochemistry, the latter being a key to the understanding and modelling of radionuclide migration.

However, beyond these specific results, three major outputs of these studies should be underlined as they are of much wider interest: (i) a better understanding of the water/gas/rock equilibrium regulating the *in situ* porewater chemistry, (ii) the demonstration of the buffer capacity of the clay rock limiting the extension of a strong biogeochemical perturbation, (iii) the ability of transport-chemistry models to describe complex biogeochemical processes. Although each geological formation and particular site are quite specific, the data, results and conclusions obtained through this programme, as well as methodologies developed at Mont Terri, may be of interest to all geoscientists investigating the properties of argillaceous rocks with other applications in mind such as, for instance, the examination of the clayey caprocks for the underground storage of CO_2 or the development of numerical models for soil chemistry.

This issue is composed of seven original papers which are largely self-contained but which, together, give a good picture of the programme of investigations carried out at the Mont Terri Rock Laboratory and of its main results. Part A gives an overview of the research programme, the experimental design and water data collected at Mont Terri. It shows that the chemical and isotopic composition of the porewater is the result of complex interactions between numerous processes occurring within the solution and at the mineral/water interfaces. Part B discusses results from overcoring and demonstrates the very extensive buffer capacity of this kind of clay against chemical perturbations introduced artificially, notably those due to microbial redox activity fuelled by a notable carbon source of initially unknown origin. Part C describes the different possible origins for this carbon contamination, on the basis of the results of leaching experiments, and attributes its most probable origin to the release of glycerol from the polymeric gel filling reference electrodes, *which were used to permanently monitor the experiment.* Part D gives a detailed account of the microbial organisms which have been identified during this porewater

0883-2927/$ - see front matter © 2011 Published by Elsevier Ltd.
doi:10.1016/j.apgeochem.2011.03.003

chemistry experiment. They include a complex mixture of heterotrophic aerobic and anaerobic organisms. Part E describes the equilibrium controls on the porewater chemistry of the Opalinus clay and underlines the major importance of a thorough understanding of mineral/water interactions to develop fully comprehensive and reliable geochemical models. Part F deals with reactive transport modelling. This paper demonstrates that the most important chemical processes controlling the porewater chemistry are ion exchange, biodegradation and specific dissolution-precipitation reactions. The high buffering capacity described in Part B is attributed here to the carbonate system and to the reactivity of clay mineral surfaces. Part G summarizes the key interpretations and conclusions which can be drawn from this programme of investigations. The specific implications for the safety of a repository in such rock formations are also presented. In particular, it has been shown that the high buffering capacity and diffusive properties of this kind of clay can efficiently limit the time span and spatial extension of a microbial perturbation which may have been introduced in the rock formation during the excavation and construction process.

Jean-Claude Petit
CEA/CAB AG, Bâtiment 447,
Centre de Saclay,
91190 Gif sur Yvette, France
E-mail address: jcpetit@cea.fr

Applied Geochemistry 26 (2011) 931–953

Contents lists available at ScienceDirect

Applied Geochemistry

journal homepage: www.elsevier.com/locate/apgeochem

Biogeochemical processes in a clay formation *in situ* experiment: Part A – Overview, experimental design and water data of an experiment in the Opalinus Clay at the Mont Terri Underground Research Laboratory, Switzerland

P. Wersin [a,i,*], O.X. Leupin [a], S. Mettler [a,j], E.C. Gaucher [b], U. Mäder [c], P. De Cannière [d], A. Vinsot [e], H.E. Gäbler [f], T. Kunimaro [g], K. Kiho [h], L. Eichinger [k]

[a] *NAGRA, Hardstrasse 73, 5430 Wettingen, Switzerland*
[b] *BRGM, 3 avenue Claude Guillemin, B.P. 36009, 45060 Orléans Cedex 2, France*
[c] *University of Bern, Institute of Geological Sciences, Baltzerstrasse 3, CH-3012 Bern, Switzerland*
[d] *SCK·CEN, Waste and Disposal Project, Boeretang 200, 2400 Mol, Belgium*
[e] *ANDRA, Laboratoire de Recherche Souterrain de Meuse/Haute-Marne, RD960 BP9, 55290 Bure, France*
[f] *BGR, Stilleweg 2, 30655 Hannover, Germany*
[g] *JAEA, Tokai-mura, Naka-gun, Ibaraki 319-1195, Japan*
[h] *CRIEPI, 1646 Abiko, Abiko-city Chiba 270-1194, Japan*
[i] *Gruner Ltd., Gellertstrasse 55, 4020 Basel, Switzerland*
[j] *Solexperts Ltd., Mettlenbachstrasse 25, 8617 Mönchaltorf, Switzerland*
[k] *Hydroisotop, 85301 Schweitenkirchen, Germany*

ARTICLE INFO

Article history:
Available online 23 March 2011

ABSTRACT

An *in situ* test in the Opalinus Clay formation, termed porewater chemistry (PC) experiment, was carried out for a period of 5 years. It was based on the concept of diffusive equilibration whereby a traced water with a composition close to that expected in the formation was continuously circulated and monitored in a packed-off borehole. The main original focus was to obtain reliable data on the pH/pCO_2 conditions of the porewater, but because of unexpected microbiologically-induced redox reactions, the objective was extended to elucidate the biogeochemical processes occurring in the borehole and to understand their impact on pH/pCO_2 and porewater chemistry in the low permeability clay formation.

The behaviour of the conservative tracers ^2H and Br^- could be explained by diffusive dilution in the clay and moreover the results showed that diffusive equilibration between the borehole water and the formation occurred within about 3 year's time. However, the composition and pH/pCO_2 conditions differed considerably from those of the *in situ* porewater. Thus, pH was lower and pCO_2 was higher than indicated by complementary laboratory investigations. The noted differences are explained by microbiologically-induced redox reactions occurring in the borehole and in the interfacial wall area which were caused by an organic source released from the equipment material. The degradation of this source was accompanied by sulfate reduction and – to a lesser extent – by methane generation, which induced a high rate of acetogenic reactions corresponding to very high acetate concentrations for the first 600 days. Concomitantly with the anaerobic degradation of an organic source, carbonate dissolution occurred and these processes resulted in high pCO_2 and alkalinities as well as drop in pH. Afterwards, the microbial regime changed and, in parallel to ongoing sulfate reduction, acetate was consumed, leading to a strong decrease in TOC which reached background levels after about 1200 days. In spite of the depletion of this organic perturbation in the circuit water, sulfate reduction and methanogenesis continued to occur at a constant rate leading to near-to-constant concentrations of sulfate and bicarbonate as well as pH/pCO_2 conditions until the end of the experiment. The main sink for sulphur was iron sulfide, which precipitated as FeS (am) and FeS_2.

The chemical and isotopic composition was affected by the complex interplay of diffusion, carbon degradation rates, mineral equilibria and dissolution rates, iron sulfide precipitation rates, and clay

* Corresponding author at: Gruner Ltd., Gellertstrasse 55, 4020 Basel, Switzerland. Tel.: +41 61 317 64 15; fax: +41 61 271 79 48.
E-mail address: paul.wersin@gruner.ch (P. Wersin).

doi:10.1016/j.apgeochem.2011.03.004

exchange reactions. The ^{13}C signals measured for different carbon species showed significant variations which could only be partly explained. The main cations, such as Na, Ca and Mg remained remarkably constant during the experiment, thus indicating the strong buffering of the formation via cation and proton exchange as well as carbonate dissolution/precipitation reactions.

1. Introduction

Porewaters in argillaceous formations have received far less attention compared to the formation waters in more conductive natural systems, such as aquifers, oil-bearing sandstones or volcanic formations. Increasing interest in clay rocks for CO_2 sequestration and as host rock for radioactive waste disposal have led fairly recently to more geochemical and microbial studies in clay formations.

The mobility and retardation of contaminants through low-permeability rocks is influenced by the composition of the porewater (e.g. pH/pCO_2, Eh conditions). In order to predict the fate of dissolved compounds, such as for example radionuclides, it is fundamental to know the porewater composition and to understand the underlying geochemical processes that regulate the *in situ* geochemical conditions of the clay. Characterizing porewater composition is however a challenging task because of the intimate clay–water association (Sacchi et al., 2000; Pearson et al., 2003).

For the disposal of radioactive waste, numerous countries are now putting a great effort in investigating the different properties of clay rocks. The main reasons for selecting such formations as host rocks for radioactive waste disposal are their good retention properties regarding migration of radionuclides, their self-sealing capacity, plastic behaviour and low hydraulic conductivity. These properties are investigated at different scales in a few underground research laboratories in Europe (Thury and Bossart, 1999; Lalieux et al., 2003; Delay et al., 2007).

A large international multidisciplinary research program on an indurated clay formation, the Opalinus Clay, located at the Mont Terri Hard Rock Laboratory in the NW of Switzerland (Fig. 1) has yielded valuable information on the mechanical, hydraulic and geochemical properties of this argillaceous rock. For example, considerable understanding of the porewater chemistry has been obtained by the development and application of new methods and techniques, such as *in situ* extraction, laboratory squeezing, leaching and geochemical modelling. As pointed out in the geochemical synthesis report of Pearson et al. (2003), all these methods suffer from different drawbacks and may induce experimental artefacts. This led to significant uncertainties in the determination of *in situ* pH/pCO_2 and Eh values.

To overcome these uncertainties, a new *in situ* test, termed porewater chemistry (PC) experiment was devised, based on the method of diffusive equilibration (as outlined in the following section). The original focus of this experiment was to obtain high-quality data on the porewater composition and thus to reduce uncertainties in pH/pCO_2 and Eh. However, microbial activity in the borehole leading to sulfate reduction was observed after about 9 months, which had never been noted in previous boreholes at Mont Terri. This unexpected result led to a revised research program with the following objectives:

i. to identify biogeochemical processes occurring in the borehole and describe these quantitatively,
ii. to obtain diffusion parameters of injected conservative tracers,
iii. to identify the source of organic carbon for microbial degradation,
iv. to draw conclusions on the findings with regard to conditions of the clay host rock around a nuclear waste repository,

In this special issue, the authors present the different research activities for the PC experiment and summarize the main findings in seven individual papers:

- This contribution (part A) has two objectives. The first objective is to provide an introduction and overview of the PC experiment. Thus, the design and setup, monitoring/sampling/chemical analyses of chemical and isotopic compounds in the circulating water during 5 years are described. The second objective is to present and to interpret from a qualitative viewpoint results from water analyses.
- In part B (Koroleva et al., 2011), the procedures of overcoring and rock sampling after the termination of the PC experiment are described. The mineralogical and chemical rock analyses are presented and interpreted.
- Part C (De Cannière et al., 2011) presents leaching tests and isotopic analyses to identify possible carbon sources fuelling microbial degradation in the *in situ* experiment.
- In part D (Stroes-Gascoyne et al., 2011) microbial analyses from sampled water and rock are summarized and compared with previous analyses from the undisturbed clay formation.
- Part E (Pearson et al., 2011) presents traditional and new chemical equilibrium concepts for describing porewater chemistry in Opalinus Clay, thus providing the basis for the reactive transport modelling applied to the PC experiment (part F).
- In part F (Tournassat et al., 2011), the geochemical evolution in the borehole of the PC experiment is simulated by a biogeochemical model which includes mineral and surface equilibria, simple microbial degradation kinetics and diffusion. The diffusion process was calibrated with aid of the non-reactive tracer data.
- Part G (Wersin et al., 2011) gives a synthesis of the results from the PC experiment and summarizes the main conclusions. Furthermore, the implications of the results are discussed in the light of the long-term safety of a high-level nuclear waste repository emplaced in Opalinus Clay.

2. Geological and geochemical background

The Mont Terri Rock Laboratory is located in a side gallery of the motorway tunnel system which transects an anticline structure of the folded Jura mountains, comprising rocks of Triassic to Jurassic age (Fig. 1). The overburden is about 300 m. The Opalinus Clay of middle-Jurassic (180 ma bp) age is bounded by the Jurensis marls (with local water flow) at the bottom and the Malm formation at the top which forms a regional aquifer.

The borehole *in situ* experiment was located in the central units of Opalinus Clay, in the so-called MI niche. The borehole itself transected a highly fractured zone of about 2 m thickness (Fig. 1). The

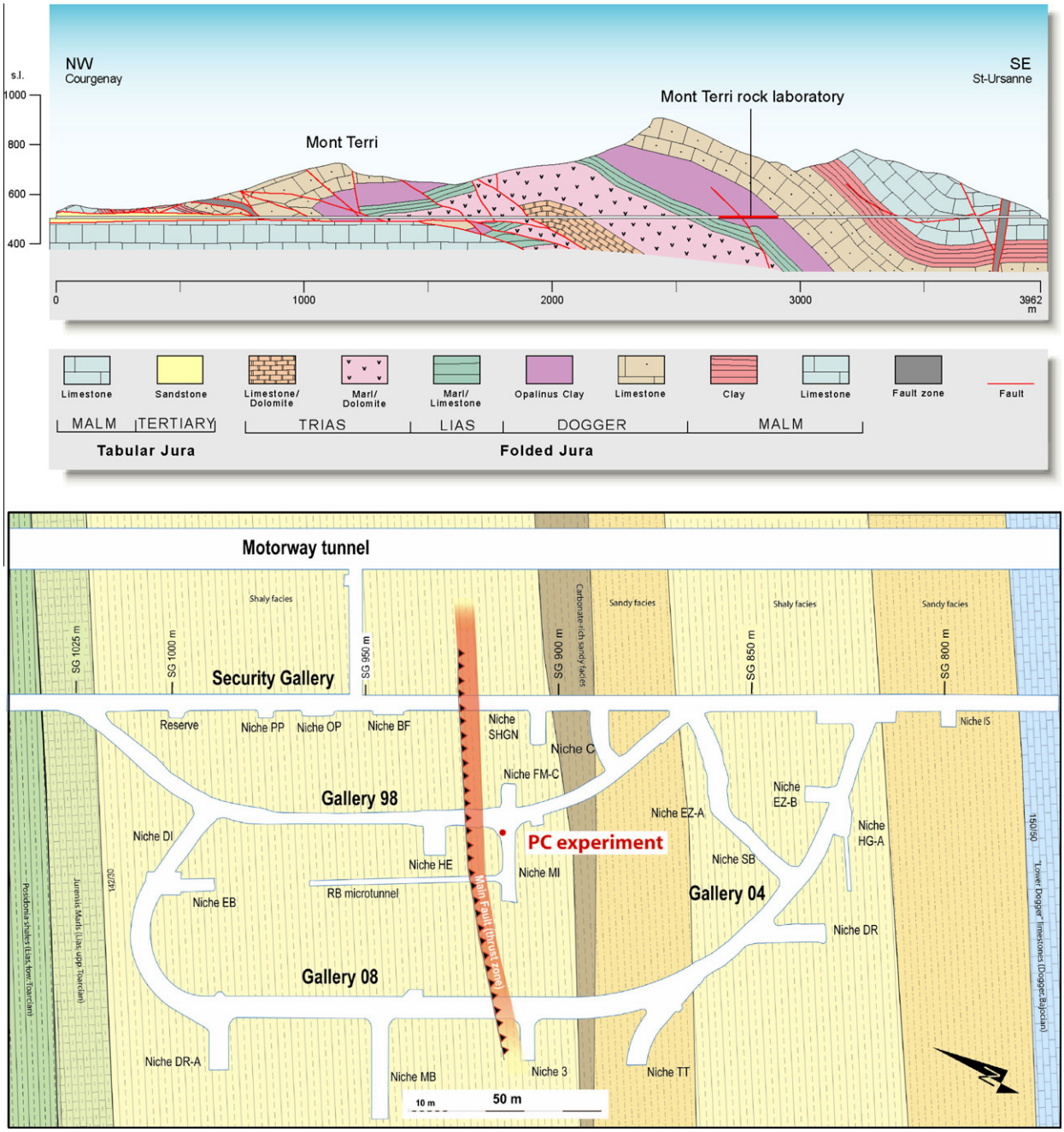

Fig. 1. Sketch of the geological profile and the Mont Terri Rock URL including location of the PC experiment.

Opalinus Clay at Mont Terri is characterised by rather homogeneous but anisotropic layers containing about 80 wt.% of clay minerals (illite, kaolinite, illite–smectite mixed layers and chlorite). Other compounds include calcite (10–15 wt.%), quartz (~10 wt.%) and trace amounts of siderite, dolomite, ankerite, pyrite, feldspar and organic carbon. The mineralogical analysis from the overcored section of the borehole is presented in Koroleva et al. (2011)). No clear mineralogical variations with depth within the section of the test interval (4.5 m) were noted. The bedding plane dips with 45° to the SE.

As outlined above, the porewater chemistry has been quite extensively studied with different lab methods and *in situ* measurements. The results of these campaigns are summarised in Pearson et al. (2003). The porewater is Na–Cl dominated and near to equilibrium with calcite and dolomite but slightly undersaturated with gypsum. The SO_4/Cl ratio of non-oxidized samples is close to that of modern seawater. The $\delta^{13}C$ values indicate that the porewater is in equilibrium with the carbonates from the formation (Pearson et al., 2003). Overall, the porewater chemistry of Opalinus Clay reveals a strong marine component. Interestingly, the salinity of the porewater is not constant across the formation: there is a clear trend of lower chloride concentrations towards the formation boundaries (Degueldre et al., 2003; Nagra, 2002), from 0.3 to about 0.06 mol/L. In fact, an asymmetric Cl^- profile was measured (Fig. 2) which has been interpreted to result from a diffusion process towards the bounding

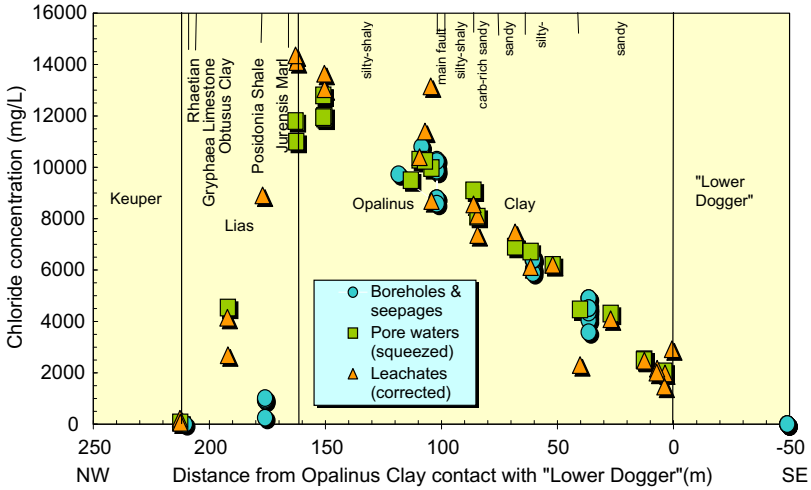

Fig. 2. Diffusion profile of chloride through the Opalinus Clay of Mont Terri (adapted from De Cannière et al. (2008)).

"fresher" limestone units, each of which shows a distinct erosion history (Mazurek et al., 2009). The pH values vary between 7 and 8, the corresponding pCO_2 values are 10^{-2} and $10^{-3.5}$ bars, respectively (Pearson et al., 2003). Recent data from a neighbouring experiment (PC-C experiment) however indicate that CO_2 partial pressures in the area of these two experiments is $\sim 10^{-2}$ bars (Vinsot et al., 2008). The Eh values are uncertain; it has been proposed by Pearson et al. (2003) that Eh is controlled by pyrite/SO_4^{2-} equilibrium.

Besides the interpretation of Cl^- profiles in the formation, a number of *in situ* migration tests at various locations have confirmed that transport in Opalinus Clay is dominated by diffusion (e.g. Palut et al., 2003; Van Loon et al., 2004; Wersin et al., 2008), even in the highly fracture main fault area (Gómez-Hernández and Guardiola-Albert, 2004).

3. Methods

3.1. Concept of diffusive equilibration

The PC experiment was based on the concept of diffusive equilibration: Synthetic porewater with a composition close to that of the formation water was circulated in a packed-off borehole. With time, this synthetic porewater should have equilibrated with the formation water via diffusion and water–rock interactions. Because of excess of formation water compared to the volume of the circulating water, equilibration was expected to occur relatively rapidly (i.e. within about 2 years). The diffusive exchange process was monitored with conservative tracers added to the synthetic water.

3.2. Drilling, installation and design

The layout of the experiment is illustrated in Fig. 3. A vertical borehole (BPC-1) of 52 mm diameter was drilled to a depth of 10.10 m. The bedding dips at an angle of about 45° to the SE. The main fault was transected at a depth of 6–8 m. The first 5 m of the borehole were drilled with air. For the remaining 5.1 m, nitrogen was used in order to minimise ingress of molecular oxygen and hence oxidation of pyrite and organic matter around the borehole wall. Immediately after drilling, the borehole was filled with Ar. The downhole equipment including the 4.5 m long screen made of porous (40 μm mesh size) low pressure polyethylene with a porosity of 0.3 and a 0.33 m long hydraulic mechanical packer was emplaced into the borehole. The remaining part of the borehole was filled with epoxy resin (Sikadur 52).

The borehole was filled with synthetic porewater (2.8 L) which had been previously saturated with an Ar/CO_2 gas mixture corresponding to a pCO_2 of $10^{-3.5}$ bar, as in air. The composition of the synthetic porewater containing the tracers deuterium, Br^- and ^{13}C is given in Table 1. The details of the preparation procedure of the synthetic water are given in Eichinger and Wersin (2004). The sum of Cl^- and Br^- concentrations in the synthetic water was prepared to correspond to that expected for chloride in the formation water. The synthetic porewater was designed by geochemical modelling to be in equilibrium with the carbonate mineralogy and the cation exchange properties of the rock (Pearson et al., 2003). The pressure recovery in the borehole was monitored via a pressure transducer (Keller PAA-23) for a period of 12 days.

After this time, the surface equipment was installed (Fig. 3), whose main components were a membrane pump (Milton roy) for circulation, flow through cells (PEEK®) equipped with a pH electrode (Xerolyt-type, Mettler Toledo), an Eh electrode (Xerolyt-type, Mettler Toledo), and a graphite-type electrical conductivity (EC) electrode (Turnhout), a pressure transducer in the water circuit (PTX 500 manufactured by Druck Ltd., UK), a data acquisition unit (Yokogawa Daqstation DX100) and three Teflon® coated 75 mL sampling cylinders (Whitey). The water circuit unit was protected by an anaerobic cabinet filled with Ar.

The installation process and emplacement of synthetic groundwater thus was carried out in two steps. The saturation of the borehole occurred on 22 March 2002. On 3 April 2002, after filling of the circulation unit with synthetic porewater, circulation was started and the borehole interval was flushed (the water volumes of the different components of circulation unit are given in Table 2). The injection of traced water thus resulted in two pulses. As derived later from Tournassat et al. (2011), the flushing was not complete, and the resulting water composition after flushing and at the start of the circulation represented a mixture of water used for the borehole saturation (which had been affected by diffusion processes) and "fresh" synthetic porewater, with a ratio of about 40/60.

Care was given that all parts in contact with the circulating water were non-metallic (screen, lines, pump, valves, electrode

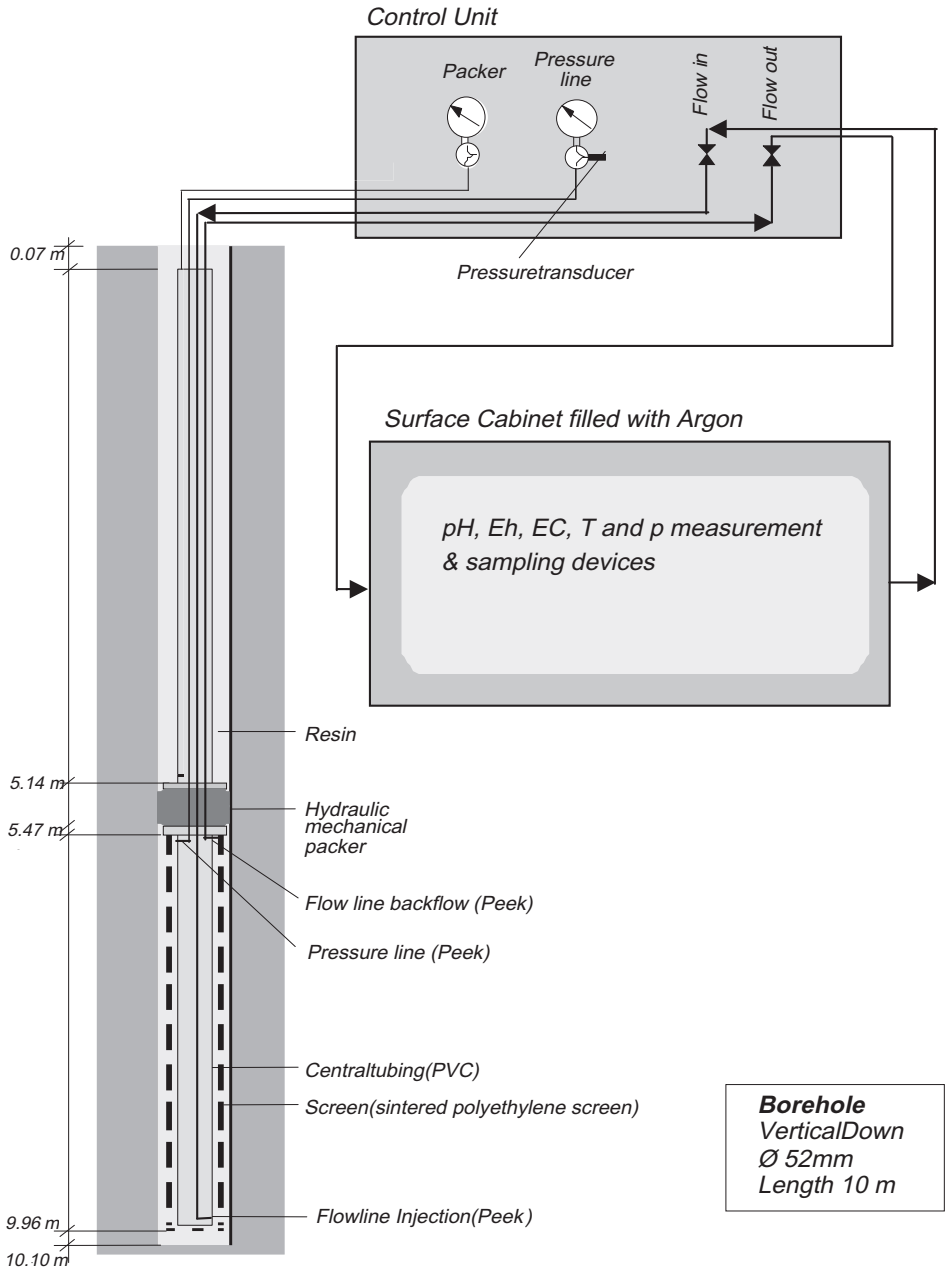

Fig. 3. Design of porewater chemistry (PC) experiment.

cells, electrodes, sample holders) in order to avoid any influence on Eh. The materials of these parts are listed in Table 2. As revealed in the course of the experiment, some of the plastic materials were not as "inert" as expected and their influence needed to be assessed in the data interpretation (see De Cannière et al., 2011). This also holds for acetone, which was used as cleaning agent for the porous filter (four washing cycles followed each time by drying under stream of nitrogen) and whose residues may have remained in the pores.

3.3. Monitoring/maintenance

After installation, the *on line* data of downhole pressure, pressure in the surface line, temperature, pH, Eh and EC were recorded via the data acquisition system and monthly downloaded and processed over the whole course of the experiment.

3.3.1. pH

The pH electrode was calibrated regularly (~ every month) via buffer solutions. After a period of about 6 months a clearly non-linear drift was noted and the electrode was replaced. The drift is due in part to the slow leakage of KCl and probably also of soluble organic compounds from the gel in the reference electrode, and in part to the reaction of sulfide and Ag within the electrode (visible as colour change). The drift was corrected in the data by manually interpolating the data points before the drift and after electrode replacement. Similar non-linear drifting of the replaced electrodes was noted over the course of the experiment whose onset however varied considerably. The uncertainty in the measured values is about 0.1 pH units.

3.3.2. Eh

The Eh electrode showed very little drift compared to the pH electrode and thus it was replaced only once (after a period of

Table 1
Concentrations of sampled waters (in mmol/L) for selected parameters.

Sample name	Test water	PC-3	PC-4	PC-5	PC-6	PC-7	PC-8	PC-9	PC-10	PC-12
Day after injection	0	116	264	529	600	837	1061	1316	1517	1846
pH (*in line*)	7.74	7.0	6.73	6.7	6.72	6.70	6.81	7.16	6.75	6.82
Eh (*in line*) mV SHE		−184	−175	−214	−227	−265	−257	−275	−240	−250
Sodium	255	253	252	247	251	253	265	247	252	243
Potassium	1.5	1.8	1.8	1.9	1.8	1.9	2.0	2.0	2.1	1.8
Magnesium	18.0	19.6	19.0	19.5	19.0	18.6	18.3	18.1	19.5	17.1
Calcium	15.9	17.4	15.8	16.0	15.3	15.4	14.9	14.0	15.5	13.5
Chloride	262	283	285	286	287	304	313	293	299	281
Bromide	29.4	12.7	8.2	7.3	6.7	2.2	3.3	3.5	3.8	4.0
Sulfate	14.7	13.3	10.5	6.6	6.2	4.9	4.3	4.1	5.0	4.3
Alkalinity	1.0	6.5	7.0	11.6	11.4	11.4	10.6	10.9	8.5	10.4
DOC/TOC	0.2	0.6	14.3	9.9	11.7	9.2	4.1	1.0	1.2	1.3
Methane	1e−4	0.038	0.035	0.029	0.026	0.044	0.12	0.72	0.25	0.084
Ammonium	0.021	0.40	0.47	0.57	0.56	0.63	0.57	0.51		0.59
Acetate			1.86	8.47	13.2	9.42	2.64	b.d.		b.d.
Org. acids (meth. Huber)			8.08	9.08	10.7	9.24	4.05	0.56	0.28	
δ^2H ‰	+370.0	+38.8	+4.3	−32.6	−37.2	−41.3	−42.5	−37	−32.7	−12.8
δ^{13}C-DIC ‰	−29.1	−11.4	−3.2	−15.9	−16.6	−15.4	−14.6	−12.3	−9.0	−11.5

b.d.: below detection limit.

Table 2
Water circuit volumes.

Equipment part	Material	Unitary volume (cm^3)	Fraction of total volume (%)
Filter screen	Polyethylene (LP)	2790.9	90.6
Water lines	PEEK™, Nylon	25.6	0.8
Valves and fittings	PEEK™, Nylon	17.0	0.5
Pump head	Polypropylene	7.9	0.3
Eh, pH, EC cells	PEEK™	15.3	0.5
Sampling vials (three vials)	PEEK™	225.0	7.3
Total water circuit		3081.7	100.0

about 3.5 years). The values (mV) were recorded relative to the Ag/AgCl electrode and are given relative to the standard hydrogen electrode (SHE).

3.3.3. EC

EC values were compensated for temperature according to:

$$K_R = \frac{K_T}{1 + \alpha(T - T_R)}$$

where K_R, K_T is the EC at reference temperature, EC at measurement temperature (mS/cm), T the measurement temperature (°C), T_R the reference temperature (25 °C), α is the dependency factor, typically 2%/°C.

The EC electrode showed anomalous behaviour which was not in line with the water composition. After inspection and replacement of the graphite-type electrode by a platinum-type one (Turnhout), it became clear that the graphite tip had almost been completely leached, presumably by some corrosion reaction. The new platinum-type electrode showed relatively constant and interpretable values (as outlined in the next section).

3.3.4. Temperature

The temperature of the circulating water was recorded with a temperature sensor integrated in the EC electrode unit.

3.3.5. Hydraulic pressures

Two independent *on line* pressure measurements were recorded: one in the surface line located directly next to the membrane pump and the other one downhole in the test interval. The membrane pulsations induced important pressure oscillation in the surface line. Adjusted pump settings (after about 1.5 year) slightly reduced this effect by reducing the amplitudes of pressure oscillations.

3.3.6. Main events and features during the in situ experiment

The *in situ* experiment was carried out for a period of 5 years (April 2002–April 2007). It was closely followed up by weekly checks of the *on line* data and, generally by biweekly checks of the equipment *on site*. In general, the technical performance of the equipment was good and, except for the technical problems listed below, no significant mishaps occurred.

Noteworthy events during lifetime of the experiment are listed in Appendix A (Table A1). In the early stage, there were two significant technical disturbances: A month after the start of the experiment, the circulation had to be stopped for 10 days due to Ar leakage in the surface cabinet. After 3½ months, a surface line was accidentally disconnected, which also led to a stop in circulation. The circulation unit was repaired a week later. Due to unexpected trends in pH and other water parameters (see results section), microbial analysis of the circulation water was conducted after 9 months, which, for the first time at the Mon Terri URL, confirmed that microbial processes were occurring in a borehole. This in fact led to a change in focus of the analytical program mentioned in the introduction. Thus, also microbial analysis was included (Stroes-Gascoyne et al., 2011). In the later stage of the experiment, the following events are noteworthy: After 4.2 years of running the surface cabinet sealing needed to be replaced and the circulation stopped for 13 days. Two months later, due to renovation work in the gallery, the circulation was stopped and the surface equipment dismantled. It was re-installed a week later and monitoring restarted. Just 2 days later, a pressure decrease due to a leakage was detected. After extensive search and testing of the different components, the leak could be finally localized in a PEEK line within the cabinet which was then replaced. As consequence of the leak, it was necessary refilling synthetic water into the circuit to make up for the pressure drop. On 11 April 2007, the circulation was stopped and the surface equipment dismantled. Overcoring of the test interval section was carried out a month later.

Table 3
Sampling schedule and analysed parameters. Underlined parameters: measured for the first time. The list includes the date of the re-emplacement of the sampling cylinders and the corresponding volume of fresh synthetic porewater added.

Sample#	Date	Days after borehole saturation	Water vol. removed/ added (mL)	Parameters	Comments
PC-0		0	+3082	pH, EC, Na, K, Mg, Ca, Sr, Cl, Br, SO_4, NH_4, NO_3, Alk, Fe, Mn, As, DOC, ^2H, ^{18}O, ^{13}C-DIC	Original synthetic porewater Saturation of the borehole with the porewater
PC-2b	03.04.02	12	−3082 +3082	pH, EC, Na, K, Mg, Ca, Cl, Br, SO_4, NH_4, NO_3, Alk, DOC, ^2H, ^{18}O, ^{13}C-DIC	Replacement of the experimental water
PC-3	16.07.02	116	−75	pH, EC, Na, K, Mg, Ca, Cl, Br, SO_4, HS, NH_4, NO_3, Alk, Fe, DOC, ^2H, ^{18}O, ^{13}C-DIC	
	23.07.02	123	+30		Re-saturation of the surface equipment after leakage
PC-4	11.12.02	264	−150 −15	pH, EC, Na, K, Mg, Ca, Sr, Cl, Br, SO_4, HS, NH_4, NO_3, Alk, Fe, Mn, Si, Al, TOC, DOC-Huber, ^2H, ^{18}O, ^{13}C-DIC, ^{13}C-DOC, organic acids, alkanes, interm. S species	Additional 15 mL were taken for microbial and SEM analyses Replacement of 1 sampling cylinder
	21.05.03	425	+75		Replacement of one sampling vial
PC-5	02.09.03	529	−2 × 75	pH, EC, Na, K, Mg, Ca, Sr, Cl, Br, SO_4, HS, NH_4, NO_3, Alk, Fe, Mn, Si, Al, TOC, DOC-Huber, DIC, ^2H, ^{18}O, ^{13}C-DIC, ^{13}C-DOC, acetate, alkanes	
PC-6	12.11.03	600	−1 × 75	pH, EC, Na, K, Mg, Ca, Cl, Br, SO_4, HS, NH_4, NO_3, Alk, TOC, DOC-Huber, DIC, ^2H, ^{18}O, ^{13}C-DIC, ^{13}C-DOC, ^{13}C-CH_4, acetate, alkanes, interm. S species	
	11.12.03	629	+3 × 75		Replacement of three sampling vials
PC-7	06.07.04	837	−3 × 75 −2 × 10	pH, EC, Na, K, Li, Mg, Ca, Ba, Sr, Cl, Br, SO_4, HS, NH_4, NO_3, Alk, Si, Al, B, Fe, TOC, DIC, TIC, ^2H, ^{18}O, ^{13}C-DIC, ^{13}C-TIC, ^{13}C-DOC, acetate, acetone, phenol$_{tot}$, alkanes	Additional volume sampled for microbial analysis
	22.11.04	976	+3 × 75		Replacement of three sampling cylinders
PC-8	15.02.05	1061	−3 × 75 −15	pH, EC, Na, K, Li, Mg, Ca, Ba, Sr, Cl, Br, SO_4, HS, NH_4, NO_3, Alk, Si, Al, B, Fe, Mn, ^2H, ^{18}O, ^{13}C-TIC, ^{13}C-TOC, ^{13}C-acetone, ^{13}C-CH_4, ^{14}C-TIC, ^{14}C-TOC, acetate, acetone, alkanes, He, H_2, O_2, N_2, Ar	Additional volume sampled for microbial analysis
	18.08.05	1245	+2 × 75		Replacement of two sampling cylinders
	25.08.05	1252	+1 × 75		Replacement of 3rd sampling vial
PC-9	28.10.05	1316	−3 × 75 −10	pH, EC, Na, K, Li, Mg, Ca, Ba, Sr, Cl, Br, SO_4, HS, NH_4, NO_3, Alk, Si, Al, B, Fe, Mn, TIC, DOC, DOC-Huber, ^2H, ^{18}O, ^{13}C-TIC, ^{13}C-CH_4, acetate, acetone, alkanes, H_2	Additional volume sampled for microbial analysis
	24.01.06	1404	+50		Re-saturation of the surface equipment after leakage
	20.04.06	1490	+3 × 75		Replacement of the three sampling cylinders
PC-10	17.05.06	1517	−3 × 75	pH, EC, Na, K, Li, Mg, Ca, Ba, Sr, Cl, Br, SO_4, HS, NH_4, NO_3, Alk, Si, Al, B, Fe, Mn, TIC, DOC, DOC-Huber, TOC-Huber, organic acids, ^2H, ^{18}O, ^{13}C-TIC, ^{13}C-CH_4, alkanes, H2	One sample vial was used for microbiological analyses, the other two for the chemical analyses
	21.07.06	1582	+3 × 75		Replacement of the three sampling vials
	02.11.06	1686	+50		Re-saturation of the surface equipment after leakage
	09.11.06	1693	+50		
	10.11.06	1694	+50		
	17.11.06	1701	+50		
PC-11	07.02.07	1783	−75	pH, EC, Na, K, Mg, Ca, Cl, Br, SO_4, NH_4, NO_3, Alk, methane, ethane	
PC-12	11.04.07	1846	−2 × 75 −1000 −150 −3 × 40 −24 −72	pH, EC, Na, K, Li, Mg, Ca, Ba, Sr, Cl, Br, SO_4, HS, S_2O_3, NH_4, NO_3, Alk, Si, Al, B, Fe, Mn, Se, I, TIC, TOC, DOC, acetate, acetone, ^2H, ^{18}O, ^{13}C-TIC, ^{34}S-SO_4, ^{18}O-SO_4, ^{34}S-H_2S, alkanes, H_2	Final sampling: first samples (2 × 75 mL) for chemical analyses, 3 × 40 mL for microbiological analyses. The others, for further chemical, isotopic and particle analyses

3.4. Water sampling and sample analysis

The circulation water was sampled with aid of the Teflon®-coated metal cylinders placed within the circuit. A cylinder with a valve at each end was removed from the circuit and sent to the laboratory, where it was opened under nitrogen atmosphere in a glove box in order to prevent reactions with oxygen. The water was then transferred into the sample vials for the different chemical and isotopic analysis. For most analyses, no filtering of the water was carried out. However, occasionally (samples PC-3 and PC-5, Table 3), for checking whether $CaCO_3$ precipitation in the cylinder had occurred, alkalinity and Ca and Mg concentrations were determined in non-filtered and filtered (0.43 μm) aliquots. No differences in the values were noted. This was confirmed by various measurements of total inorganic carbon (TIC) and dissolved inorganic carbon (DIC), as outlined below. After each sampling, the sample cylinders were filled with "fresh" synthetic porewater and re-connected to the circulation unit. Some samples were used

for solid (PC-4) and microbiological analyses (PC-4 and PC-9). Also for microbiological analyses, additional samples were taken in sterile tubes from the circuit line directly (about 10 mL each for samples PC-7, PC-8, PC-9 and PC-10).

The sequence of the sampling and the corresponding analytical parameters for each sample and the re-insertion of the sample vials (including corresponding water volumes) are given in Table 3. This illustrates that during the course of the *in situ* test, the analytical program was expanded for a number of organic and inorganic compounds including isotopic parameters and microbiological analyses because of the unexpected evolution of the porewater (bio)geochemistry.

Major components (Na, K, Ca, Mg, Cl, SO_4, Br) and nitrate were analysed by ion chromatography (Dionex DX-100). Sr, Si, Al and Se were analysed by ICP–OES (Perkin Elmer Optima 3000). Ammonium, Fe and Mn were analyzed by standard spectrophotometric methods. Total sulfide was also measured photometrically after fixation with Zn acetate. Thiosulfate, sulphite, polysulfides and sulfide were determined by HPLC after extraction into a HEPES, acetonitrile and monobrombian cocktail. Arsenic was determined with AAS (graphite furnace). DIC/TIC, were analyzed after acidification and vacuum extraction by infrared spectroscopy, ^{13}C-DIC was analysed by isotope ratio mass spectrometry (IRMS, Finnigan MAT 250). Upon elimination of DIC/TIC, TOC/DOC was analysed by quantitative oxidation (TOC analyser), ^{13}C-TOC was analysed by IRMS. ^{18}O-H_2O was analysed by IRMS. ^{2}H-H_2O was analyzed after distillation by IRMS (Finnigan Delta E). The sulphur isotopes, ^{34}S-SO_4 and ^{34}S-H_2S were analyzed by IRMS after precipitation of $BaSO_4$ (sulfate) and ZnS (sulfide), respectively.

The speciation of TOC and DOC was analyzed by size exclusion chromatography combined with liquid chromatography (method developed by the DOC-laboratory of Dr. Huber, Germany; Huber and Frimmel, 1991a, 1991b). It allowed separate determination of the fraction of low molecular weight organic acids (in the text shortened to "organic acids"). Carboxylic acids (acetate, formate, propionate, butanoate) were additionally analyzed by HPLC (Ion Pac ICE-AS 6, Dionex). The alkane gases extracted from the water-filled sampling cylinders were determined by GC (Shimadzu 17-A), dissolved acetone by GC-FID. Analytical uncertainties for the different parameters are presented in Tables A2.

Microbiological analyses techniques are presented together with the results in the summary study by Stroes-Gascoyne et al. (2011).

3.5. CO_2 measurements on core samples and isotopic analysis on gas and carbonates

Gas extraction was performed with two core samples taken from the BPC-1 borehole and CO_2 partial pressure measurements were carried by the outgassing method described in Lassin et al. (2003): Core MT7-1 from 6.46 to 7.27 m depth and core MT7-2, from 8.71 to 9.20 m. MT7-1 and MT7-2 were equilibrated 40 days in a stainless steel vessel under controlled atmosphere: MT7-1 in a N_2 atmosphere of low pressure (0.256 bar < P < 0.266 bar), MT7-2 in a He atmosphere (1.032 bar < P < 1.057 bar). Gas samples were taken and measured periodically within this time. The obtained headspace pCO_2 should correspond to the pCO_2 at equilibrium with the rock (Lassin et al., 2003). It should be pointed out that because of the rather small core volumes and large surface area some drying-out of the cores may have occurred, which would induce a lowering of pCO_2 compared to saturated conditions.

Furthermore, isotopic composition of the extracted CO_2 as well as of the carbonates calcite, dolomite and siderite of the core sample MT7-1 was determined. The carbonate minerals were extracted from a powdered bulk rock sample by conventional phosphoric acid digestion, followed by the selective dissolution technique of Al-Aasm et al. (1990). The δ^{13}C and δ^{18}O measurements of extracted CO_2 and of the carbonates were performed by IRMS.

3.6. Porewater extraction by advective displacement

A drill core sample was extracted from a neighbouring borehole BPC-A1 at 10 m depth. The sample was inserted in a pressure vessel where a high confining pressured with He is applied. Traced synthetic porewater was forced via the large hydraulic gradient through the sample. The first water samples collected at the low pressure end represent the original porewater if care in sample preparation is taken. The details of the sampling and the method are reported in Mäder (2004). pH was measured *in line*. Samples for determination of the major constituents by standard analytical techniques were taken. Samples #5–7 were considered the less disturbed according to the interpretation of Mäder (2004). Here, only pH and calculated pCO_2 data from these samples are reported.

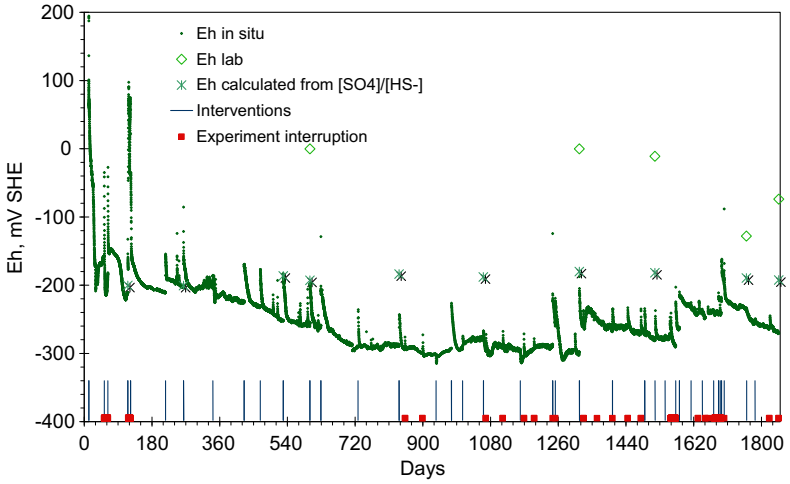

Fig. 4. Measured Eh versus time ("days" refers to days after borehole saturation); continuously measured "*in situ*" values and laboratory values measured on the sampled water as well as Eh values calculated from the concentrations of the redox couple SO_4^{2-}/HS^-.

4. Results and discussion

The complete set of data for the sampled waters is given in the Appendix A, where also *on line* data for pH, Eh and EC for these samples are indicated.

4.1. On line data

4.1.1. Eh

The Eh data of the circulating water (Fig. 4) showed an initially rapid decrease from above 100 mV to about −200 mV (with respect to SHE) in the first 6 months, followed by a slower decrease to close to −280 mV after 2 years. Afterwards, values remained rather constant for about 1.5 years and then slightly increased again. The later increase could be related to experimental disturbances, which occurred more frequently in the last year of the experiment (see Section 3). The circuit water thus displayed reducing conditions, which however were offset by short disturbances caused by maintenance activities (calibration of the probes, repair; Fig. 4). Generally, reducing conditions were re-established a few days after the interruptions. Fig. 4 shows that the laboratory measured Eh were above the field Eh, but still negative, suggesting slight oxidation of the samples. According to previous investigation on Opalinus Clay porewater (Pearson et al., 2003), the redox couple SO_4/HS^- (pyrite) appears to control redox conditions, the corresponding Eh is about −180 ± 20 mV SHE. As can be seen, the measured Eh decreased below −200 mV SHE after 350 days. The figure also shows that the *in situ* measured Eh matched the Eh calculated from the sulfate and sulfide concentrations of the first samples (days 116 and 264), but decreased below the calculated Eh for the later samples. The latest measured Eh was still somewhat below the expected equilibrium redox conditions.

4.1.2. pH

In spite of the noise in the data induced by sampling, experimental disturbances and drift of the reference electrode, the "smoothed" *in situ* measurements (see Section 3) yielded good quality data (uncertainty of ~0.1 units). The initial pH of 7.7

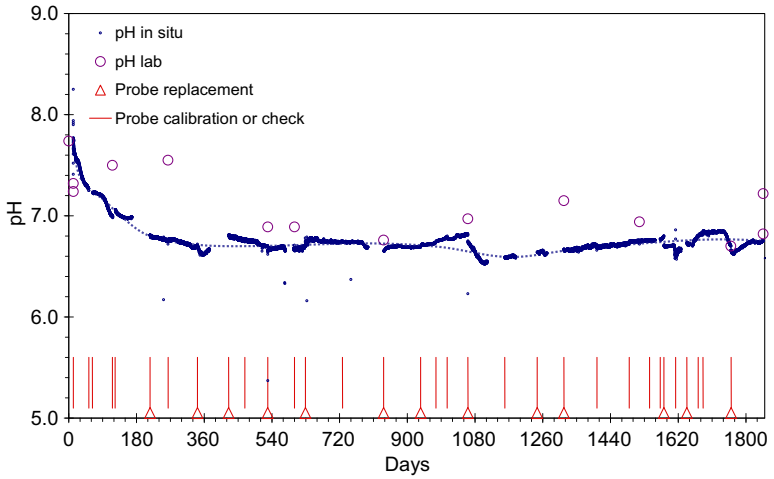

Fig. 5. Measured pH versus time ("days" refers to days after borehole saturation); continuously measured "*in situ*" values and laboratory values measured on the sampled water.

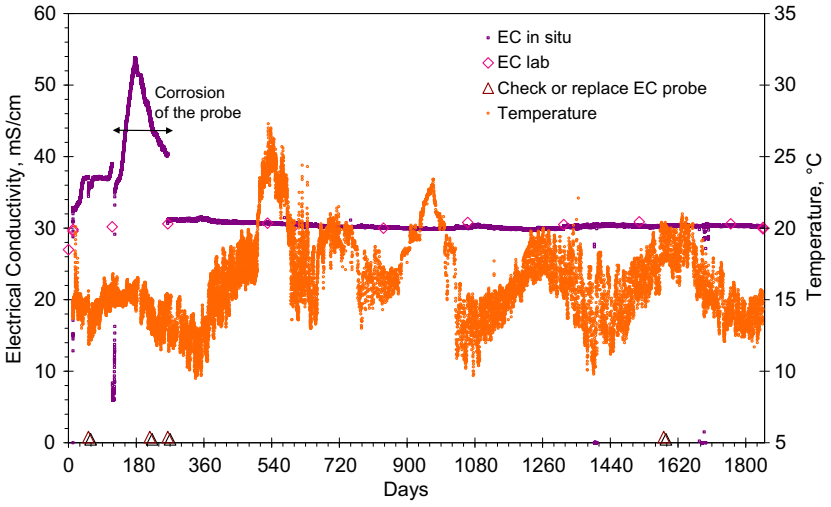

Fig. 6. Temperature and electrical conductivity versus time ("days" refers to days after borehole saturation); for EC only: continuously measured "*in situ*" values and laboratory values measured on the sampled water.

showed a steady decrease to 6.8 after 1 year after which the values remained constant within 0.2 units (Fig. 5). The corresponding lab data of the water samples showed comparable values, except for the initial ones. This may be explained by CO_2 outgassing that probably occurred during transfer of the first samples for the analyses in the laboratory environment. It could be verified that field pH was consistent with the composition of the sample, especially with regard to the alkalinity – carbonate system. As discussed in Section 3.4, the measured pH values were lower than those expected in the porewater.

4.1.3. EC

As mentioned above, the first graphite electrode did not produce reliable data. Subsequent values measured by the platinum-based EC electrodes showed relatively constant values of about 30 mS/cm (Fig. 6). Some disturbance occurred during the latest experimental period due to leakage in the surface line (see Section 3). In general, the *in situ* measurements showed good agreement with lab measurements of the different water samples.

4.1.4. Temperature

Temperature evolves as sinusoidal curve, which reflects the seasonal temperature variation in the gallery, with a maximum around 20 °C in summer and a minimum around 10 °C, in winter (Fig. 6). In the second and third year, this trend was disturbed by an experiment conducted nearby. The heat generated by the corresponding experimental devices *on site* induced temperatures as high as 28 °C in the circuit cabinet.

4.1.5. Pressure (not shown)

The interval pressure was adjusted to the hydraulic pressure of the formation around the PC borehole to keep diffusive conditions. The interval pressure ranged mostly between 3.5 and 4.2 bars; it increased to 4.5 bars in the second year and went up to 6–7 bars, simultaneously to the rise of temperature caused by the activities in the neighbourhood of the experiment. Leakage in the circuit towards the end of the experiment resulted in a temporary pressure drop down to atmospheric pressure. Important pressure oscillations of several bars amplitude between 2 and 10 and even 12 bars, were registered by the pressure transducer located in the surface circuit next to the pulsating membrane pump. In the borehole, oscillations disappeared almost completely; their amplitude was 0.2 bars, 0.5 bars at most.

4.2. Tracer evolution

The tracers HDO and bromide were added to the synthetic porewater in order to follow the dilution occurring by diffusive exchange with the adjacent porewater. The initial tracer concentrations were $\delta^2H + 370.0‰$ and 30.0 mM bromide. Formation water concentrations of deuterium and bromide are $\delta^2H -52.9‰$ and ~0.4 mM Br^- (Pearson et al., 2003). The evolution of the tracer data is represented as relative concentration of the measured concentration, with respect to the added tracer concentrations, C/C_0, in Fig. 7. The conservative tracers (HDO, Br) showed a steady decrease until day 837, which can be explained by diffusive dilution with the adjacent porewater. Faster dilution of HDO relative to bromide reflects the larger accessible porosity of HDO compared to bromide, the anion being affected by electrostatic repulsion of the negatively charged clay surface. Periodic replacement of the sampled water volume with fresh synthetic porewater (see Table 3) kept the tracer concentrations at a higher level and explained why tracer concentrations never reached the formation concentration, but even increased slightly during the second half of the experiment (from day 1061). When tracer replenishment was taken into account, the temporal evolution could be successfully modelled assuming diffusive mixing. This indicates that diffusive equilibration with the formation water in fact occurred with no notable contribution of advective transport (Tournassat et al., 2011).

4.3. Evolution of the chemical composition

Chloride, the main anionic component, showed the mirror trend of bromide, thus increasing to levels of about 0.3 M in the circuit water within about 2 years (not shown). This corresponds to the expected concentration of the formation water (Pearson et al., 2003). It should be noted however that the chloride data during the later part of the experiment reveals a notable decrease again which only partly may be explained by dilution with replaced synthetic porewater from sample replacements. Sulfate, on the other hand, did not follow the expected trend. As depicted in Fig. 8, this anion showed an initial rapid decrease during the first 500 days, followed by a slower one to about 800 days. Thereafter, the sulfate concentration remained relatively constant at about one third of its initial value. The according SO_4/Cl ratios after this period were considerably lower

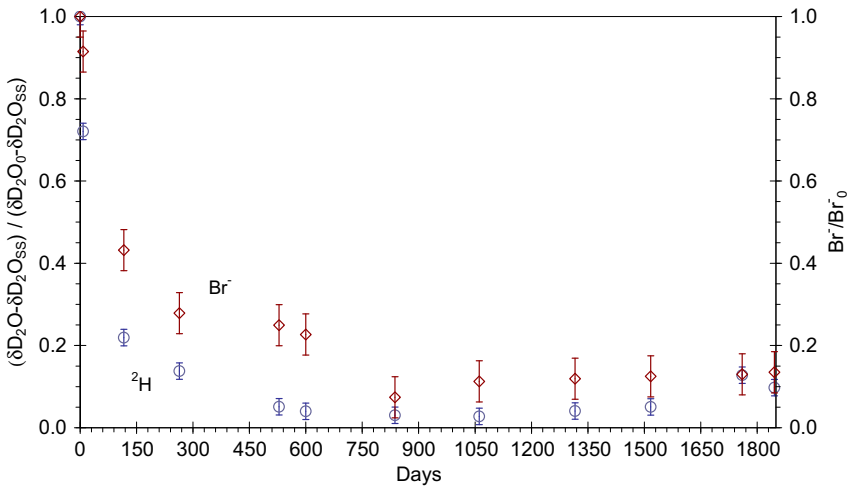

Fig. 7. Evolution of the tracer bromide and deuterium measured in the sampled water, which were added to the synthetic porewater injected at the beginning of the experiment (relative error bars Br 5%; D, 3%).

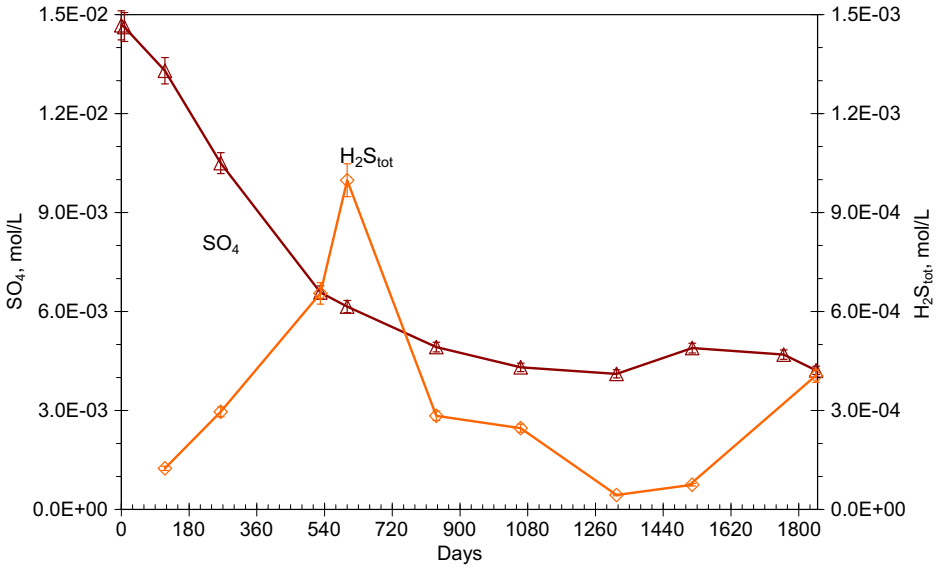

Fig. 8. Evolution of the dissolved sulfate and sulfide concentrations (error bars SO_4^{2-} 3%; HS^- 5%).

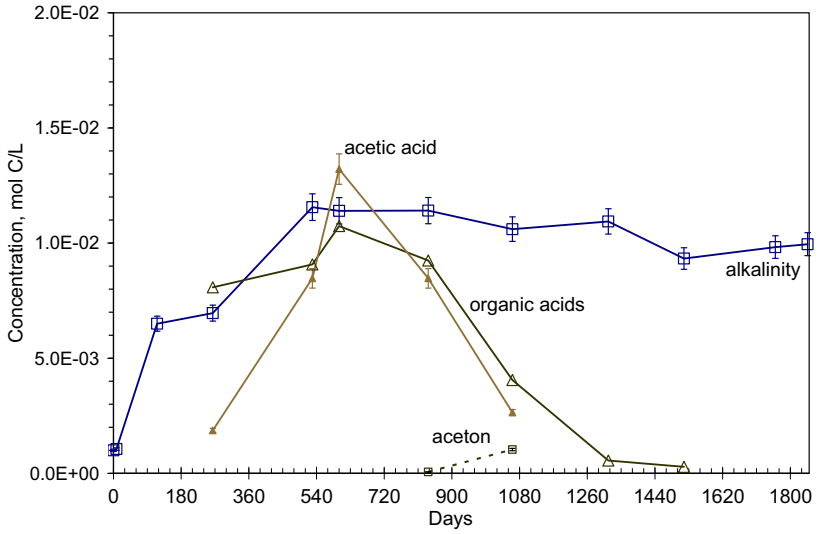

Fig. 9. Evolution of the dissolved organic species, DOC or TOC, small organic acid and acetic acid, acetone, dissolved alkanes (C_1 to C_4) as well as dissolved and total inorganic carbon, and carbonate alkalinity (error bars 5% of the concentration; DIC concentrations of day 0–264 are calculated concentrations, error bar 10% of the concentration).

than had ever been observed in Mont Terri formation waters (e.g. Pearson et al., 2003). In parallel to the initial SO_4 decrease, sulfide increased strongly to about 0.9 mM after 540 days, but decreased afterwards to lower, but clearly detectable levels again. This evolution of sulphur indicates (i) sulfate reduction to sulfide and (ii) loss of total sulphur from the water circuit. The fate of sulphur and associated redox processes are discussed in more detail below.

The evolution of total alkalinity as well as the principal inorganic and organic carbon species is illustrated in Fig. 9. Total alkalinity showed more than a 10-fold increase after the first 540 days, thus reaching levels of about 11 mM after which values remained rather constant. Interestingly, this behaviour seems mirror that of sulfate (see below). TOC, on the other hand, showed an even more significant increase, peaking after 250 days at 15 mM, remaining high till 840 days, and decreasing strongly afterwards to levels of ~1 mM. These low levels correspond in fact to DOC concentrations in the formation water, as recently shown by Courdouan et al. (2007). As indicated by chemical analysis for low molecular weight organic acids (LMWOA) performed on samples taken after day 540, virtually all of TOC comprised these organic acids. The main compound was acetate which contributed to 100% of LMWOA within analytical uncertainties at the peak concentration and showed parallel decrease to TOC and LMWOA afterwards. It is noteworthy, that the first analysis of acetate after 264 days indicated concentrations corresponding to only about 10% of TOC, thus suggesting a higher fraction of other LMWOA or perhaps of larger organic compounds.

Thus, the total alkalinity determined by acid titration consisted of both carbonate alkalinity ($HCO_3^- + 2CO_3^{2-}$) and non-carbonate alkalinity (other species neutralized by acids to pH c. 4.3 such as

de-protonated, weak organic acids and HS^- (e.g. Stumm and Morgan, 1996). Measurements of these other components were necessary in order to describe HCO_3^- evolution. Because organic acids were not determined during the initial period of the experiment, their effect on alkalinity can only be estimated and the bicarbonate concentrations are thus affected by a large uncertainty. However, after this period, i.e. after 420 days, when TOC concentrations are still high and acetate (Ac) is the dominant contributor (Fig. 9), then $Alk \approx [HCO_3^-] + [Ac^-] + [HS^-]$, and $[HCO_3^-]$ can be calculated from the measured concentrations of the other two compounds. The resulting bicarbonate concentration as a function of time showed a parabolic increase up to day 540, after which it remained constant. This is contrary to the behaviour of organic carbon which clearly showed a decrease to low levels after the concomitant increase with DIC.

Major cations Na^+, Ca^{2+} and Mg^{2+} did not show significant change with time (not shown). This indicates (i) that the cation composition of the synthetic water agrees well with that of the *in situ* porewater and, in view of the strong changes revealed from SO_4^{2-}, HCO_3^- and pH, (ii) the strong buffering capacity of the clay via cation exchange and carbonate dissolution/precipitation reactions.

4.4. Comparison of CO_2 partial pressures with laboratory studies

A major aim of the PC experiment was to obtain reliable dissolved CO_2 concentrations, respectively the pCO_2 at equilibrium with the porewater, which together with the solution composition controls the pH of the porewater (Pearson et al., 2003). The topic

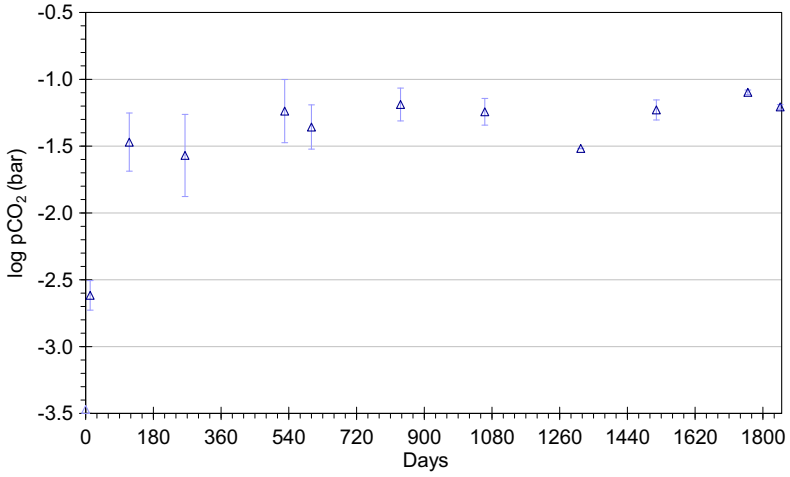

Fig. 10. Evolution of the pCO_2 in equilibrium with the porewater composition. The pCO_2 was calculated from the chemical composition of the samples. Error bars correspond to the difference between pCO_2 calculated from alkalinity or DIC.

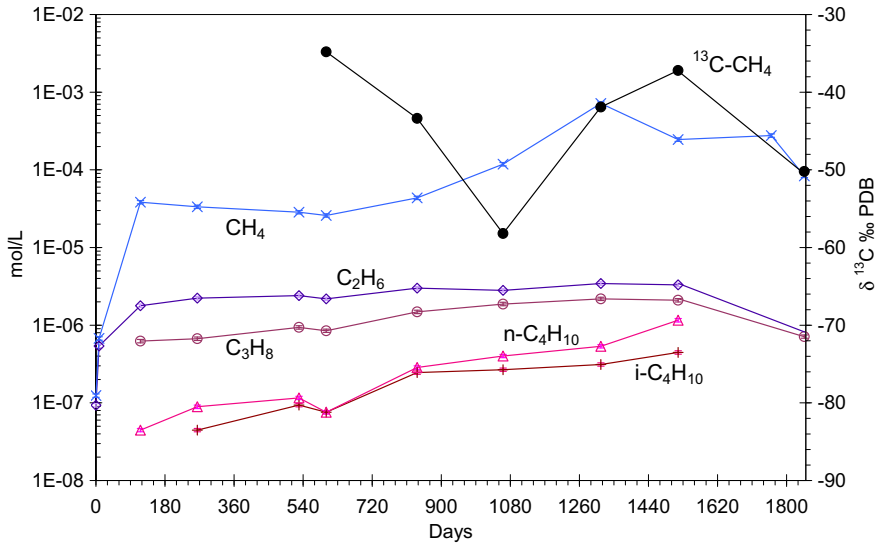

Fig. 11. Dissolved alkane compositions (left axis) and isotopic signal of methane (right axis) versus time (error bars 5% of the concentration; $\delta^{13}C$-CH_4: 5‰ PDB). Concentration of butane in the sample taken day 1846 was below detection limit (n-butane); i-butane was not measured.

was also addressed in parallel to the PC experiment by two laboratory studies performed with clay cores drilled from Mont Terri, the gas extraction study by Gaucher et al. (2003) and the study on porewater sampling by advective displacement (Mäder, 2004), as outlined in Section 3.

The gas extraction study yielded a log pCO_2 of −2.81 bar for the sample MT7-1 equilibrated under N_2 ($-2.86 < \log pCO_2 < -2.76$) and log pCO_2 −2.88 bar for the sample MT7-2 equilibrated under He ($-2.95 < \log pCO_2 < -2.85$). The advective displacement study yielded *on line* pH values of 7.5 ± 0.2. The pCO_2 values were modelled using the measured pH and alkalinity values and adjusting TIC values for calcite saturation. The corresponding calculated log pCO_2 values ranged from −2.61 to −2.94. Thus, a remarkable agreement between the results of these two lab studies was noted, yielding a pCO_2 of $10^{-2.75\pm0.15}$ bar for the porewater. It should be pointed out however, that the measured pCO_2 values from gas extraction may reflect too low values because of possible drying-out effects (cf. Section 3.5.). In the nearby *in situ* PC-C experiment, somewhat higher CO_2 partial gas pressures ranging from $10^{-2.4}$ to $10^{-1.7}$ bar were calculated from water analyses (Vinsot et al., 2008).

The pCO_2 determined from the composition of the sampled PC water is represented in Fig. 10. This illustrates, that except for the first sample (PC-1) equilibrated for 12 days, the log pCO_2 ranged between $-1.8 < \log pCO_2 < -1.1$ bar. The final sample showed a log pCO_2 −1.21 ± 0.02 bar. Thus, the pCO_2 in circuit was distinctly higher than inferred from lab data or from results from the nearby PC-C experiment (Vinsot et al., 2008). This is a clear indication of the effect of microbiologically-induced redox reactions within the *in situ* experiment.

4.5. Evolution of selected minor compounds and dissolved gases

The concentration of dissolved Fe shows a similar trend as sulfide, thus increasing from about 2 μM to rather high levels (~0.1 mM) at day 1061 and decreasing then down to low levels of a few μM, similar to those expected in the porewater (Pearson et al., 2003). At these low Fe levels, slight undersaturation with siderite (SI ≈ −1.0) and near to equilibrium with FeS(am) (SI ≈ 0.5) is calculated, whereas at the higher levels, the waters are significantly oversaturated with FeS(am) (SI = 1.0–1.9) and near to equilibrium with $FeCO_3$ (SI ≈ 0.4). Manganese concentrations show less variation than Fe and are in the range of 2–9 μM, close to equilibrium with rhodochrosite (SI = −0.4–0.0).

Strontium and ammonium, both known to be part of the cation exchanger of the Opalinus Clay (Pearson et al., 2003), show similar concentrations and remained relatively constant with time (not shown). The Sr concentrations became increasingly undersaturated with respect to celestite (SI = −0.1 to −0.8).

The concentrations of alkanes are illustrated in Fig. 11. The dominant compound is methane which showed an initial rapid increase, followed by a slow but steady increase to 0.7 mM to day 1316. During the last stage a slight decreasing trend is noted. For the higher alkanes much lower concentrations, but also an increasing trend to day 1316, followed by a decreasing one was observed.

Table 4
Isotopic composition $\delta^{13}C$ and $\delta\ ^{18}O$ of several carbon components as well as $\delta^{34}S$ and $\delta^{18}O$ of sulfate in the Opalinus Clay system according to Pearson et al. (2003) and Gaucher et al. (2003).

$\delta^{13}C$ in ‰ PDB	Pearson et al. (2003)	Gaucher et al. (2003)
$\delta^{13}C$ C_{org}	−27.7 to −26.6	
$\delta^{13}C$ CO_2		−10.2 ± 0.1 (sample MT7-1)
		−10.5 ± 0.1 (sample MT7-2)
$\delta^{13}C$-DIC	−10.93	
$\delta^{13}C$-CH_4	−40.4	
$\delta^{13}C$ carbonate	−0.08–0.21	
$\delta^{13}C$ calcite		−0.2 ± 0.1
$\delta^{13}C$ dolomite		−1.2 ± 0.1
$\delta^{13}C$ siderite		−4.2 ± 0.1
$\delta^{34}S$ in ‰ CDT		
$\delta^{34}S$ SO_4	16.3–25	
$\delta^{18}O$ ‰ SMOW		
$\delta^{18}O$ CO_2		29.0 ± 0.1 (sample MT7-1)
		31.5 ± 0.1 (sample MT7-2)
$\delta^{18}O$ carbonate	23.16–25.28	25.0 ± 0.1
$\delta^{18}O$ calcite		27.4 ± 0.1
$\delta^{18}O$ dolomite		28.4 ± 0.1
$\delta^{18}O$ siderite		25.0 ± 0.1
$\delta^{18}O$ SO_4	3.1–12.3	

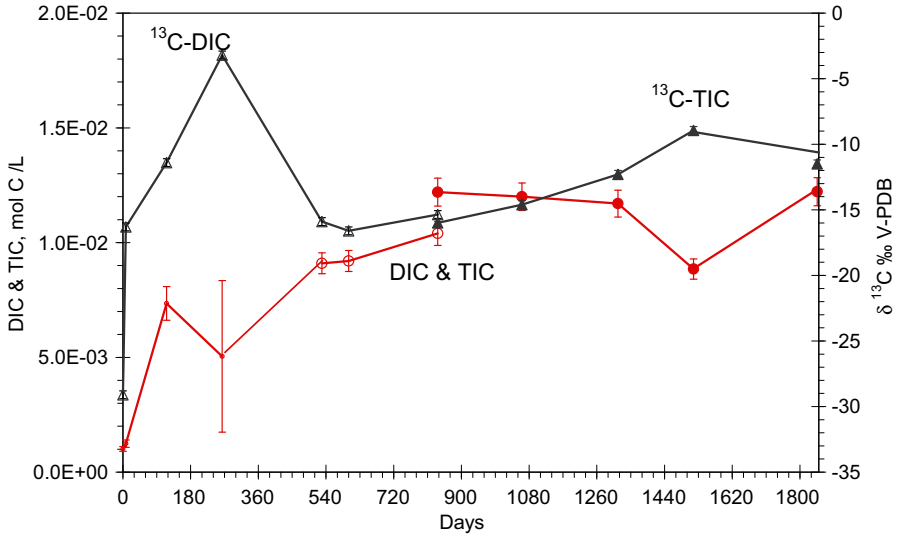

Fig. 12. Evolution of the isotopic signal (right axis) and of the concentrations (left axis) of the dissolved inorganic and total inorganic carbon (error bars: 5% of the concentration; $\delta^{13}C$-IC: 0.3‰ PDB).

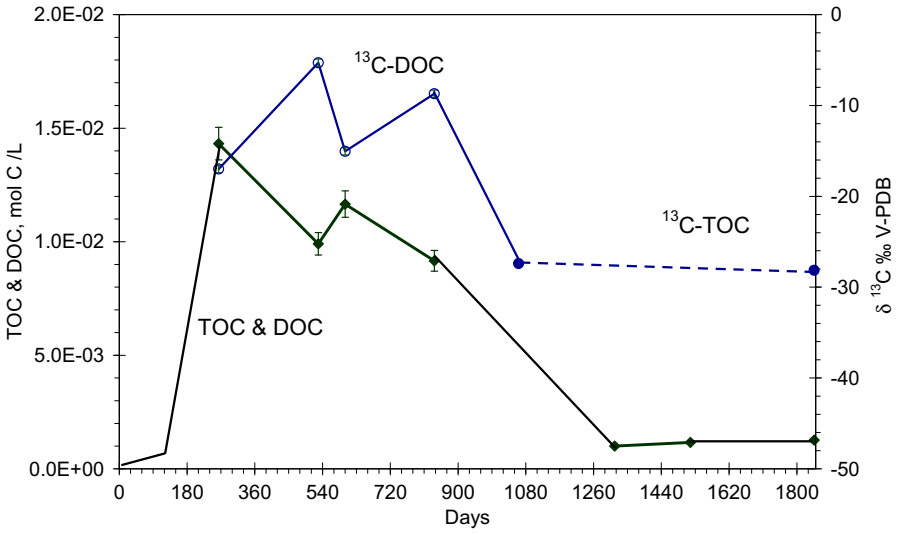

Fig. 13. Evolution of the isotopic signal (right axis) and of the concentrations (left axis) of the dissolved and total inorganic carbon (error bars: 5% of the concentration, δ^{13}C-IC: 0.3‰ PDB).

Hydrogen concentrations (not shown) were determined only during the last part of the experiment, following day 1061. They show a notable increase from a few μM to 14 μM at the end of the experiment.

4.6. Evolution of carbon and sulphur isotopes

The evolution of δ^{13}C-DIC of the circuit water, originally traced with a low value of −29.1‰ PDB, was followed over the entire experiment. In addition, due to the unexpected microbiologically-induced disturbance (discussed below), δ^{13}C-DOC, δ^{13}C-CH_4, δ^{14}C-DIC and δ^{14}C-DOC were measured during the later stages of the experiment.

The δ^{13}C-DIC evolution (Fig. 12) cannot be explained by diffusive mixing, except perhaps during the initial 200 days where a similar behaviour as that for δ^{2}H was noted. Afterwards instead, significant variations between −4‰ and −15‰, with an average value of about −12‰ occurred which indicate important fractionation due to carbon degradation reactions. The expected δ^{13}C-DIC of the *in situ* porewater is about −10‰ (Pearson et al., 2003; Gaucher et al., 2003; Table 4), the values for carbonates in the clay are higher (−0.2‰ for calcite, −1.2‰ for dolomite and −4–2‰ for siderite). The organic material in Opalinus Clay has a δ^{13}C of −26.9‰ (Pearson et al., 2003), the δ^{13}C of synthetic plastic materials may vary considerably. Thus, for example, δ^{13}C of plastics manufactured from aliphatic petroleum range from −26‰ to -40‰ (Murray et al., 1994; Höhener, 2005). For the polymer gel-filling of the reference electrodes, a δ^{13}C value of −32.0‰ was determined (De Cannière et al., 2011). No fractionation is expected during mineralization of either natural or synthetic organic material (Boutton, 1991). The observed average δ^{13}C of −12‰ is considerably heavier than expected from mineralization of organic material, but lighter than that in the natural carbonate. This suggests that values are the result of both carbonate dissolution and degradation of organic material. Support for this is provided by the ^{14}C analysis which indicate that about 50% of DIC represents modern carbon, whereas for DOC 100% were found to be modern carbon. This result moreover indicates a modern carbon source, which points to a degradation of some equipment material. As discussed in detail in De Cannière et al. (2011), acetone, a possible candidate for the carbon source, is not expected to contain a modern carbon signal, whereas organics from the gel-filling of the reference electrode (e.g. glycerol) do show a modern carbon signal (see Section 3). Support for this source is provided mass balance considerations given in Wersin et al. (2011).

δ^{13}C-DOC values which were measured starting from day 200 (Fig. 13) show rather heavy and similar values (−15‰ to −5‰) as those for δ^{13}C-DIC until day 900, but decrease afterwards to values of around −28‰. The heavy values are not consistent with a simple organic carbon degradation process, since as noted above, carbon sources are expected to be considerably lighter. On the other hand, processes which may increase δ^{13}C DOC are methanogenesis (e.g. Hunkeler et al., 1999) or carboxylation, (e.g. Platen and Schink, 1987). In fact, increase in methane in the circuit water was observed (Fig. 11), but the trend noted cannot be directly related to that of δ^{13}C-DOC. The signals of δ^{13}C-CH_4 show decreasing values from −32‰ to −60‰ from day 540 to day 1'000, but then increase during the latest stage of the experiment. The decreasing values are in line with methanogenesis in the borehole, whereas during the last stage, δ^{13}C-CH_4 suggests methane oxidation reactions.

In summary, carbon isotopes clearly indicate carbon transformation and degradation as well as reactions involving methane as well as carbonate dissolution, but the different signals observed cannot be explained in a consistent way. This is partly due to the fact that the open system under consideration requires concomitant consideration of diffusional processes, kinetics and equilibrium reactions (Tournassat et al., 2011).

The analysis of the isotopic ratios of δ^{34}S with 51.0‰ CDT and δ^{18}O with 12.4‰ SMOW in sulfate as well δ^{34}S in sulfide (8.1‰) at the end of the experiment indicate significant fractionation due to microbial redox processes. The corresponding ratios in the original synthetic water were 7.1‰ for δ^{34}S and 10.7 for δ^{18}O. Previous analyses in the porewater (Pearson et al., 2003) also showed lower values in δ^{34}S in the range of 16–25‰, but a similar value for δ^{18}O (Table 4).

4.7. Evidences of microbiologically-mediated sulfate reduction

The results show clear evidence of sulfate reduction coupled to microbial degradation of organic carbon. Sulfate reducing and to a

lesser degree methanogenic bacteria were consistently detected in the circuit water from the beginning of the microbial measurements (at day 264), as outlined in Stroes-Gascoyne et al. (2011). The produced sulfide reacted with Fe(II) to form iron sulfides such as X-ray amorphous FeS and pyrite, as determined from analysis of black precipitates (Koroleva et al., 2011; Stroes-Gascoyne et al., 2011). A further evidence of sulfate reduction is provided by the $\delta^{34}S$ data determined at the end of the experiment.

From the patterns of the carbon data, a number of different carbon degradation and mineralization processes were active at different times during the experiment. Four main stages can be identified. At the initial stage (~first 100 days), little DOC was released. In the 2nd stage (~100–600 days), considerable microbiologically-driven sulfate reduction coupled to the degradation of an organic source occurred, which led to a concomitant increase in DOC. As discussed in De Cannière et al. (2011), glycerol released from the gel-filling of the electrodes is the most likely candidate for this organic disturbance. This organic carbon got first transformed to organic acids, most of which are of larger molecular weight than acetate. After about 200 days, however the reaction products shifted primarily to acetate. Assuming glycerol as source, this pathway can be described as:

$$C_3H_8O_3 + 0.25SO_4^{2-} \rightarrow 1.5CH_3COO^- + 0.25H_2S + H^+ + H_2O \quad (1)$$

Some of the organic acids are further mineralized to CO_2 and fermented to methane, but these reaction pathways proceed at a lower rate relative to reaction (1). The production of acidity leads to carbonate dissolution and increase in pCO_2, as indicated from the increase in $\delta^{13}C$-DIC.

During the 3rd stage (600–1000 days) acetate decrease can be explained by out-diffusion and degradation process, such as acetate mineralization and fermentation which leads to a strong decrease in TOC and a moderate increase in methane:

$$CH_3COO^- + SO_4^{2-} + 3H^+ \rightarrow 2CO_2 + H_2S + 2H_2O \quad (2)$$

$$CH_3COO^- + H^+ \rightarrow CH_4 + CO_2 \quad (3)$$

Sulfide concentrations remained low, pointing to the relatively fast precipitation of iron sulfides. During this stage, DIC remained high. The main overall reaction pathway can be written as:

$$CH_3COO^- + SO_4^{2-} + Fe^{2+} \rightarrow FeS + 2HCO_3^- + H^+ \quad (4)$$

During the 4th stage (1000 days till end of experiment), sulfate reduction continued in spite of the near-to-depletion of TOC, sulfate being provided by the rock via diffusion, resulting in a steady-state between sulfate influx and sulfate reduction. The source of organic carbon during this stage is not clear. It may either be a new non-soluble source or previously formed non-soluble organic species (e.g. bacterial organic matter).

In addition to X-ray amorphous FeS, pyrite was formed. The proportion of the sulfide products is not known. The Fe(II) diffusing from the rock may have originated from the dissolution of Fe-rich carbonate (siderite, ankerite) or release of surface-bound Fe(II) to the clay.

5. Conclusions

Synthetic porewater traced with deuterium, bromide and negative $\delta^{13}C$ was circulated in a borehole for 5 years. As evidenced from the behaviour of the conservative tracers, diffusive equilibration with the surrounding porewater of the clay formation was reached after about 3 years. However, the composition and pH/pCO_2 conditions differed considerably from those of the *in situ* porewater. Thus, pH was lower and pCO_2 was higher than indicated by complementary laboratory investigations and also different from conditions in near-by boreholes. The noted differences are explained by microbiologically-induced redox reactions occurring in the borehole and in the interfacial wall area which were caused by one or several degrading organic sources.

As indicated by ^{14}C analysis, the microbial perturbation was induced by modern organic carbon released from some equipment material. The most probable source displaying a modern carbon signal is the polymer-filling of the reference electrode which released glycerol into the water circuit. The degradation of this source was accompanied by sulfate reduction and induced a high production rate of acetate for the first 600 days. Concomitantly, carbonate dissolution occurred and high pCO_2 and alkalinities and lowering in pH resulted. Afterwards, the microbial regime changed and, in parallel to ongoing sulfate reduction, acetate was consumed, leading to a strong decrease in TOC which reached background levels after about 1200 days. In spite of the end of this organic disturbance in the circuit water, sulfate reduction continued to occur at a constant rate, fuelled probably by insoluble organic species. This induced near-to-constant concentrations of sulfate and bicarbonate and of pH/pCO_2 conditions until the end of the experiment. The main sink for sulphur was iron sulfide, which precipitated as FeS (am) and as FeS_2.

The chemical and isotopic composition was affected by the complex interplay of diffusion, carbon transformation rates, mineral equilibria and dissolution rates (e.g. Fe carbonates), iron sulfide precipitation rates, and exchange reactions with the clay. The ^{13}C signals measured for different carbon species showed significant variations which could only be partly explained by the main degradation processes inferred from chemical analysis.

It is interesting to note that main cation concentration, such as Na, Ca and Mg, remained remarkably constant during the experiment, thus indicating the strong buffering of the formation via cation exchange and carbonate dissolution/precipitation reactions. For quantitative interpretation, a coupled diffusion, chemical equilibria, and reaction kinetics model is required (Tournassat et al., 2011).

Acknowledgements

This work was carried out within the Mont Terri Project in close co-operation with the Mont Terri Consortium. We especially appreciate the support of Thomas Fierz (Solexperts), Hugo Moers (SCK-CEN), Paul Bossart, Christophe Nussbaum, Heinz Steiger, Olivier Meier (Geotechnical Institute/Swisstopo) and the COREIS team for the field work. The support of Lorenz Eichinger (Hydroisotop) for the analytical work is acknowledged. The manuscript has benefited from fruitful discussions with Joe Pearson (New Berne, USA), Christophe Tournassat (BRGM), and Sim-Stroes-Gascoyne (AECL).

Appendix A

See Tables A1 and A2.

Table A1
Important events during the experiment.

Date	Days after borehole saturation	Summary of the activities
22.03.02	0	Saturation of the borehole test interval with synthetic porewater
03.04.02	12	Flush surface installation with Argon and complete infill with synthetic porewater Complete replacement of the borehole water; sampling of the old borehole water Start circulation between downhole test interval and surface equipment
04.04.02	13	Simulation of power failure (on and off of the circulation pump)
12.04.02	21	Loss of Argon used to feed the anaerobic surface cabinet
14.05.02	53	Leak detected at the windows of the anaerobic surface cabinet, the reason for the Argon loss. The window was removed for repair Stop experimental circulation
24.05.02	63	Window of the anaerobic surface cabinet was re-emplaced Re-start the experimental circulation
16.07.02	116	Sampling of one 75 mL vial
17.07.02	117	Accidental disconnection of the circulation line during activities at a neighbor experiment; air increased in the surface lines No circulation
23.07.02	123	The lines to the borehole were shut closed as consequence of the line disconnection Immediate pressure response after injection of a few mL of synthetic porewater shows that the borehole interval was not de-saturated The surface circuit was re-saturated with synthetic porewater after it had been flushed with Argon gas The system pressure is adjusted to 3.5 bar and the circulation re-started
11.12.02	264	Sampling of two 75 mL vials. In addition, two microbiological samples were taken (5 mL and 10 mL) in recipients flushed with Argon Replacement of the electrical conductivity probe
27.02.03	342	Re-connection of the downhole pressure sensors (test interval pressure and packer pressure). No pressure data between 11th of December and 27th of February
02.09.03	529	Sampling of three 75 mL vials, noticeable smell of H_2S Change the pump settings (31 pulse/min, 20% stroke length instead of formerly 15 pulse/min, 50% stroke length) to try to reduce pressure oscillation in the surface line
12.11.03	600	Sampling one 75 mL vial
06.07.04	837	Sampling three 75 mL vials for chemical analyses. In addition, two 10 mL samples in sterile tubes as well as pieces of line tubing and the replaced pH probe were taken for microbiological analyses
15.02.05	1061	Sampling three 75 mL vials as well as one microbiological sample in a sterile tube (5 mL waste + 10 mL)
18.08.05	1245	A small leak was detected in a PEEK fitting on the circuit line and replaced (temporary interruption of the circulation)
25.08.05	1252	Again, a PEEK circuit line was leaking (hole in the line) and replaced (temporary interruption of the circulation)
28.10.05	1316	Sampling three 75 mL vials and one microbiological sample in a sterile tube (10 mL)
14.12.05	1363	Repair of a broken fitting on the line feeding the anaerobic surface cabinet with Argon (temporary interruption of the circulation)
24.01.06	1404	Replacement of the PEEK borehole inlet after a small crack was detected, which partly de-saturated the surface equipment (“0” reading on the EC probe). Surface circuit needed to be refilled and the pressure adjusted by addition of about 50 mL synthetic porewater Repair of the windows sealing of the anaerobic surface cabinet (temporary interruption of the circulation)
17.03.06	1456	Pressure sensor of the test interval is defective
22.03.06	1461	Installation of a new pressure transducer for the test interval
17.05.06	1517	Sampling three 75 mL vials: 1 vial for microbiological analyses, two vials for chemical analyses
28.06.06	1559	The window sealing of the anaerobic surface cabinet was not tight anymore. The window was removed for repair Stop the experimental circulation
11.07.06	1572	Restart the circulation after installation of the cabinet window
29.09.06	1652	Dismantling of the surface equipment for the shotcrete renovation of the gallery Stop circulation
05.10.06	1658	Re-installation of surface equipment. Check circuit lines, adjust the pressure of the system (pressure sensors were still not re-connected due to the work in the gallery) Re-start experimental circulation
20.10.06	1673	Connection of all the lines to the data acquisition
22.10.06	1675	Interruption of the circulation, interval pressure dropped to atmospheric level, surface equipment partly de-saturated (EC cell reading “0 mS/cm”)
02.11.06	1686	Stop circulation pump, close the borehole A first re-saturation of the surface circuit failed due to clogging at the inlet of the EC measuring cell. After cleaning the equipment, it was re-saturated and the pressure, adjusted Re-start experimental circulation
06.11.06	1690	Interval pressure dropped again to atmospheric level and the electrical conductivity reading to “0 mS/cm” Stop circulation pump, close the borehole No leak could be detected on the surface circuit, even after cleaning the surface circuit lines. Still, the interval pressure dropped. So the borehole was closed and isolated from the surface circuit and the interval pressure monitored to check if the downhole lines were not leaking Interruption of the experimental circulation
09.11.06	1693	No leaking of the downhole lines Connection of the surface and the downhole circuit, adjust the pressure, re-start circulation
10.11.06	1694	Interval decline to atmospheric level and the electrical conductivity reading was “0 mS/cm”. Stop circulation pump, close the borehole Replace existing pump, adjust the pressure and re-start circulation
17.11.06	1761	Again, interval pressure at atmospheric level, EC reading on “0 mS/cm”. Stop circulation pump Replace a leaking PEEK line. Re-saturate the surface circuit and adjust the pressure. Re-start circulation
07.02.07	1783	Sampling one 75 mL vial
11.04.07	1846	Final dismantling and sampling of the experimental porewater

Table A2a
Analyses of water samples: selected on line data, dissolved compounds.

Sample description	Mol weight	Unit	Analytical error	PC01J10000	PC 01J02.0000	PC-0	PC-0b	PC-3	PC-4	PC-5
Sample number				135917	182549	136419	136421	138465	143261	148380
Sample date + time				22 March 02	11/April 02	3/April 02	3/April 02	16/July 02	11/December 02	2/September 03
Sample description				Test water	Final test water		18:50–19:00	ca. 10:00	ca. 12:00	ca. 10:00
Sample volume		L			1.0	0.5		0.075	0.15	0.15
Days after start of the experiment				0	1846	0	0.5	116	264	529
Field observations										
Appearance				Clear	Clear	Clear	Clear	Susp. particles	Susp. particles	Clear
Odor				None	None	None	None	Light smell of H_2S	Romg smell of H:	Trong smell of H_2
Online measurements					None					
Time								6:12	10:56	10:36
Eh SHE		mV				No circulation through the online instruments	No circulation through the instruments	−184.00	−175.00	−214.00
pe calc								−3.20	−3.10	−3.60
pH								7.00	6.73	6.70
EC		mS/cm						Broken electrode	Broken electrode	30.70
Temperature		°C		20.00				15.90	14.20	24.70
Pressure in the piezometer		bar					2.90	3.61	3.37	4.33
Dissolved constituents										
EC		mS/cm	3%	27.00	29.90	29.60	29.83	30.20	30.60	30.70
pH			0.10	7.74	7.22	7.24	7.32	7.50	7.55	6.89
Eh		mV SHE	2 mV		436.00					
Lithium	6.94	mol/L	5%		7.20E−07					
Sodium	22.99	mol/L	3%	2.55E−01	2.58E−01		2.58E−01	2.53E−01	2.52E−01	2.47E−01
Potassium	39.10	mol/L	3%	1.45E−03	1.45E−03		1.52E−03	1.79E−03	1.77E−03	1.89E−03
Ammonium	18.04	mol/L	5%	2.16E−05	<5.54E−06		2.77E−05	3.99E−04	4.71E−04	5.71E−04
Magnesium	24.31	mol/L	3%	1.80E−02	1.80E−02		1.84E−02	1.96E−02	1.90E−02	1.95E−02
Magnesium tot (acid)	24.31	mol/L	3%							2.00E−02
Calcium	40.08	mol/L	3%	1.59E−02	1.58E−02		1.60E−02	1.74E−02	1.58E−02	1.60E−02
Calcium tot (acid)	40.08	mol/L	3%							1.59E−02
Strontium	87.62	mol/L	5%	4.45E−04	2.17E−04				4.34E−04	4.68E−04
Barium	137.33	mol/L	5%		4.806E−07					
Chloride	35.45	mol/L	3%	2.62E−01	2.61E−01		2.67E−01	2.83E−01	2.85E−01	2.86E−01
Bromide	79.90	mol/L	3%	2.94E−02	2.87E−02		2.69E−02	1.27E−02	8.20E−03	7.33E−03
Iodide	126.90	mol/L	3%		5.04E−07					
Sulphate	96.06	mol/L	3%	1.47E−02	1.49E−02		1.46E−02	1.33E−02	1.05E−02	6.58E−03
Sulfide (tot) as S	32.07	mol/L	5%						2.96E−04	6.55E−04
Nitrate	62.00	mol/L	3%	<1.61E−05	<1.61E−05		<8.06E−06	<8.06E−06	<8.06E−06	<8.06E−06
Alkalinity	61.02	mol/L	5%	1.00E−03	1.094E−03	1.252E−03	1.056E−03	6.500E−03	6.960E−03	1.156E−02
Boron	10.81	mol/L	5%		1.39E−05					
Silicon	60.08	mol/L	5%		<1.66E−06				6.99E−05	2.03E−04
Aluminium	26.98	mol/L	5%		8.89E−06				1.04E−06	7.41E−07
Iron	55.85	mol/L	4%	2.33E−06	<1.79E−06			3.58E−07	4.48E−06	2.33E−06
Manganese	54.94	mol/L	4%	4.00E−06	1.51E−06				3.28E−06	2.18E−06
Selenium	78.96	mol/L	5%		2.79E−08					

(*continued on next page*)

Table A2a (*continued*)

Sample description	Mol weight	Unit	Analytical error	PC01J10000	PC 01J02.0000	PC-0	PC-0b	PC-3	PC-4	PC-5
Sample number				135917	182549	136419	136421	138465	143261	148380
Sample date + time				22 March 02	11/April 02	3/April 02	3/April 02	16/July 02	11/December 02	2/September 03
Sample description				Test water	Final test water		18:50–19:00	ca. 10:00	ca. 12:00	ca. 10:00
Sample volume		L			1.0	0.5		0.075	0.15	0.15
Days after start of the experiment				0	1846	0	0.5	116	264	529
Reduced sulfur species										
Sulfide	33.07	mol/L	5%					1.22E−03		
Sulfur (0)	32.07	mol/L						1.56E−05		
Thiosulfate	112.13	mol/L						2.70E−04		
Sulfite	80.06	mol/L						1.70E−04		
Carbon species										
Toc	12.01	mol C/L	10%		2.00E−04				1.43E−02	9.91E−03
TOC-Huber	12.01	mol C/L	10%							
DIC	12.01	mol C/L	10%							9.10E−03
TIC	12.01	mol C/L	10%		1.30E−03					
DOC	12.01	mol C/L	10%	<1.67E−05	1.67E−04	1.50E−04	1.33E−04	6.49E−04		
DOC-Huber	12.01	mol C/L	10%							
Organic acids (LC/spectr; Huber)	12.01	mol C/L	10%						8.08E−03	9.08E−03
Acetic acid	59.04	mol C/L							1.86E−03	8.47E−03
Formic acid	45.02	mol C/L							6.66E−05	
Aceton	58.08	mol C/L								
2-Hydroxy-5-methylanisol (C8)	122.16	mol C/L								
Total phenols		mol C/L								
Isotopes										
2H		‰SMOW	1.5%	+370.0	+368.8		+251.5	+38.8	+4.3	−32.6
^{18}O		‰SMOW	0.15%	−10.46	−10.45		−10.08	−9.02	−8.43	−8.62
^{13}C-CO_2		‰PDB	0.3%							
^{13}C-DIC		‰PDB	0.3%	−29.1			−163	−114	−3.2	−15.9
^{13}C-TIC		‰PDB	0.3%		−11.5					
^{13}C-DOC		‰PDB	0.4%						−17	−5.3
^{13}C-TOC		‰PDB	0.4%		Not possible					
^{13}C-aceton		‰PDB	0.3%							
$2HCH_4$		‰PDB								
^{13}C-CH_4		‰PDB	0.3%							
^{13}C-C_2H_6		‰PDB	0.3%							
^{14}C-TIC		%	var.		94.9 ± 0.9					
^{14}C-DOC		%	var.		Not possible					
$\delta\ ^{34}S$-SO_4		‰CDT	0.3		7.10					
$\delta\ ^{18}O$-SO_4		‰SMOW	0.2%		10.70					
$\delta\ ^{34}S$-H_2S		‰CDT	0.2%							
Gas analysis	N ml/ mol									
Helium	22400.00	mol/L	5%	n.m.	n.m.	n.m.	n m	n.m.	n.m..	n.m.
Hydrogen	22400.00	mol/L	5%	n.m.	n.m.	n.m.	n.m.	n.m.		n.m.
Oxygen	22400.00	mol/L	5%	n.m.	n.m.	n.m.	n.m.	n.m.		n.m.
Nitrogen	22400.00	mol/L	5%	n.m.	n.m.	n.m.	n.m.	n.m.		n.m.
Argon	22400.00	mol/L	5%	11.111.	n.m.	n.m.	n.m.	n.m.	n.m..	n.m.
Methane	22400.00	mol/L	5%	1.24E−07	n.m.	6.76E−07	n.m.	3.84E−05	3.35E−05	2.86E−05

Ethane	22400.00	mol/L	5%	9.31E−08	n.m.	5.40E−07	n.m.	1.79E−06	2.23E−06	2.41E−06
Propane	22400.00	mol/L	5%	n.m..	n.m.	n.m.	n.m.	6.25E−07	6.70E−07	9.38E−07
i-butane	22400.00	mol/L	5%	n.m..	n.m..	n.m.	n.m.	<4.46E−08	4.46E−08	9.38E−08
n-butane	22400.00	mol/L	5%	n.m..	n.m..	n.m.	n.m.	<4.46E−08	8.93E−08	1.16E−07
Ethene	22400.00	mol/L	5%	n.m..	n.m..	n.m.	n.m.	8.93E−08	<4.46E−08	<4.46E−08
Calculated parameters										
Charge balance (Cat-|An|)/(Cat+|An|)		%		0.54	1.20		0.56	−0.34	0.58	0.46
Charge Balance		eq/L		3.50E−03	7.76E−03		3.62E−03	−2.22E−03	3.77E−03	2.92E−03
Total salt		meq/L		0.65	0.65		0.65	0.66	0.65	0.64
si_Calcite		SI		0.26	−0.22	−0.12	−0.12	0.38	0.04	0.10
si_Dolomite(dis)		SI		0.19	−0.76	−0.55	−0.56	0.44	−0.20	−0.07
si_Dolomite(ord)		SI		0.74	−0.21	0.00	−0.01	0.99	0.35	0.48
si_Gypsum		SI		−0.51	−0.51	−0.52	−0.52	−0.53	−0.66	−0.85
si_Celestite		SI		0.01					−0.14	−0.31
si_Siderite		SI		−1.20					−1.17	−1.41
si_Rhodochrosite		SI		−0.72	−1.62				−1.06	−1.19
si_Quartz		SI							−0.03	0.11
si_Pyrite		SI							17.88	18.19
si_Pyrrhotite		SI							0.40	0.41
si_Troilite		SI							0.50	0.51
si_Goethite		SI		4.93					2.15	1.77
si_Fe(OH)3(am)		SI		−1.08					−3.86	−4.23
si_Fe(OH)3(mic)		SI		0.92					−1.86	−2.23
si_Kaolinite		SI							4.41	4.33
si_Gibbsite		SI			2.65				1.94	1.77
si_CO_2(g)		SI		−3.15	−2.59	−269	−2.54	−1.59	−1.35	−1.25

Table A2b
Analyses of water samples: isotope and gas compositions, calculated values (charge balance, saturation index of selected minerals).

Sample description	Mol weight	Unit	Analytical error	PC-6	PC-7	PC-8	PC-9	PC-10	PC-11	PC-12
Sample number				149804	155031	160724	167347	172539	180363	182554
Sample date + time				14 November 03	6 July 04	15 February 05	28 October 05	17 May 06 02	15 January 2007	11 April2007
Sample description				ca. 10:00	ca. 12:00	14:00	ca. 14:30	ca. 16:30	11:00	13:45
Sample volume		L		0.075	0.225	0.245	0.235	0.225	0.075	0.150
Days after start of the experiment				600	837	1061	1316	1517	1760	1846
Field observations										
Appearance				Clear	Clear	Black solids	Black solids	Significant black solids, no color	Clear, black solids, no	Clear, no color
Odor				Stromg smell of H_2S	Stromg smell of H_2S	Stromg smell of H_2S	No smell	Significant H_2S	Very stromg smell of H_2S	Stromg H_2S
Online measurements										
Time				11:44	10:44	13:44	14:30	14:10	11:10	8:10
Eh SHE		mV		−227	−265	−257	−275	−256	−233	−250
pe calc				−4.0	−4.6	−4.5	−4.8	−4.4	−4.1	−4.4
pH				6.72	6.65–6 70	6.81	Drift	6.75	6.70	6.75
EC		mS/cm		30.60	30.00	30.05	30.03	30.26	30.30	30.20
Temperature		°C		15.80	16.80	1460	15.50	17.60	13.70	14.30
Pressure in the piezometer		bar		4.48	4.77	5.93	6.56	3.92	3.40	1.88
Dissolved constituents										
EC		mS/cm	3%	30.30	30.00	30.80	30.50	30.90	30.60	30.10
pH			0.10	6.89	6.76	6.97	7.15	6.94	6.70	6.82
Eh		mV SHE	2 mV	−0.29			−0.29	−11	−128	−74
Lithium	6.94	mol/L	5%		3.89E−05	6.34E−05	6.63E−05	6.05E−05		
Sodium	22.99	mol/L	3%	2.51E−01	2.53E−01	2.65E−01	2.47E−01	2.48E−01	2.43E−01	2.38E−01
Potassium	39.10	mol/L	3%	1.83E−03	1.91E−03	2.04E−03	2.00E−03	2.07E−03	1.93E−03	1.76E−03
Ammonium	18.04	mol/L	5%	5.60E−04	6.26E−04	5.71E−04	5.60E−04	5.10E−04	5.77E−04	5.88E−04
Magnesium	24.31	mol/L	3%	1.90E−02	1.86E−02	1.83E−02	1.81E−02	1.92E−02	1.85E−02	1.68E−02
Magnesium tot (acid)	24.31	mol/L	3%							
Calcium tot (acid)	40.08	mol/L	3%							
Strontium	87.62	mol/L	5%		3.99E−04	4.45E−04	4.45E−04	4.79E−04		2.05E−04
Barium	137.33	mol/L	5%		5.68E−07	5.10E−07	8.01E−07	2.26E−07		
Chloride	35.45	mol/L	3%	2.87E−01	3.04E−01	3.13E−01	2.93E−01	2.93E−01	2.91E−01	2.76E−01
Bromide	79.90	mol/L	3%	6.67E−03	2.18E−03	3.32E−03	3.50E−03	3.68E−03	3.82E−03	3.97E−03
Iodide	126.90	mol/L	3%							1.18E−05
Sulphate	96.06	mol/L	3%	6.15E−03	4.92E−03	4.31E−03	4.11E−03	4.89E−03	4.69E−03	4.22E−03
Sulfide (tot) as S	32.07	mol/L	5%	9.98E−04	2.84E−04	2.46E−04	4.37E−05	7.48E−05		4.05E−04
Nitrate	62.00	mol/L	3%	<8.06E−06	<8.06E−06	<8.06E−5	<3.22E−05	<8.06E−5	<8.06E−5	<8.06E−06
Alkalinity	61.02	mol/L	5%	1.140E−02	1.1409E−02	1.06E−02	1.09E−02	9.33E−03	9.83E−03	9.95E−03
Boron	10.81	mol/L	5%		5.92E−04	4.81E−04	4.81E−04	2.68E−04		4.35E−04
Silicon	60.08	mol/L	5%		9.49E−05	9.65E−05	9.65E−05	3.83E−05		8.49E−05
Aluminium	26.98	mol/L	5%		1.85E−06	<3.71E−07	9.27E−07	7.78E−06		1.19E−05
Iron	55.85	mol/L	4%		8.42E−06	1.02E−04	2.90E−05	8.95E−06		3.04E−06
Manganese	54.94	mol/L	4%			3.46E−06	9.28E−06	9.28E−06		2.37E−06
Selenium	78.96	mol/L	5%							1.27E−08
Reduced sulfur species										
Sulfide	33.07	mol/L	5%	1.72E−05						
Sulfur (0)	32.07	mol/L		6.39E−06						
Thiosulfate	112.13	mol/L		1.14E−04						1.14E−04
Sulfite	80.06	mol/L								

Carbon species										
TOC	12.01	mol C/L	10%	1.17E−02	9.16E−03	n.m.		1.17E−03		1.27E−03
TOC-Huber	12.01	mol C/L	10%				9.99E−04	1.32E−03		
DIC	12.01	mol C/L	10%	9.20E−03	1.04E−02	n.m.				
TIC	12.01	mol C/L	10%		1.22E−02		1.17E−02	8.85E−03		8.85E−03
DOC	12.01	mol C/L	10%	1.08E−02	7.91E−03	n.m.	9.57E−04	8.33E−04		1.27E−03
DOC-Huber	12.01	mol C/L	10%					1.24E−03		
Organic acids (LC/spectr , Huber)	12.01	mol C/L	10%	1.07E−02	9.24E−03	4.05E−03	5.58E−04	2.83E−04		
Acetic acid	59.04	mol C/L		1.32E−02	9.42E−03	2.64E−03	<3.39E−04			<8.47E−05
Formic acid	45.02	mol C/L		6.61 E−03	4.71E−03					
Aceton	58 08	mol C/L			6.20E−05	1.03E−03	<1.72E−06			<8.61E−06
2-Hydroxy-5-methylanisol (C8)	122.16	mol C/L			1.09E−06					
Total phenols		mol C/L			4.66E−05	Detection limit				
Isotopes										
2H		‰ SMOW	1.5‰	−37.2	−41.3	−42.5	−37	−32.7		−12.8
^{18}O		‰ SMOW	0.15‰	−8.47	−8.71	−8.45	−8.41	−8.66		−5.93
^{13}C-CO_2		‰ PDB	0.3‰	−18.85						
^{13}C-DIC		‰ PDB	0.3‰	−16.6	−15.36					
^{13}C-TIC		‰ PDB	0.3‰		−15.99	−14.6	−12.3	−8.95		−11.5
^{13}C-DOC		‰ PDB	0.4‰	−15.05	−13.8					
^{13}C-TOC		‰ PDB	0.4‰			−27.4 ± 0.85				−28.14
^{13}C-aceton		‰ PDB	0.3‰			−25.2 ± 0.6				
2H CH4		‰ PDB								not possible
^{13}C-CH4		‰ PDB	0.3‰	−34.8	−43.36	−58.2	−41.9	−37.2 + −2		−50.2
^{13}C-C_2H_6		‰ PDB	0.3‰							−41.8
^{14}C-TIC		%	var		53.61	64.57 ± 0.69				19.4 ± 0.4
^{14}C-DOC		%	var.			101.76 ± 1.83				not possible
$\delta^{34}S$-SO_4		‰ CDT	0.3							51.00
$\delta^{18}O$-SO_4		‰ SMOW	0.2‰							12.40
$\delta^{34}S$-H_2S		‰ CDT	0.2‰							8.1 ± 0.23
Gas analysis	N ml/mol									
Helium	22400.00	mol/L	5%	n.m.	n.m.	<4.46E−07	n.m.	n.m.	n.m.	n.m.
Hydrogen	22400.00	mol/L	5%	n.m.	n.m.	3.57E−06	2.23E−06	<8.93E−06	1.38E−05	n.m.
Oxygen	22400.00	mol/L	5%	n.m.	n.m.	<4.46E−07	n.m.	n.m.	n.m.	n.m.
Nitrogen	22400.00	mol/L	5%	n.m.	n.m.	3.22E−04	n.m.	n.m.	n.m.	n.m.
Argon	22400.00	mol/L	5%	n.m.	n.m.	6.19E−04	n.m.	n.m.	n.m.	n.m.
Methane	22400.00	mol/L	5%	2.59E−05	4.37E−05	1.18E−04	7.16E−04	2.46E−04	2.76E−04	8.37E−05
Ethane	22400.00	mol/L	5%	2.19E−06	3.00E−06	2.81E−06	3.44E−06	3.30E−06	3.62E−06	1.56E−06
Propane	22400.00	mol/L	5%	8.48E−07	1.49E−06	1.88E−06	2.19E−06	2.10E−06	n.m.	7.14E−07
i-butane	22400.00	mol/L	5%	7.59E−08	2.46E−07	2.68E−07	3.13E−07	4.46E−07	n.m.	<4.46E−08
n-butane	22400.00	mol/L	5%	7.59E−08	2.86E−07	4.02E−07	5.36E−07	1.16E−06	n.m.	n.m.
Ethene	22400.00	mol/L	5%	<4.46E−08	n.m.	<4.46E−08	n.m.	n.m.	n.m.	n.m.
Calculated parameter										
Charge balance (Cat-|An|)/(Cat+|An|)		%		0.56	−0.43	−0.07	−0.25	0.58	−0.15	0.41
Charge balance		eq/L		3.61E−03	−2.78E−03	−4.74E−04	−1.60E−03	3.67E−03	−9.48E−04	2.43E−03
Total salt		meq/L		0.64	0.65	0.67	0.63	0.64	0.63	0.60
si_Calcite		SI		−0.10	0.06	0.30	0.70	0.25	0.23	0.30
si_Dolornite(dis)		SI		−0.47	−0.16	0.32	1.14	0.24	0.19	0.33
si_Dolomite(ord)		SI		0.08	0.39	0.87	1.69	0.79	0.74	0.88
si_Gypsum		SI		−0.90	−0.99	−1.07	−1.10	−1.00	−1.01	−1.09
si_Celestite		SI			−0.50	−0.52	−0.52	−0.42		−0.83
si_Sidente		SI			−0.87	0.44	0.31	−0.67		−1.04

(*continued on next page*)

Table A2b (*continued*)

Sample description	Mol weight	Unit	Analytical error	PC-6	PC-7	PC-8	PC-9	PC-10	PC-11	PC-12
Sample number				149804	155031	160724	167347	172539	180363	182554
Sample date + time				14 November 03	6 July 04	15 February 05	28 October 05	17 May 06 02	15 January 2007	11 April2007
Sample description				ca. 10:00	ca. 12:00	14:00	ca. 14:30	ca. 16:30	11:00	13:45
Sample volume		L		0.075	0.225	0.245	0.235	0.225	0.075	0.150
Days after start of the experiment				600	837	1061	1316	1517	1760	1846
si_Rhodochrosite		SI				−0.80	0.04	−0.41		−0.91
si_Quartz		SI			0.11	0.12	0.11	−0.30		0.04
si_Pynte		SI			18.02	19.29	18.20	17.03		18.24
si_Pyrrhotite		SI			0.61	1.78	0.95	0.12		0.49
si_Troihte		SI			0.71	1.88	1.05	0.22		0.59
si_Goethite		SI			2.34	3.73	4.22	2.49		2.24
si_Fe(OH)3(am)		SI			−3.67	−2.28	−1.79	−3.51		−3.77
si_Fe(OH)3(mic)		SI			−1.67	−0.28	0.21	−1.51		−1.77
si_Kaohnite		SI					3.74	5.73		6.48
si_Gibbsite		SI					1.47	2.87		2.90
si_CO_2(g)		SI		−1.47	−1.28	−1.24	−1.52	−1.18	−1.10	−1.22

References

Al-Aasm, I.S., Taylor, B.E., South, B., 1990. Stable isotope analysis of multiple carbonate samples using selective acid extraction. Chem. Geol. 80, 119–125.

Boutton, T.W., 1991. Stable carbon isotope ratios of natural materials: II atmospheric, terrestrial, marine and freshwater environments. In: Coleman, D.C., Fry, B. (Eds.), Carbon Isotope Techniques. Academic Press, San Diego, pp. 173–185.

Courdouan, A., Christl, I., Meylan, S., Wersin, P., Kretzschmar, R., 2007. Characterization of dissolved organic matter in anoxic rock extracts and *in situ* pore water of the Opalinus Clay. Appl. Geochem. 22, 2926–2939.

De Cannière, P., et al., 2008. Geochemistry and microbiology experiments. In: Bossart, P., Thury, M. (Eds.), Mont Terri Rock Laboratory Project, Programme 1996 to 2007 and Results, Rep. Swiss Geol. Surv. 3, pp. 69–86 (Chapter 6).

De Cannière, P., Schwarzbauer, J., Höhener, P., Lorenz, G., Salah, S., 2011. Biogeochemical processes in a clay formation *in-situ* experiment: Part C – organic contamination and leaching data. Applied Geochem.

Degueldre, C., Scholtis, A., Laube, A., Turrero, M.J., Thomas, B., 2003. Study of pore water chemistry through an argillaceous formation. A hydropaleochemical approach. Appl. Geochem. 18, 55–73.

Delay, J., Vinsot, A., Krieguer, J.-M., Rebours, H., Armand, G., 2007. Making of the underground scientific experimental programme at the Meuse/Haute-Marne underground research laboratory, North Eastern France. Phys. Chem. Earth 32, 2–18.

Eichinger, L., Wersin, P., 2004. Porewater Chemistry (PC) Experiment: Results of Chemical and Isotopic Measurements. Sampling Period 2002–2003. Mont Terri Project, Technical Note TN 2004-78.

Gaucher, E., Crouzet, C., Flehoc, C., Girard, J.P., Lassin, A., 2003. Porewater Chemistry (PC) Experiment: Measurement of Partial Pressure and Isotopic Composition of CO_2 on Two Core Samples from the Mont Terri Rock Laboratory, Borehole BPC-1. Mont Terri Project Technical Note TN 2002-22.

Gómez-Hernández, J.J., Guardiola-Albert, C., 2004. Flow Mechanism (FM-C) Experiment: Three-dimensional Model Predictions of Tracer Evolution of HTO and Iodine in the Main Fault. Mont Terri Project, Technical Report TR 2000-08.

Höhener, P., 2005. Porewater Chemistry (PC) Experiment: Interpretation of Test Data from July 2004 and Conclusions on Unknown Carbon Source. Mont Terri Project, Technical Report TN 2005-22.

Huber, S.A., Frimmel, F.H., 1991a. Flow injection analysis of organic and inorganic carbon in the low-ppb range. Anal. Chem. 63, 2122–2130.

Huber, S.A., Frimmel, F.H., 1991b. A liquid chromatographic system with multi-detection for the direct analysis of hydrophilic organic compounds in natural waters. Fresen. J. Anal. Chem. 342, 198–200.

Hunkeler, D., Höhener, P., Bernasconi, S., Zeyer, J., 1999. Engineered *in situ* bioremediation of a petroleum hydrocarbon-contaminated aquifer: assessment of mineralization based on alkalinity, inorganic carbon and stable carbon isotope balances. J. Contam. Hydrol. 37, 201–223.

Koroleva, M., Lerouge, C., Mäder, U., Claret, F., Gaucher, E.C., 2011. Biogeochemical processes in a clay formation *in situ* experiment: Part B – Insights and data from the overcoring – evidence of strong buffering by the rock formation. Appl. Geochem.

Lalieux, P., Bernier, F., Volckaert, G., Cornelis, B., 2003. Rôle du laboratoire de recherche souterrain HADES pour le programme belge de mise en dépôt de déchets radioactifs au sein d'une formation argileuse. Géologues No. 148.

Lassin, A., Gaucher, E., Crouzet, C., 2003. Dissolved carbon dioxide and hydrocarbon extraction. In: Pearson et al. (Eds.), Annex 6 Geochemistry of Water in the Opalinus Clay Formation at the Mont Terri Rock Laboratory, Geology Series No. 5, Swiss Federal Office for Water and Geology, pp. 253–262.

Mäder, U., 2004. Porewater Chemistry (PC) Experiment: A New Method of Porewater Extraction from Opalinus Clay with Results for a Sample from Borehole BPC-A1. Mont Terri Project Technical Note TN2002-25.

Mazurek, M., Alt-Epping, P., Bath, A., Gimmi, T., Waber, H.N., 2009. Natural Tracer Profiles Across Argillaceous Formations: The CLAYTRAC Project: Paris. Nuclear Energy Agency, OECD. 361 p.

Murray, A.P., Summons, R.E., Boreham, C.J., Dowling, L.M., 1994. Biomarker and n-alkane isotope profiles for tertiary oils – relationship to source-rock depositional setting. Organ. Geochem. 22, 521–542.

Nagra, 2002. Projekt Opalinuston: Synthese der geowissenschaftlichen Untersuchungsergebnisse. Nagra Technical Report NTB 02-03, Wettingen, Switzerland (in German).

Palut, J.-M., Montarnal, Ph., Gautschi, A., Tevissen, E., Mouche, E., 2003. Characterisation of HTO diffusion properties by an *in situ* tracer experiment in Opalinus clay at Mont Terri. J. Contam. Hydrol. 61, 203–218.

Pearson, F. J., Arcos, D., Boisson, J.-Y., Fernandez, A.M., Gäbler, H.-E., Gaucher, E., Gautschi, A., Griffault, L., Hernan, P., Waber, H.N., 2003. Mont Terri Project – Geochemistry of Water in the Opalinus Clay Formation at the Mont Terri Rock Laboratory. Report of the FOWG, Berne. Geology Series No. 5.

Pearson, F.J., Tournassat, C., Gaucher, E., 2011. Biogeochemical processes in a clay formation *in situ* experiment: Part E – equilibrium controls on chemistry of pore water from the Opalinus Clay, Mont Terri Underground Laboratory, Switzerland. Appl. Geochem.

Platen, H., Schink, B., 1987. Methanogenic degradation of acetone by an enrichment culture. Arch. Microbiol. 149, 136–141.

Sacchi, E., Michelot, J.-L., Pitsch, H., 2000. Porewater Extraction from Argillaceous Rocks for Geochemical Characterisation. Nuclear Energy Agency, OECD, Paris.

Stroes-Gascoyne, S., Schippers, C., Sergeant, A., Hamon, C.J., Neble, S., Vesvres, M.-H., Barsotti, V., Poulain, S., Le Marrec, C., 2011. Biogeochemical processes in a clay formation in situ experiment: Part D – microbial analyses – synthesis of results. Appl. Geochem.

Stumm, W., Morgan, J.J., 1996. Aquatic Chemistry, third ed. John Wiley & Sons, New York.

Thury, M., Bossart, P., 1999. Mont Terri Rock Laboratory. Results of Hydrogeological, Geochemical and Geotechnical Experiments Performed in 1996 and 1997. Swiss National Hydrological and Geological Survey, Bern, Switzerland.

Tournassat, C., Alt-Epping, P., Gaucher, E.C., Gimmi, T., Leupin, O.X., Wersin, P., 2011. Biogeochemical processes in a clay formation in situ experiment: Part F – reactive transport modelling. Appl. Geochem.

Van Loon, L.R., Wersin, P., Soler, J.M., Eikenberg, J., Gimmi, Th., Hernán, P., Dewonck, S., Matray, J.-M., 2004. *In situ* diffusion of HTO, $^{22}Na^{+}$, Cs^{+} and I^{-} in Opalinus Clay at the Mont Terri underground rock laboratory. Radiochim. Acta 92, 757–763.

Vinsot, A., Appelo, C.A.J., Cailteau, C., Wechner, S., Pironon, J., De Donato, P., De Cannière, P., Mettler, S., Wersin, P., Gäbler, H.-E., 2008. CO_2 data on gas and pore water sampled *in situ* in the Opalinus Clay at the Mont Terri rock laboratory. In: Proceedings of the International Meeting on Clay in Natural and Engineered Barriers for Radioactive Waste Confinement, Lille, 2007, Physics and Chemistry of the Earth, vol. 33, pp. S54–S60.

Wersin, P., Soler, J.M., Van Loon, L., Eikenberg, J., Baeyens, B., Grolimund, D., Gimmi, T., Dewonck, S., 2008. Diffusion of HTO, Br^{-}, I^{-}, Cs^{+}, $^{85}Sr^{2+}$ and $^{60}Co^{2+}$ in a clay formation: results and modelling from an *in situ* experiment in Opalinus Clay. Appl. Geochem. 23, 678–691.

Wersin, P., Stroes-Gascoyne, S., Pearson, F.J., Tournassat, C., Leupin, O.X., Schwyn, B., 2011. Biogeochemical processes in a clay formation in situ experiment: Part G – key interpretations & conclusions. Implications for repository safety. Appl. Geochem.

Applied Geochemistry 26 (2011) 954–966

Contents lists available at ScienceDirect

Applied Geochemistry

journal homepage: www.elsevier.com/locate/apgeochem

Biogeochemical processes in a clay formation *in situ* experiment: Part B – Results from overcoring and evidence of strong buffering by the rock formation

M. Koroleva [a,1], C. Lerouge [b], U. Mäder [a,*], F. Claret [b], E. Gaucher [b]

[a] Institute of Geological Sciences, University of Bern, Baltzerstrasse 3, CH-3012 Bern, Switzerland
[b] BRGM, French Geological Survey, 3 Avenue Claude Guillemin, B.P. 36009, 45060 Orléans Cedex 2, France

ARTICLE INFO

Article history:
Available online 17 March 2011

ABSTRACT

An *in situ* Porewater Chemistry (PC) experiment in the Opalinus Clay formation was carried out at the Mont Terri underground rock laboratory (Jura Mountains, Switzerland) for a period of 5 a. A traced water with a composition close to that expected in the formation was continuously circulated and monitored in a packed-off borehole to achieve diffusive equilibration. An unwanted microbial perturbation changed the water composition, characterized by reduction of SO_4 combined with increasing sulfide, increasing alkalinity, decreasing pH and increasing $P(CO_2)$. In contrast, the main cations (Na, Ca, Mg) remained remarkably constant during the experiment, thus indicating the strong buffering of the formation via cation and proton exchange as well as carbonate dissolution/precipitation reactions.

After 5 a, the 4.5 m long vertical test interval was overcored and Opalinus Clay samples were analyzed along ca. 15 cm long radial profiles. The analytical investigations included mineralogy (XRD, SEM-EDX), bulk parameters (water content, density, C, S), cation exchange capacity and occupancy, aqueous leachates for Cl^-, Br^-, SO_4^{2-} and water and carbonate stable isotopes. Emphasis was put on best sample preparation and conservation techniques. Results show that the distribution of non-reactive tracers (Br^- and ^2H) follows the expected out/in-diffusion profiles compatible with the time-dependent boundary conditions in the test interval of the borehole. Although some experimental features remain unresolved (e.g. high content of leachable SO_4^{2-} compared to the test interval), the distribution of reactive tracers (in porewater, on the clay exchanger and in the solid phase) demonstrate the very extensive buffer capacity of the Opalinus Clay formation towards chemical disturbances, such as those induced by microbial SO_4 reduction and oxidation of an organic C source.

1. Introduction

Argillaceous formations are being considered as potential host rocks for the deep geological disposal of radioactive waste due to their low permeability and large sorption capacity. Diffusion properties and reactive transport have been examined with *in situ* experiments at the Mont Terri Rock Laboratory for more than 10 a (Pearson et al., 2003; Soler et al., 2008; Wersin et al., 2009). The Porewater Chemistry (PC) Experiment was a 5-a diffusion experiment (2002–2007) carried out in a 4.5 m long test interval that also crossed a zone containing faulted rocks, and it was equipped with a fluid circulation system. Details of the set-up and geochemical evolution of the test water is described by Wersin et al. (2011-a).

The experiment initially aimed at constraining *in situ* pore water conditions, but microbial activity perturbed the chemical system, and the characterization and understanding of the perturbation and its effects then became a main focus (Stroes-Gascoyne et al., 2011; Tournassat et al., 2011; Wersin et al., 2011-b). The objective of the overcoring was to examine the extent to which the Opalinus Clay surrounding the test interval responded to the complex geochemical evolution of the fluid composition within the test interval.

The sampling strategy was to excavate the entire test interval by overcoring and sub-sample along radial profiles at different depths. In addition to mineralogy, geochemistry and physical properties, information to constrain pore water chemistry was sought, namely by aqueous leaching and the determination of cation exchange capacity and selectivity, as well as stable isotope composition determined by different methods.

2. Initial and boundary conditions of the *in situ* experiment

A full description of the experiment is provided by Wersin et al. (2011-a). Here, the key parameters relevant for the understanding and interpretation of the analytical results from the

* Corresponding author. Tel.: +41 31 631 87 61; fax: +41 31 631 48 43.
E-mail address: urs.maeder@geo.unibe.ch (U. Mäder).
[1] Present address: Geologisch-Paläontologisches Institut, Universität Hamburg, Bundesstrasse 55, D-20146 Hamburg, Germany.

0883-2927/$ - see front matter © 2011 Elsevier Ltd. All rights reserved.
doi:10.1016/j.apgeochem.2011.03.005

Table 1
Concentrations (mmol/L) in the test interval for select parameters at initial time and at the final stage of the PC experiment (Wersin et al., 2011-b).

	Test water	PC-8	PC-9	PC-10	PC-12
Day after injection	0	1061	1316	1517	1846
pH (in line)	7.74	6.81	7.16	6.75	6.82
Eh (in line) mV SHE		−257	−275	−240	−250
Na	255	265	247	252	243
K	1.5	2.0	2.0	2.1	1.8
Mg	18.0	18.3	18.1	19.5	17.1
Ca	15.9	14.9	14.0	15.5	13.5
Fe	0.0023	0.1021	0.0290	0.0089	0.0030
Cl^-	262	313	293	299	281
Br^-	29.4	3.3	3.5	3.8	4.0
SO_4^{2-}	14.7	4.3	4.1	5.0	4.3
Total sulfides	0	0.246	0.044	0.075	
Alkalinity	1.0	10.6	10.9	8.5	10.4
DOC/TOC	0.2	4.1	1.0	1.2	1.3
CH_4	1e−4	0.12	0.72	0.25	0.084
$\delta^2H‰$	+370.0		−37	−32.7	−12.8
$\delta^{13}C$-DIC‰	−29.1		−12.3	−9.0	−11.5

samples obtained from overcoring are summarized. Artificial pore water with a composition to match the expected major components of the *in situ* pore water, was circulated for 5 a. A gas mixture was used in the head space of the circulation reservoir to prescribe a partial pressure of CO_2 of $10^{-3.5}$ bar. Bromide and ^2H were used as tracers to observe loss over time to due to diffusion.

Sulfate-reducing bacteria became active and this led to a marked decrease of SO_4^{2-} concentrations over time (Table 1). Contamination by organic C (glycerol and possibly minor acetone; De Cannière et al., 2011) and graphite electrodes occurred initially, and this led to the production of inorganic C by bacterial activity (oxidation of organic C and reduction of SO_4). The pH decreased over time to a value of ~6.7 while SO_4^{2-} concentration decreased, and sulfide and alkalinity increased due to bacterial SO_4 reduction. The full data set is included in Wersin et al. (2011-a).

The test interval was sampled and emptied 16 days before overcoring, and a slight Ar overpressure was locked in (Table 1, and analyses in Wersin et al., 2011-a). There was a strong smell of H_2S, and in-line filtration was performed to sample suspended black material. The interval was emptied again before the pressure had to be released followed by cutting fluid lines for preparing overcoring one week before recovering the first core segment. Some in-flow to the interval occurred during this last week, and some of this water was recovered with the deepest core segment containing the end of the test interval.

3. Overcoring and sample material

3.1. Overcoring

The 4.5 m long vertical test interval at 5.5–10 m depth consisted of a segmented porous polyethylene hollow cylinder (50 mm OD, 30 mm ID) with a solid PVC core, topped by a mechanical packer, and a service tube for flow lines to the surface (Fig. 1). The annular space between the service tube and the claystone was filled with epoxy resin to provide a permanent seal. Overcoring was initially not foreseen and a borehole survey was not performed.

A 200 mm diameter borehole was first drilled off-centre along the service tube in order to cut the equipment at depth with a down-hole side cutter above the packer (Fig. 1). This borehole was back-filled with mortar, and the service tube was overcored and removed. Powdered claystone and epoxy resin were used to stabilize and seal the top of the cut equipment.

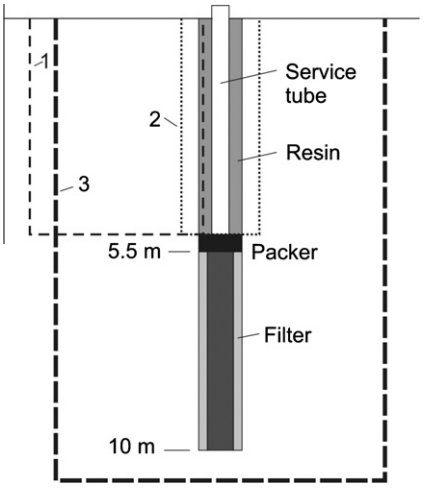

Fig. 1. Schematic of underground installation and excavation procedure, with exaggerated horizontal scale: (1) Auxiliary borehole (200 mm OD), (2) overcoring of service tube and resin infill, and (3) overcoring of test interval (384 mm OD). See Wersin et al. (2011-a) for details of surface installations.

The overcoring equipment employed was an adaptation of heavy triple-barrel equipment used at the Grimsel Test Site (http://www.grimsel.com/) for granite, with a 386 mm outer diameter and a 284 mm core diameter. The second (inner) barrel was suspended from the cross-over at the top to ensure rotation-free conditions. Inside this second barrel, a heavy-walled segmented acrylic liner was placed to further protect the core. This liner was simply slid over the core as drilling progressed, and the liner stayed on the core during extraction and handling of core segments. The adaptation from previous applications at the Grimsel Test Site included conversion to air-cooled dry drilling and the ability to retrieve an overcore of 5.5 m length in a single core pull, i.e. the entire test interval.

Drilling to 5.3 m depth was carried out on April 26, 2007. Unfortunately, the top part of the equipment (packer, topmost filter cylinder, central PVC tube) was pulled out with the overlaying core. The borehole was flooded with Ar, and the packer re-installed at depth to protect the test interval. Overcoring started the following day, but came to a halt when penetrating the fault zone ("Main Fault") due to extra moisture contained in the faulted rock and resultant clogging of the core and barrels. The top half of the interval (5.3–7.4 m) was retrieved, but the fault section (7.4–9 m) was lost (ground and exhausted). The bottom part (9–10.5 m) was cored and recovered the following morning.

The filter section was well preserved from 6.5–7 m, but completely mashed towards the fault section below due to the aforementioned drilling difficulties. Filters were well preserved in the lower core. Argon flushing was provided during idle time, and also during core recovery. The core segments were left in the acrylic liners, sealed off with caps, and preserved under Ar until further handling.

3.2. Profile locations and sampling procedures

Three radial profiles (A, B and C) were sampled from oval segments which were collected from different depth levels parallel to bedding (Fig. 2). Profile A was taken from a depth of 6.6 m by BRGM, profiles B and C were collected by the University of Bern from a depth of 6.7 and 9.7 m.

Downsizing of the large overcore segments (>100 kg) preserved in their acrylic liners was performed by a combination of cutting with a large low-speed mechanical whip saw, and cleaving along

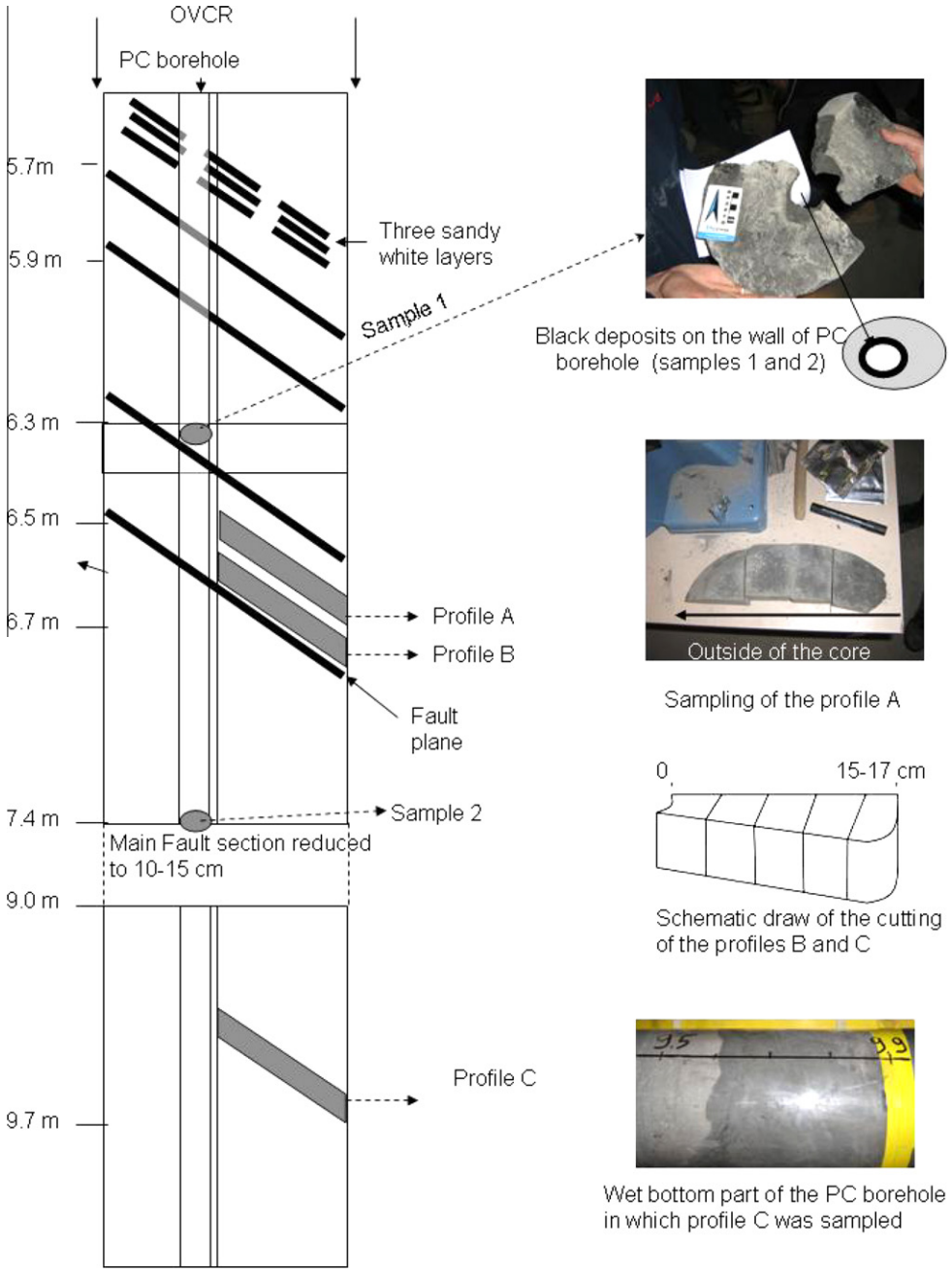

Fig. 2. Scheme of the overcoring and sample locations, including profiles A, B and C, and two samples of black deposit scraped off the wall of the PC borehole.

bedding planes or bedding-parallel fracture planes. Argon flushing and wrapping with tin foil or plastic film was employed during cutting to minimize drying and exposure to atmosphere. Subsamples were then transported in plastic wraps to an adjacent processing site equipped with a band saw, cleaving tools, vacuum-sealing equipment and liquid N_2 for further sub-sampling and sample preservation. Special care was taken for samples intended for microbiological studies, by disinfecting cutting equipment and core liners with burning alcohol, wearing breathing masks, and using filters for Ar flushing.

The segment for radial profile A was divided into two parts with sample storage adapted to the analysis type. For the aqueous leaching measurements, half of the segment was cut and immediately stored in liquid N_2 until transfer into a glove box (<1 ppm O_2 atmosphere) at the BRGM laboratory in order to avoid any O_2 contamination. For the mineralogical characterization, the equivalent half part of the segment was stored in plasticized Al bags sealed under vacuum and previously purged under an Ar atmosphere. Black "slimy" material was scraped off the borehole wall and also preserved by sealing in vacuum.

Samples from radial profiles B and C were dry cut using a small band saw (Fig. 2). Afterwards, the sub-samples were divided into 4 pieces each: (1) for aqueous and Ni-en extraction tests, (2) for bulk density measurements, (3) for water isotope determinations, and (4) for gravimetric water content measurements. Each sub-sample was moderately evacuated and sealed in a thick-walled plastic bag. Each plastic bag was inserted into a plasticized Al bag, which was again evacuated and then sealed. The initial wet mass of the samples required for gravimetric water content was determined immediately after sampling. The samples for pore water investigations were further processed in the laboratory after 2–3 days of cold storage.

Small samples from the residual borehole fluid that accumulated in the bottom core sample were taken by BRGM for analysis of black suspended material, and these were preserved by sealing in vacuum. Observations on a filter residue taken during the final interval sampling campaign are also included in this report. This sample was obtained by in-line filtration during sampling, and preservation of the filter cartridge by evacuation and sealing in plastic. The sample was analyzed within a few days at the University of Bern prior to overcoring.

4. Methods

4.1. Mineralogical characterization

X-ray diffraction (XRD) measurements were performed on profile A sub-samples with a SIEMENS D5000 X-ray diffractometer with Co $K\alpha_{1+2}$ radiation operating at 40 kV and 100 mA, and on profile B sub-samples with a Philips PW 1800 diffractometer. The complete mineralogy was obtained by XRD measurement of bulk-rock powder, whereas the clay fraction was determined by XRD of oriented samples of the <2 μm fraction that were air-dried, saturated with ethylene glycol, and heated at 550 °C. Mineral identification was performed using standard X-ray diffraction libraries. Mineral quantification from X-ray patterns was performed on samples of profile B using laboratory internal standardisation. The content of sheet silicates (clay minerals) was calculated by difference: total clay = 100 wt.% $-\sum$ wt.% (quartz, feldspars, carbonates, pyrite, C_{org}).

The contents of total S, total C and inorganic C were determined in samples from profiles B and C with a CS-mat 5500 element analyzer (Ströhlein GmbH, Germany). The carbonate contents were determined in the samples from profile A using the calcimetry method NF P 94-048 with a BERNARD calcimeter. The carbonate contents (calcite, dolomite and siderite) for profile B and C were calculated from the inorganic C content combined with the XRD data. The pyrite content was calculated from the total S content assuming that pyrite is the only S-bearing phase.

Scanning electron microscope (SEM) observations, EDX analyses and elemental mapping were performed with a JEOL JSM 6100 instrument coupled with an energy-dispersive spectrometer (Kevex Quantum) operated at 25 kV at BRGM. Prior to analysis, a thin C layer was sputter-coated on the samples (Edwards Auto 306). SEM analyses at the university of Bern were performed on uncoated samples in low vacuum (10 Pa) with a Zeiss EVO50 XVP instrument, operated at 20 keV and a beam current of 100–1400 nA for EDX analysis (EDAX Sapphire light element detector).

Transmission electron microscope (TEM) observations and analyses were performed at the Orléans University on a Philips CM20 with a CCD Gatan camera, at 200 kV. The TEM samples were prepared by dispersing powdered samples in alcohol by ultrasonic treatment, dropping them onto a porous C film supported on a Cu grid, and then drying them in air.

Electron microprobe chemical analyses were performed using a Camebax SX50 instrument and ZAF correction. Analyses of silicates and carbonates were performed with 15 kV acceleration voltage, a beam current of 12 nA and a 1–2 μm beam width. Analyses of sulfides were performed with 20 kV acceleration voltage and 20 nA. Counting time was 10 s for major elements and 20 s for trace elements. Standards used included both well-characterized natural minerals and synthetic oxides.

4.2. Water content and bulk density

The water content was determined by drying sample aliquots of approximately 17–52 g to constant mass at 105 °C. The bulk wet densities were determined by the Paraffin oil displacement method. From these quantities the water-loss porosity and bulk dry density were calculated (Pearson et al., 2003; Gimmi, 2003; Nagra, 2002).

The water content is also obtained from the isotope diffusive-exchange method (Rübel et al., 2002), but is of lesser accuracy and it is used as a consistency test for the isotope determinations (see below).

4.3. Aqueous leaching and cation exchange properties

An aqueous extraction was performed to quantify the amounts of soluble salts present in the rock. All extraction tests were conducted under an O_2-free atmosphere in order to minimize pyrite oxidation.

The powdered sub-samples of profile A were leached with deionized water that was boiled and degassed. Extraction tests were performed at a solid:liquid ratio of 0.001, 0.01, 0.1, and 1 (kg rock per kg water) over 10 min and 24 h. After the leaching procedure, the liquid was filtered at 0.1 μm prior to analysis. Chloride, Br^- and SO_4^{2-} concentration were measured by ion chromatography. Dissolved organic and inorganic C were measured using a Shimadzu TOC carbon analyser.

The sub-samples of profile B were dried prior the aqueous extraction and cation occupancy determinations, followed by crushing by hand to a grain size of approx. 5 mm in order to minimize possible contributions from fluid inclusions. Drying and crushing were conducted under a N_2 atmosphere inside a glove box at room temperature. Extraction tests were performed at solid:liquid ratios of 0.1, 0.25, 0.5 and 1 (kg rock per kg water) using deionized O_2-free water that was prepared in a glove box by N_2 bubbling for 30 min. Each sample was shaken end-over-end for 7 days in polypropylene tubes in order to equilibrate the extract solution with calcite and dolomite of the rock (Bradbury and Baeyens, 1998; Pearson et al., 2003). After filtration (0.45 μm) the supernatant solutions were immediately analyzed for pH and alkalinity by titration. Anions and cations in the extract solutions were determined by ion chromatography with a Metrohm 861 Compact IC-system.

Cation exchange capacity (CEC) and cation occupancies were determined by displacement with Ni ethylenediamine (Ni-en) (Bradbury and Baeyens, 1998). This displacement was carried out using 30 g of rock powder at solid:liquid ratios (S:L) of 0.25, 0.5, 1.0, 1.5 (kg rock per kg solution) using deionized O_2-free water that was prepared in a glove box. Each sample was shaken end-over-end for 7 days under a N_2 atmosphere inside a glove box. After solid separation by centrifugation, the supernatant leachate was filtered to <0.45 μm. Analyses including Na, K, Ca, Mg, Sr and Ni were performed using atomic absorption spectrometry.

4.4. Stable isotope ratios of carbonates and pore water

Calcite was extracted by an acid attack with phosphoric acid (100% anhydrous) at a temperature of 70 °C for 3 min on an automated line ("carbo device") coupled with a Finnigan Mat delta S mass spectrometer for determining $\delta^{13}C$ and $\delta^{18}O$. The fractionation coefficient used for the calculations is from Swart et al. (1991). The results are reported in δ units relative to international standards VSMOW for O and PDB for C. The reproducibility was ±0.2‰ for O and C.

The stable isotopic composition of pore water was determined using the diffusive-exchange technique (Rübel et al., 2002). The method is based on diffusive exchange via the vapor phase between the preserved pore water of a rock sample and two different test waters of known but contrasting isotopic composition in a sealed container at room temperature.

Saturated rock pieces of approximately 2 cm in size from the radial profiles B and C (200–300 g) were placed in a vapor-tight container together with a small crystal dish containing a known mass of test water with known isotopic composition. The two different test waters used are de-ionized laboratory water (LAB) and glacial melt water (SSI). In order to prevent mass transfers and isotope fractionation (e.g., Horita et al., 1993a,b) between the test water and the pore water of the rock through desiccation–condensation mechanisms, the water activity of the test water must be adjusted to fit the water activity in the rock samples, which depends on the type and concentration of salts, and on the proportion of water bound to the mineral surfaces (Sposito, 1990). Therefore, 0.3 M NaCl was added to the test water to match the water activity of 0.98, a typical value for the Opalinus Clay. The 3-reservoir system (rock sample, test water and the air inside the container) was equilibrated for 30 days at room temperature in order to achieve complete isotope equilibrium (Rübel et al., 2002). After equilibration, the test water was removed from the crystallization dish and analyzed by IRMS at the Hydroisotop GmbH laboratory. The rock material was dried in an oven to constant mass at 105 °C in order to obtain the gravimetric water loss of the samples. The error of the equilibration experiment was calculated applying Gaussian error propagation.

The observed shift of the isotopic compositions of the test waters allows the calculation of the isotopic composition of the pore water. The water contents of the samples used in the LAB and SSI experiments are identical, and the $\delta^{18}O$ and $\delta^{2}H$ of the pore water is calculated according to:

$$c_{pw(t=0)} = \frac{m_{twLAB}c_{twSSI(t=\infty)}m_{rockSSI}(c_{twLAB(t=\infty)} - c_{twLAB(t=0)}) - m_{twSSI}m_{rockLAB}c_{twLAB(t=\infty)}(c_{twSSI(t=\infty)} - c_{twSSI(t=0)})}{m_{rockSSI}(m_{twLAB}c_{twLAB(t=\infty)} - m_{twLAB}c_{twLAB(t=0)}) - m_{rockLAB}(m_{twSSI}c_{twSSI(t=\infty)} - m_{twSSI}c_{twSSI(t=0)})} \quad (1)$$

where m_{pw} and m_{tw} are the masses of pore water and test water, m_{rock} is the mass of the rock sample, c_{pw} is the original (*in situ*) isotopic composition of pore water, and c_{tw} is the isotopic composition of the test water at the beginning ($t = 0$) and at the end ($t = \infty$) of the equilibration with LAB or SSI test water.

The initial $\delta^{18}O$ or $\delta^{2}H$ values in pore water in the experiments LAB and SSI are identical, and, therefore, the water content is found according to:

$$WC = \frac{(c_{tw(t=\infty)SSI} - c_{tw(t=0)SSI})m_{twSSI}m_{rockLAB} - (c_{tw(t=\infty)LAB} - c_{tw(t=0)LAB})m_{twLAB}m_{rockSSI}}{m_{rockLAB}m_{rockSSI}(c_{tw(t=\infty)LAB} - c_{tw(t=\infty)SSI})} \quad (2)$$

This value can be compared to the directly measured water content as an independent check of the success of the experiment.

5. Results

5.1. Mineral characterization of the Opalinus Clay close to the water/rock interface

The total clay fraction in profile B is quite homogeneous, ranging from 66 to 67 wt.%. It is composed of illite (25–35%), illite/smectite mixed-layers (12–14%), chlorite (5–9%), and kaolinite (13–20%), without any systematic trend related to the distance of the interface to the test interval (data reported in Koroleva and Mäder (2008)).

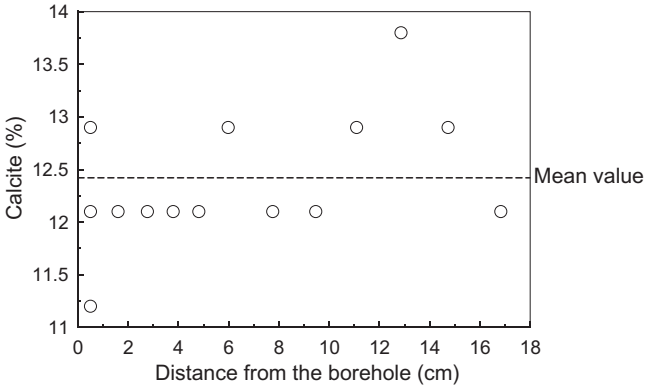

Fig. 3. Distribution of the carbonate content as a function of distance (profile A).

The carbonate fractions obtained for both profiles, A and B, are comparable. They consist of calcite (12–14%) with minor siderite (~3%) and dolomite (<2%). The variations of calcite content along both profiles are small and reflect the heterogeneity of the rock (Fig. 3). Carbonates occur as a detrital fraction (calcitic and aragonitic bioclasts), micritic calcite and rare euhedral calcite grains, whereas siderite and dolomite occur as disseminated 10–50 μm-sized euhedral grains.

Pyrite is the only observed S-bearing phase, occurring as disseminated framboids and clusters of framboids in all samples. Pyrite content ranges between 1.5 and 1.7 wt.%.

Microscopic observations of polished thin sections and bulk rock EDX spectra using SEM do not show significant mineralogical, textural and chemical variations along all radial profiles. This is consistent with previous data obtained for Opalinus Clay (Pearson et al., 2003).

Elemental mapping of major elements, which was performed adjacent to the water/rock interface (within 300 μm), also shows no significant changes in chemical and mineralogical composition (Fig. 4). Framboidal pyrite present in the Opalinus Clay formation remained stable at the water/rock interface (Fig. 5a). Euhedral grains of carbonate close to the water/rock interface do not exhibit any dissolution or growth features on surfaces (Fig. 5b and c). Calcite was observed as micro-coatings on the wall of the PC-borehole, suggesting precipitation of calcite at the water/rock interface (Fig. 5f). Gypsum was also identified at the interface,

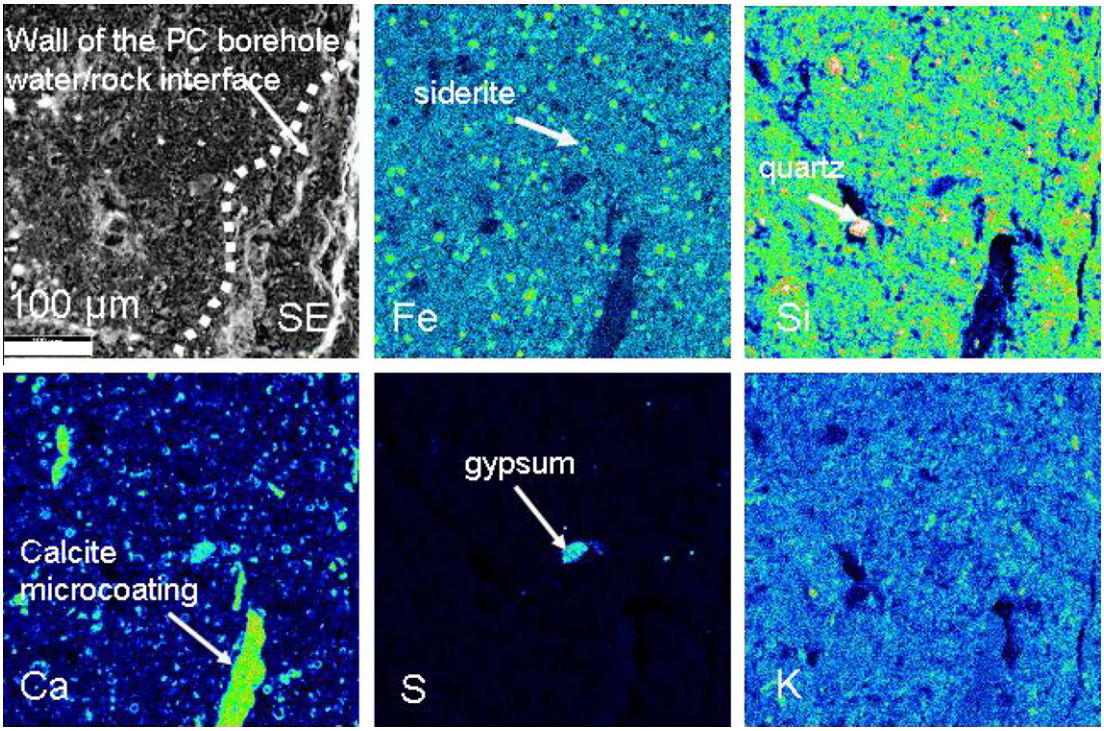

Fig. 4. Secondary electron (SE) image and corresponding (Fe, Si, Ca, S, K) elemental maps of the region within 300 µm of the water/rock interface with interpreted mineral distribution. The morphology of the interface is visible on the SE image on the right. Combined K and Si maps show the homogeneous distribution of clay minerals at the interface. Combined Ca, Fe and S maps show the distribution of primary euhedral calcite, dolomite and siderite at the interface, but also the neoformation of calcite, and the presence of gypsum close to the interface.

whereas it is absent further away from the interface. Complementary TEM observations on particles leached by alcohol from the sub-sample close to the PC-borehole wall confirmed the neoformation of carbonates, and provided evidence of a S-bearing phase and euhedral small Ca-phosphates. Although samples were preserved in liquid N_2 until examination in order to preserve redox conditions, a possible rapid oxidation of labile sulfides into gypsum during preparation of the sample cannot be excluded. Small changes in rock texture with disorientation of clay minerals and occurrence of microporosity were observed close to the water/rock interface (<300 µm from the border) (Fig. 5d and e). Calcite neoformation was also observed in the microporosity (Fig. 5f). It was impossible to determine the origin of the microporosity. It could be an artifact due to mechanical damage induced by drilling the PC-borehole and subsequent convergence, or it could also be due to limited mineral dissolution.

5.2. Mineral characterization of mud and precipitates formed in the borehole fluid

Comparison of X-ray diffraction results from mud collected from the test borhole with those obtained on profile A shows that the mineralogy of the mud is quite similar to the Opalinus Clay but indicates a slightly higher carbonate content in the mud (Fig. 6).

Precipitates were also observed in the water sample taken from the bottom of the borehole. The precipitates were deposited on a thin section, covered with C coating and directly observed and analyzed under vacuum to minimize oxidation processes. SEM observations, EDX spectra combined with EPMA analyses of the precipitates provide evidence of two major sulfide phases with different Fe/S ratios (Fig. 7a and b): (a) a dominant sulfide phase characterized by a Fe/S ratio close to 1, comparable to greigite (Fe_3S_4), and (b) a sulfide phase characterized by a Fe/S ratio close to 0.5 and invariably containing Na, independent of Cl content. This latter phase could correspond to pyrite mixed with Na salts. Sulfate particles are less common (Fig. 7c). They consist of Na and Na–Ca sulfate occurring as platy grains and elongate flakes, respectively. The mixing of Fe–S phases with salts renders analysis difficult. The sulfate phases are suspected to have formed during core recovery, storage and sample preparation due to oxidation of the labile sulfides, because the pore water itself is undersaturated with respect to gypsum.

Similar observations were made on a black filter residue obtained during the final sampling campaign prior to overcoring; it consisted of a mixture of salts from drying, and Fe–S phases. Some very small cubes of suspected pyrite were observed. In contrast to the sample described above, the filter residue contained abundant biofilm. Other samples preserved in vacuum turned brown after a couple of weeks owing to some O_2 diffusion and the labile nature of the different Fe–sulfide phases.

In summary, combined observations and analyses indicate substantial precipitation of Fe sulfide phases and minor calcite in the test interval, but no significant changes in the wall–rock adjacent to the test interval.

5.3. Water content and density

The average water content relative to its dry and wet mass obtained by drying at 105 °C varies in the range of 8.02–8.40 wt.% and 7.42–7.75 wt.%, respectively. The absolute uncertainty between duplicate samples is less than 0.07 wt.%. Water contents calculated by the isotope diffusive-exchange range between 9 and 12 wt.% and are higher than those obtained by drying the same samples after the experiment at 105 °C. For profile B they range between 9 and 12 wt.% and for profile C between 8 and 15 wt.%. Previous studies of the Opalinus Clay explained such differences of about 10–20% by possible isotopic exchange with bound water on the

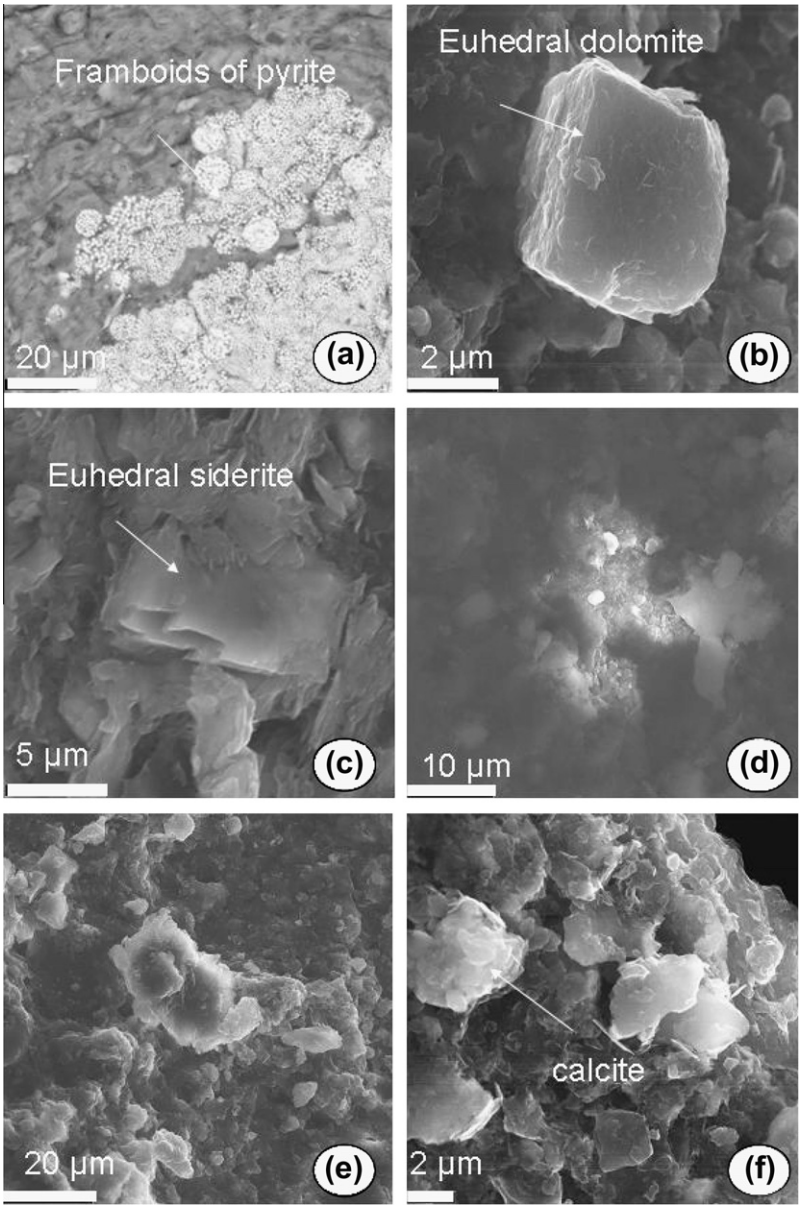

Fig. 5. Secondary electron images of primary minerals at the water/rock interface: (a) pyrite close to the interface; (b) dolomite crystal close to the interface; (c) siderite in a relatively oriented clay matrix; (d) microporosity with calcite neoformation; and (e and f) disorientation of clay minerals at the water/rock interface.

clay surfaces that may differ in its isotopic composition from that of the capillary water (Rübel et al., 2002).

The bulk wet density varies between 2.38 and 2.40 g/cm^3. The water-loss porosity (or volumetric water content, φ_{WL}) can be calculated according to:

$$\phi_{WL} = WC_{wet}\rho_{b.wet}/\rho_{water}, \quad (3)$$

where WC_{wet} is water-loss relative to its wet mass, $\rho_{b.wet}$ is bulk wet density and ρ_{water} is the density of water. Commonly, the density of pore-water of the Opalinus Clay at Mont Terri is taken as 1.00 g/cm^3 (Pearson et al., 2003) because the salinity of the pore water is distinctly less than that of seawater.

The water-loss porosities vary between 17.8 and 18.6 vol.%. Bulk dry density can be calculated from water content and bulk wet density. The bulk dry densities vary in the range of 2.20–2.22 g/cm^3. Assuming that the samples were fully saturated, the water-loss porosity value is equal to the total porosity, and the grain density can be estimated to approximately 2.71 g/cm^3 in agreement with previous measurements (Pearson et al., 2003).

The water contents relative to the dry mass and the bulk dry densities as a function of the distance to the water/rock interface do not vary significantly along radial profiles (Fig. 8).

5.4. Anion contents in aqueous leachates

The composition of an aqueous extract solution represents the sum of: (a) the constituents originally dissolved in the pore water, (b) the mineral components dissolving during the leaching process, (c) any constituents contributed from cracked fluid inclusions, and (d) effects of cation-exchange with the exchanger population of expandable clays. Aqueous extractions (profile A and B) were performed at different solid:liquid (S:L) ratios, and for profile A also at different contact times (10 min and 24 h), in order to control the possible effect of celestite dissolution.

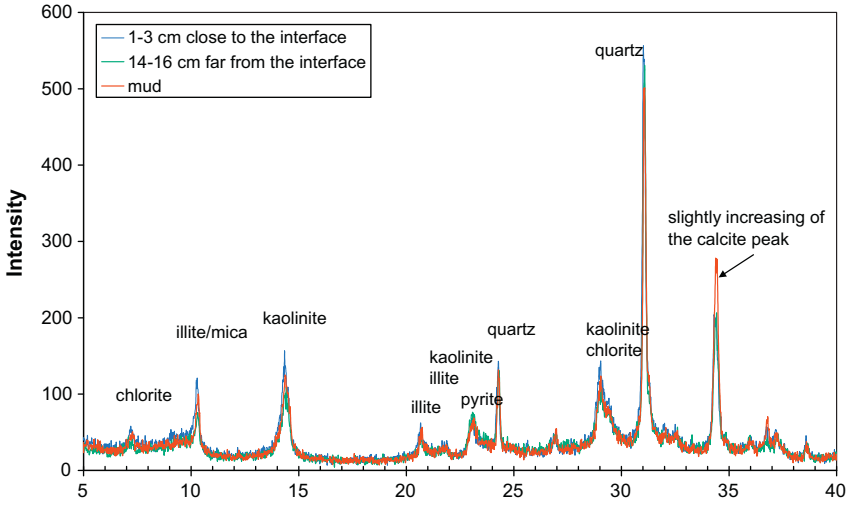

Fig. 6. X-ray diffraction pattern of mud collected in the borehole, compared with X-ray diffraction patterns of Opalinus Clay samples of radial profile A.

Chloride, Br^- and SO_4^{2-} concentrations are given in Table 2 in $mmol/kg_{rock}$. No variation is observed as a function of different S:L ratios for these three ions. Assuming that all Cl^-, Br^- and SO_4^{2-} leached in the aqueous extracts originates from pore water, anion concentrations in pore water can be calculated from the aqueous leaching data, grain density and the geochemical porosity using:

$$A_{\text{pore water}} = \frac{A_{\text{b.rock}}\rho_{\text{b.wet}}}{\phi_A} \quad (4)$$

where $A_{\text{b.rock}}$ is the anion concentration in $mmol/kg_{rock}$ (based on aqueous leaching), $A_{\text{pore water}}$ is the anion concentration in $mmol/kg_{H2O}$ in pore water, $\rho_{\text{b.wet}}$ is the bulk wet density, and ϕ_A is the anion-accessible porosity.

Chloride and Br^- concentrations (Fig. 9) and SO_4^{2-} concentrations (Fig. 10) in pore water recalculated from aqueous extracts were reported as a function of the radial distance away from the test interval. Br^- in pore water decreases toward the outer rim, while Cl^- is almost constant within uncertainties. Sulfate in porewater increases toward the outer rim of the profile.

5.5. Cation exchange capacity and cation site occupancy

The CEC is determined from the consumption of a highly selective cation (Ni) onto the exchanger and also as the sum of cations displaced from the exchange sites into solution. The measured cation concentrations (Table 3) represents the sum of cations displaced from mineral surfaces, the dissolution of salts precipitated from pore water during desiccation of the samples, and a minor contribution from the dissolution of sparsely soluble minerals, such as carbonates. Therefore, the derivation of the *in situ* cation exchange population requires a correction of the measured cation concentration in the Ni-en extract with the cation contribution from the pore water. The aqueous extracts are affected by ion exchange and mineral dissolution, and therefore, some assumptions have to be made for correcting the Ni-en data since the pore water composition is not known a priori. Bradbury and Baeyens (1998) suggest a relatively simple correction for the Opalinus Clay based on the dominant aqueous speciation to associate Na^+ with Cl^- measured in the aqueous extracts, and SO_4^{2-} with Ca^{2+}. The SO_4^{2-} correction could be further refined to account for any Mg–SO_4 and Na–SO_4 complexation, and to compensate for the cation charge-balancing the extra-alkalinity generated from calcite dissolution. Chloride carries 90% of the anion charge in normal Opalinus Clay pore water, and Na^+ 80% of the cation charge. Note that the source of SO_4^{2-} in the aqueous extracts appears to be dominantly mineral dissolution (+/− minor pyrite oxidation/calcite dissolution) and, therefore, the counter-ions associated with extra SO_4^{2-} are not primarily pore water components but more likely Ca^{2+}. Corrections were, therefore, made by subtracting an amount of Na^+ equivalent to Cl^- in the aqueous extract and an amount of Ca^{2+} equivalent to SO_4^{2-}.

The measured CEC, as the sum of the exchangeable cations, ranges from 10.4 to 11.6 meq/100 g for all samples applying corrections as discussed above (Fig. 11). The Ni consumption balances the CEC within the analytical uncertainties.

The fractional cation occupancies on the exchanger (X_i) were calculated (Table 4) according to $X_i = C_i/\text{CEC}$, where C_i is the quantity of cation in milli-equivalents (Na^+, K^+, Mg^{2+}, Ca^{2+}, Sr^{2+}) on the permanent charge sites after corrections, and CEC is the sum of exchangeable cations.

5.6. Stable isotope composition of carbonates and pore water

The $\delta^{13}C$ and $\delta^{18}O$ of calcite along profile A vary between −0.6 and −0.4‰ PDB, and between +24.8 and +25.1‰ VSMOW, respectively (Fig. 12). The isotopic variations cover the same range as the analytical error. Moreover, $\delta^{13}C$ and $\delta^{18}O$ of calcite measured at the end of the experiment are quite similar to $\delta^{13}C$ and $\delta^{18}O$ of calcite previously analyzed in the initial borehole at the same depth: $\delta^{13}C = -0.2‰$ and $\delta^{18}O = +25.0‰$ (Gaucher et al., 2002). In contrast, calcite at the water/rock interface of the PC-borehole with a $\delta^{13}C$ of −1‰ and a $\delta^{18}O$ of +23.1‰ is significantly ^{18}O-depleted relative to the calcite in the Opalinus Clay.

The $\delta^{18}O$ values of pore water obtained from the isotope diffusive-exchange method range from −7.46‰ to −8.20‰ for a 5-point profile at level C without showing a gradient (data not given). Cumulative errors range from ±0.35‰ to ±1.1‰ for the individual experiments. Due to one failed experiment (leaky container), only a 3-point profile is available for level B, ranging from −6.38‰ to −8.55‰, showing more scatter but no trend. The δ^2H values range from −36.7‰ to −66.6‰ for profile C defining a near-linear gradient (Fig. 13), but are inconclusive for the partial profile at level B. The full data set is given in Koroleva and Mäder (2008).

6. Discussion

6.1. Water content and density

The water content does not vary significantly along radial profiles (Fig. 8). However, the value is highest in the sample adjacent

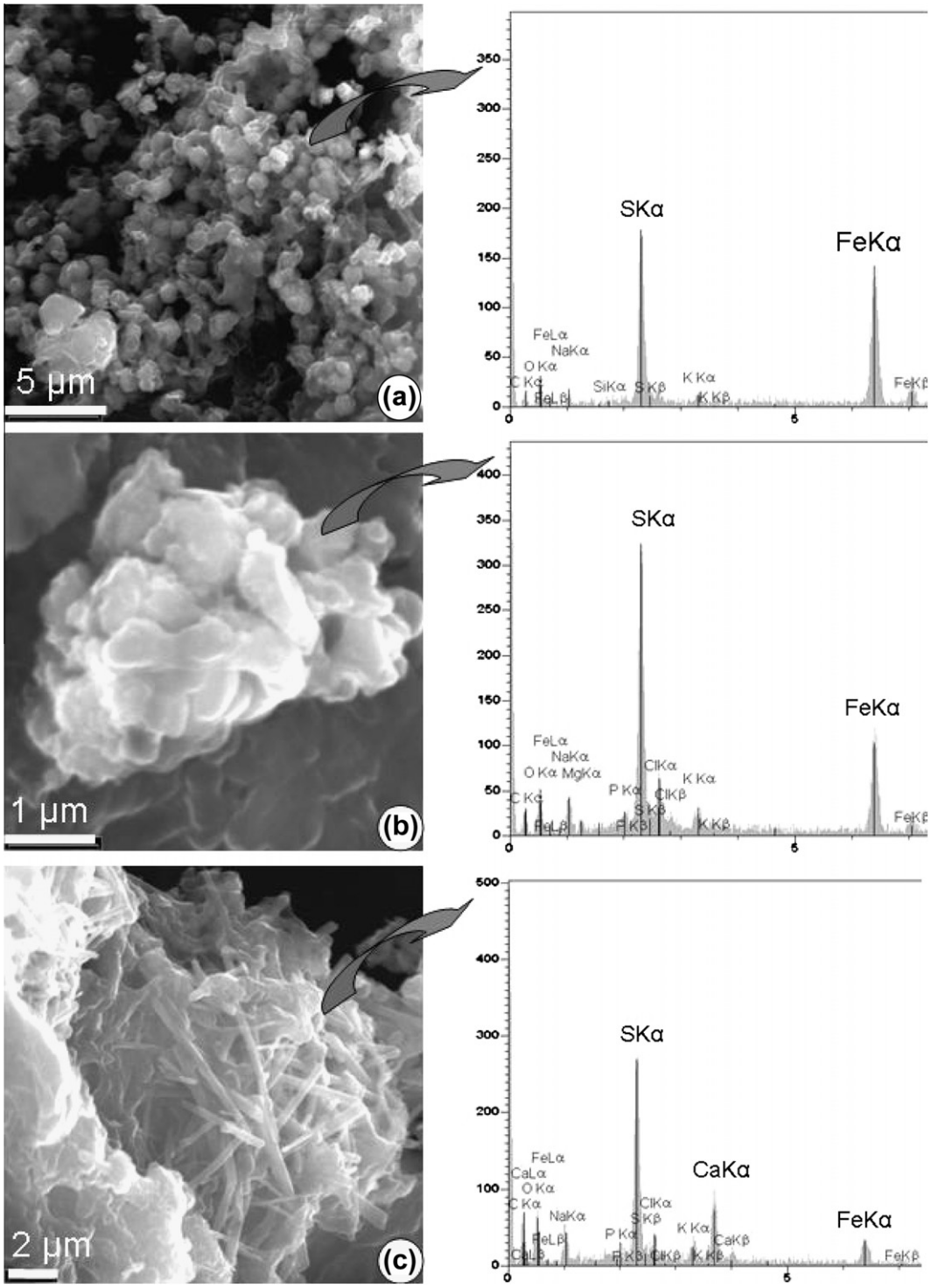

Fig. 7. Back-scattered electron images and corresponding EDX spectra of sulfide- and sulfate-phases in suspension in the water from the borehole: (a) Fe–S sulfide-phase with a Fe/S ratio ~ 1; (b) Fe–S sulfide-phase with a Fe/S ratio ~ 0.5; and (c) Ca–Na sulfate.

to the PC-borehole and lowest at the outer rim. This is likely an effect of a disturbed zone with a slightly higher porosity surrounding the test interval. The water content values obtained by drying of the rock material after the isotope diffusive-exchange experiment as well as the calculated water content from isotopic composition show the same decreasing trend away from the borehole. This may be attributed to some swelling effects. Nevertheless, the physical properties are rather uniform and do not vary by much that could be related to water–rock interaction processes. Even bulk wet densities are not significantly lower or higher adjacent to the test interval (Fig. 8) where the most prominent changes might be expected.

6.2. Gradients in pore water composition

Due to electrostatic repulsion at negatively charged clay surfaces, porosity accessible to anions is lower than for water or cations in claystones. Comparison of Cl^- and Br^- data in aqueous

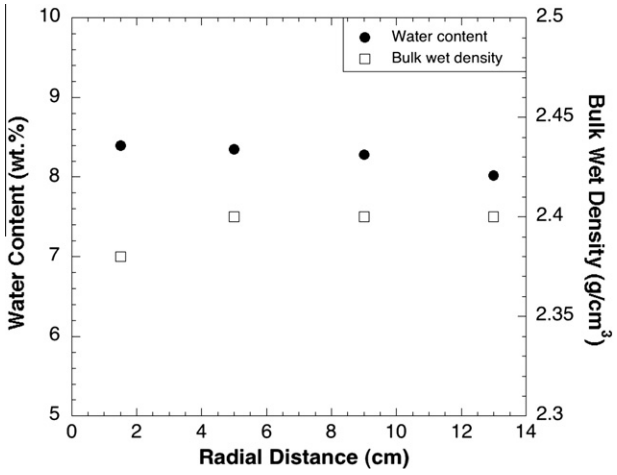

Fig. 8. Water content relative to dry mass and bulk wet density as function of distance (profile B).

extract solutions with those in the test interval present for the last 300 days ($Cl \approx 276$ mmol/kg$_{H2O}$, $Br \approx 3.97$ mmol/kg$_{H2O}$, Table 1) shows that the anion-accessible porosity is approximately 75% of the total porosity. Previous measurements at Mont Terri yielded ratios of Cl^- porosity to the water-loss porosity of ~0.6 with a range of reliable values from 0.5 to 0.7 (Pearson 1999; Pearson et al., 2003, Fig. A10.8). Measurements of diffusion of both water (measured using HTO) and Cl^- have also been made on several samples from Mont Terri. The ratio of the diffusion porosity for Cl^- to that of HTO is also between 0.5 and 0.7 (Pearson et al., 2003, Table A10.8; Van Loon et al., 2003, 2004). As a consequence, the value obtained from the overcore samples is the highest reliable value measured on Opalinus Clay samples. The reason for this high value could not be correlated to any rock parameter but may be due to some relaxation effect close to the borehole affecting the clay micro fabric but not bulk properties. There was a small annular gap of 1 mm present initially when the equipment was inserted into the open borehole, and this gap did close during the experiment implying some relaxation.

While Cl^- concentration in the test interval was very similar to the *in situ* Cl^- concentration in the porewater, Br^- concentration was much higher in the test interval than in the formation. As a consequence, Cl^- and Br^- concentration profiles (Fig. 9) are in agreement with what is expected from a diffusion process (see Tournassat et al. (2011) for modeling details). The Br/Cl molal ratio obtained at 17 cm distance ($6 \cdot 10^{-3}$) is still higher than the one

Table 2
Aqueous leaching data at different S:L ratios, with concentrations scaled to dry rock mass.

Radial distance (average) (cm)	Segment depth (m)	Profile ID	S:L ratio	Time of shaking (h)	Number of measurements	Cl^- (mmol/kg$_r$)	Br^- (mmol/kg$_r$)	SO_4^{2-} (mmol/kg$_r$)
0.5	6.5	A	0.001	0.1	3	19.8	<0.002	<0.003
0.5	6.5	A	0.01	0.1	3	16.6	0.21	1.50
0.5	6.5	A	0.10	0.1	8	16.8	0.20	1.55
0.5	6.5	A	0.10	24	5	17.8	0.20	1.65
1.5	6.7	B	0.10	168	1	16.0	0.15	2.28
1.5	6.7	B	0.25	168	1	16.0	0.17	2.28
1.5	6.7	B	0.50	168	1	16.3	0.18	2.27
1.5	6.7	B	1.00	168	1	17.0	0.19	1.89
1.6	6.5	A	0.10	0.1	1	14.6	0.17	1.43
1.6	6.5	A	0.10	24	1	15.0	0.16	1.57
2.8	6.5	A	0.10	0.1	3	14.7	0.17	1.45
2.8	6.5	A	0.06	24	1	15.2	0.17	1.59
2.8	6.5	A	0.10	24	1	15.3	0.17	1.59
2.8	6.5	A	0.09	24	1	17.1	0.20	1.85
3.8	6.5	A	0.10	0.1	1	14.8	0.17	1.60
3.8	6.5	A	0.10	24	1	15.2	0.17	1.66
4.8	6.5	A	0.10	0.1	1	14.4	0.16	2.29
4.8	6.5	A	0.10	24	1	14.8	0.16	2.35
5	6.7	B	0.10	168	2	15.2	0.12	2.27
5	6.7	B	0.25	168	2	15.1	0.15	2.33
5	6.7	B	0.50	168	2	15.5	0.16	2.32
5	6.7	B	1.00	168	2	16.2	0.16	2.21
6	6.5	A	0.10	0.1	1	14.4	0.15	2.00
6	6.5	A	0.10	24	1	14.4	0.15	2.06
7.8	6.5	A	0.10	0.1	3	14.1	0.13	2.95
7.8	6.5	A	0.10	24	1	14.2	0.13	4.75
9	6.7	B	0.10	168	2	15.6	<0.01	2.67
9	6.7	B	0.25	168	2	15.1	0.11	2.68
9	6.7	B	0.50	168	2	15.5	0.14	2.66
9	6.7	B	1.00	168	2	16.2	0.13	2.59
9.5	6.5	A	0.10	0.1	1	13.6	0.11	2.27
9.5	6.5	A	0.10	24	1	14.0	0.11	2.38
11.1	6.5	A	0.10	0.1	1	12.8	0.09	2.13
11.1	6.5	A	0.10	24	1	12.8	0.09	2.35
12.9	6.5	A	0.10	0.1	1	12.4	0.08	2.27
12.9	6.5	A	0.10	24	1	12.5	0.08	2.46
13	6.7	B	0.10	168	2	15.1	<0.01	2.74
13	6.7	B	0.25	168	2	14.7	0.09	2.83
13	6.7	B	0.50	168	2	15.1	0.12	2.79
13	6.7	B	1.00	168	2	15.8	0.11	2.70
14.7	6.5	A	0.10	0.1	3	13.3	0.08	3.11
14.7	6.5	A	0.10	24	3	13.4	0.08	4.73
16.8	6.5	A	0.001	0.1	3	16.7	<0.002	3.59
16.8	6.5	A	0.01	0.1	3	15.1	<0.002	2.69
16.8	6.5	A	0.10	0.1	3	14.7	0.08	2.52

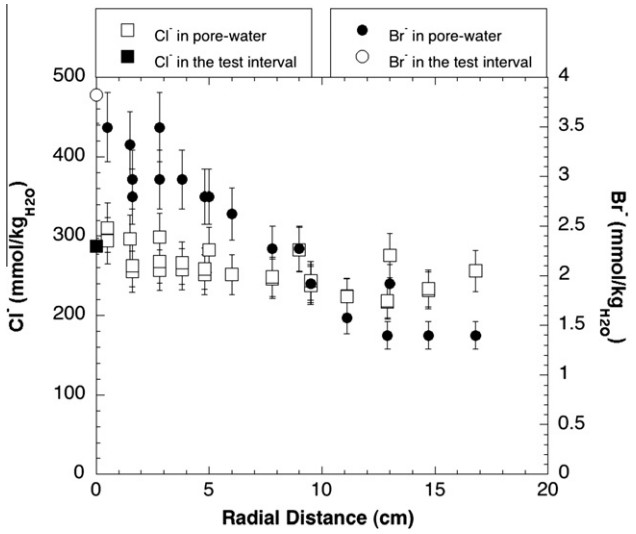

Fig. 9. Cl^- and Br^- in pore water and in the test interval as a function of radial sample distance (profiles A and B). Estimated errors are ±10%.

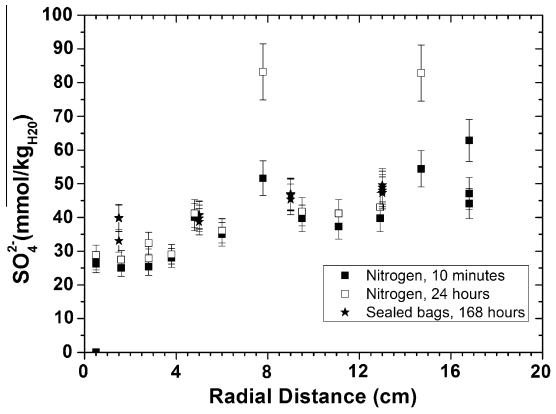

Fig. 10. SO_4^{2-} concentrations in pore water computed from aqueous leachates as function of radial sample distance (profiles A and B), and coded for leaching duration and sample preservation technique (liquid N_2, sealed in vacuum).

Table 3
Ni-en extraction data at S:L ratio equal to 1 (profile B) and CEC as sum of cations.

Radial distance (average) (cm)	Ca^{2+} (meq/100 g)	Mg^{2+} (meq/100 g)	Na^+ (meq/100 g)	K^+ (meq/100 g)	Sr^{2+} (meq/100 g)	Sum of cations (meq/100 g)	Ni^{2+} (meq/100 g)
1.5	2.6	2.0	7.2	0.8	0.13	12.8	10.5
5	2.7	1.9	7.1	0.8	0.12	12.7	10.7
9	2.8	1.9	7.0	0.8	0.13	12.5	10.8
13	2.8	1.9	7.0	0.8	0.13	12.6	10.9

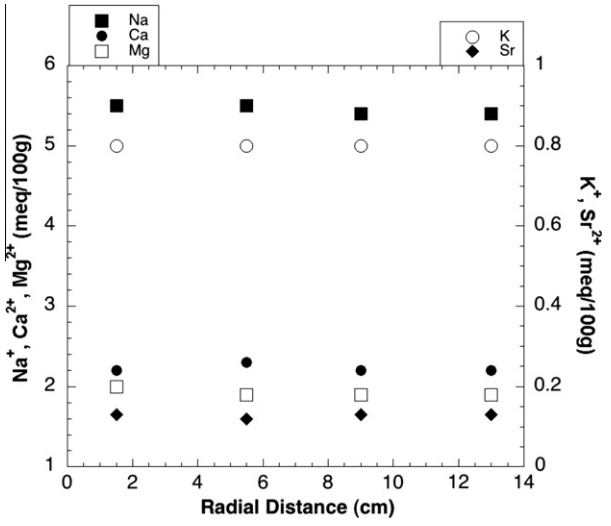

Fig. 11. Cation occupancy as function of distance (profile B).

Table 4
Fractional cation occupancies on the exchanger (profile B).

Radial Distance (average) (cm)	X_{Ca}	X_{Mg}	X_{Na}	X_K	X_{Sr}
1.5	0.21	0.19	0.51	0.08	0.012
5	0.21	0.18	0.52	0.08	0.012
9	0.22	0.18	0.52	0.07	0.012
13	0.21	0.18	0.52	0.08	0.012

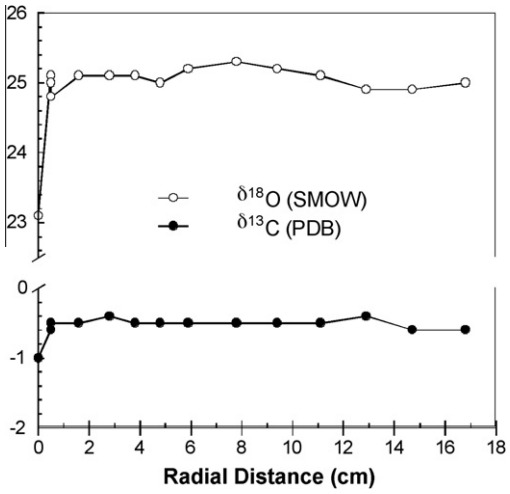

Fig. 12. Carbon and O isotopic composition of calcite as a function of distance (profile A).

typically observed for the Opalinus Clay formation at Mont Terri (Br/Cl ratio $\sim 3 \cdot 10^{-3}$, Pearson et al., 2003). This indicates that the diffusion profile extends beyond 17 cm.

In contrast to Cl^- and Br^-, the SO_4^{2-} concentrations in pore water calculated from aqueous leachates are significantly higher than those observed in the test interval. Sub-samples located adjacent to the test interval yield a recalculated SO_4^{2-} concentration in pore water of 27 mmol/kg$_{H2O}$ (liquid N_2 preservation, 10-min extract) and 33–40 mmol/kg$_{H2O}$ (vacuum-sealed, 7-day extract), but the test interval contains only 4.6 mmol/kg$_{H2O}$ at the end of the field experiment (Fig. 10, Table 1). Samples at the far end of the profile yield 45–63 mmol/kg$_{H2O}$ SO_4^{2-} which is a factor of 3–4 higher than the expected value of ca. 15 mmol/kg$_{H2O}$ used for the initial pore water composition (Table 1). It is concluded that there must be either (1) a significant amount of dissolution of a soluble sulfate mineral during the aqueous leaching test or (2) a slight oxidation of the sample material (e.g., pyrite, or secondary sulfides). Gaucher et al. (2009) observed extracted SO_4^{2-} values that were three times too high compared to pore water for Callovian–Oxfordian claystone from Bure, France, and explained this by celestite dissolution during the extractions. Here, the good agreement between extractions performed at 10 min, 24 h and 7 days do not indicate the presence of celestite. Secondary sulfides similar to those described

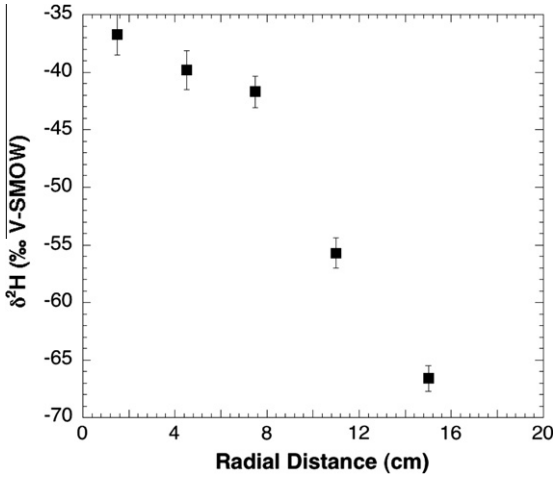

Fig. 13. δ^2H in pore water as a function of radial sample distance (profile C).

from the borehole interface may have formed due to the increasing in-diffusion of dissolved sulfide following its concentration increase in the test interval. Although the sample preservation methods chosen were previously shown to prevent oxidation of pre-existing pyrite (Pearson et al., 2003; Gaucher et al., 2009), newly-formed Fe–sulfides may be more labile and are likely more difficult to preserve. Partial oxidation of the sample (pyrite, other Fe–sulfides) can, therefore, not be excluded. The oxidation of less than 0.2 g of pyrite per kg of rock is sufficient for explaining the observed discrepancies, i.e. approximately 1% of the total pyrite content of the sample. These results confirm that it is very difficult to obtain reliable SO_4^{2-} concentrations from leaching experiments of core samples due to side reactions that are very difficult to prevent completely. Despite these limitations, a SO_4^{2-} gradient can be observed in the data. Although recalculated concentrations are not consistent with concentrations in the test water, the gradient is in accord with the substantial reduction in SO_4^{2-} concentrations over time in the test interval, from near 15 to 4–5 mmol/kg, leading to a strong gradient and associated flux of SO_4^{2-} towards the test interval.

The artificial pore water was initially traced for a large positive δ^2H of +370‰, and δ^{18}O was at a laboratory water value of −10.46‰. The final sampling campaign (17 days before overcoring) yielded values of −13‰ and −5.93‰ for δ^2H and δ^{18}O, respectively. Slow but continuous in-flow of pore water occurred to the interval after final sampling, and this may have especially affected the δ^2H profile. The δ^{18}O values show no variation with radial distance for the profile at 9.7 m depth (C) with an average of −7.8‰ (range: −7.5‰ to −8.2‰). This range partially overlaps with values obtained by the same method from a nearby borehole BWS-A2 (1 sample, −7.7‰) and a somewhat more distant borehole BWS-A5 (9 samples, crossing the Main Fault, −7.1‰ to −7.6‰) reported in Pearson et al. (2003, Table A4.3). Values around −9.0‰ measured in the inflow from long-term pore water sampling in BWS-A2 appear enigmatic and the discrepancy remains unexplained (Pearson et al., 2003, Table A1.14). Data, therefore, suggest that the δ^{18}O remained largely undisturbed in the rock matrix during the PC experiment.

In contrast, δ^2H (Fig. 13, profile at 9.5 m depth) shows an approximately regular decrease from −36‰ near the borehole to −67‰ at a radial distance of ca. 15 cm measured along bedding. This latter value is consistent with values of −59‰ to −66‰ measured on the inflow in a borehole at a similar structural position (Pearson et al., 2003, borehole BWS-A2, Table A1–14), but more negative than a value obtained from core material from the same borehole by diffusive exchange (Pearson et al., 2003, Table A4–3). While reasons for this latter discrepancy between different methods remains unclear, the profile obtained for ^{2}H is in agreement, like those for Cl^- and Br^-, with diffusion processes having taken place during the 5 a of the experiment. The pattern obtained for a 4-sample profile at 6.7 m depth is less clear due to the fact that one experiment apparently leaked as documented by an erroneously high apparent water content.

The combined O and H data of the test porewater monitored over 5-a and of the Opalinus Clay overcored at the water/rock interface were plotted in a δ^{18}O – δ^2H diagram (Fig. 13). The figure shows the slight ^{2}H diffusion into the Opalinus Clay and the strong buffering of the Opalinus Clay formation.

6.3. Stability of the clay exchanger and of the mineral assemblage

Fig. 11 illustrates the cation occupancies on the exchanger as a function of radial distance from the borehole. For all samples the occupancy is approximately 5.5 meq/100 g for Na^+, 2.2 meq/100 g for Ca^{2+}, 2.0 meq/100 g for Mg^{2+}, approximately 0.8 meq/100 g for K^+, and the Sr^{2+} data shows a very narrow spread at a value of 0.13 meq/100 g. The fractional cation occupancies on the exchanger are, therefore, identical in all investigated samples. Furthermore, the data obtained for the profiles compare quite well with undisturbed Opalinus Clay as reported in Pearson et al. (2003, Table A3.11) for the locations in a comparable position (BWS-A3) and obtained by a comparable Ni-en method with similar corrections applied: 9.5–10.4 meq/100 g for the sum of exchangeable cations, 4.8–5.0 meq/100 g for Na^+, 2.5–2.7 meq/100 g for Ca^{2+}, 1.6–1.9 meq/100 g for Mg^{2+}, and ca. 0.1 meq/100 g for Sr^{2+}. The occupancy obtained in BWS-A3 for K^+ (0.5–0.7 meq/100 g) is somewhat less than the value obtained from the PC samples.

The mineralogy of the mud collected on the wall of the borehole and precipitates in the borehole fluid provide evidence of neoformation of Fe-bearing sulfides (pyrite, and probably greigite and/or mackinawite) and calcite, induced by the microbial perturbation (Stroes-Gascoyne et al., 2011; Tournassat et al., 2011; Wersin et al., 2011-a,b). A source of Fe^{2+} is required for this Fe-bearing mineral precipitation. Iron(II) originates ultimately from the formation pore water by diffusion (neither initial test water nor equipment devices contained Fe). In the formation, Fe^{2+} can originate from the clay exchanger (Tournassat et al., 2009; Pearson et al., 2011) or from a dissolving solid phase (pyrite, siderite, clay minerals or detrital phases such as biotite, Pearson et al., 2003). There was, however, no notable decrease in siderite towards the test interval. Pyrite dissolution is not possible from a thermodynamic and mass balance point of view: first, the bacterial perturbation led to more reducing conditions than those present *in situ* (Pearson et al., 2011) and second, the stoichiometric dissolution of pyrite would produce one Fe for two S while precipitation of the observed Fe–sulfides required more than one Fe atom for two S atoms. As a consequence, Fe in pore water (Table 1) and Fe from the exchanger are the most likely sources.

The ^{18}O depletion in calcite in the mud collected from the wall of the borehole could be due to water/calcite isotopic exchange or precipitation of calcite from the borehole water. The δ^{13}C and δ^{18}O of the fluid at equilibrium with the calcite of the mud was calculated using the calcite-water O isotope fractionation of O'Neil et al. (1969) and the calcite–HCO_3^- carbon isotope fractionation of Deines et al. (1974), and a formation temperature between 15 and 25 °C, i.e. the maximum range of temperatures measured in the borehole during the PC experiment. Calculated equilibrium δ^{13}C and δ^{18}O of ca. −3‰ PDB and ca. −7‰ to −5‰ VSMOW, respectively, are significantly different from the observed isotopic signature of the initially injected synthetic porewater (δ^{13}C and δ^{18}O of −29.1‰ and −10.5‰, respectively). But the calculated

isotopic composition is quite close to the pore water after 264 days. This is after major changes of the chemical parameters of the borehole water occurred as a consequence of bacterial perturbations (SO_4 reduction), and the observed carbonates are inferred to have formed as a consequence of this.

Mineralogical, textural and chemical variations of bulk rock as well as of the clay fraction and (C, O) isotopes of carbonates along the radial profiles are small and may be considered as representative of the heterogeneity of the rock. Euhedral grains of carbonates (calcite, dolomite and siderite) at the water/rock interface do not provide any evidence of surface dissolution or growth. Pyrite framboids and clusters also remained stable. There is no visible evidence of precipitation/dissolution processes which could be linked to the effects of water–rock interaction during the PC experiment in the Opalinus Clay adjacent to the test interval.

7. Conclusions

Mineralogical, chemical and isotopic analyses were performed on samples from overcoring a 5-a *in situ* diffusion experiment carried out in Opalinus Clay, and that was microbially disturbed. No mineralogical, chemical, physical and isotopic changes were observed in the Opalinus Clay bulk rock except for the immediate interfacial region and a very slight increase in water content next to the test interval. This is despite that the sulfate–sulfide system was heavily perturbed in the test interval.

Results show that the distribution of non-reactive tracers (Br^- and ^2H) in pore water display clear radial diffusion profiles and follows the expected out/in-diffusion compatible with the time-dependent boundary conditions in the borehole. Bromide concentration decreases with distance from the test interval, and thus also Br/Cl ratios. The Br/Cl ratio does not reach a plateau in the range of 0–17 cm.

The determined apparent anion-accessible porosity ratio of ~0.75 is slightly higher than the range of 0.5–0.7 of existing data. It is not clear if this is due to a physico-chemical disturbance induced by the experiment.

In summary, only very minor effects in the wall rock resulted from a 5-a microbially perturbed *in situ* test (SO_4 reduction and oxidation of organicC). This attests to the expected relatively rapid buffering processes and large buffering capacity of Opalinus Clay provided by its mineralogy and ion exchange complex.

Acknowledgements

Financial support by the partners of the Mont Terri Consortium participating in the PC Experiment (ANDRA, BGR, CRIEPI, JAEA, Nagra, SCK-CEN) is acknowledged. The support of field work by Christophe Nussbaum and Thierry Theurillat (Geotechnical Institut AG / Swisstopo) and the excellent drilling work supported by Bernd Frieg (Nagra) and carried out by Schützeichel Kernbohrgesellschaft is highly appreciated. Chr. Tournassat (BRGM) and F.J. Pearson (New Bern, consultant) provided a review of an earlier version. E. Sacchi (Università di Pavia) and an anonymous reviewer improved clarity of arguments and presentation.

References

Bradbury, M.H., Baeyens, B., 1998. A physicochemical characterization and geochemical modeling approach for determining porewater chemistries in argillaceous rocks. Geochim. Cosmochim. Acta 62, 783–795.

De Cannière, P., Schwarzbauer, J., Höhener, P., Lorenz, G., Salah, S., Leupin, O.X., Wersin, P., 2011. Biogeochemical processes in a clay formation *in situ* experiment: part C – organic contamination and leaching data. Appl. Geochem.

Deines, P., Langmuir, D., Harmon, R.S., 1974. Stable carbon isotope ratios and the existence of a gas phase in the evolution of carbonate groundwaters. Geochim. Cosmochim. Acta 38, 1147–1164.

Gaucher, E.C., Crouzet, C., Flehoc, C., Girard, J.P., Lassin, A., 2002. Measurement of Partial Pressure and Isotopic Composition of CO_2 on Two Core Samples from the Mont Terri Rock Laboratory, Borehole BPC-1. Report BRGM/RP-51771-FR, BRGM, France.

Gaucher, E.C., Tournassat, C., Pearson, F.J., Blanc, P., Crouzet, C., Lerouge, C., Altmann, S., 2009. A robust model for clayrock porewater chemistry. Geochim. Cosmochim. Acta 73, 6470–6483.

Gimmi, T., 2003. Porosity, Pore Structure, and Energy State of Pore Water of Opalinus Clay from Benken. Nagra Internal Report NIB 93-09. Nagra, Wettingen, Switzerland.

Horita, J., Cole, D.R., Wesolowski, D.J., 1993a. The activity-composition relationship of oxygen and hydrogen isotopes in aqueous salt solutions: II. Vapor–liquid water equilibration of mixed salt solutions from 50 to 100 °C and geochemical implications. Geochim. Cosmochim. Acta 57, 4703–4711.

Horita, J., Wesolowski, D.J., Cole, D.R., 1993b. The activity-composition relationship of oxygen and hydrogen isotopes in aqueous salt solutions: I. Vapor–liquid water equilibration of single salt solutions from 50 to 100 °C. Geochim. Cosmochim. Acta 57, 2797–2817.

Koroleva, M., Mäder, U., 2008. PC-Experiment: Geochemical Analysis of Sample Material from Overcoring BPC-1. Mont Terri Project. Technical Note 2006-68.

NAGRA, 2002. Projekt Opalinuston: Synthese der geowissenschaftlichen Untersuchungsergebnisse. Entsorgungsnachweis für abgebrannte Brennelemente, verglaste hochaktive sowie langlebig-mittelaktive Abfälle. Nagra Technical Report NTB 02–03. Nagra, Wettingen, Switzerland.

O'Neil, J.R., Clayton, R.N., Mayeda, T.K., 1969. Oxygen isotope fractionation in divalent metal carbonates. J. Chem. Phys. 51, 5547–5558.

Pearson, F.J., 1999. What is the porosity of a mudrock? In: Aplin, A.C., Fleet, A.J., Macquaker, J.H.S. (Eds.), Muds and Mudstones: Physical and Fluid Flow Properties. Geol. Soc. London Spec. Publ. 158, 9–21.

Pearson, F.J., Arcos, D., Bath, A., Boisson, J.Y., Fernandez, A.M., Gaebler, H.E., Gaucher, E.C., Gautschi, A., Griffault, L., Hernan, P., Waber, H.N., 2003. Mont Terri Project – Geochemistry of Water in the Opalinus Clay Formation at the Mont Terri Rock Laboratory. Reports of the Federal Office of Water and Geology (FOWG). Geology Series No. 5.

Pearson, F.J., Tournassat, C., Gaucher, E., 2011. Biogeochemical processes in a clay formation *in situ* experiment: part E – equilibrium controls on chemistry of pore water from the Opalinus Clay, Mont Terri Underground Laboratory, Switzerland. Appl. Geochem.

Rübel, A., Sonntag, Ch., Lippmann, J., Pearson, F.J., Gautschi, A., 2002. Solute transport in formations of very low permeability; profiles of stable isotope and dissolved noble gas contents of pore water in the Opalinus Clay, Mont Terri, Switzerland. Geochim. Cosmochim. Acta 66, 1311–1321.

Soler, J.M., Samper, J., Yllera, A., Hernández, A., Quejido, A., Fernández, M., Yang, C., Naves, A., Hernán, P., Wersin, P., 2008. The DI-B *in situ* diffusion experiment at Mont Terri: results and modelling. Phys. Chem. Earth 33, 196–207.

Sposito, G., 1990. Molecular models of ion adsorption on mineral surfaces. In: Hochella, M.F., White, A.F. (Eds.), Mineral–Water Interface Geochemistry. Rev. Mineral. 23, 261–279.

Stroes-Gascoyne, S., Sergeant, C., Schippers, A., Hamon, C.J., Nèble, S., Vesvres, M.-H., Barsotti, V., Poulain, S., Le Marrec, C., 2011. Biogeochemical processes in a clay formation *in situ* experiment: part D – microbial analyses – synthesis of results. Appl. Geochem.

Swart, P.K., Burns, S.J., Leder, J.J., 1991. Fractionation of the stable isotopes of oxygen and carbon in carbon dioxide during the reaction of calcite with phosphoric acid as a function of temperature and technique. Chem. Geol. 86, 89–96.

Tournassat, C., Gailhanou, H., Crouzet, C., Braibant, G., Gautier, A., Gaucher, E.C., 2009. Cation exchange selectivity coefficient values on smectite and mixed-layer illite/smectite minerals. Soil Sci. Soc. Am. J. 73, 928–942.

Tournassat, C., Alt-Epping, P., Gaucher, E.C., Gimmi, T., Leupin, O.X., Wersin, P., 2011. Biogeochemical processes in a clay formation *in situ* experiment: part F – Reactive transport modelling. Appl. Geochem.

Van Loon, L.R., Soler, J.M., Jakob, A., Bradbury, M.H., 2003. Effect of confining pressure on the diffusion of HTO, $^{36}Cl^-$ and $^{125}I^-$ in a layered argillaceous rock (Opalinus Clay): diffusion perpendicular to the fabric. Appl. Geochem. 18, 1653–1662.

Van Loon, L.R., Soler, J.M., Muller, W., Bradbury, M.H., 2004. Anisotropic diffusion in layered argillaceous rocks: a case study with Opalinus Clay. Environ. Sci. Technol. 38, 5721–5728.

Wersin, P., Gaucher, E., Gimmi, Th., Leupin, O., Mäder, U., Pearson, F.J., Thoenen, T., Tournassat, Ch., 2009. Geochemistry of Pore Waters in Opalinus Clay at Mont Terri: Experimental Data and Modelling. Mont Terri Project. Technical Report 2008-06.

Wersin, P., Leupin, O.X., Mettler, S., Gaucher, E., Mäder, U., Vinsot, A., De Cannière, P., Gäbler, H.-E., Kunimaro, T., Kiho, K., 2011. Biogeochemical processes in a clay formation *in situ* experiment: part A – overview, experimental design and water data of an experiment in the Opalinus Clay at the Mont Terri Underground Research Laboratory, Switzerland. Appl. Geochem.

Wersin, P., Stroes-Gascoyne, S., Pearson, F.J., Tournassat, C., Leupin, O.X., Schwyn, B., 2011. Biogeochemical processes in a clay formation *in situ* experiment: part G – key interpretations and conclusions. Implications for repository safety. Appl. Geochem.

Applied Geochemistry 26 (2011) 967–979

Contents lists available at ScienceDirect

Applied Geochemistry

journal homepage: www.elsevier.com/locate/apgeochem

Biogeochemical processes in a clay formation *in situ* experiment: Part C – Organic contamination and leaching data

P. De Cannière [a,g,*], J. Schwarzbauer [b], P. Höhener [c], G. Lorenz [d], S. Salah [a], O.X. Leupin [e], P. Wersin [e,f]

[a] SCK·CEN, Environment, Health and Safety Institute, Waste and Disposal Project, Boeretang 200, BE-2400 Mol, Belgium
[b] RWTH Aachen University, Institute of Geology and Geochemistry of Petroleum and Coal Laboratory for Organic-geochemical Analysis, Lochnerstrasse 4-20, DE-52056 Aachen, Germany
[c] Université de Provence-CNRS, UMR 6264 LCP, 3 place Victor Hugo – Case 29, FR-13331 Marseille Cedex 3, France
[d] Hydroisotop GmbH, Woelkestrasse 9, DE-85301 Schweitenkirchen, Germany
[e] NAGRA, Hardstrasse 73, CH-5430 Wettingen, Switzerland
[f] Gruner Ltd., Gellertstrasse 55, CH-4020 Basel, Switzerland
[g] FANC – AFCN, Rue Ravenstein 36, BE-1000 Brussels, Belgium

ARTICLE INFO

Article history:
Available online 17 March 2011

ABSTRACT

Data interpretation of the Porewater Chemistry (PC) experiment at the Mont Terri Rock Laboratory has led to unexpected observations of anaerobic microbial processes which caused important geochemical perturbations of the Opalinus Clay water in the borehole. The increases of acetate to 146 mg C/L, of DIC to 109 mg C/L and of CH_4 to 0.5 mg C/L were unexpected and could not be explained without the presence of a C source in the system. The organic C fuelling the observed microbial activity was until then unknown. Leaching tests were performed on several polymers used for the fabrication of the PC equipment to identify the source of organic matter (OM). Polyethylene (PE) appears to be very inert and does not release detectable concentrations of dissolved organic C (DOC) (<1 ppb) into the water. Polyurethane (PU) leaches out a dozen different organic compounds accounting for only 13 μg DOC/g PU. Under the conditions of the leaching tests, 1 g of polyamide (PA, Nylon) also releases ~512 μg of the plasticizer N-Butyl-Benzene-Sulfonamide (NBBS). Soaking tests with polyethylene samples immersed in acetone under conditions similar to those used to remove grease spots on the porous PE filter prior to installation showed that acetone could have been trapped in the PE filter, corresponding to an initial concentration of 1.5 g acetone/L of water. However, the accumulated amount of organic C taken into account from all these components was insufficient to satisfactorily explain the observed microbially mediated reducing perturbation. Finally, large amounts of dissolved organic C were found to be released in the system by the jelly polymer filling the reference compartment of the pH and E_h electrodes permanently installed over 5 years in flow-through cells on the water circulation loop of the PC experiment. Glycerol was further identified by chromatographic analysis as the main organic compound released by the electrodes. From the analysis results, as well as from the geochemical calculations, the most likely primary organic C source fuelling the microbial perturbation was glycerol released from the polymeric gel filling the reference electrodes (1.6 g glycerol/electrode). Other sources, such as acetone, may also have contributed to microbial processes, but only to a minor extent.

1. Introduction

In order to gain deeper insight into geochemical processes regulating pH and E_h, the Porewater Chemistry (PC) experiment was started at the Mont Terri Rock Laboratory in 2002. This *in situ* experiment was based on the diffusive equilibration method. Synthetic porewater was recirculated in a packed-off borehole and allowed to equilibrate with the formation water via diffusion (Wersin et al., 2011a). The diffusive exchange process was monitored by conservative tracers (^2H, Br^-) (Waber, 2002; Eichinger, 2003, 2004). Throughout the experiment disturbance by atmospheric O_2 was minimised. In particular, the borehole was drilled with N_2 and filled with Ar prior to equipment installation (Drouiller and Vinsot, 2002; De Cannière and Fierz, 2002; Wersin et al., 2011a). All parts contacting the circulating water were non-metallic to avoid any influence on redox potential measurements (E_h). The non-preservable parameters, such as pH, E_h, temperature, and hydraulic pressure, were continuously monitored *in situ*. Water samples were taken periodically and analysed for their chemical and isotopic composition. In addition, microbial analyses

* Corresponding author. Present address: FANC – AFCN, Rue Ravenstein 36, BE-1000 Brussels, Belgium. Tel.: +32 (0)2 289 20 86; fax: +32 (0)2 289 21 12.
E-mail address: pierre.decanniere@fanc.fgov.be (P. De Cannière).

0883-2927/$ - see front matter © 2011 Elsevier Ltd. All rights reserved.
doi:10.1016/j.apgeochem.2011.03.006

were also performed (Battaglia and Gaucher, 2003; Daumas, 2004; Ishii, 2004; Mauclaire, 2005; Stroes-Gascoyne et al., 2007, 2011) along with isotope analysis of the CO_2 gas and the carbonate minerals in the samples (Waber, 2002; Eichinger, 2003, 2004; Wersin et al., 2011a; Tournassat et al., 2011).

The chemical composition of the water sampled from the PC experiment showed significant changes with time, especially for the major anions, pH, E_h, pCO_2, dissolved inorganic and organic C (DIC, DOC), and the stable isotope composition ($\delta^{13}C$). In particular, the concentrations of SO_4^{2-} and HCO_3^- were strongly affected. After a period of 2.3 a, HCO_3^- concentrations showed a 7-fold increase and SO_4^{2-} concentrations decreased by a factor of 3 (Mettler, 2004; Wersin et al., 2011a). Concomitantly, pH values decreased from 7.8 to 6.7 and sulphide concentrations showed a strong rise. E_h values showed an initial rapid decrease, which was followed by a slow steady decrease down to −220 mV (SHE). The concentrations of DOC rose from 2–5 mg C/L to values >150 mg C/L of which most was acetic acid.

^{13}C-DIC and ^{13}C-DOC values showed some variations with time, but both parameters appear to have reached stable values at about −15‰ (Waber, 2002; Eichinger, 2003, 2004; Wersin et al., 2011a). ^{13}C–CH_4 showed strongly negative values of about −43‰ after 2.3 a. Microbial analysis indicated the presence of SO_4-reducing and of some methanogenic bacteria in the circulating water (Battaglia and Gaucher, 2003; Ishii, 2004; Mauclaire, 2005; Stroes-Gascoyne et al., 2011).

Surprisingly also, the *in situ* data indicated pCO_2 values as high as $10^{-1.3}$ bar in the latter stages of the PC experiment. These values were not consistent with CO_2 measurements from core samples (pCO_2 of about $10^{-2.7}$ bar) obtained by Gaucher (2002) and porewater data from a column infiltration experiment (Mäder, 2002, 2005; Mäder and Gimmi, 2007), nor with other Mont Terri experiments suggesting lower *in situ* pCO_2 values ($10^{-3.5}$ bar) (Pearson et al., 2003, 2011; Gaucher, 2004a,b; Vinsot et al., 2005; De Cannière et al., 2008).

The chemical and isotopic data (Eichinger, 2003, 2004b; Wersin et al., 2011a) as well as geochemical modelling (Arcos, 2003; Gaucher, 2003, 2004a,b; Pearson, 2003, 2005; Pearson et al., 2011; Tournassat et al., 2011) confirmed the significance of microbially-mediated SO_4-reduction occurring in the borehole. The reducing agent appears to be principally organic C. Although CH_4 oxidation is commonly associated with SO_4-reduction, the role of CH_4 within this redox process is not conclusive, but both methanogenic fermentation and CH_4 oxidation reactions appear to occur. The measured $\delta^{13}C$ data in the circulating water are interpreted to be a result of concomitant organic C degradation and carbonate dissolution (Höhener, 2004; Tournassat et al., 2011; Pearson et al., 2011). Data indicate that glycerol (propane-1,2,3-triol) released from the polymer gel of pH–E_h electrodes emplaced in the water circulation loop served as a degrading C source fuelling the microbial processes. Acetone and organic matter released by the PE filter screen and other parts of the equipment made exclusively of polymeric materials could have contributed to the microbial degradation only to a minor extent.

1.1. Objective and motivation

The objective of the present work was to identify, or to exclude, possible sources of organic C released by different plastic materials, pH electrodes, or solvents, used in the equipment, or component cleaning of the PC experiment. This characterisation study was launched after the interpretation of test data obtained from the PC experiment and a literature survey on the biodegradation of synthetic materials done by Höhener (2004, 2005). Of particular interest were first the plasticizers that might have leached from soft polyurethane (PU) and polyamide (PA, Nylon).

Another initially suspected source of dissolved organic C in the water of the PC experiment was acetone. Indeed, the polyethylene (PE) filter for the PC experiment was washed with acetone before installation in order to remove traces of grease that were left from the manufacturing process. So, it might have been possible that the polyethylene was still soaked with acetone. Acetone is known to be biodegraded by fermentative (Platen et al., 1994) and SO_4-reducing bacteria (Janssen and Schink, 1995a,b), or other complex degradation pathways (Platen and Schink, 1987).

Finally, the continuous increase of DOC observed by Leupin (unpublished data, pers. comm.) in the water circuit of another *in situ* Diffusion Retention (DR) experiment at Mont Terri gave a decisive clue to solve the long puzzling enigma related to the unidentified C source in the system. DOC accumulation in water of the DR experiment showed that the organic polymer gel used in the reference compartment of on-line pH and E_h electrodes was also likely the main contributor to the organic C inventory in the PC experiment. Hence, an essential and ultimate objective was to determine the nature and the concentration of organic C released by the electrodes and to establish a C mass balance with a consistent geochemical hypothesis for the C turnover in the system (see also Tournassat et al., 2011).

2. Materials and methods

2.1. Nature and properties of equipment materials

The experimental setup and the installation procedure of the Mont Terri Porewater Chemistry (PC) experiment are described in detail by De Cannière and Fierz (2002) and by Wersin et al. (2011a). The borehole equipment consisted of a single packer system with a 4.5 m long filter section between the bottom of the hole and the packer, and an upper section sealed with epoxy resin (Sikadur 52) above the packer (Fig. 1) to isolate the test interval from the gallery and to prevent gas exchanges (O_2, CO_2, CH_4, etc.) with atmosphere. The filter section (test interval) was equipped with hollow cylindrical sintered low-density polyethylene (LDPE) filters supported by a central rod made of polyvinylchloride (PVC). The stacked porous filters were connected to poly-ether-ether-ketone (PEEK) water lines located at the bottom and the top of the test interval to allow continuous water circulation in the system. At the surface, in the gallery, a solenoid diaphragm metering pump (Milton Roy P-74501-15) with a polypropylene head connected to downhole PEEK water lines and surface nylon tubing recirculated water through PEEK flow-through cells isolated from atmospheric oxygen in a gas-tight anaerobic cabinet slightly pressurised under Ar. The PEEK flow-through cells hosted pH, E_h, electrical conductivity electrodes and temperature sensors. The materials used in the different components of the PC experiment are summarised in Table 1. The total volume of circulating water was 3.082 L (De Cannière and Fierz, 2003).

2.2. Short description of the work

Amongst other polymer materials, Höhener (2004) recommended performing leaching tests of polyethylene (PE), polyurethane (PU) and polyamide (PA, Nylon), and also to study the processes of absorption/desorption of acetone by porous polyethylene from the filter screen. PE was used in the porous filter screen, PU for the packer sleeve, and PA for water tubings of the surface setup.

Leaching tests with pure water were performed and the released organic products after extraction from water with dichloromethane were determined by gas chromatography (GC) and gas chromatography coupled to mass spectrometry (GC/MS). In

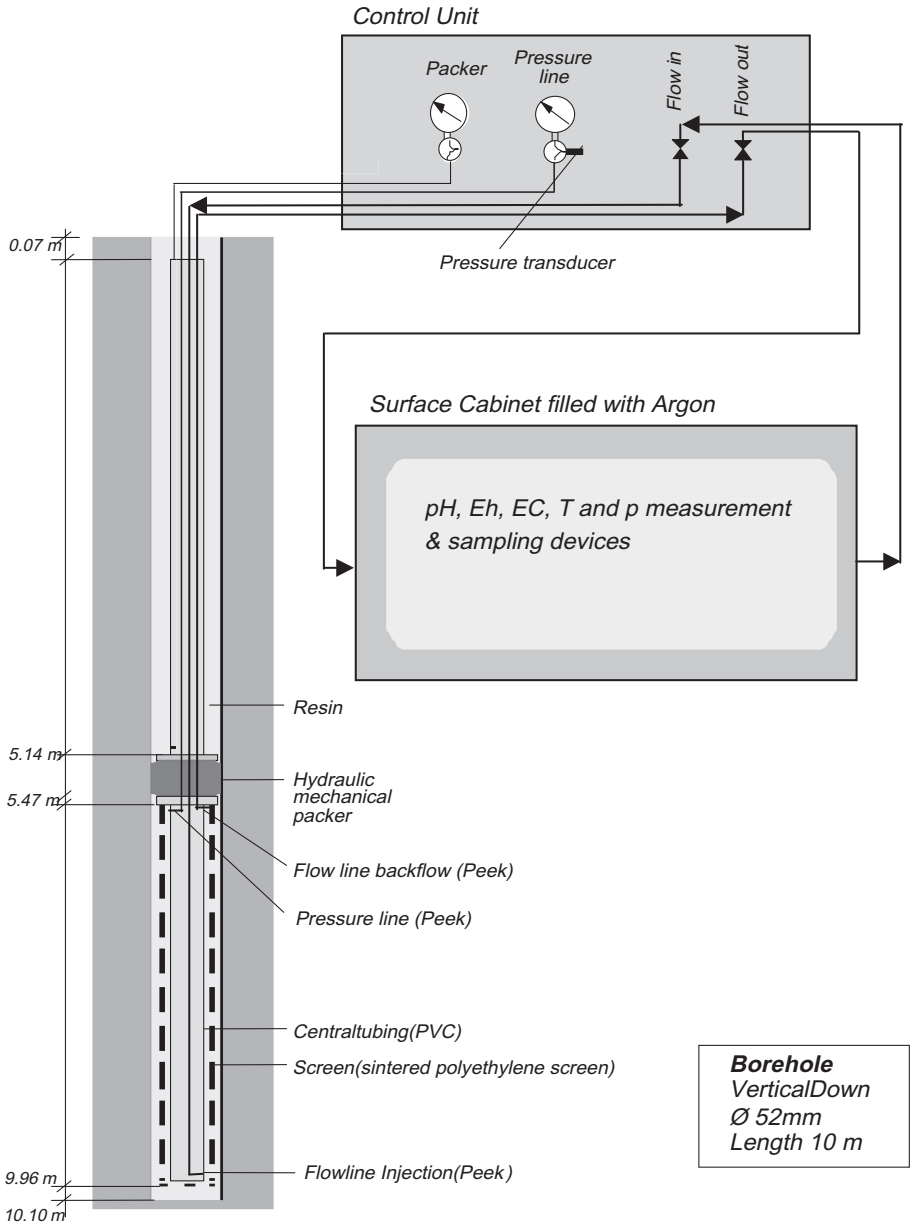

Fig. 1. Schematic drawing of the test setup (down-hole equipment) of the Porewater Chemistry (PC) experiment.

Table 1
Synthetic materials used in the different components of Mont Terri PC experiment. Volume refers to the volume of the plastic materials only, not to the volume of the water circuit.

Component (–)	Material and component dimensions outer, inner diameter, thickness, length (mm)	Material volume (cm^3)	Density ($g\ cm^{-3}$)	Mass (g)
Packer sleeve	Polyurethane (PU) OD = 50 mm, thickness = 2 mm, L = 200 mm	63	0.90	56.5
Porous filter screen	Low-density polyethylene (LDPE) porosity = 0.30; mesh 40 μm, OD = 50 mm, ID = 30 mm, L = 4500 mm	3958[a]	0.93	3681
Tubing: downhole	Poly-ether-ether-ketone (PEEK, 1/8″) OD = 3.175 mm, ID = 2.05 mm, L = 20 500 mm	90	1.29	116
Tubing: surface equipment	Polyamide (PA, Nylon) OD = 4 mm, ID = 2 mm, L = 3000 mm	28	1.07	30.2
Central casing	Polyvinylchloride (PVC) OD = 30 mm, thickness = 3 mm, L = 4500 mm	604	1.30–1.50	785–900

All component lengths are given in millimetres scale, even for elements and tubings with a length of several metres.
[a] 3958 cm^3 corresponds to the volume of the porous LDPE filter screen, not to the volume of water it contains.

parallel, the presence of possible residues of cleaning acetone in the porous PE filter was assessed by soaking PE samples in triplicate in acetone, rinsing the PE with pure water, and allowing the sample to dry sufficiently. Solid phase micro-extraction (SPME) and head-space chromatography were used to detect acetone residues.

Finally, after Leupin (2008, pers. comm.) realised that pH–E_h electrodes permanently installed online over 5 a in the water circulation system could be a considerable source of DOC in water, it was decided to perform leaching tests with electrodes immersed in pure water to determine the DOC release rate from these electrodes. GC/MS analyses and C (^{14}C and $\delta\ ^{13}C$) isotope measurements were also applied to characterise the polymer gel of their reference compartment and to identify the nature of the organic matter (OM) released.

2.3. Leaching of selected polymer materials

The choice of the polymers selected for the leaching tests was motivated by the potential organic matter (OM) release (depending on their susceptibility to leaching), the amounts used (inventory), and their location in the Porewater Chemistry (PC) experiment (accessibility). Amongst other polymer materials recommended by Höhener (2004) for performing leaching tests, polyethylene (PE), polyurethane (PU) and polyamide (PA, Nylon) were selected. Polyethylene, although very inert by nature as a paraffin material (*parum affines*, poor affinity) was also selected because it was the material with the larger mass and the highest surface in contact with water in the test interval. The very flexible polyurethane used for the inflatable packer sleeve was suspected to contain plasticizers, or many chemical additives. Finally, polyamide (Nylon) used only in the surface cabinet waterlines was also found to release a plasticizer (NBBS) in a piezometer using the same type of tubing at the underground research laboratory in Mol (Belgium) (Van Geet, 2004).

The second part of the work dealt with the search for soluble small organic molecules: acetone possibly absorbed by the porous polyethylene screen and glycerol (propane-1,2,3-triol) released by the polymer gel from pH and E_h reference electrodes.

In order to prevent oxidation, the leaching tests were done under an inert atmosphere of N_2 as *in situ*. The time span selected for the leaching tests of polymers was no longer than 2 weeks because microbial growth could start to interfere if an excessively long time was chosen. To check the background "contamination" in water and from glassware, a fourth leaching test was run without any plastic material – as a blank.

As light and photolysis could affect the degradation of polymers in the *in vitro* leaching tests and could create artefacts with respect to the conditions prevailing *in situ* in the field test at Mont Terri, all polymer leaching tests were performed in the dark.

2.3.1. Leaching experiment protocol

Aliquots of approximately 32 g of each polymer (PA, PE and PU) were placed separately in precleaned glass vials, which were filled with 500 mL of bidistilled water. After flushing the head space with N_2 the vials were closed and left at room temperature (RT) in the dark for 16 days. In parallel, a blank experiment was performed under the same conditions, but without sample material. After the leaching time period, the polymer sample was removed and two successive liquid/liquid extractions with 50 mL of dichloromethane (CH_2Cl_2) and 50 ml dichloromethane after water acidification to pH 2 were applied to the remaining water samples, respectively. After drying the CH_2Cl_2 extracts over granulated anhydrous Na_2SO_4 their volume was reduced to 100 μL using a rotavapor, and each fraction was analysed separately by gas chromatography (GC) and gas chromatography coupled to mass spectrometry (GC/MS). After addition of an internal standard (IS: 100 μL of ethylpalmitate, 83.4 ng/μL) quantitative gas chromatographic analyses were carried out by means of GC/MS using internal and external standard methods.

2.3.2. Gas chromatography–mass spectrometry analyses

The experimental conditions applied in the GC and GC/MS analyses were the following:

GC conditions:

- GC8000 series, Fisons Instruments.
- ZB5 capillary column; 30 m × 0.25 mm ID × 0.25 μm df (film thickness).
- Temperature programme: 60 °C for 3 min, with 5 °C/min to 300 °C.
- Split/splitless-injection at 270 °C, split ratio 1:40, splitless time 60 s.
- Detector: Flame Ionisation Detector (FID); T = 270 °C.
- Carrier gas: H_2; flow rate: 35 cm s^{-1} – injection volume: 1 μL.

GC/MS conditions:

Chromatographic separation:

- HP5890 GC, Hewlett Packard.
- BPX5 capillary column; 30 m × 0.22 mm ID × 0.25 μm df (film thickness).
- Temperature programme: 60 °C for 3 min, with 5 °C/min to 300 °C.
- Split/splitless-injection at 270 °C, split ratio 1:35, splitless time 60 s.

Mass spectrometry detection:

- Finnigan MAT 8222 mass spectrometer.
- Low resolution (1000) in EI^+-mode, 70 eV (EI^+ positive ion Electron Impact ionisation mode).
- Full scan mode from m/z 35 to m/z 700.
- Source heat 200 °C.

2.4. Analysis of acetone residues trapped in polyethylene

Several experiments were performed to determine the residual acetone trapped in porous polyethylene (PE) after soaking in acetone for some time. After that, the polyethylene samples were dried at room temperature (RT), or at 60 °C, to assess the effect of drying conditions on the residual acetone quantities. Acetone was then recovered by solid phase micro-extraction (SPME) and further analysed by gas chromatography (GC). These experiments were accompanied by a spike calibration experiment and blank tests to obtain semi-quantitative results and to validate the experimental procedure. The two protocols made at room temperature and 60 °C were as follows.

2.4.1. Experiment 1 (RT)

A piece of 0.7 g of polyethylene (PE) was soaked in 50 mL acetone (technical grade). After 2 h the PE sample was removed and rinsed three times with 250 mL of bidistilled water. Then the sample was dried at room temperature (RT) for 30 min. Afterwards, the sample was transferred to a closed 12 mL glass vial, and a head space solid phase micro-extraction (SPME) procedure was applied. This experiment was repeated once.

2.4.2. Experiment 2 (60 °C)

A similar piece of PE as used in experiment 1 was prepared and analysed in the same way as described above. However, one step in the procedure differed. The drying process was carried out at 60 °C in an oven, while all other conditions were kept constant.

2.4.3. Spike experiment

A piece of 0.7 g of PE was placed in a closed vial of 12 mL volume and spiked with 0.2 μL of acetone (technical grade). After 10 min a head space SPME procedure was applied.

2.4.4. Blank experiments

In addition, blank experiments were performed in order to identify artefacts and laboratory derived contamination. The procedure was performed under the same conditions as described for experiments 1 and 2, but without using a PE sample.

2.4.5. Solid phase extractions and gas chromatography analyses

Solid phase micro-extraction (SPME) is a common analytical technique to extract lipophilic organic compounds dominantly from water phases. Additionally, it can be applied to head space analysis in order to concentrate volatile compounds from water or solid samples. In principle, an accumulation of lipophilic compounds takes place at the surface of the coated fibre of the SPME equipment as the result of steady-state conditions with respect to the distribution behaviour of the analytes between the different phases. After accumulation on the fibre, the analytes can be thermally desorbed directly in the GC injector and in the following, be analysed by gas chromatography. The experimental conditions applied in the SPME and GC analyses were the following:

Extraction conditions:

- Extraction time: 45 min.
- Extraction temperature: room temperature (RT).
- SPME phase: polydimethylsiloxane/divinylbenzene (PDMS/DVB) fibres (Supelco (USA), 57326-U).
- Desorption temperature (injector temperature): 270 °C.

GC conditions:

- GC8000 series, Fisons Instruments.
- ZB5 capillary column; 30 m × 0.25 mm ID × 0.25 μm df (film thickness).
- Temperature held isothermally at 60 °C.
- Split-injection at 270 °C, split ratio 1:40.
- Detector: Flame Ionisation Detector (FID); T = 270 °C.
- Carrier gas: H_2; flow rate 35 cm s^{-1}.
- Injection volume: 1 μL.

2.5. Analyses of polymer-filled pH electrodes

The DOC present in the gel of 3 identical Mettler–Toledo (Ingold) polymer-filled pH electrodes (HA405-DXK-S8/120 Combination pH Xerolyt electrodes) was determined by means of three complementary methods: DOC leaching test by immersion of a pH electrode in pure water; chromatographic/mass spectrometry analyses of the organic constituents present in the electrode gel; and ^{14}C and $\delta^{13}C$ measurements of the organic C present in the polymer filling the electrode.

2.5.1. Leaching of DOC from polymer-filled pH electrodes

Laboratory tests were performed to assess the leaching rate of the mobile organic substances present in the pH electrode polymer gel and suspected to have contaminated the water circuit of the Porewater Chemistry (PC) experiment as was evidenced by Leupin (2008, pers. comm.) in the Diffusion Retention (DR) experiments at Mont Terri. A polymer-filled Xerolyt (Mettler–Toledo) pH electrode was immersed in 400 mL of pure deionised water (Milli-Q water; electrical resistivity: 18 MΩ cm) at room temperature under ambient air and constant stirring rate to leach out DOC. A water sample of about 20 mL was taken at regular time interval (up to 155 days) and the following analyses were performed: concentration of DOC, K^+ and Cl^- (released from the reference compartment filled with 3 M KCl), and pH monitoring. DOC was determined by CO_2 infra-red measurement after complete combustion of the sample in a total organic C (TOC) analyser instrument. Potassium was determined by ICP-AES and Cl^- by anion chromatography, while the pH drift was continuously recorded as a function of time on a portable Knick datalogger.

2.5.2. Analysis of glycerol in polymer-filled pH electrodes

Qualitative screening analyses (GC/MS) of extractable organic constituents of the polymer filling (gel) were first performed to identify the different sources of organic C released from pH electrodes. They were followed by the quantitative determination of glycerol identified as the main low-molecular weight constituent of the polymer infill. The experimental working procedure consisting of three steps is briefly summarised hereafter.

2.5.2.1. Working-up: Isolation of the polymer filling gel. The glass casing of a Xerolyt pH electrode was gently cut and the gel was isolated and dried at 105 °C until constant weight. This dried resin material was further used for qualitative and quantitative analyses.

2.5.2.2. Qualitative screening analyses. Ultrasonic-assisted extraction of an aliquot of pre-dried resin material using dichloromethane as solvent; Gas chromatography (GC); qualitative GC/MS analysis.

2.5.2.3. Quantitative analyses of glycerol in resin filling.

(i) *Gas chromatography/mass spectrometry (GC/MS) analysis*: Ultrasonic-assisted extraction of an aliquot of pre-dried resin material using methanol as solvent; Quantitative GC/MS analysis of target substance glycerol after derivatisation with acetanhydride (generating triacetine to improve the quality of following GC/MS analysis); Calibration with reference material.

(ii) *Liquid chromatography/mass spectrometry (LC/MS) analysis*: Ultrasonic-assisted extraction of an aliquot of pre-dried resin material using a mixture of water/methanol (50:50 v:v) as solvent; quantitative LC/MS analysis of target substance glycerol using an APCI source; calibration with reference material.

2.5.3. Analysis of ^{14}C and $\delta^{13}C$ of the polymer-resin filling pH electrodes

As C-isotope data made on pore water samples 7 and 8 (2004–2005) during the PC experiment revealed an unexpected high level of modern C in water (Wersin et al., 2011a; Pearson et al., 2011; Tournassat et al., 2011), it was decided to also perform C-isotope analyses on the gel material filling the electrodes to verify if the electrodes were the source of this anomaly.

Table 2
Main compounds detected and their respective amount released in water by the polyurethane (PU) sample. The peak number refers to the chromatogram of Fig. 2d.

Compound detected	Released amount (ng/g PU)	Peak number[a]
Phenylisocyanate	800	1
(butoxyethoxy)ethanol	760	2
Phenoxyethanol/	1130	3
benzothiazol		3, 9
Cyclohexanethioisocyanate	410	4
Phenoxypropionic acid	4680	5
Caprolactam	390	6
2-(2-Butoxyethoxy)-ethyl acetate	115	7
Unknown	3710	8
1,6-Dioxacyclo-dodecane-7,12-dione	377	9
Triethylcitrate	151	10
Unknown	300	11
Sum	12,823	–

C_6-phenols and alkylsulfonic acid phenylesters were also identified in minor concentrations.

[a] Peaks from Fig. 2d, PU, first extract.

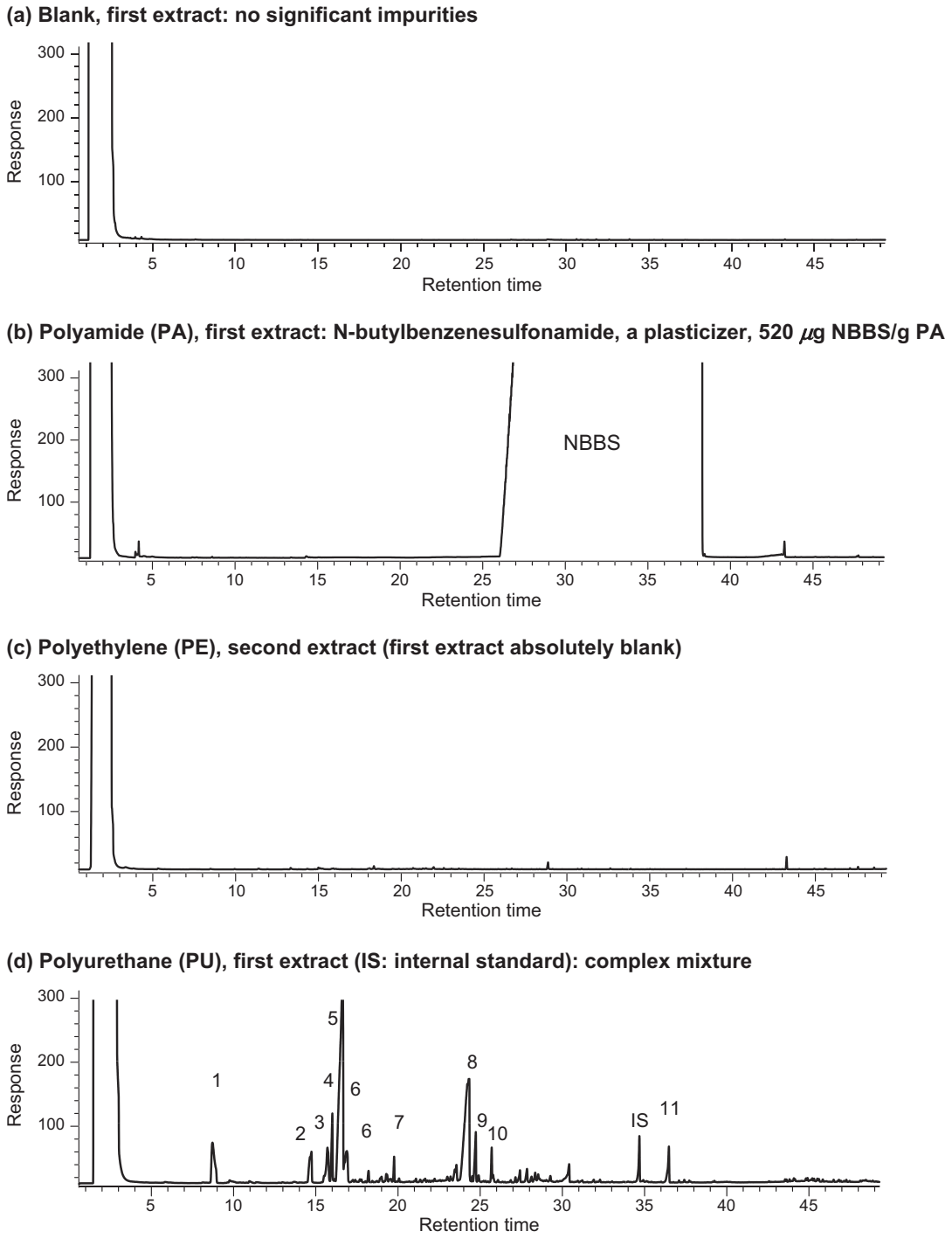

Fig. 2. Gas chromatograms of selected leaching extracts. PA: N-Butyl-Benzene-Sulfonamide: 520 μg NBBS/g PA. PE: No significant contaminant detected. PU: complex mixture of a dozen of constituents determined by addition of an internal standard (IS). All retention times are given in minute.

Table 3
Results of the analyses for acetone extracted from polyethylene (PE) after drying under different conditions.

Experiment	Drying T (°C)	Detection of acetone	Peak area (a.u.)	Ratio[a] to the lowest area	μL acetone per g PE
Blank experiment 1	RT	–	–	–	–
Experiment 1	RT	+++	433 600	53.2	1.61
Experiment 1 (repetition)	RT	+++	389 550	47.8	1.44
Blank experiment 2	60	–	–	–	–
Experiment 2	60	+	8150	1.0	0.03
Spike experiment	RT	++	77 050	9.5	0.29

The signs –, +, ++, and +++ indicate the quality of the acetone detection.
RT: room temperature.
[a] Normalized to the lowest area (8150 from experiment 2).

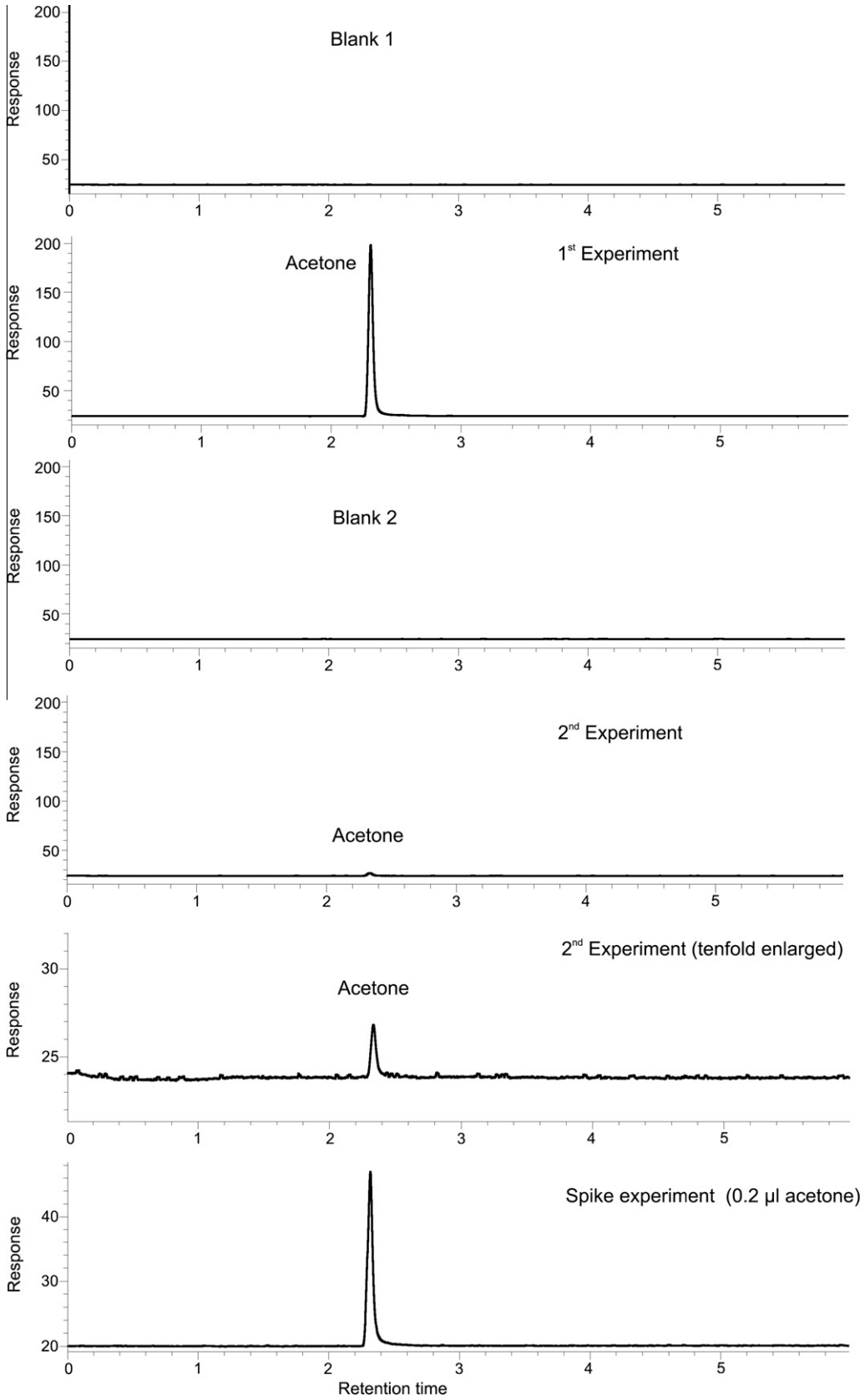

Fig. 3. Experiments of acetone uptake by porous polyethylene. Residues of acetone determined by gas chromatography after acetone recovery by solid phase micro-extraction (SPME).

The glass shell of a polymer-filled *Xerolyt* pH electrode was cut with a corundum-made blade to prevent any C contamination. The gel was then dried at around 50 °C for 5 days in an oven. The whole gel was ashed in a glow-wire equipped combustion bomb, so that all organic C was converted to CO_2. Around 0.9 g C were collected from the gel. Part of the pure CO_2 was separated for direct measurement by isotope ratio mass spectrometry (IRMS) for the $\delta^{13}C$ value (related to VPDB-Std: ±0.3‰). The majority of the pure CO_2 was dissolved in an absorber liquid for low-level ^{14}C measurements. After addition of a scintillation cocktail, the sample was analysed in a liquid scintillation counter (LSC) over several days (double standard deviation; 100%-modern = 0.226 Bq/g C).

3. Results and discussion

3.1. Leaching of selected polymer materials

The analyses reveal that polyethylene (PE) from the porous screen does not release any detectable quantity of contaminants into the bidistilled water. As observed on Fig. 2d, polyurethane (PU) from the packer sleeve releases many constituents (about a dozen have been identified and quantified) in water after leaching, but it accounts for only about 12.8 μg/g of dissolved organic matter. Finally, the polymer most prone to leaching is polyamide (PA). N-Butyl-Benzene-Sulfonamide (NBBS, CID: 19241), a plasticizer added to nylon tubing, is by far the main compound leached out of PA in the highest detected quantity (520 μg/g). The results of the quantitative analyses for the compounds released by polyurethane are given in Table 2.

For polyamide, an important conclusion must be drawn from the huge peak of NBBS observed on Fig. 2b. Indeed, even at low concentration of DOC (<1 mg L^{-1} water), the peak of NBBS completely saturates the detector of the gas chromatograph for about 15 min. During this time NBBS dazzles the system and creates a "blind detection window" for GC/MS in the useful concentration range (μg L^{-1}). Thus, no constituents of natural organic matter with a retention time comprised inside this window can be detected. The same interference also hampered analyses of Boom Clay humic and fulvic acids at the Mol underground laboratory where a piezometer was rigged with the same polyamide tubing (Van Geet, 2004).

3.2. Acetone residues trapped in polyethylene porous screen

3.2.1. Analysis results

The results of the gas chromatography analyses of acetone extracted from polyethylene (PE) after drying at room temperature (RT), or at 60 °C, are summarised in Table 3 and illustrated in Fig. 3.

Table 4
Dimensions and volume of porous filter with polyethylene and acetone data.

Dimensions and parameters	Value	Unit
Filter outer radius: $R_o = ½D_o$	2.5	cm
Filter inner radius: $R_i = ½D_i$	1.5	cm
Filter height (4.5 m)	450	cm
Filter volume (5.6 L)	5655	cm^3
PE porosity: 30%	0.30	–
Pure PE volume (4.0 L)	3958	cm^3
PE density	0.93	g/cm^3
PE mass	3681	g
Acetone density	0.7908	g/ml
Acetone MW	58	g/mol
% C_{org} in acetone	62.1%	–
Volume of water in circuit	3.082	L

LDPE density: 0.92–0.93.
HDPE density: 0.95–0.96.

Table 5
Acetone quantity trapped in the polyethylene filter and then released in the water circuit.

μL Acetone per g PE	g Acetone in PE filter	Acetone in water (mg/L)	Acetone in water (mol/L)	DOC in water (mg C/L)
1.61	4.687	1521	2.62E−02	944
1.53	4.454	1445	2.49E−02	897
1.44	4.192	1360	2.35E−02	844
0.03	0.087	28	4.89E−04	18

The calculations for the concentration of acetone in water assume that all acetone was completely released by polyethylene in the water circuit.

After soaking PE with acetone and drying it at room temperature (RT), a huge amount of acetone residues were detected. Applying a higher drying temperature of 60 °C lowered this contamination to approximately 2% as compared to the first contamination (drying at RT). Hence, a higher drying temperature and extended drying time can minimise the acetone residues. Based on the data obtained for a defined amount of acetone applied on the same amount of PE, the concentrations on the soaked PE pieces can be roughly estimated to be ~1.53 μL/g PE for experiment 1 (RT) and ~0.03 μL/g PE for experiment 2 (60 °C), respectively. Noteworthy, is that the blank experiments revealed no artefact or laboratory contamination.

3.2.2. Mass balance calculations for acetone

Table 4 presents the values of the parameters needed to calculate the initial acetone inventory trapped in the porous polyethylene filter, i.e., the dimensions and the volume of the polyethylene filter along with data on polyethylene and acetone density.

The details of the mass balance calculations of the total quantity of acetone trapped in the polyethylene of the piezometer porous screen are given in Table 5 in order to determine the maximum concentration of acetone in the system that could have fuelled the microbial activity observed in the experiment.

In the case of 1.61 μL acetone/g PE about 6 mL or 4.7 g of acetone were trapped in the porous polyethylene filter. If all this acetone was released in the circuit water, it would correspond to a very high acetone concentration in water: 1.5 g acetone/L water, or 2.6×10^{-2} mol dm^{-3} of acetone, or 944 mg C/L. Such a concentration could have fuelled the microbial activity observed in the Porewater Chemistry experiment. Even, in the more favourable case, where the residual concentration of acetone in PE after drying at 60 °C was only 0.03 μL acetone/g PE, after complete release in water this would correspond to 28 mg acetone/L, or 4.9×10^{-4} mol dm^{-3} of acetone, or 18 mg C L^{-1}, i.e., a value higher than the normal background level (1.2–15.8 ± 0.5 mg C L^{-1}) of natural DOC measured in undisturbed Opalinus Clay pore water (Scholtis et al., 1999; Boisson, 2005; Courdouan et al., 2007a,b,c; Courdouan – Merz, 2008). Given these results, residual acetone trapped in the porous polyethylene screen was first considered a good candidate as an electron donor for fuelling the microbial activity observed in the Porewater Chemistry experiment. Indeed, according to Höhener (2004, 2005), the results of several works published by Platen and Schink (1987, 1989), Janssen and Schink (1995a,b), Platen et al. (1990, 1994) attest that SO_4-reducing bacteria (SRB) are able to metabolise acetone. The isotopic composition of the acetone used for washing the PE sleeve could not be determined because no acetone was left over. Nevertheless, it could be established through a literature survey (Höhener, 2005) that acetone was most probably of fossil origin and thus contained no ^{14}C, since its most probable manufacturing process was the cumene route based on petroleum hydrocarbons as precursors.

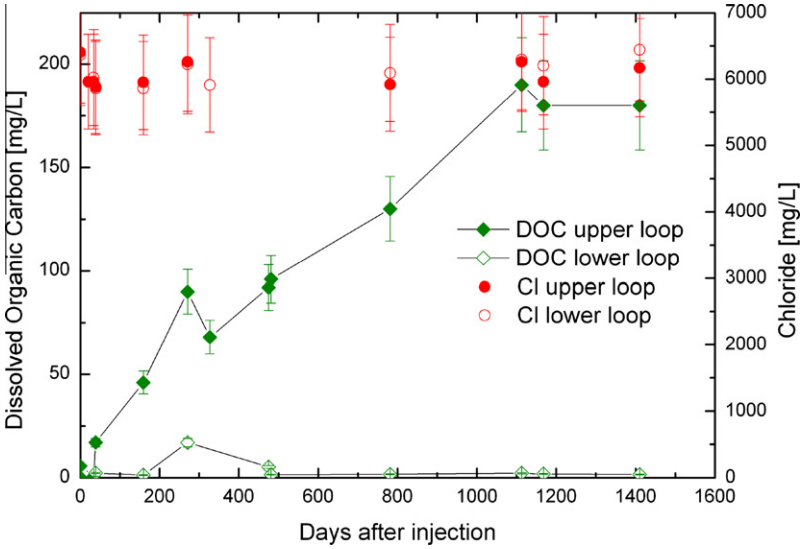

Fig. 4. Continuous leaching with time of dissolved organic carbon (DOC, mg C L^{-1}) from the pH–E_h electrodes (Xerolyt, Mettler–Toledo) observed in the upper loop of the *in situ* Diffusion and Retention (DR) experiment at the Mont Terri Rock Laboratory (Leupin, pers. comm., unpublished data). The upper water circulation loop contained pH–E_h electrodes while this was not the case of the lower loop (shown as reference curve below for DOC).

3.3. Release of OM observed in other in situ experiments

Besides the polymeric materials used for the equipment and the problem related to acetone cleaning of equipment prior to installation, it became clear that another source of C was likely to have been overlooked. Unexplained DOC anomalies developing in other *in situ* experiments suggested that on-line pH–E_h electrodes could also be incriminated as a source of organic C.

As indicated by the upper curve of Fig. 4, unexpected high and steadily increasing concentrations of DOC (mg C L^{-1}) have also been measured in the water circuit-I of the *in situ* Diffusion and Retention (DR) experiment ongoing at the Mont Terri Rock Laboratory. In contrast, the DOC concentrations measured in water from a second water circuit-II are representative of DOC levels found in water sampled from other boreholes under anaerobic conditions: they are in good agreement with the values given by Glaus et al. (2005) and Courdouan – Merz (2008) who measured DOC concentrations in Opalinus Clay pore waters and rock extracts in the range 1–20 mg C L^{-1}, or even lower: 1.2–15.8 ± 0.5 mg C L^{-1}.

The evolution of DOC measured in water circuit-I clearly reflects an anomaly: the DOC concentration progressively increases from 0 up to ~190 mg C L^{-1} within a period of about 3 years (Leupin, pers. comm., unpublished data). The last determined DOC value is more than 13 times higher than the normal value selected by Boisson (2005) for Opalinus Clay: ~14 mg C L^{-1}. Concomitantly, microbially-mediated SO_4-reduction appeared to have also taken place in this water circuit as indicated by the characteristic H_2S smell still detectable at the end of the experiment.

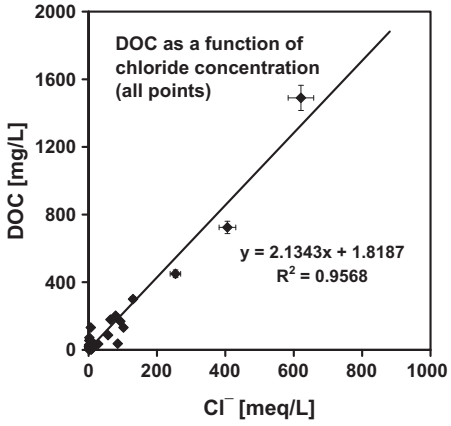

Fig. 5. Leached dissolved organic carbon (DOC, mg C L^{-1}) from the pH–E_h electrodes (Xerolyt, Mettler–Toledo) as a function of the leached chloride concentration (meq L^{-1}) observed in the *in situ* Coralus experiment at the Mol Underground Research Laboratory (Belgium) (Valcke et al., 2007).

The main difference between the two water circuits is the presence, or absence, of on-line pH and E_h electrodes. Flow-through cells equipped with electrodes were installed on circuit-I, but not on the circuit-II. Therefore, another possible source of organic matter release could arise from the E_h–pH electrodes. The electrodes used for the Porewater Chemistry and the diffusion experiments were the same (Xerolyt, Mettler–Toledo), thus a similar perturbation as in the DR experiment could be expected in the Porewater Chemistry experiment. Indeed, to withstand *in situ* hydraulic pressure, their reference compartments are fully filled with an electrolyte polymer that could also contain glycerol (propane-1,2,3-triol). A continuous increase of DOC was also observed by Valcke et al. (2007) during pH and E_h measurements with identical electrodes in the frame of the *in situ* Coralus experiment (Mol Underground Research Laboratory, Belgium). Fig. 5 illustrates the high correlation between DOC and Cl^- concentrations. Such a relationship becomes straightforward if both non-sorbed substances are simultaneously released in water from the organic gel filled KCl 3 M reference compartment of the electrodes. The low background concentration of Cl^- in Boom Clay porewater allowed this observation. The sorption of K^+ onto clay minerals makes the same correlation between DOC and K^+ more difficult to detect in experiments installed *in situ*.

3.4. Release of OM by polymer-filled pH electrodes

The results of three independent series of tests performed to characterise the organic matter released into the water by the pH electrodes are presented hereafter: DOC leaching test; GC/MS analyses of the organic constituents of the electrode gel; and ^{14}C and $\delta^{13}C$ measurements of the organic C of the gel.

3.4.1. Leaching of DOC from polymer-filled pH electrode

Fig. 6 presents the results of the leaching test made with a Xerolyt pH electrode immersed in pure water. From Fig. 6, one

clearly observes a continuous leaching of DOC, K^+ and Cl^- coupled with a progressive pH increase (6.4 → 8) with time.

The cumulative amounts (mmol) of DOC, K^+ and Cl^- leached out from the pH electrode asymptotically increase from zero at the beginning of the experiment to a pseudo plateau value of about 13–14.5 mmol as illustrated by Fig. 6.

The leaching rate (μmol/day) is highest at the beginning of the experiment, when the concentration gradient between the inner and the outer parts of the electrode is highest, and exponentially decreases with time. The leaching rate decrease is likely due to the drop of the concentration gradient (the driving force) which was not directly accessible for measurement in the experimental setup used. The leaching rate decreased from ~300 μmol/day for DOC and ~1000 μmol/day for K^+ and Cl^-, respectively, down to approximately ~50 μmol/day, or less, for all analysed species.

3.4.2. Analysis of glycerol in polymer-filled pH electrode

Non-target screening qualitative analysis revealed one major constituent within the low-molecular weight fraction of the resin filling material of the pH electrode. Glycerol was identified as a major component, associated with two substances in the trace level range (see molecular structures in Fig. 7), which exhibit structural similarity to glycerol and, therefore, can be considered as glycerol derivatives. Further compounds appearing in very low concentrations remained unidentified (Fig. 7).

The glycerol content in the pH electrode resin filling material was determined by quantitative GC/MS and LC/MS analyses performed independently and the results are summarised hereafter. As indicated by the calibration standard deviation and reproducibility, the GC/MS data were of higher analytical precision, whereas the less precise LC/MS results could only be considered of being indicative for a certain concentration level, but not as accurate values. Hence, in summary, the total amount of glycerol (mean value from three GC/MS measurements) in the polymer-gel filling material (8.087 g, dry weight) of one electrode is approximately 1.601 g or 19.8 wt.% (based on dry weight of the gel). This high concentration was confirmed by the independent LC/MS analyses.

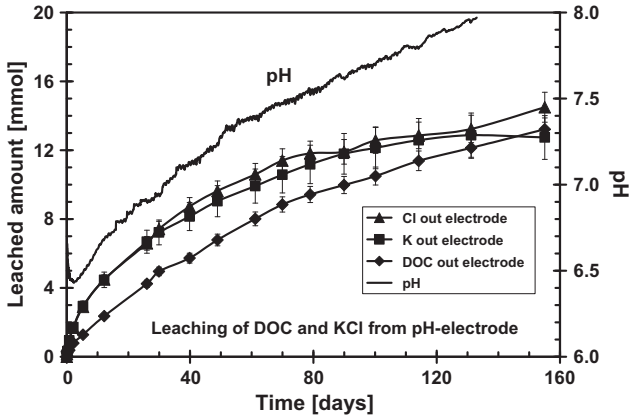

Fig. 6. Cumulated leached amounts (mmol) of dissolved organic carbon (DOC, mmol C), K^+ and Cl^- ions released from a polymer-filled pH electrode (Xerolyt, Mettler–Toledo) immersed in pure water, and concomitant pH drift observed with time.

3.4.3. Glycerol fabrication route

From the reviews of Ma and Hanna (1999) and Meher et al. (2006) it appears that the main source of glycerol (propane-1,2,3-triol, CID: 753) in the world market is the trans-esterification process of vegetable oil and animal fat used as renewable feedstock for the production of biodiesel. Trans-esterification is needed to transform easily biodegradable triglycerides in more stable methyl esters of fatty acids and glycerol is a major by-product presently available as a chemical commodity in large quantities (Zheng et al., 2008; da Silva et al., 2009). An ancient synthesis of glycerol from fossil fuel was based on the hydrolysis of epichlorohydrin (CID: 7835). The epichlorohydrin route is now abandoned because of the overwhelming worldwide production of glycerol from biofuel. Thus, a modern carbon ^{14}C-signature is quite logically expected for the glycerol contained in the pH–E_h electrodes (Pearson et al., 2011; Tournassat et al., 2011).

3.4.4. Analysis of ^{14}C and $\delta^{13}C$ of the polymer-resin filling pH electrode

According to the ^{14}C result of 100.5 ± 5.2%-modern (double standard deviation), the whole gel material is constituted of recent organic matter. However, the $\delta^{13}C$ value of −32‰ is relatively low for organic matter of biogenic production, but not uncommon. According to the most widespread production mode of glycerol today (by-product of biodiesel fabrication), a result of 100%-modern C is consistent with the presence of glycerol in the gel filling the

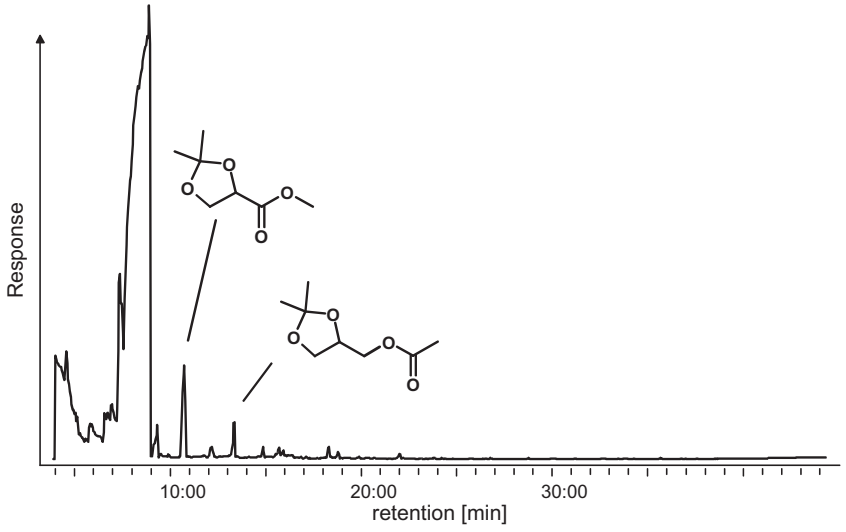

Fig. 7. GC/MS chromatogram of the extractable, low-molecular weight fraction of the resin filling pH electrode. Molecular structures of two major trace components are given as insets.

reference compartment of pH and E_h electrodes. The continuous release of glycerol by these electrodes permanently installed online for 5 a in the PC experiment can thus straightforwardly explain the high percentage of modern C measured in the water sample PC-6 (^{14}C-DOC = 101.76 ± 1.83%-modern on 15 February 2005) and in the water sampled at the end of the PC experiment when emptying the test interval just before overcoring: ^{14}C-TIC = 94.9 ± 0.9%-modern. In a similar way, the δ^{13}C value of −32‰ measured on the whole polymer gel recovered from a brand new identical electrode can also easily account for the δ^{13}C DOC = −28.14‰ measured in the last water sample PC01J02.0000 taken on 11 April 2007 at the end of PC experiment. For more details, see the supporting data given in the appendix in Wersin et al. (2011a).

3.4.5. Carbon budget of the system

The respective contributions of the various organic materials used in the PC experiment to the total C budget of the system are the following:

- The large PE screen and the PEEK cells and tubing are inert and release no detectable water-soluble organic compounds.
- The polyamide tubing (PA) and the polyurethane (PU) of the packer sleeve released detectable amounts of soluble, degradable compounds but their quantities were too low to account for the observed degradation process in the system.
- Acetone – that might have been trapped in the PE screen following cleaning – may have initially contributed to fuel the bacterial activity observed in the system, but just at the start of the experiment and only to a minor extent. Moreover, the ^{14}C modern signal measured for dissolved organic and inorganic C was not compatible with compounds synthesised from fossil C as is often the case for acetone. The maximum amount of residual acetone (∼5 g) assumed to be trapped in the PE screen was less than half of the quantity (∼11 g acetone) needed to reduce all the SO_4 lost during the PC experiment.
- Glycerol was released from the polymer-gel filling the reference compartment of pH and E_h electrodes continuously in contact for ∼5 a with the water circulating in the PC experiment. The proportion of glycerol measured in the dried gel was 19.8 wt.% of the polymer filling material, i.e., about 1.6 g of glycerol per electrode. ^{14}C-data (100% modern C) and modelling results of Tournassat et al. (2011) also support glycerol as the main C source fuelling microbial activity. The amount of glycerol necessary to reduce all the SO_4 (∼17 g glycerol) is in line with the total quantity of glycerol present in the pH and E_h electrodes used in the PC experiment over ∼5 a. Indeed, 15 Xerolyt (Mettler–Toledo) electrodes were successively put in permanent contact with the water circuit, corresponding to a total inventory of ∼24 g of glycerol available in their fresh polymer gel. This represents the maximum glycerol quantity that could have been leached in the system over the lifetime of the PC experiment if all the electrodes were fully depleted in glycerol after the leaching of the latter in the water continuously circulating in the test interval.

Therefore, glycerol is the most likely organic compound to have fuelled sulphate reduction in PC experiment. Other sources, mainly acetone residues initially trapped in the PE screen, may also have contributed to the degradation process, but only to a minor extent.

4. Main lessons learned

Synthetic polymers have been extensively used to fabricate the equipment of the Porewater Chemistry (PC) experiment. The main reason of this choice was to avoid any contact of water with metals, such as C-steel or stainless steel, which hamper the delicate measurements of redox potential (E_h) in porewater with low levels of dissolved electro-active species due to the presence of metals such as Fe, Ni and Cr (Fernandez, 2003).

In addition to its good mechanical and corrosion resistance, the main merit of stainless steel is certainly its tightness to gases: it is a total barrier against atmospheric O_2 ingress, and it also prevents loss of gases present in the porewater such as CO_2 and CH_4.

By replacing stainless steel in the system by polymers, their limitations were also discovered. On the one hand, polymers blends can release non-negligible quantities of plasticizers, such as phthalate, or NBBS. On the other hand, solvents such as acetone, or ethanol, used for cleaning or disinfecting surfaces, can easily diffuse into the polymer matrix and remain trapped in their structure, especially if the latter is porous.

To design the next generation equipment for the Porewater Chemistry experiment, the construction materials should be carefully selected to avoid the release of organic matter fuelling a reductive perturbation mediated by SO_4-reducing or methanogenic bacteria. Any significant source of dissolved organic C should be eliminated from the polymer materials, from equipment cleaning operations, and from pH electrodes.

Tubing materials should be free of plasticizers. As the presence of NBBS in Nylon strongly interferes with the analyses of dissolved natural organic matter (NOM), poly-ether-ether-ketone (PEEK) should be preferred to polyamide for tubing.

Organic solvents must be used with discernment to clean large pieces of equipment, especially of porous material and special care must be taken to avoid solvent residues remaining trapped in critical parts.

To minimise the development of micro-organisms in water, the growth of biofilms should be prevented. Adhesion of living cells onto polymer surfaces depends on interfacial tension and surface properties. In this way, the selection of polyethylene was probably not the best option, because polyethylene is known to favour biofilm formation. Polyvinylchloride (PVC), which is less prone to biofilms would have been a better choice.

5. Conclusions

The results of the leaching tests performed on three polymers (polyethylene, PE; polyurethane, PU; and polyamide, PA) selected from the plastic materials used for the fabrication of the equipment of the Porewater Chemistry (PC) experiment have shown that for a pure polymer, such as polyethylene (addition polymerisation) leaching of DOC into water is insignificant, while for condensation polymers containing plasticizers a high release of organic compounds is exhibited. Polyethylene used for the large porous filter screen is very inert. Polyurethane, used for the packer sleeve sealing the borehole head, is a very flexible elastomer. Many ingredients take part in its formulation and a dozen of them have been identified by gas chromatography–mass spectrometry (GC/MS). Isocyanate-bearing compounds, aliphatic, and aromatic, molecules with oxygenated functions (a.o., alcohol, ether, and carboxylic groups) are more readily released in water. In the experimental conditions of the leaching tests performed in this study about 13 μg of organic matter were leached/g of polyurethane. However, the polymer contributing most to the release of organic matter in solution in the leaching tests is polyamide (Nylon), which was used for the water tubing inside the surface anaerobic cabinet. This polyamide (PA) releases significant quantities of NBBS (520 μg/g PA). NBBS (CID: 19241) is a neurotoxic plasticising agent of Nylon aimed at improving the flexibility of PA tubing.

Head-space/SPME analyses have confirmed that the porous polyethylene filter used in the packed-off interval of PC

Experiment could have initially contained large amounts of residual acetone trapped in the small diameter sintered polyethylene beads. Indeed, acetone residues are effectively present at high concentration (1.61 mL acetone/kg PE) in polyethylene samples soaked in acetone and dried in conditions representative of those used to clean the porous screen of the Porewater Chemistry (PC) experiment prior to installation. If this amount of trapped acetone is rapidly and completely released into the circuit water, it could give a very high initial concentration: 1.5 g acetone/L water, i.e., 2.6×10^{-2} mol dm^{-3} of acetone, or 944 mg C/L.

Finally, the build-up of DOC in the water circuit of another *in situ* diffusion experiment equipped with the same pH–E_h electrodes, along with the results of leaching tests performed on these electrodes, and the analytical data from GC/MS and C isotopic analyses made on their gel filling, revealed the importance of glycerol contamination in the water of the Porewater Chemistry experiment. From C mass balance calculations and isotopic analyses (Pearson et al., 2011; Tournassat et al., 2011), it can be inferred that glycerol is probably the primary C source in the system.

The most likely answer to the question which C source fuelled the microbial processes in the Mont Terri PC experiment is thus that both, acetone and glycerol, contributed about equally. Acetone fuelled fossil C into the pore water, whereas glycerol contributed modern C, so that the result was a mixed C signal of 53.6% modern C. The interpretation of the stable C isotopes is less straightforward. Both, acetone and glycerol, have a strongly negative $\delta^{13}C$ in the range of −27 to −32‰ (typical range for petroleum precursors for acetone manufacturing, and measured value for glycerol). In contrast, measurements in the pore water showed that DIC reached a $\delta^{13}C$ of −15‰ at the end of the experiment. The much higher $\delta^{13}C$ can still easily be explained by the methanogenic activity in the pore water, fuelling light C isotopes into CH_4 which reached very negative $\delta^{13}C$, thus enriching the non-CH_4 carbon pool to more positive $\delta^{13}C$ values than the original source.

The implications for repository safety are developed in detail by Wersin et al. (2011b) and are similar to these recently expressed by Van Humbeeck et al. (2009). To minimise microbially-mediated processes in and around galleries of deep geological repositories, it is important to minimise the quantity of organic compounds left after construction work and to completely fill all residual voids. Indeed, if free space, water and organic C are locally present, they will fuel the development of bacteria. On the one hand bacterial activity can have beneficial effects by quickly restoring reducing conditions and immobilising redox-sensitive radionuclides, but on the other hand the metabolism by-products generated by bacterial activity could damage metallic barriers. Indeed, thiosulphate ($S_2O_3^{2-}$) and sulphide (HS^-) produced by SO_4-reducing bacteria (SRB) are aggressive species increasing the localised corrosion of steel canisters and Cu overpacks as mentioned by Stroes-Gascoyne et al. (2011).

Acknowledgements

This work is undertaken in close co-operation with the operator of the rock laboratory (BWG/Swisstopo) and the project management team (Geotechnical Institute until 2006), namely Paul Bossart and Christophe Nussbaum, and with the financial support of the Mont Terri Consortium. The fruitful discussions on organic contamination in the PC experiment with Suzanne Mettler (SolExperts), Simcha Stroes-Gascoyne (AECL), Urs Mäder (Uni Bern), Joe Pearson (GWG), Christophe Tournassat (BRGM) and Lorenz Eichinger (Hydroisotop GmbH) during the Porewater Chemistry Experiment have been highly appreciated. Thomas Fierz (SolExperts) is gratefully acknowledged for his friendly assistance during the whole experiment. We are also indebted to Louis Van Ravenstyn (SCK·CEN) for his contribution to the electrode leaching tests and to Elie Valcke (SCK·CEN) for providing porewater data from the Coralus *in situ* test made at Mol (B).

References

Arcos, D., 2003. Porewater Chemistry (PC) experiment: results of the geochemical modelling. TN 2003-18. QuantiSci/Enviros. August 03. TN2003_18.pdf. Mont Terri Project, Bern (CH) Technical Note. <http://www.mont-terri.ch/ids/default.asp?TopicID=97>.

Battaglia, F., Gaucher E., 2003. Porewater Chemistry (PC) experiment: microbial and particle characterisation in the borehole water. BRGM/RP-52226-FR. Public Document with Restricted Access. TN 2003-23. BRGM. January 04. TN2003_23.pdf. Mont Terri Project, Bern (CH) Technical Note. <http://www.mont-terri.ch/ids/default.asp?TopicID=97>.

Boisson, J., 2005. Clay Club catalogue of characteristics of argillaceous rocks. OECD/NEA Report No. 4436, 71. See Switzerland, Mont Terri, Excel file with parameter values.

Courdouan – Merz, A., 2008. Nature and reactivity of dissolved organic matter in clay formations evaluated for the storage of radioactive waste. Doctor of Sciences Dissertation ETH. Diss. ETH N 17723. Thesis available in electronic format from the ETH E-collection: (see typical DOC (mg L^{-1}) concentration in Opalinus Clay pore water in Table 3.4 on p. 71 and on rock extracts in Table B.1 on p. 109). <http://e-collection.ethbib.ethz.ch/view/eth:30819>.

Courdouan, A., Christl, I., Meylan, S., Wersin, P., Kretzschmar, R., 2007a. Isolation and characterization of dissolved organic matter from the Callovo–Oxfordian formation. Appl. Geochem. 22, 1537–1548.

Courdouan, A., Christl, I., Meylan, S., Wersin, P., Kretzschmar, R., 2007b. Characterization of dissolved organic matter in anoxic rock extracts and in situ pore water of the Opalinus Clay. Appl. Geochem. 22, 2926–2939.

Courdouan, A., Christl, I., Wersin, P., Kretzschmar, R., 2007c. Nature and reactivity of dissolved organic matter in the Opalinus Clay and Callovo-Oxfordian Formations [Oral presentation: O/05/3]. In: Proc. Clays in Natural and Engineered Barriers for Radioactive Waste Confinement – Lille 2007 – 3rd Internat. Meeting. Organised by Andra in Lille (France), 17–20 September 2007.

da Silva, G.P., Mack, M., Contiero, J., 2009. Glycerol: a promising and abundant carbon source for industrial microbiology. Biotechnol. Adv. 27, 30–39.

Daumas, S., 2004. Porewater Chemistry (PC) experiment: microbial and technical assistance and initial characterisation of the Opalinus Clay. Field report. Field campaign from 16 to 25 February 2004. Assistance microbiologique lors de l'expérimentation PC-C: Caractérisation initiale de l'argile (report written in French/English). TN 2004-21 PC-C. CFG Services. September 04 TN2004_21.pdf. Mont Terri Project, Bern (CH) Technical Note. <http://www.mont-terri.ch/ids/default.asp?TopicID=97>.

De Cannière, P., Fierz, T., 2002. Porewater Chemistry (PC) experiment: experimental setup and compilation of the test data. TN 2002-12. SCK•CEN and SolExperts. April 03. TN2002_12.pdf. Mont Terri Project, Bern (CH) Technical Note. <http://www.mont-terri.ch/ids/default.asp?TopicID=97>.

De Cannière, P., Fierz, T., 2003. Pore Water Chemistry (PC) experiment: compilation of the test data. Phase 8. TN 2003-07. SCK·CEN and Solexperts. August 03. TN2003_07.pdf. Mont Terri Project, Bern (CH) Technical Note. <http://www.mont-terri.ch/ids/default.asp?TopicID=97>.

De Cannière, P., Aoki, K., Arcos, D., Bath, A., Boisson, J.-Y., Courdouan, A., Degueldre, C., Fernández, A.M., Fierz, T., Gäbler, H-E., Gaucher, E., Gautschi, A., Griffaut, L., Hernán, P., Mäder, U., Mazurek, M., Mettler, S., Pearson, F.J., Schippers, A., Scholtis, A., Schwyn, B., Sergeant, C., Stroes-Gascoyne, S., Tournassat, C., Turrero, M.J., Vinsot, A., Waber, H.N., Wersin, P., 2008. Geochemistry and microbiology experiments. In: Bossart, P., Thury, M. (Eds.), Mont Terri Rock Laboratory – Project, Programme 1996 to 2007 and Results. Rep. Swiss Geol. Surv., vol. 3, pp. 69–86 (Chapter 6). <http://www.swisstopo.ch>.

Drouiller, Y., Vinsot, A., 2002. PC & PC-A experiments: geochemical objectives and data about the nitrogen drilling: boreholes BPC-1 and BPCA1 (report written in French). TN 2002-29. ANDRA. Sep 02. TN2002_29.pdf. Mont Terri Project, Bern (CH) Technical Note. <http://www.mont-terri.ch/ids/default.asp?TopicID=97>.

Eichinger, L., 2003. Porewater Chemistry (PC) experiment: results of chemical and isotopic measurements. Sampling period 2002 (the annex file is written in German). TN 2003-48. Hydroisotop. August 03. TN2003_48.pdf. Mont Terri Project, Bern (CH) Technical Note. <http://www.mont-terri.ch/ids/default.asp?TopicID=97>.

Eichinger, L., 2004. Porewater Chemistry (PC) experiment: results of chemical and isotopic measurements. Sampling period 2002–2003. TN 2004-78. Hydroisotop. October 04. TN2004_78_part1.pdf and TN2004_78_part2.pdf. Mont Terri Project, Bern (CH) Technical Note. <http://www.mont-terri.ch/ids/default.asp?TopicID=97>.

Fernandez, A.M., 2003. Porewater Chemistry (PC) experiment: results of the redox-measurements. TN 2003-29. Ciemat. August 03. Mont Terri Project, Bern (CH) Technical Note. <http://www.mont-terri.ch/ids/default.asp?TopicID=97>.

Gaucher, E., 2002. Porewater Chemistry (PC) experiment: measurement of partial pressure and isotopic composition of CO_2 on two core samples from the Mont Terri Rock Laboratory, borehole BPC-1. TN 2002-22. BRGM. Mar 03. TN2002_22.pdf. Mont Terri Project, Bern (CH) Technical Note. <http://www.mont-terri.ch/ids/default.asp?TopicID=97>.

Gaucher, E., 2003. Porewater Chemistry (PC) experiment: progress in modelling PC-experiment results. Diffusion and bacterial effects. Final Report. TN 2003-22. BRGM May 04. TN2003_22.pdf. Mont Terri Project, Bern (CH) Technical Note. <http://www.mont-terri.ch/ids/default.asp?TopicID=97>.

Gaucher, E., 2004a. PC-C experiment (gas and pore water equilibration): pCO_2 on core samples, CO_2 gas isotopes, calcite, dolomite & siderite isotopes. Report of experiments. TN 2004-52. BRGM. Jan 05. TN2004_52.pdf. Mont Terri Project, Bern (CH) Technical Note. <http://www.mont-terri.ch/ids/default.asp?TopicID=97>.

Gaucher, E., 2004b. Porewater Chemistry (PC) experiment: progress in modelling PC experiment results including thermodynamics, kinetics, micro-organism activity and isotopic fractionation considerations. Final Report. TN 2004-72. BRGM. February 04. TN2004_72.pdf. Mont Terri Project, Bern (CH) Technical Note. <http://www.mont-terri.ch/ids/default.asp?TopicID=97>.

Glaus, M.A., Baeyens, B., Lauber, M., Rabung, T., Van Loon, L.R., 2005. Influence of water-extractable organic matter from Opalinus Clay on the sorption and speciation of Ni(II), Eu(III) and Th(IV). Appl. Geochem. 20, 443–451.

Höhener, P., 2004. Porewater Chemistry (PC) experiment: interpretation of test data and literature survey on biodegradation of synthetic material. Final Report, June 28, 2004. TN 2004-62. BioRem + Consulting. Jul 04. TN2004_62.pdf. Mont Terri Project, Bern (CH) Technical Note. <http://www.mont-terri.ch/ids/default.asp?TopicID=97>.

Höhener, P., 2005. Porewater Chemistry (PC) experiment: interpretation of test data from July 2004 and conclusions on unknown carbon source. Final Report. TN 2005-22. BioRem + Consulting. Jan 05. TN2005_22.pdf. Mont Terri Project, Bern (CH) Technical Note. <http://www.mont-terri.ch/ids/default.asp?TopicID=97>.

Ishii, 2004. Porewater Chemistry (PC) experiment: quantification (and qualification) of microbial communities. TN 2004-76. Max Planck Institute. Mar 05. TN2004_76.pdf. Mont Terri Project, Bern (CH) Technical Note. <http://www.mont-terri.ch/ids/default.asp?TopicID=97>.

Janssen, P.H., Schink, B., 1995a. Catabolic and anabolic enzyme-activities and energetics of acetone metabolism of the sulfate-reducing bacterium *Desulfococcus biacutus*. J. Bacteriol. 177, 277–282.

Janssen, P.H., Schink, B., 1995b. Metabolic pathways and energetics of the acetone-oxidizing, sulfate-reducing bacterium, *Desulfobacterium cetonicum*. Arch. Microbiol. 163, 188–194.

Ma, F., Hanna, M., 1999. Biodiesel production: a review. Bioresour. Technol. 70, 1–16.

Mäder, U., 2002. Porewater Chemistry (PC) experiment: a new method of porewater extraction from Opalinus Clay with results for a sample from borehole BPC-A1. TN 2002-25. Uni Be. January 04. TN2002_25.pdf. Mont Terri Project, Bern (CH) Technical Note. <http://www.mont-terri.ch/ids/default.asp?TopicID=97>.

Mäder, U., 2005. Porewater Chemistry (PC) experiment: ion-specific transport properties derived from a core infiltration experiment from borehole BPCA1. TN 2004-85. Uni Bern. Mar 05. Mont Terri Project, Bern (CH) Technical Note. <http://www.mont-terri.ch/ids/default.asp?TopicID=97>.

Mäder, U., Gimmi, Th., 2007. Species-specific transport and reactive transport modelling of a long-term core infiltration experiment on Opalinus Clay. Presentation P/MTPM/47, Extended Abstracts 3rd Internat. Meeting Organised by Andra on Clays in Natural and Engineered Barriers for Radioactive Waste Confinement, September 17–20, 2007, Lille, France, pp. 515–516.

Mauclaire, L., 2005. Porewater Chemistry (PC) experiment: sampling in test interval of borehole BPC-1, sample preparation and microbial analyses. TN 2004-71. ETH. April 05. Mont Terri Project, Bern (CH) Technical Note. <http://www.mont-terri.ch/ids/default.asp?TopicID=97>.

Meher, L., Vidya Sagar, D., Naik, S., 2006. Technical aspects of biodiesel production by transesterification – a review. Renew. Sustain. Energy Rev. 10, 248–268.

Mettler, S., 2004. Porewater Chemistry (PC) experiment: raw data report March 2002–January 2004. TN 2004-77. Nagra. September 04. TN 2004_77-pdf. Mont Terri Project, Bern (CH) Technical Note. <http://www.mont-terri.ch/ids/default.asp?TopicID=97>.

Pearson, F.J, 2003. Porewater Chemistry (PC) experiment: overview and interpretation of selected results through January 2005. TN 2003-01. Pearson. March 05. TN2003_01.pdf. Mont Terri Project, Bern (CH) Technical Note. <http://www.mont-terri.ch/ids/default.asp?TopicID=97>.

Pearson, F.J., 2005. Porewater Chemistry (PC) experiment: overview and interpretation of selected results through January 2005. TN 2003-01. Pearson. March 05. TN2003_01.pdf. Mont Terri Project, Bern (CH) Technical Note. <http://www.mont-terri.ch/ids/default.asp?TopicID=97>.

Pearson, F.J., Arcos, D., Bath, A., Boisson, J.Y., Fernandez, A.M., Gäbler, H.E., Gaucher, E., Gautschi, A., Griffault, L., Hernan, P., Waber, H.N., 2003. Geochemistry of water in the Opalinus Clay Formation at the Mont Terri Rock Laboratory. Report of the Swiss Federal Office for Water and Geology, Geology Series. No. 5. ISBN 3-906723-59-3.

Pearson, F.J., Tournassat, C., Gaucher, E., 2011. Biogeochemical processes in a clay formation in-situ experiment: Part E – equilibrium controls on chemistry of pore water from the Opalinus Clay, Mont Terri Underground Laboratory, Switzerland. Appl. Geochem., 2011.

Platen, H., Schink, B., 1987. Methanogenic degradation of acetone by an enrichment culture. Arch. Microbiol. 149, 136–141.

Platen, H., Schink, B., 1989. Anaerobic degradation of acetone and higher ketones via carboxylation by newly isolated denitrifying bacteria. J. General Microbiol. 135, 883–891.

Platen, H., Temmes, A., Schink, B., 1990. Anaerobic degradation of acetone by *Desulfococcus biacutus* Spec Nov. Arch. Microbiol. 154, 355–361.

Platen, H., Janssen, P.H., Schink, B., 1994. Fermentative degradation of acetone by an enrichment culture in membrane-separated culture devices and in cell-suspensions. FEMS Microbiol. Lett. 122, 27–32.

Scholtis, A., Jones, M., Schwark, Vliex, M., 1999. Organic matter characterisation of rocks and pore waters. In: Thury, M., Bossart, P. (Eds.), Results of the Hydrogeological, Geochemical and Geotechnical Experiments Performed in the Opalinus Clay (1996–1997). Geologische Berichte – Rapports Géologiques – Geological Report No. 23 Landeshydrologie und Geologie – Service Hydrologique et Géologique National – Swiss National Hydrological and Geological Survey, Bern (Chapter 6.4).

Stroes-Gascoyne, S., Schippers, A., Schwyn, B., Poulain, S., Sergeant, C., Simonoff, M., Le Marrec, C., Altmann, S., Nagaoka, T., Mauclaire, L., McKenzie, J., Daumas, S., Vinsot, A., Beaucaire, C., Matray, J.-M., 2007. Microbial community analysis of Opalinus Clay drill core samples from the Mont Terri Underground Research Laboratory, Switzerland. Geomicrobiol. J. 24, 1–17.

Stroes-Gascoyne, S., Sergeant, C. Schippers, A., Hamon, C.J., Nèble, S., Vesvres, M.-H., Barsotti, V., Poulain, S., Le Marrec. C., 2011. Biogeochemical processes in a clay formation in-situ experiment: Part D – microbial analyses – synthesis of results. Appl. Geochem., 2011.

Tournassat, C., Alt-Epping, P., Gaucher, E.C., Gimmi, T., Leupin, O.X., Wersin, P., 2011. Biogeochemical processes in a clay formation in-situ experiment: Part F – reactive transport modelling. Appl. Geochem., 2011.

Valcke, E., Smets, S., Labat, S., Lemmens, K., Van Iseghem, P., Gysemans, M., Thomas, P., Van Bree, P., Vos, B., and Van den Berghe, S. Godon, N., Jollivet, P., Mestre, J.P., Parisot, G., Bojat, M., Boubals, J.M., Deschanels, X., Jockwer, N., Wieczoreck, K., Pozo, C., Petronin, J.C., Raynal, J., 2007. CORALUS-II. An integrated in situ corrosion test on alpha-active HLW glass – phase II. Detailed final report of SCK·CEN for the EC project CORALUS II. – Mol, Belgium: SCK·CEN. European Commission, 5th Euratom Framework Programme 1998–2002, 135 pp. Key action: Nuclear Fission – Contract FIKW-CT-2000-00011. Reporting period: 2000-October-01 to 2005-July-31. External Report of the Belgian Nuclear Research Centre; ER-27 – ISSN 1782-2335. Persistent URL: <http://hdl.handle.net/10038/475>, <http://publications.sckcen.be/dspace/bitstream/10038/475/1/er_27.pdf>. Dissolved organic carbon was also released from the on line E_h and pH electrodes. See p. 10: 2.1.2.2.2 On-line measurement of pH and redox potential – Tables A.17 and A.18, pp. 105–114. See also: <http://cordis.europa.eu/>.

Van Geet, M., 2004. Characterisation of Boom Clay organic matter: mobile and immobile fraction, 35 pp. Interim report for the period 2001–2003, June, 2004. DS 2.82: Characterisation of Boom Clay organic matter: mobile and immobile fraction. See on the Chromatogram Presented at Fig. 20 of p. 23 the Large Peak of NBBS a Plasticizer of Nylon (Polyamide) Tubings Jeopardizing the Morpheus Piezometer. SCK·CEN Report R-3884 (04/MVGe/P-37).

Van Humbeeck, H., Verstricht, J., Li, X.L., De Cannière, P., Bernier, F., Kursten, B., 2009. The OPHELIE mock-up. Final Report. EURIDICE report 09-134, January 2009. <http://www.euridice.be/>.

Vinsot, A., Fierz, T., Cailteau, C., de Donato, P., Pironon, J., Pepa, S., Wersin, P., De Cannière, P., Gäbler, H.-E., Badertscher, N., Eichinger, L., 2005. Gas equilibration and pore water sampling experiment in the Opalinus Clay at the Mont Terri rock laboratory. In: Oral presentation at the 2nd International Meeting on "Clays in Natural and Engineered Barriers for Radioactive Waste Confinement" organised by Andra (Andra 2005 International Meeting held in Tours, France, on 14–18 March 2005). Tours Conf. 2005, Abstracts.

Waber, N., 2002. Pore Water Chemistry (PC) experiment: evaluation of the diffusive exchange method for the determination of $\delta^{18}O$ and $\delta^{2}H$ in Opalinus Clay pore water from Mont Terri. TN 2002-24. Uni Be. Dec 02. TN2002_24.pdf. Mont Terri Project, Bern (CH) Technical Note. <ttp://www.mont-terri.ch/ids/default.asp?TopicID=97>.

Wersin, P., Leupin, X.O., Mettler, S., Gaucher, E., Mäder, U., Vinsot, A., De Cannière, P., Gäbler, H. E., Kunimaro, T., Kiho, K., 2011a. Biogeochemical processes in a clay formation in-situ experiment: Part A – overview, experimental design and water data. Appl. Geochem., 2011.

Wersin, P., Stroes-Gascoyne, S., Pearson, F.J., Tournassat, C., Leupin, O.X., Schwyn, B., 2011b. Biogeochemical Processes in a clay formation in-situ experiment: Part G – key interpretations and conclusions. Implications for repository safety. Appl. Geochem., 2011.

Zheng, Y., Chen, X., Shen, Y., 2008. Commodity chemicals derived from glycerol, an important biorefinery feedstock. Chem. Rev. 108, 5253–5277.

Applied Geochemistry 26 (2011) 980–989

Contents lists available at ScienceDirect

Applied Geochemistry

journal homepage: www.elsevier.com/locate/apgeochem

Biogeochemical processes in a clay formation *in situ* experiment: Part D – Microbial analyses – Synthesis of results

S. Stroes-Gascoyne [a,*], C. Sergeant [b], A. Schippers [c], C.J. Hamon [a], S. Nèble [b,d], M.-H. Vesvres [b], V. Barsotti [b], S. Poulain [b,e], C. Le Marrec [f]

[a] *Atomic Energy of Canada Limited (AECL), Whiteshell Laboratories, Pinawa, Manitoba, Canada R0E 1L0*
[b] *University Bordeaux/CNRS UMR 5084, Laboratoire de Chimie Nucléaire Analytique et Bioenvironnementale (CNAB) –19 Chemin du Solarium, B.P.120 – F-33175 Gradignan cedex, France*
[c] *Bundesanstalt für Geowissenschaften und Rohstoffe (BGR), Geomicrobiology, Hannover, Germany*
[d] *Helmholtz Zentrum München, Institute of Groundwater Ecology, Neuherberg, Germany*
[e] *Department of Microbiology & Immunology, Stanford University School of Medicine, 299 Campus Drive, West – Fairchild D317, Stanford, CA 94305-5124, USA*
[f] *Institut Polytechnique de Bordeaux/INRA UMR 1219, Institut de la Vigne et du Vin, 210 Chemin de Leysotte – F-33882 Villenave d'Ornon, France*

ARTICLE INFO

Article history:
Available online 17 March 2011

ABSTRACT

The purpose of the Porewater Chemistry (PC) experiment at the Mont Terri (MT) Underground Rock Laboratory (URL) was to measure geochemical parameters, such as pH, Eh and pCO_2, in the porewater of the Opalinus Clay formation. Although the PC experiment was designed and implemented carefully from a geochemical perspective, conditions were not sterile and some microbial and nutrient contamination likely occurred. Microbial activity in the added synthetic porewater in the borehole was apparent shortly after initiation of the experiment and affected the geochemical parameters observed in the porewater. This paper summarizes the results from microbial analyses of post-termination PC water and overcore clay samples, conducted to attempt to elucidate the role of microbial activity in the evolution of the geochemical conditions in the PC experiment. Microbial analyses of the PC borehole water, and of clay overcore samples from around the borehole, were carried out at three laboratories and included both molecular biology and culturing methods.

Results indicated the presence of heterotrophic aerobic and anaerobic organisms that resulted likely from the initial, non-sterile conditions, sustained by suspected contamination with organic matter (glycerol, acetone). The results also indicated the presence of NO_3-reducers, Fe-reducers, SO_4-reducers and methanogens (i.e., *Bacteria* as well as *Archaea*), suggesting a reducing environment with Fe(III)- and SO_4 reduction, and methanogenesis occurring in the PC water and adjacent clay. A black precipitate containing pyrite (identified by XRD and SEM) and a strong H_2S smell in the porewater confirmed the occurrence of SO_4 reduction. Microorganisms identified in the porewater included *Pseudomonas stutzeri*, *Bacillus licheniformis*, *Desulfosporosinus* spp. and *Hyphomonas* spp. Species identified in enrichment cultures from the overcore samples included *Pseudomonas stutzeri*, three species of *Trichococcus* spp., *Caldanaerocella colombiensis*, *Geosporobacter subterrenus* and *Desulfosporosinus lacus*. Overall the results indicated a thriving microbial community in the PC water and adjacent clay in contrast to "undisturbed" Opalinus Clay for which limited evidence for a small viable microbial community has been given in a previous study.

1. Introduction

Opalinus Clay is a candidate host rock for a deep geological repository (DGR) for high-level radioactive waste (HLW) in Switzerland. Microbial activity in a HLW repository is of concern for a number of reasons (e.g., Stroes-Gascoyne and West, 1996; Pedersen, 2000). Such activity may result in microbially influenced corrosion (MIC) which could affect the longevity of the containers holding the waste, through the formation of corrosion-inducing aggressive environments under biofilms or through the production of corrosive metabolites. In addition, mobile microbes may sorb radionuclides released from breached containers and act as colloids, potentially increasing the migration of radionuclides. Microbial gas production is also of potential concern because a build-up of a gas phase in a repository could possibly reduce the effectiveness of the multi-barrier containment system (Stroes-Gascoyne and West, 1996).

Studies have been carried out on Opalinus Clay drill cores to investigate the occurrence of indigenous microbes and their

* Corresponding author. Tel.: +1 204 753 2311; fax: +1 204 753 2690.
E-mail address: stroesgs@aecl.ca (S. Stroes-Gascoyne).

0883-2927/$ - see front matter Crown Copyright © 2011 Published by Elsevier Ltd. All rights reserved.
doi:10.1016/j.apgeochem.2011.03.007

community size and structure in "undisturbed" Opalinus Clay (Mauclaire et al., 2007; Stroes-Gascoyne et al., 2005, 2007, 2008; Poulain et al., 2008). The cores were drilled with aseptic techniques in the Mont Terri (MT) Underground Rock Laboratory (URL), Switzerland. The results provided limited evidence that a small viable microbial community is present in Opalinus Clay. This evidence included five positive culture results (including for SO_4-reducing bacteria, SRB) out of 20 culture attempts; extraction of phospholipid fatty acids (PLFA) corresponding to $\sim 10^5$ to 10^6 viable cells/g dry weight; detection of PLFA biomarkers for anaerobic Gram-negative bacteria and SRB; and the presence of sufficient nutrients to support growth of indigenous and non-indigenous microorganisms for two months. Concurrently, these studies also provided evidence against the presence of a large thriving, active microbial community in Opalinus Clay, including 15 negative culture results out of 20 attempts; lack of visible or active cells by application of microscope techniques (phase contrast, acridine orange (AO) staining; catalyzed reported deposition – fluorescence *in situ* hybridization (CARD-FISH)); consistent failure to extract polymerase chain reaction (PCR)-amplifiable DNA from the core; the presence of 14 times higher amounts of lipids indicative of cell debris than those indicative of viable cells (i.e., PFLA); very small pore sizes; and very low water content in the core.

The microbial characterization of Opalinus Clay suggests, therefore, that unperturbed Opalinus Clay contains only a small viable microbial community, which is probably metabolically (almost) inactive (dormant), due to space and water restrictions. However, it was also concluded from these studies that any disturbances that would provide space, water and nutrients, as could be the case during repository excavation and construction, could revive the dormant organisms, especially in the disturbed parts of the host rock.

This paper reports the results of the microbial analyses carried out on water and clay samples from the Porewater Chemistry (PC) experiment. Wersin et al. (2011-a) give a detailed description of the PC experiment. Briefly, the objective of the PC experiment conducted at the MT URL was to measure *in situ* a number of non-conserved important physical–chemical parameters, such as pH, E_h and pCO_2, within the porewater of the Opalinus Clay formation. It became apparent quickly after the start of the PC experiment that microbial activity was affecting the borehole water geochemistry. Therefore, samples were analyzed for microbial characteristics on several occasions during 2003–2006 (Table 3 in Wersin et al., 2011-a), to attempt to establish the role of microbial activity in the evolution of the geochemical conditions in the PC experiment. Results have been recorded by Battaglia and Gaucher (2003), Ishii (2004), Schippers (2006) and Mauclaire and McKenzie (2006). Table 1 gives a summary of the results for total cell counts (microscopic counts after staining) and the percentage of active cells (FISH or CARD-FISH) during the period 2003 to 2006. Total cell counts varied from 6×10^3 to 2×10^6 cells/mL over time. The percentage of active cells varied from 8% to 73%. Active *Bacteria* and *Archaea* including SRB and methanogens were detected, giving evidence for a substantial amount of organic substances in the PC water supporting the growth of heterotrophic prokaryotes.

Table 1
Summary of microbial cell counts and activity in PC porewater (2003–2006).

Sample date	DAPI (cells/mL)	FISH/CARD-FISH (% active cells)	Source of data
May 2006	1×10^4–3×10^5	0–22	Mauclaire and McKenzie (2006) and Schippers (2006)
November 2005	2×10^5	44	Mauclaire and McKenzie (2006)
February 2005	6×10^3	73	Mauclaire and McKenzie (2006)
July 2004	$3.5 (\pm 0.7) \times 10^5$	41	Ishii (2004)
2003	2×10^6	Not analyzed	Battaglia and Gaucher (2003)

DAPI: 4′,6-diamidino-2-phenylindole.
FISH: fluorescence *in situ* hybridisation.
CARD-FISH: CAtalyzed Reporter Deposition – fluorescence *in situ* hybridisation.

The objective of the current further analysis of both porewater and overcore clay samples taken at the termination of the PC experiment was to comprehensively determine and characterize the influence of microbial metabolism on the geochemistry of the PC experiment.

2. Materials and methods

2.1. The porewater chemistry experiment

The borehole in which the PC experiment was located was drilled with N_2, to minimize pyrite and clay mineral oxidation, but microbiological conditions were not perfectly aseptic. Likewise, the down-hole equipment placed in the borehole was chemically clean but not sterile.

The borehole was filled immediately after drilling with synthetic (but not sterilized) "Pearson" porewater with a chemical composition close to that expected at the borehole location ("main fault" zone) (Pearson et al. 2003). The water was labelled with ^2H and Br^- and circulated in the borehole for about 5 a, while equilibrating through diffusion with the porewater in the surrounding host rock. The experimental set-up was free of any metallic components to avoid artefacts on redox measurements (Wersin et al., 2011-a). The borehole interval was 4.69 m long, located between 5.41 m and the bottom of the borehole (10.10 m) and was lined with a stack of cylindrical sintered (low pressure) polyethylene filter screens (with a mesh width of 40 μm, a porosity of 30%, an inner diameter of 30 mm and an outer diameter of 50 mm). These screens allowed for a free exchange between the synthetic water filling the borehole interval and the Opalinus Clay formation porewater. Microbes would be able to freely move through such screens. The filter screens were cleaned with acetone before emplacement to remove grease residue. Although the screens were rinsed subsequently with distilled water and dried with N_2 gas prior to installation in the borehole, it is possible that some acetone residue remained in the pores of these screens and was, therefore, introduced into the PC experiment (De Cannière et al., 2011).

The test interval was equipped with three lines, one with the inlet at the bottom and two with their ports at the top of the interval. All lines consisted of PEEK 1/8″ tubes (outer diameter 3.175 mm, inner diameter 2.05 mm). Two lines (the bottom line and one of the top lines) were part of the closed circulation circuit. The second top line was used for interval pressure monitoring. The PC water was sampled at regular intervals for chemical (and microbial) analyses over the duration of the experiment (5 a). The interval fluid was pumped in closed circuit and the pH and E_h electrodes were installed on-line at the surface in a system where they were easily accessible for calibration and maintenance. The use of flow-through cells containing the electrodes, placed in a cabinet at the surface, which was flushed continuously with pure Ar, allowed the continuous monitoring of these parameters in the absence of air (Wersin et al., this issue-a). However, the gel-filled electrodes in this experiment are thought to have leaked glycerol into the PC system, creating the anaerobic microbial disturbance observed (De Cannière et al., 2011).

2.2. Sampling and sample distribution

At the termination of the PC experiment (11 April 2007), all of the porewater was retrieved for various analyses, using metal flow-through vials (sterilized for microbial samples), to maintain *in situ* (anoxic) conditions in the water. A black precipitate was observed in the PEEK tubing. Several of these sterilized metal vials containing borehole water, and a precipitate sample, were shipped by courier to the following three laboratories: BGR: The Federal Institute for Geosciences and Natural Resources in Hannover, Germany (Geomicrobiology unit); CNAB: University Bordeaux/CNRS UMR 5084, Laboratoire de Chimie Nucléaire Analytique et Bioenvironmentale, Gradignan, France, and AECL: Atomic Energy of Canada Limited, Whiteshell Laboratories, Pinawa, Manitoba, Canada.

After removal of all water, careful overcoring of the PC borehole was carried out, using procedures designed to minimize or avoid disturbance of the Opalinus Clay surrounding the borehole, as described by Koroleva et al. (2011). Samples of undisturbed overcore (10 cm segments) most suitable for microbial analyses (BPC-OC) were retrieved from the bottom part (9.0–10.5 m) of the borehole and shipped to the three laboratories, partly frozen with dry ice, partly kept cool with blue ice packages.

Table 2 summarizes the various PC water and overcore samples shipped to, and analyzed by, the three laboratories. BGR sub-sampled the clay inside the filter screen (which likely consisted of clay from directly outside the filter screen from higher up in the overcore that fell into the borehole), directly outside the filter screen, and in the much drier part of BPC-OC1 (9:30–9:40 m). CNAB subsampled BPC-OC2 (7:00–7:10 m) and BPC-0C3 (9:20–9:30 m) directly adjacent (i.e., 0–2 cm) to the outside of the filter screen. AECL took sub-samples from directly adjacent to the outside of the filter screen (i.e., 0–2 cm) and in the outer much drier part of BPC-OC5 (9:10–9:20 m). AECL also sent a water sample (PC01J01.0020–0023; Table 2) and a large subsample from BPC-05 (100 g, taken from the clay adjacent the filter screen, 0 to ~5 cm) to Microbial Insights (MI), Rockport, Tennessee, USA, for analysis. Detailed subsample locations (for the core samples) are given elsewhere (Stroes-Gascoyne et al., 2008). Immediately upon arrival at the different laboratories, the PC water and solid core samples were sub-sampled for different analyses. Samples were fixed in formaldehyde for total cell counting and CARD-FISH or kept frozen until DNA extraction for molecular biological analysis. For culturing, the samples were diluted and the different media were inoculated immediately.

Table 2
Samples distributed to the three laboratories BGR, CNAB and AECL.

Sample number	Type of sample	Observations/comments
BGR		
PC01J01.0019	Water sample (40 mL)	Black, H_2S
BPC-0C1	Overcore 9:30–9:40 m, $I_{(1)}$, $I_{(2)}$, O	Screen in place
CNAB		
PC01J01.0017	Water sample (40 mL)	Uncolored, black precipitate
BPC-0C2	Overcore 7:00–7:10 m	Partial screen in place
BPC-0C3	Overcore 9:20–9:30 m, $I_{(2)}$	Screen in place
AECL (and MI)		
PC01J01.0018	Water sample (40 mL)	Black, strong smell of H_2S
PC01J01.0020–0023[a]	Four water samples (combined)	Black, strong smell of H_2S
PC01S01.0002	PEEK tubing (20 cm)	Black precipitate
BPC-0C5	Overcore (9:10–9:20 m), $I_{(3)}$, O	Screen in place

$I_{(1)}$ = Inside filter screen; $I_{(2)}$ = Mud + clay, 0–2 cm outside filter screen; $I_{(3)}$ = Filter screen outside scrapings + 2 cm outside filter screen; O = "reference" (dry) clay.
[a] Water samples combined (12 + 72 + 114 + 107 mL).

2.3. Total cell numbers and CARD-FISH

At BGR, 20 mL of the PC water sample were fixed in 4% formaldehyde in phosphate buffered saline (PBS-buffer, i.e., 0.01 M NaCl buffered to pH 7.6 with 9 mM Na_2HPO_4 and 1 mM $NaH_2PO_4{\cdot}H_2O$) as previously described (Pernthaler et al., 2001) for total cell count and CARD-FISH analysis.

Total cell number determination was carried out by depositing cells on filters (Weinbauer et al., 1998), staining with the bright fluorescent dye SYBR Green II and counting using a fluorescence microscope. Living Bacteria (probes EUB338 I-III) and Archaea (probe ARCH915) were quantified by CARD-FISH on filters as previously described (Pernthaler et al., 2002; Schippers et al., 2005). Hybridized cells were stained with the fluorescent dye CY3 and all cells were counterstained with DAPI (4′,6-diamidino-2-phenylindole). The detection limit for the microscopic methods was 10^5 cells/mL.

2.4. Cultivation methods

2.4.1. Liquid media

To check for qualitative enrichment of microorganisms, six liquid media were prepared at CNAB according to the recommendations of the Deutsche Sammlung von Mikroorganismen und Zellkulturen (DSMZ) (http://www.dsmz.de/): Aerobic Medium 1 (AEM1) for aerobic organotrophic microorganisms; Anaerobic Medium 1 (ANM1) for anaerobic organotrophic microorganisms; Anaerobic Medium 2 (ANM2) for anaerobic organotrophic microorganisms that reduce inorganic electron acceptors; Anaerobic Medium 3 (ANM3) for anaerobic lithotrophic microorganisms that reduce inorganic electron acceptors; Anaerobic Medium 4 (ANM4) for methanogenic archaea; and Anaerobic Medium 5 (ANM5) for SO_4-reducing bacteria (SRB). AQDS, which was added to media ANM2 and ANM3, is a humic acid analog that turns color from yellow to orange when reduced by microorganisms (Lovley et al., 1996).

Initial solid sample suspensions were prepared for every medium. A 1 cm^3 clay sample was crushed under N_2 in a mortar and pestle. The resulting powder was suspended in 10 mL of each medium devoid of substrate. Anaerobic initial suspensions were prepared in a glove box while aerobic ones were prepared under laminar flow. One mL of every solid sample suspension was used to inoculate 10 mL of each enrichment medium, except for ANM5 (0.5 mL of initial suspension in 5 mL of media). Three incubation temperatures were tested for every culture: 30, 60 and 80 °C. Enrichment assays in ANM5 medium were also incubated at 12 °C.

At AECL, various physiological groups of microorganisms were enumerated using different media by the most probable number (MPN) method (Stroes-Gascoyne et al., 2008). Suspensions of the solid samples (10 g in 100 mL of PBS-buffer) were stirred or shaken for 30 min, followed by serial diluting to 10^{-4} in PBS. The dilutions were used for the inoculation of different media. Sulfate-reducing bacteria were enumerated in degassed modified Postgate's B medium (Atlas, 1993). Tubes were incubated at room temperature and scored after 4 weeks. Nitrate-utilizing bacteria (NUB, that convert NO_3^- to NO_2^-) and NO_3-reducing bacteria (NRB, that convert NO_3^- to N_2) were enriched in R2A medium, amended with 0.1% NO_3^-, and scored for N_2 gas production (in inverted Durham tubes) or the presence of NO_2^- after 4 weeks of incubation at 30 °C. Iron-reducing bacteria (IRB) were enumerated using the method of Gould et al. (2003). Tubes were incubated at 30 °C and scored after 4 weeks.

2.4.2. Solid media (agar plates)

At AECL, BGR and CNAB, R2A-agar plates (Reasoner and Geldreich, 1985) and media AEM1, ANM1 and ANM5 supplemented with agar, 1.5% Bacto-agar (Eurobio, France) were inoculated to enumerate cultivable microorganisms. In addition, Pearson R2A medium, consisting of regular R2A medium but prepared with Pearson water (which closely resembles the *in situ* porewater composition in Opalinus Clay, Mauclaire et al., 2007; Stroes-Gascoyne et al., 2008) was inoculated. Serial dilutions to 10^{-4} from water and solid samples were prepared for inoculation, using PBS-buffer or 0.9% NaCl solution. The agar plates were incubated at 12 °C and 30 °C for up to 4 weeks under aerobic and anaerobic conditions (glove box) and colonies were counted subsequently. Different colonies (according to macroscopic observations) from selected initial agar plate cultures were isolated until a pure culture of each colony was obtained, before DNA was extracted for phylogenetic analysis (at CNAB). Non-diluted and diluted PC water sub-samples were also plated on Petri dishes and covered with agar AEM1 media at 50 °C and isolated bacteria were then cultivated in liquid AEM1 media.

2.5. Molecular biology methods

2.5.1. PFLA-analysis

The lipid extraction procedure as employed by MI was a modified Bligh and Dyer method (White et al., 1979) and involved extraction of PLFA in organic solvents, followed by analysis using capillary gas chromatography and mass spectrometry (Stroes-Gascoyne et al., 2008).

2.5.2. Phylogenetic analysis of microorganisms

The FastDNA Spin Kit for Soil (MP Biomedicals) with slight modifications (at CNAB) or a bead-beating method (Stephen et al., 1999; at MI) were used to extract DNA from liquid enrichment and agar plate pure cultures (at CNAB) or the whole PC water sample (at MI) (Poulain et al., 2008; Stroes-Gascoyne et al., 2007, 2008). PCR reactions were performed into 25 μL final volumes with universal primers for the bacterial 16S rRNA gene (Bact8F3, Univ1492A and Bact907r; Weisburg et al., 1991; Muyzer et al. 1996; at CNAB). At MI, PCR amplification of 16S rRNA gene fragments was performed as described in Muyzer et al. (1993), with some modifications (Stroes-Gascoyne et al., 2008). Two primer sets were used in a nested PCR approach, *E. coli* bp positions 27 and 1492 and *E. coli* positions 341–534 of the 16S rRNA gene. Negative controls for external contaminations were included at each step of every series of experiments. DNA from a known bacterial strain was used as a positive control for PCR amplification. The PCR products were separated using Denaturing Gradient Gel Electrophoresis (DGGE). Sequencing assays were performed directly on PCR products by Genome Express. DGGE bands were excised, purified, and the 16S rRNA genes were amplified and sequenced (Stroes-Gascoyne et al., 2008). BLASTn software was used to compare our sequences to known sequences in the NCBI database (http://www.ncbi.nlm.nih.gov/BLAST; Altschul et al., 1997).

2.5.3. Quantitative, real-time PCR

At BGR, high-molecular-weight DNA was extracted from the solid samples (which were first pounded in a mortar and pestle), following a modified FastDNA Spin Kit for Soil protocol (Webster et al., 2003) for quantitative, real-time PCR (Q-PCR) analysis. *Bacteria* and *Archaea* were quantified via their 16S rDNA gene (Nadkarni et al., 2002; Takai and Horikoshi, 2000). To convert 16S rDNA gene copy numbers to cell numbers conversion factors of 4.1 for *Bacteria* and 1.5 for *Archaea* were used (Kock and Schippers, 2008). Sulfate-reducing bacteria were quantified by targeting their functional gene dissimilatory sulfite reductase (*dsrA*; Schippers and Neretin, 2006), and methanogenic *Archaea* were quantified by targeting their functional gene methyl coenzyme M reductase (*mcrA*; Wilms et al., 2007).

2.6. Physical parameters

At AECL, water activity (i.e., the partial pressure of water vapor in equilibrium with the sample) was measured on a sub-sample of clay using a Decagon™ WP4 Dewpoint PotentiaMeter (Decagon Devices, Pullman, WA) and water content was determined by drying the water activity sub-sample at 110 °C to constant weight.

The black precipitate in the PEEK tubing sample (Table 2) was removed with sterile plastic pipette tips and examined by X-ray diffraction. Data were collected using a Rigaku RU-300 diffraction system equipped with a thin-film diffractometer and a pole-figure goniometer. Conventional $\theta/2\theta$ scans were collected (at AECL).

3. Results

Table 3 summarizes all results of the microbial analyses except the phylogenetic data which are presented in (Tables 4a and 4b).

3.1. PC water samples

For the water samples total cell counts based on cell staining and counting with two different dyes ranged from 2×10^8 (DAPI) to 7×10^8 (SYBR Green) cells/mL, with the active bacterial population (CARD-FISH) an order of magnitude lower (6×10^7 bacteria/mL). The active Archaeal population (CARD-FISH) was again an order of magnitude lower (3×10^6 cells/mL). Numbers of viable (live) cells based on PLFA analysis (2.4×10^7 cells/mL) were similar to the active bacterial population found. These results suggest that of the total cells visible in the water sample, between 10% and 30% were viable and active. Table 1 suggests that in the 2006 water samples, between 8% and 22% of the total cells were active and that over the period 2003–2006 active cell percentages ranged from as little as 0% to as much as 73%. The fact that total cell numbers in PC water at termination were two to three orders of magnitude higher than during the experiment could suggest that upon removal of all the water, biofilm material was dislodged and contributed to the overall cell count. The PLFA profile (data not shown) suggested the presence of a diverse population in the PC water sample, including large percentages of *Firmicutes* and *Proteobacteria* and smaller percentages of SRB and anaerobic metal reducers (Stroes-Gascoyne et al., 2008; Wersin et al., 2011-b).

Culture results for the water samples (Table 3) for heterotrophic aerobes (on regular R2A medium) ranged from 1×10^6 to 7×10^6 CFU/mL. Numbers of heterotrophic aerobes on more saline Pearson solution-based R2A medium were an order of magnitude lower (about 3×10^5 CFU/mL) than on regular R2A medium. Heterotrophic anaerobes (on R2A medium) were 2–3×10^5 CFU/mL on regular R2A and 8–9×10^5 CFU/mL on Pearson R2A, suggesting that the heterotrophic anaerobes present in the PC water possibly preferred a higher salinity. The MPN culture results for SRB ranged from 2–8×10^3 cells/mL, while IRB ranged from 5×10^2 to $>10^4$ cells/mL. NUB were $>10^5$ MPN/mL and NRB ranged from 5×10^2 to $>10^4$ cells/mL. Qualitative positive culture results for the water sample were found for heterotrophic aerobes (in AEM1), heterotrophic anaerobes (in ANM1) and SRB (in ANM5), especially at 30 and 80 °C.

DNA was extracted from 27 colonies obtained on agar plates from the water sample, followed by 16S rRNA gene PCR amplification and sequencing at CNAB (Stroes-Gascoyne et al., 2008). Of the 14 positive identification results, 12 indicated the presence of *Pseudomonas stutzeri* (100%; GenBank accession number EF530571) and

Table 3
Results from the microbial analyses of the PC water and PC overcore clay samples.

Analysis	Results				
	Water	$I_{(1)}$	$I_{(2)}$	$I_{(3)}$	O
Direct cell counting (visualized cells/mL)					
DAPI (total cells)	2×10^8				
SYBR Green (total cells)	7×10^8				
CARD-FISH Bacteria (active cells)	6×10^7				
CARD-FISH Archaea (active cells)	3×10^6				
Enrichment cultures agar plates or MPN (CFU or cells/mL or g) or qualitative (positive/total (Temp °C))					
Aerobic Heterotrophs	$1–7 \times 10^6$ $2–3 \times 10^5$*		5/6(30);1/6(60);0/6(80)	$1–3 \times 10^6$	3×10^2
Anaerobic Heterotrophs	$2–3 \times 10^5$ $8–9 \times 10^5$*		3/6(30);0/6(60);0/6(80)	$0.05–1 \times 10^7$	1×10^2
Anaerobic Heterotrophs (inorg. EA)			6/6(30);0/6(60);3/6(80)		
Sulfate-reducing Bacteria	$2–8 \times 10^3$		5/6(30);0/6(60);6/6(80)	$>2 \times 10^3$	1×10^1
Nitrate-utilizing Bacteria	$>1 \times 10^5$			$>2 \times 10^5$	3×10^3
Nitrate-reducing Bacteria	$>2 \times 10^4$ to $>1 \times 10^5$			$1–>2 \times 10^5$	$<4 \times 10^0$
Iron-reducing Bacteria	5×10^2 to $>1 \times 10^4$			$0–>2 \times 10^3$	1×10^1
Anaerobic Lithotrophs (inorg. EA)			6/6(30);3/6(60);6/6(80)		
Methanogens			6/6(30);2/6(60);6/6(80)		
Molecular biology methods					
PLFA (cells/mL or g)	2×10^7			2×10^5	1×10^5
Q-PCR Bacteria (cells/g)		5×10^6	ND		ND
Q-PCR Archaea (cells/g)		1×10^5	ND		ND
Q-PCR SRB (cells/g)		ND	ND		ND
Q-PCR Methanogens (cells/g)		<100	ND		ND
DNA extr./PCR/DGGE/sequencing	See Table 4a		See Table 4b		
Physical parameters					
Water content (%)				25.7–11.0	8.6
Water activity (a_w)				0.990–0.986	0.962
X-ray diffraction (XRD)	Pyrite precipitate in PEEK tubing			(traces of pyrite)	(traces of pyrite)

$I_{(1)}$ = Inside filter screen; $I_{(2)}$ = Mud + clay, 0–2 cm outside filter screen; $I_{(3)}$ = Filter screen outside scrapings + 2 cm outside filter screen; O = "reference" (dry) clay.
DAPI = 4′, 6-diamidino-2-phenylindole; CARD-FISH = Catalyzed reporter deposition – fluorescence *in situ* hybridisation; MPN = Most probable number; CFU = Colony-forming units; inorg. EA = Inorganic electron acceptor; PLFA = Phospholipid fatty acids; (Q)-PCR = (Quantitative) polymerase chain reaction; DGGE = Denaturing gradient gel electrophoresis; ND = Not detected.
* On "Pearson"-based R2A medium; 5/6 (30) = 5 positive results out of 6 (at 30 °C).

Table 4a
Identification of microorganisms in the PC water sample and from enriched colonies based on 16S rRNA gene sequencing.

Sample	Identification (% Identity; GenBank accession number)
PC water sample	*Desulfosporosinus* spp. (100%; AY007667) *Hyphomonas* spp. (100%; AJ557850) *Pelotomaculum* (86.5%; AB154390) *Clostridia* (89.7%; EF063613)
Colonies on 1.5% Bacto-agar	*Bacillus licheniformis* (99%; AB305267) *Pseudomonas stutzeri* (100%; EF530571)

two the presence of *Bacillus licheniformis* (99–100%; AB305267) (Table 4a). DNA extraction followed by PCR, DGGE and 16S rRNA gene sequencing on the whole PC water sample indicated the presence of *Desulfosporosinus* spp. (100%; a Gram-positive spore-forming SRB; AY007667) and *Hyphomonas* (100%; a Gram-negative aerobic non-spore-forming alphaproteobacterial species that divides by asymmetric budding; AJ557850), as well as two sequences related (with much lower homologies) to *Pelotomaculum* (86.5%; AB154390) and *Clostridia* (89.7%; EF063613) (Table 4a).

X-ray Diffraction (XRD) on the black precipitate in the PEEK tubing (Table 3) indicated the presence of pyrite. This precipitate contained abundant very distinct gold flecks (visible by naked eye) and scored positive for SRB (data not shown, Stroes-Gascoyne et al., 2008). The black precipitates were also analyzed by scanning electron microscopy (SEM) and both FeS and FeS_2 were observed (Koroleva et al., 2011).

3.2. PC core section samples

Table 3 also summarizes the microbial results for the PC overcore clay samples (including results for water content, water activity and XRD). The phylogenetic data for the overcore clay samples are summarized in Table 4b. Note that results for sub-samples denoted $I_{(1)}$ in Table 3 refer to clay taken from inside the filter screen and $I_{(2)}$ or $I_{(3)}$ refer to clay sub-samples taken from directly outside ($\leqslant$2 cm) the filter screen. Results for sub-samples denoted O refer to clay sub-samples taken further away (>10 cm) from the filter screen, in the much drier part of the overcore samples.

The quantitative culture results (agar plates and MPN) show considerable cultivable populations in the (wet) clay samples taken from outside but near the filter screen (0–2 cm), in contrast to much lower culturable populations in the drier part of the overcore. Heterotrophic aerobic populations ranged from $1–3 \times 10^6$ CFU/g in the wet clay, in contrast to about 3×10^2 CFU/g in the drier clay. Similarly, anaerobic heterotrophs ranged from 5×10^5 to 1×10^7 CFU/g in the wet clay, in contrast to 1×10^2 CFU/g in the drier clay and much larger SRB, NUB, NRB and IRB populations were found in the wet clay samples compared to the drier sample.

The qualitative enrichment culture results obtained for wet clay sub-samples taken from near the outside of the filter screen were largely positive at 30 °C with 31 out of 36 cultures showing growth, suggesting a diverse and active microbial population in the wet clay. The enrichment cultures at 60 °C were mostly negative, with only 6 out of 36 cultures showing growth, suggesting the presence of few (moderately) thermophilic organisms. However, the enrichment cultures at 80 °C were surprisingly positive with 21 out of 36

Table 4b
Identification of microorganisms in enrichment cultures from PC overcore samples based on 16S rRNA gene sequencing.

Medium	Identification (% Identity; GenBank accession number)
Heterotrophic Aerobes (AEM1), liquid	*Pseudomonas* spp.(100%; EF530571)
Heterotrophic Anaerobes (ANM1), liquid	*Trichococcus collinsii* (100%; EF111215) *Nostocoida limicola* I (100%; AF255736) *Trichococcus flocculiformis* (100% ; AJ306611) *Trichococcus pasteurii* (100%; X87150)
Heterotrophic Anaerobes (ANM2), liquid	*Caldanaerocella colombiensis* (93–97%; AY464940)
(Inorganic electron acceptor)	*Geosporobacter subterrenus* (93–97%; (DQ643978)
Anaerobic Lithotrophs (ANM3), liquid	*Geosporobacter subterrenus* (98%; DQ643978)
(Inorganic electron acceptor)	*Caldanaerocella colombiensis* (97%; AY464940)
Sulfate-reducing bacteria (ANM5), liquid	*Pseudomonas* spp. (82–93%; HM142823)
Methanogens (ANM4), liquid	*Trichococcus collinsii* (100%; EF111215) *Nostocoida limicola* I (100%; AF255736) *Trichococcus flocculiformis* (100%; AJ306611) *Trichococcus pasteurii* (100%; X87150) *Desulfosporosinus lacus* (100%; AJ582757)
Heterotrophic Aerobes (AEM1), solid (agar)	*Trichococcus collinsii* (100%; EF111215) *Nostocoida limicola* I (100%; AF255736) *Trichococcus flocculiformis* (100%; AJ306611) *Trichococcus pasteurii* (100%; X87150)
Heterotrophic Anaerobes (ANM1), solid (agar)	*Pseudomonas stutzeri* (100%; EF530571) *Kocuria palustris* (98%; EU333884)
Sulfate-reducing bacteria (ANM5), solid (agar)	*Pseudomonas stutzeri* (100%)(EF530571)

cultures showing growth. This suggests the presence of a variety of thermophilic organisms which are often found in cold environments for unknown reasons (Hubert et al., 2009).

PLFA results indicated a viable population of about 2×10^5 cells/g in the wet clay near the filter screen and about 1×10^5 cells/g in the drier part of the clay, suggesting that, although culturability drops off by two to five orders of magnitude in the drier clay, the number of viable cells decreased by only a factor of two. The PLFA results also indicated a very non-diverse population in the PC clay samples (data not shown, Stroes-Gascoyne et al., 2008; Wersin et al., 2011-b). Table 3 shows that culturability appears to be higher than the PLFA-based cell counts in the samples taken adjacent to the filter screen. However, this is probably due to a sampling artefact: the weight of the clay sample required for PLFA analysis was much higher (up to 100 g) than the weight of clay sample used for culturing (5–10 g), and the "wet clay" PLFA sample, because of its size, likely contained some drier materials from further (>2 cm from the outside of the filter screen) into the clay, towards the much drier outer edge of the core. There was a steep drop in water content in the clay core with distance from the filter screen (Table 3; Stroes-Gascoyne et al., 2008).

Q-PCR results indicated the presence of 5×10^6 *Bacteria*/g, 1×10^5 *Archaea*/g, $<10^2$ methanogens/g and no SRB in the overcore clay sample taken from within the filter screen ($I_{(1)}$). The clay material within the filter screen was probably wet overcore clay material from higher up in the overcore that fell into the filter screen during retrieval. It is curious that no SRB were found with Q-PCR in this sample. However, the Q-PCR primers used had some mismatches with some strains of Gram-positive *Desulfotomaculum* species (Kondo et al., 2004), thus the Q-PCR primers may not have detected some Gram-positive SRB which appear more abundant than Gram-negative SRB from the sequencing results (Table 4b). All Q-PCR results were negative for samples taken directly outside the filter screen and in the drier clay further removed from the filter screen. While the latter result is in agreement with previous results for undisturbed Opalinus Clay (i.e., noted difficulty with extracting DNA from Opalinus Clay samples (Stroes-Gascoyne et al., 2007)), it is curious that Q-PCR could not extract any DNA from the sample directly adjacent to the filter screen because considerable culturability was found in corresponding samples. However, the samples originated from different core sections which may explain incongruent results. It is also possible that very high cell numbers are required for a positive DNA extraction from this clay, which probably strongly adsorbed free DNA. On the other hand the sample ($I_{(1)}$) contained considerable cell numbers based on Q-PCR analysis.

XRD analysis of wet clay and drier clay samples showed only a trace of pyrite, in contrast to the black precipitate in the PEEK tubing which indicated very strong peaks for pyrite. This could suggest that most SO_4-reducing activity occurred in the actual water phase of the PC experiment, or that the XRD signal for pyrite was obscured by the presence of other minerals (e.g., kaolinite, illite, quartz and calcite, Stroes-Gascoyne et al., 2008).

Table 4b summarizes the phylogenetic results for DNA extractions from both the whole liquid enrichment cultures and from the cultured isolates obtained from plating the liquid enrichment cultures onto solid agar media. The identifications from the whole enrichment cultures indicated the presence of *Pseudomonas spp.* (100%; EF530571) in AEM1 medium. A 16S rRNA gene sequence related to *Pseudomonas spp.* (82–93%; HM142823) was detected in ANM5. Three species of *Trichococcus* (*T. collinsii*, *T. flocculiformis* and *T. pasteurii*) (100%; EF111215; AJ306611 and X87150, respectively) and *Nostocoida limicola I* (100%; AF255736) were found in both ANM1 and ANM4 media, suggesting that these species are anaerobic. According to Liu et al. (2002), *Trichococcus* contains members of aero-tolerant species. Sequences related to *Caldanaerocella colombiensis* (93–98%; AY464940) and *Geosporobacter subterrenus* (93–98%; DQ643978) were found in both ANM2 and ANM3 media. *Geosporobacter* spp. is a Gram-positive, strict anaerobic, halotolerant organism that forms endospores (Klouche et al., 2007). These results suggest that the species present in the PC clay samples are not very fastidious but can be supported in a range of culture media and redox conditions. Although the SRB enrichment medium did not indicate the presence of identifiable SRB, a 16S rRNA gene sequence related to the SRB *Desulfosporosinus lacus* (100%; AJ582757) was found in the methanogenic medium. *Desulfosporosinus* spp. is a strictly anaerobic, spore-forming SRB (Stackebrandt et al., 2003).

The identification of isolates based on 16S rRNA gene sequencing also showed the presence of the 3 same species of *Trichococcus* (*T. collinsii*, *T. flocculiformis* and *T. pasteurii*) (100%; EF111215; AJ306611; X87150, respectively) and *Nostocoida limicola I* (100%; AF255736), this time in colonies from AEM1 agar plates, confirming that these organisms are aero-tolerant and can thrive in both aerobic and anaerobic environments. *Pseudomonas stutzeri* (100%; EF530571) was identified from agar colonies on ANM1 and ANM5 media, confirming that this organism can thrive under a range of (aerobic and anaerobic) conditions, i.e., thrive with both O_2 and NO_3^- but not with SO_4^{2-} as electron acceptor (Lalucat et al., 2006). *Kocuria palustris* (98%; EU333884) was identified from colonies on ANM1 medium, suggesting that this species is anaerobic.

4. Discussion

4.1. Development of microbiologically driven geochemically reducing conditions in the PC experiment

The cultivation and molecular biological results of this study both indicate a thriving microbial community in the PC water

and adjacent clay. These results are in sharp contrast to the largely negative microbiological results obtained for aseptically-drilled "undisturbed" Opalinus core in earlier studies (i.e., Mauclaire et al., 2007; Stroes-Gascoyne et al., 2005, 2007, 2008; Poulain et al., 2008). The here obtained total cell counts and quantitative culture results are higher by up to several orders of magnitude than generally found in oligotrophic deep groundwaters (e.g., Haveman and Pedersen, 2002; Haveman et al., 1998; 1995), and corroborate the conclusion by Ishii (2004) that organic substances must be present in the PC water, either leached from the Opalinus Clay or inadvertently added as contamination, to sustain such microbial communities.

The microbial community analyses summarized in Tables 3, 4a and b were conducted to attempt to establish the role of microbial activity in the evolution of the geochemical conditions in the PC experiment. Even if the applied methods give rather incomplete information about the complexity of the microbial community, it became apparent that the PC water and clay contained active microbial populations that likely played a role in the rapid establishment of strongly reducing redox conditions in the PC experiment.

The positive culture results for SRB and a 100% 16S rRNA gene homology to known, spore forming SRB (*Desulfosporosinus* spp.; *Desulfosporosinus lacus*), the H_2S smell and black color of the water sample and the presence of pyrite and SRB in the black precipitate in the PEEK tubing, all are positive proof of the occurrence of active SO_4 reduction in the PC porewater. The positive identification of *Desulfosporosinus* spp. in the PC porewater suggests an agreement with the earlier indication of the presence of *Desulfotomaculum* spp. in the PC water, reported by Ishii (2004) because of the reclassification of some *Desulfotomaculum* species as *Desulfosporosinus* species which are obligate anaerobic spore-forming SRB (Stackebrandt et al., 1997, 2003; Robertson et al., 2001). In its spore-form, it would be resistant to unfavorable conditions in the clay and also would less likely be affected negatively by exposure to O_2 (air). In addition, some SRB species have been found to resist damage from air exposure, even in vegetative state (Krekeler et al., 1998; Dilling and Cypionka, 1990).

The origin of the microorganisms in the PC water and clay samples cannot be determined clearly on the basis of the results of this study. Some species likely resulted from contamination, but revival of indigenous microbes also needs to be considered. It is possible that SRB (e.g. spore-forming *Desulfosporosinus* species) and the other species identified in the PC water and clay samples could result from an indigenous (possibly dormant) population in Opalinus Clay (e.g., Mauclaire et al., 2007; Poulain et al., 2008). Although the 100% homology with known sequences is probably not in favor of an indigenous origin, the opposite, i.e., finding an unpublished microbial sequence or culture, does not necessarily imply its authenticity (Willerslev et al., 2004).

Revival of dormant SRB (in particular *Desulfosporosinus* spp.) upon changing nutrient (and water) conditions in subsurface environment samples has been observed elsewhere. Suzuki et al. (2002, 2003) reported the presence of anaerobic spore-forming *Desulfosporosinus* spp. in sediment and water samples from an U-contaminated mine sediment, but only after anaerobic incubation with added organic substrate (lactate, acetate, ethanol, benzoic acids and glucose), to create anaerobic conditions in the incubations. This species was not detected in the original sediments by the RNA-based molecular biology techniques used. The study by Suzuki et al. (2003) showed that, as a result of the change from microaerophilic and oligotrophic conditions in the original mine sediment and water samples, to anaerobic and nutrient-rich conditions during the incubations in the laboratory, significant changes occurred in the microbial population in these sediments, with an abundant increase in active *Desulfosporosinus* spp. in the incubated sediments. Because the original sediment was microaerophilic, it is likely that *Desulfosporosinus* spp. were present in small amounts (perhaps as spores) in the original sediment and were, therefore, not detected initially by the RNA-based molecular biology techniques (spores are not active and, therefore, have no ribosomal activity and little ribosomal nucleic acids), but only after stimulation of activity and subsequent multiplication.

It can be hypothesized that a similar process could have occurred in the artificially created environment of the PC experiment. The original (anaerobic) Opalinus Clay surrounding the borehole contained little water, space and nutrients. Through the drilling process, more pore space was created, in the borehole, in the form of micro-fractures in the excavation-damaged zone around the borehole and in the porous filter screen. Also, although drilling was carried out under N_2 and measurements conducted under Ar, some air was introduced inadvertently into the borehole during short accidental situations during the 5 a of the PC experiment (Wersin et al. 2011-a; e.g. on day 117 of the PC experiment an accidental disconnection of a PEEK line occurred at the surface while the pump was still operating and aspirating air into the system for several days). Therefore, it is very likely that the PC experiment was contaminated with air (from sampling incidents), with aerobic or facultative aerobic bacteria (from the artificial porewater and clean but not sterile equipment), and nutrients (from organic contaminants such as glycerol and acetone (as discussed in Section 2.1). As a result, aerobic and NO_3-reducing microbial activity likely was stimulated (aerobes or facultative anaerobic organisms were found in abundance in both the PC water and PC wet clay surrounding the borehole). Subsequently, this caused the rapid development of (strictly) anaerobic conditions, suitable for the growth (and perhaps revival) of anaerobic (introduced and/or indigenous) species such as *Desulfosporosinus* spp. in the borehole water and environments (filter screen and wet clay). Under these circumstances, a progressive reduction of electron acceptors (e.g., Mn(IV), Fe(III), SO_4^{2-}) would have occurred and the results presented here are ample proof that SO_4^{2-} reduction (and pyrite formation) was indeed occurring in the PC borehole water and environments.

Furthermore, the geochemical analysis of the PC experiment indicated the presence of CH_4, indicative of strongly reducing conditions. Earlier microbial analysis (Mauclaire and McKenzie, 2006; Ishii, 2004) showed the presence of *Archaea* and in particular active *Methanosarcina* spp. in the PC water. In the present study, the analysis of the PC borehole water found a large active *Archaea* population (10^6 cells/mL) using the CARD-FISH technique. Based on Q-PCR analysis the presence of *Archaea* (10^5 cells/g clay) was also suggested in the clay from inside the filter screen, where the use of a specific Q-PCR assay showed <100 methanogens/g clay (Table 3) (although finding specific methanogens in culture media was less successful, Table 4b). Therefore, the occurrence of active methanogenesis in the PC borehole water can be concluded from the data reported here and previously.

The geochemical consequences of the microbial reactions that occurred in the PC experiments have been modelled by Tournassat et al. (2011).

4.2. Origin of organic carbon in PC borehole water

The previous study (Stroes-Gascoyne et al., 2005, 2007) showed that suspensions with sterile-drilled Opalinus Clay core material were able to support a variety of introduced bacteria for two months without addition of nutrients. Therefore, organic matter inherently present in Opalinus clay could have leached from the clay into the PC water through the filter screen and this could in principle have contributed to supporting microbial activity and growth in this experiment. Opalinus Clay contains about 1 wt.%

organic matter that is thermally immature with negligible hydrocarbon-producing potential (Pearson et al., 2003). Only a small portion of the organic material is humic material (~0.15%) and the rest is assumed to be kerogen or uncharacterized organic matter. The dissolved organic matter concentration is low (~14 mg/L) (Boisson, 2005). The work of Courdouan et al. (2007) and Courdouan-Metz (2008) on the nature and reactivity of dissolved organic C (DOC) in Opalinus Clay indicated that about 30% of DOC consists of hydrophilic low molecular weight organic acids such as acetate, 20% of higher molecular weight and about 50% of unknown hydrophobic matter.

Ishii (2004) concluded that the PC porewater must contain organic matter to support the microbial species present. Although the artificial porewater did not contain added organic matter, organic material likely entered the PC experiment in the form of contamination. The most likely source was glycerol leaking from the gel in the pH and Eh electrodes (De Cannière et al., 2011). The anaerobic respiration (oxidation) of glycerol (electron donor) occurs in many organisms in the presence of an external electron acceptor (e.g., SO_4^{2-}). An additional potential source was a residue of acetone that could inadvertently have been left in the pores of the filter screen. In the absence of O_2, acetone can be degraded by denitrifying, SO_4-reducing or fermenting bacteria (Höhener, 2005 and references therein). In the presence of SO_4^{2-} and SO_4-reducing bacteria of the genus *Desulfotomaculum*, acetate is oxidized to CO_2, H_2S and H_2O. The genus *Desulfosporosinus* (formerly *Desulfotomaculum*) was identified in PC water and clay. Other SRB such as *Desulfovibrio* are not capable of utilizing acetate as a C source (Höhener, 2005 and references therein).

Other sources of organic C, such as plasticizers (n-butyl-benzene-sulfonamide, NBBS) from polyamide tubing and phenols (a by-product of the epoxy resin used for sealing the borehole), were also possible (Höhener, 2004). None of these compounds were found in squeeze waters from pristine Opalinus Clay but the PC borehole water contained phenol (28 μg/L) and a variety of other phenolic compounds (methyl-, ethyl-, di-, and tri-methylphenols) in concentrations between 3 and 150 μg/L, whereas phthalates were below detection limits (200–400 μg/L). The acetone concentration was 1.2 mg/L at maximum, the acetate concentration 250 mg/L and the creosol concentration 150 μg/L (Höhener, 2005). Analysis of ^{14}C in the dissolved inorganic C (DIC) showed that 53.6 ± 0.4% of the DIC in the PC borehole water was modern C. This suggested that predominantly modern C fuelled the microbial processes in the porewater (and not the old C in the Opalinus Clay) (Höhener, 2005). Glycerol and acetone appeared to be the most likely candidates for this C source. Acetone can be manufactured from both modern and fossil C while glycerol generally is produced from modern C. It is, therefore, most likely that glycerol was the primary contaminating C source (De Cannière et al., 2011; Tournassat et al., 2011). The pattern of phenolic compounds including the creosol resembling that found in coal tar-contaminated groundwater, and the origin of these phenols found in the PC borehole water is, therefore, not explained (if derived from wood creosote, the compounds could be of modern origin). Plasticizer (NBBS) concentration from tubing was relatively low and plasticizers likely can be excluded as the main source of unknown C in the system (see also discussion in De Cannière et al. (2008, 2011)).

4.3. Repository considerations

Although a rapid development of (strongly) reducing conditions is generally desirable in a future nuclear waste repository environment (e.g., because of slower container corrosion and HLW dissolution processes, and decreased mobility of radionuclides at low redox potentials), the products of SO_4 reduction (H_2S, m^-, $S_2O_3^{2-}$) may in fact increase corrosion of Cu or steel waste containers. While it must be emphasized that the PC experiment does not constitute a realistic HLW repository environment, the microbial processes that occurred in the PC experiment are in fact an illustration of the potential for microbial processes that may be stimulated or initiated locally in the Opalinus Clay (and other clay formations) upon disturbance by drilling and subsequent introduction of water, nutrients and microbes. A similar unanticipated development of microbial activity was apparent in the Belgian OPHELIE experiment that was filled with FoCa Clay bentonite (Van Humbeeck et al., 2009). During the operating phase of that experiment, corrosion problems occurred that could be attributed to the development of microbial activity, likely fuelled by organic matter leaking from load cells and by an increase in space and water availability in the experiment as a result of its geometry (Van Humbeeck et al., 2009).

Although stimulating microbial processes may have both positive and negative effects, it seems prudent at present to keep such stimulation to a minimum in a HLW repository environment because of concerns for enhanced container corrosion and gas production. Therefore, stringent precautions would need to be taken, especially in the environments around and close to the waste containers, for which microbially influenced corrosion (e.g., as a result of the production of sulfide and thiosulfate from SO_4 reduction) is of concern (i.e., stress corrosion cracking and pitting induced, respectively, by the HS^- and $S_2O_3^{2-}$ species). The events in the PC experiment are indicative of the potential consequences of stimulating or introducing microbial activity and need to be considered when designing and building *in situ* large experiments, and ultimately a HLW repository.

5. Summary and conclusions

The porewater chemistry (PC) experiment was conducted at the Mont Terri Underground Research Laboratory to measure *in situ* a number of non-conserved important physico-chemical parameters, such as pH, E_h and pCO_2, within the porewater of the Opalinus Clay formation. It became apparent that the PC experiment contained an active, highly dynamic microbial community that evolved during the 5-a duration of the experiment and most likely caused the rapid establishment of strongly reducing redox conditions in the PC experiment. The origin of the microorganisms in the PC water and clay samples cannot be determined clearly on the basis of the results of this study. It is likely that some microbial contamination occurred when the experiment was initiated. Contamination with organic material occurred as well, most likely in the form of glycerol leaking from pH and E_h electrodes and possibly from residues of acetone (in the pores of the filter screen), but also (to a much lesser extent) from phenolic compounds including creosol. Revival of indigenous microbes (possibly surviving in spore or dormant (anabiotic) form) also needs to be considered.

Microbial analyses of the PC borehole water and of clay samples from around the borehole, obtained via overcoring, were carried out at three laboratories, using a large number of different techniques, including both molecular biology and culturing methods. Results indicated the presence of heterotrophic aerobic, facultative and obligate anaerobic organisms that resulted likely from the initial, suspected contamination. The results also indicated the presence of active SO_4 reduction, methanogenesis and possibly Fe(III) reduction in these samples.

With respect to the geochemical evolution in the borehole water, the microbial results reported here provide a strong indication and some actual proof (H_2S, pyrite, CH_4) of the *in situ* ecological sequence of microbial activity that took place. This sequence rapidly would have created more anaerobic conditions, which then allowed for a progressive sequence of microbial processes with

increasingly negative redox potentials, from NO_3-reduction and Fe-reduction to SO_4-reduction and finally CH_4 production. It is also possible that these microbial processes took place simultaneously, but in different ecological niches in the PC environment. It should be emphasized that the microbial processes observed in the PC borehole water were a result of the artificial environment created by the PC experiment and are not a realistic representation of microbial processes occurring in undisturbed Opalinus Clay.

The previous studies (Stroes-Gascoyne et al., 2007; Poulain et al., 2008) concluded that: (i) undisturbed Opalinus Clay appears to contain, at most, only a small viable microbial community, which is probably metabolically almost inactive or dormant; (ii) this *in situ* suspended state is most likely due to space and water restrictions in this environment; and (iii) any disturbances that would provide space, water and nutrients, as would be the case during repository excavation and construction, would support any introduced organisms and may perhaps revive any dormant organisms (if present). The microbial processes that occurred in the PC experiment (and also in the OPHELIE experiment, van Humbeeck et al., 2009) are, therefore, in fact an illustration of the potential for microbial processes that may be stimulated or initiated locally in clay host rock upon disturbance by drilling and the concomitant introduction of water, nutrients and microbes. If such processes are to be kept to a minimum in a HLW repository environment, stringent precautions need to be taken, especially around the waste containers, where microbially influenced corrosion is of concern. The potential consequences of stimulating or introducing microbial activity need to be considered when designing and building large *in situ* experiments and ultimately a HLW repository in clay formations.

Acknowledgements

CNAB would like to thank CNRS, University Bordeaux I and the Mont Terri project consortium for funding this work and for financial assistance to S. Nèble. AECL would like to thank the Nuclear Waste Management Organization (NWMO) for financial support of this work. We are grateful to Rizlan Bernier-Latmani (EPFL, Ecole Polytechnique Fédérale de Lausanne, Switzerland) for discussions on microbial degradation of glycerol; to Neil Miller (AECL) for performing the XRD analyses; and to Pierre De Cannière (FANC, Federal Agency of Nuclear Control, Belgium) for a detailed and very helpful review of this manuscript. The Mont Terri project consortium provided funds for the PLFA/DGGE analysis at Microbial Insights, Rockport, Tennessee, USA.

References

Altschul, S.F., Madden, T.L., Schaffer, A.A., Zhang, J., Zhang, Z., Miller, W., Lipman, D.J., 1997. Gapped BLAST and PSI-BLAST: a new generation of protein database search programs. Nucleic Acids Res. 25, 3389–3402.

Atlas, R.M., 1993. In: Parks, L.C. (Ed.), Handbook of Microbiological Media. CRC Press Inc..

Battaglia, F., Gaucher, E., 2003. Mont Terri Project Porewater Chemistry Experiment. Microbial Characterisation and Particle Transport. Mont Terri Project Technical Note TN 2002-23, Bern (CH). <http://www.mont-terri.ch/ids/default.asp?TopicID=97>.

Boisson, J., 2005. Clay Club Catalogue of Characteristics of Argillaceous Rocks. OECD/NEA Report No; 4436, 71.

Courdouan, A., Christl, I., Wersin, P., Kretzschmar, R., 2007. Nature and reactivity of dissolved organic matter in the Opalinus Clay and Callovo-Oxfordian Formations. In: Proc. Clays in Natural End Engineered Barriers for Radioactive Waste Confinement, Lille, France, September 17–20, 2007.

Courdouan-Metz, A., 2008. Nature and Reactivity of Dissolved Organic Matter in Clay Formations Evaluated for the Storage of Radioactive Waste. Doctoral dissertation. ETH, Zurich, Switzerland.

De Cannière, P., Vinsot, A., Schwyn, B., Mettler, S., Fernandez, A.M., Turrero, M.J., Hernan, P., Boisson, J.-Y., Stroes-Gascoyne, S., Sergeant, C., Schippers, A., Mäder, U., Mazurek, M., Waber, H.N., Gaucher, E., Tournassat, C., Aoki, K., Arcos, D., Gabler, H.-E., Courdouan, A., Gautschi, A., Wersin, P., Bath, A., Pearson, F.J., 2008. Geochemistry and microbiology experiments. In: Bossart, P., Thury, M. (Eds.), Mont Terri Rock Laboratory – Project, Programme 1996 to 2007 and Results. ISBN:978-3-302-40016-7 (Chapter 6). <http://www.swisstopo.admin.ch/internet/swisstopo/en/home/docu/pub/geology/reports.html> and <http://www.toposhop.admin.ch/en/shop/products/publications/geology/reports>.

De Cannière, P., Schwarzbauer, J., Höhener, P., Lorenz, G., Salah, S., Leupin O.X., Wersin, P., 2011. Biogeochemical processes in a clay formation in situ experiment: part C – Organic contamination and leaching data. Appl. Geochem.

Dilling, W., Cypionka, H., 1990. Aerobic respiration in sulphate-reducing bacteria. FEMS Microbiol. Lett. 71, 123–128.

Gould, W.D., Stichbury, M., Francis, M., Lortie, L., Blowes, D.W., 2003. An MPN method for the enumeration of iron-reducing bacteria. In: Proc. The Mining and Environment Conference III, Session 2A Bacteria. Sudbury, Ontario, Canada.

Haveman, S.A., Pedersen, K., 2002. Microbially mediated redox processes in natural analogues for radioactive waste. J. Contam. Hydrol. 55, 161–174.

Haveman, S.A., Stroes-Gascoyne, S., Hamon, C.J., Delaney, T.L., 1995. Microbial Analysis of Groundwaters from Seven Boreholes at AECL's Underground Research Laboratory. Technical Record, TR-677, COG-95-017. Atomic Energy of Canada Limited.

Haveman, S.A., Pedersen, K., Ruotsalainen, P. 1998. Geomicrobial Investigations of Groundwaters from Olkiluoto, Hastholmen, Kivetty and Romuvaara, Finland. Report Posiva 98-09, Posiva Oy, Finland.

Höhener, P., 2004. Porewater Chemistry (PC) Experiment: Interpretation of Test Data and Literature Survey on Biodegradation of Synthetic Materials. Mont Terri Project Technical Note TN2004-62, Bern (CH). Federal Office of Water and Geology. <http://www.mont-terri.ch/ids/default.asp?TopicID=97>.

Höhener, P., 2005. Porewater Chemistry (PC) Experiment: Interpretation of Test Data from July 2004 and Conclusions on Unknown Carbon Source. Mont Terri Project Technical Note TN2005-22, Bern (CH). <http://www.mont-terri.ch/ids/default.asp?TopicID=97>.

Hubert, C., Loy, A., Nickel, M., Arnosti, C., Baranyi, C., Brüchert, V., Ferdelman, T., Finster, K., Mønsted Christensen, F., Rosa de Rezende, J., Vandieken, V., Jørgensen, B.B., 2009. A constant flux of diverse thermophilic bacteria into the cold arctic seabed. Science 325, 1541–1544.

Ishii, K., 2004. Porewater Chemistry (PC) Experiment: Quantification (and Qualification) of Microbial Communities. Mont Terri Project Technical Note TN 2004-76, Bern (CH). <http://www.montterri.ch/ids/default.asp?TopicID=97>.

Klouche, N., Fardeau, M.L., Lascourrèges, J.F., Cayol, J.L., Hacene, H., Thomas, P., Magot, M., 2007. *Geosporobacter subterraneus* gen. Nov., sp. Nov., a spore-forming bacterium isolated from a deep subsurface aquifer. Internat.. J. Syst. Evol. Microbiol 57, 1757–1761.

Kock, D., Schippers, A., 2008. Quantitative microbial community analysis of three different sulfidic mine tailings dumps generating acid mine drainage. Appl. Environ. Microbiol. 74, 5211–5219.

Kondo, R., Nedwell, D.B., Purdy, K.J., de Queiroz Silva, S., 2004. Detection and enumeration of sulphate-reducing bacteria in estuarine sediments by competitive PCR. Geomicrobiol. J. 21, 145–157.

Koroleva, M., Lerouge, C., Mäder, U., Claret, F., Gaucher, E., 2011. Biogeochemical processes in a clay formation in situ experiment: part B – results from overcoring and evidence of strong buffering by the rock formation. Appl. Geochem.

Krekeler, D., Teske, A., Cypionka, H., 1998. Strategies of sulphate-reducing bacteria to escape oxygen stress in a cyanobacterial mat. FEMS Microbiol. Ecol. 25, 89–96.

Lalucat, J., Bennasar, A., Bosch, R., Garcia-Valdes, E., Palleroni, N.J., 2006. Biology of *Pseudomonas stutzeri*. Microbiol. Mol. Biol. Rev. 70, 510–547.

Liu, J.R., Tanner, R.S., Schumann, P., Weiss, N., McKenzie, C.A., Janssen, P.H., Seviour, E.M., Lawson, P.A., Allen, T.D., Seviour, R.J., 2002. Emended description of the genus *Trichococcus*, description of *Trichococcus collinsii* sp. nov., and reclassification of *Lactosphaera pasteurii* as *Trichococcus pasteurii* comb. nov. and of *Ruminococcus palustris* as *Trichococcus palustris* comb. nov. in the low-G+C Gram-positive bacteria. Int. J. Syst. Evol. Microbiol. 52, 1113–1126.

Lovley, D.R., Coates, J.D., Blunt-Harris, E.L., Phillips, E.J.P., Woodward, J.C., 1996. Humic substances as electron acceptors for microbial respiration. Nature 328, 445–448.

Mauclaire, L., McKenzie, J., 2006. Mont Terri Project: Microbial Activity and Identification within PC, PC-C Porewaters. Mont Terri Project Technical Note TN 2006-61, Bern (CH). <http://www.mont-terri.ch/ids/default.asp?TopicID=97>.

Mauclaire, L., McKenzie, J.A., Schwyn, B., Bossart, P., 2007. Detection and cultivation of indigenous microorganisms in Mesozoic claystone core samples from the Opalinus Clay Formation (Mont Terri Rock Laboratory). Phys. Chem. Earth 32, 232–240.

Muyzer, G., De Waal, E.C., Uitterlinden, A.G., 1993. Profiling of complex microbial populations by denaturing gradient gel electrophoresis analysis of polymerase chain reaction-amplified genes coding for 16S rRNA. Appl. Environ. Microbiol. 59, 695–700.

Muyzer, G., Hottenträger, S., Teske, A., Wawer, C., 1996. Denaturating gradient gel electrophoresis of PCR-amplified 16S rDNA – a new molecular approach to analyze the genetic diversity of mixed microbial communities, 1–23. In: Akkermans, A.D.L., Van Elsas, J.D., de Bruijn, F.J. (Eds.), Molecular Microbial Ecology, Manual3.4.4. Kluwer Academic Publishers, Dordrecht, The Netherlands.

Nadkarni, M., Martin, F.E., Jacques, N.A., Hunter, N., 2002. Determination of bacterial load by real-time PCR using a broad range (universal) probe and primer set. Microbiology 148, 257–266.

Pearson, F.J., Arcos, D., Bath, A., Boisson, J.Y., Fernandez, A.M., Gabler, H.E., Gaucher, E., Gautschi, A., Griffault, L., Herman, P., Waber, N.H., 2003. Geochemistry of Water in the Opalinus Clay Formation at the Mont Terri Rock Laboratory.

Synthesis Report. Reports of the Swiss Federal Office for Water and Geology (FOWG), Geology Series, No. 5, Bern, Switzerland.
Pedersen, K., 2000. Microbial Processes in Radioactive Waste Disposal. Technical Report Tr-00-04. Swedish Nuclear Fuel and Waste Management Co., Stockholm.
Pernthaler, J., Glöckner, F., Schönhuber, W., Amann, R., 2001. Fluorescence in situ hybridization (FISH) with rRNA-targeted oligonucleotide probes. In: Paul, J. (Ed.), Methods in Microbiology: Marine Microbiology, vol. 30. Academic Press Ltd., London, pp. 207–226.
Pernthaler, A., Pernthaler, J., Amann, R., 2002. Fluorescence in situ hybridization and catalyzed reporter deposition for the identification of marine bacteria. Appl. Environ. Microbiol. 68, 3094–3101.
Poulain, S., Sergeant, C., Simonoff, M., Le Marrec, C., Altmann, S., 2008. Microbial investigation of Opalinus Clay, an argillaceous formation under evaluation as a potential host rock for a radioactive waste repository. Geomicrobiol. J. 25, 240–249.
Reasoner, D.J., Geldreich, E.E., 1985. A new medium for the enumeration and subculture of bacteria from potable water. Appl. Environ. Microbiol. 49, 1–7.
Robertson, W.J., Bowman, J.P., Franzmann, P.D., Mee, B.J., 2001. *Desulfosporinus meridiei* sp. nov., a spore-forming sulphate-reducing bacterium isolated from gasoline-contaminated groundwater. Int. J. Syst. Evol. Microbiol. 51, 133–140.
Schippers, A., 2006. Microbial Activity in Opalinus Clay (MA-experiment): Microbiological Analysis of Porewater Samples from the PC and PC-C Experiments Report BGR Tagebuch-No. 10873/06.
Schippers, A., Neretin, L.N., 2006. Quantification of microbial communities in near-surface and deeply buried marine sediments on the Peru continental margin using real-time PCR. Environ. Microbiol. 8, 1251–1260.
Schippers, A., Neretin, L.N., Kallmeyer, J., Ferdelman, T.G., Cragg, B.A., Parkes, R.J., Jørgensen, B.B., 2005. Prokaryotic cells of the deep sub-seafloor biosphere identified as living bacteria. Nature 433, 861–864.
Stackebrandt, E., Sproer, C., Rainey, F.A., Burghart, J., Pauker, O., Hippe, H., 1997. Phylogenetic analysis of the genus *Desulfotomaculum*: evidence for the misclassification of *Desulfotomaculum guttoideum* and description of *Desulfotomaculum orientis* as *Desulfosporinus orientis* gen. Nov, comb. nov. Int. J. Syst. Bacteriol. 47, 1134–1139.
Stackebrandt, E., Schumann, P., Schüler, E., Hippe, H., 2003. Reclassification of *Desulfotomaculum auripigmentum* as *Desulfosporosinus auripigmenti* corrig., comb. nov.. Int. J. Syst. Evol. Microbiol. 53, 1439–1443.
Stephen, J.R., Chang, Y-J., MacNaughton, S.J., Whitaker, S.L., Hicks, C.L., Leung, K.T., Flemming, C.A., White, D.C., 1999. Fate of a metal-resistant inoculum in contaminated and pristine coils assessed by denaturing gradient gel electrophoresis. Environ. Toxicol. Chem. 18, 1118–1123.
Stroes-Gascoyne, S., West, J.M., 1996. An overview of microbial research related to high-level nuclear waste disposal with emphasis on the canadian concept for the disposal of nuclear fuel waste. Can. J. Microbiol. 42, 349–366.
Stroes-Gascoyne, S., Schwyn, B., Schippers, A., Poulain, S., Sergeant, C., Le Marrec, C., Simonoff, M., Altmann, S., Nagaoka, T., Mauclaire, L., Vasconcelos, C., McKenzie, J., Daumas, S., Vinsot, A., Beaucaire, C., Matray, J.M., 2005. MA Experiment: Microbial Investigations on Unperturbed Opalinus Clay Samples. Mont Terri Project Technical Note TN2004-44, Bern (CH). <http://www.mont-terri.ch/ids/default.asp?TopicID=97>.
Stroes-Gascoyne, S., Schippers, A., Schwyn, B., Poulain, S., Sergeant, C., Le Marrec, C., Simonoff, M., Altmann, S., Nagaoka, T., Mauclaire, L., McKenzie, J., Daumas, S., Vinsot, A., Beaucaire, C., Matray, J.M., 2007. Microbial community analysis of Opalinus Clay drill core samples from the Mont Terri Underground Research Laboratory, Switzerland. Geomicrobiology 24, 1–17.
Stroes-Gascoyne, S., Sergeant, C., Schippers, A., Hamon, C.J., Nèble, S., Vesvres, M.-H. Poulain, S., Le Marrec, C., 2008. Microbial Analyses of PC Water and Overcore Samples: Synthesis of Results. Mont Terri Project Technical Note TN2006-69, Bern (CH). <http://www.mont-terri.ch/ids/default.asp?TopicID=97>.
Suzuki, Y., Kelly, S.D., Kemnert, K.M., Banfield, J.F., 2002. Nanometre-size products of uranium bioreduction. Nature 419, 134.
Suzuki, Y., Kelly, S.D., Kemnert, K.M., Banfield, J.F., 2003. Microbial populations stimulated for hexavalent uranium reduction in uranium mine sediment. Appl. Environ. Microbiol. 69, 1337–1346.
Takai, K., Horikoshi, K., 2000. Rapid detection and quantification of members of the archaeal community by quantitative PCR using fluorogenic probes. Appl. Environ. Microbiol. 66, 5066–5072.
Tournassat, C., Alt-Epping, P., Gaucher, E.C., Gimmi, T., Leupin, O.X., Wersin, P., 2011. Biogeochemical processes in a clay formation in situ experiment: part F – reactive transport modelling. Appl. Geochem..
Van Humbeeck, H., Verstricht, J., Li, X.L., De Cannière, P., Bernier, F., Kursten, B., 2009. The OPHELIE Mock-up. Final Report. EURIDICE Report 09-134, January 2009.
Webster, G., Newberry, C.J., Fry, J., Weightman, A.J., 2003. Assessment of bacterial community structure in the deep sub-seafloor biosphere by 16S rDNA-based techniques: a cautionary tale. J. Microbiol. Method 55, 155–164.
Weinbauer, M.G., Beckmann, C., Höfle, M.G., 1998. Utility of green fluorescent nucleic acid dyes and aluminium oxide membrane filters for rapid epifluorescence enumeration of soil and sediment bacteria. Appl. Environ. Microbiol. 64, 5000–5003.
Weisburg, W.G., Barns, S.M., Pelletier, D.A., Lane, D.J., 1991. 16S ribosomal DNA amplification for phylogenetic study. J. Bacteriol. 173, 697–703.
Wersin, P., Leupin, O.X., Mettler, S., Gaucher, E., Mäder, U., De Cannière, P., Vinsot, A., Gabler, H.E., Kunimaro, T., Kiho, K., Eichinger, L., 2011-a. Biogeochemical processes in a clay formation in situ experiment: part A – overview, experimental design and water data of an experiment in the Opalinus Clay at the Mont Terri Underground Research Laboratory, Switzerland. Appl. Geochem.
Wersin, P., Stroes-Gascoyne, S., Pearson, F.J., Tournassat,C., Leupin, O.X., Schwyn, B., 2011-b. Biogeochemical processes in a clay formation in situ experiment: part G – key interpretations and conclusions. Implications for repository safety. Appl. Geochem.
White, D., Davis, C.W.M., Nickels, J.S., King, J.D., Bobbie, R.J., 1979. Determination of the sedimentary microbial biomass by extractable lipid phosphate. Oecologia 40, 51–62.
Willerslev, E., Hansen, A.J., Poinar, H.N., 2004. Isolation of nucleic acids and cultures from fossil ice and permafrost. Trends Ecol. Evol. 19, 141–147.
Wilms, R., Sass, H., Köpke, B., Cypionka, H., Engelen, B., 2007. Methane and sulphate profiles within the subsurface of a tidal flat are reflected by the distribution of sulphate-reducing bacteria and methanogenic archaea. FEMS Microbiol. Ecol. 59, 611–621.

Applied Geochemistry 26 (2011) 990–1008

Contents lists available at ScienceDirect

Applied Geochemistry

journal homepage: www.elsevier.com/locate/apgeochem

Biogeochemical processes in a clay formation *in situ* experiment: Part E – Equilibrium controls on chemistry of pore water from the Opalinus Clay, Mont Terri Underground Research Laboratory, Switzerland

F.J. Pearson [a,*], Christophe Tournassat [b], Eric C. Gaucher [b]

[a] Ground-Water Geochemistry, 5108 Trent Woods Dr., New Bern, NC 28562, USA
[b] BRGM, B.P. 36009, 45060 Orleans Cedex 2, France

ARTICLE INFO

Article history:
Available online 17 March 2011

ABSTRACT

The chemistry of pore water (particularly pH and ionic strength) is an important property of clay rocks being considered as host rocks for long-term storage of radioactive waste. Pore waters in clay-rich rocks generally cannot be sampled directly. Instead, their chemistry must be found using laboratory-measured properties of core samples and geochemical modelling. Many such measurements have been made on samples from the Opalinus Clay from the Mont Terri Underground Research Laboratory (URL). Several boreholes in that URL yielded water samples against which pore water models have been calibrated. Following a first synthesis report published in 2003, this paper presents the evolution of the modelling approaches developed within Mont Terri URL scientific programs through the last decade (1997–2009). Models are compared to the composition of waters sampled during dedicated borehole experiments. Reanalysis of the models, parameters and database enabled the principal shortcomings of the previous modelling efforts to be overcome. The inability to model the K concentrations correctly with the measured cation exchange properties was found to be due to the use of an inappropriate selectivity coefficient for Na–K exchange; the inability to reproduce the measured carbonate chemistry and pH of the pore waters using mineral–water reactions alone was corrected by considering clay mineral equilibria. Re-examination of the measured Ca/Mg activity ratios and consideration of the mineralogical composition of the Opalinus Clay suggested that Ca/Mg cation exchange rather than dolomite saturation may control the ratio of these ions in solution. This re-examination also suggests that the Ca/Mg ratio decreases with increasing pore-water salinity. Several possible reasons for this are proposed. Moreover, it is demonstrated that feldspar equilibria must not be included in Opalinus Clay modelling because feldspars are present only in very small quantities in the formation and because Na/K ratios measured in pore water samples are inconsistent with feldspar saturation. The principal need to improve future modelling is additional or better data on rock properties, in particular: (i) a more detailed identification of phases in the Opalinus Clay that include redox-sensitive elements together with evaluation of their thermodynamic properties; (ii) an improved understanding of the distribution of celestite throughout the Opalinus Clay for Sr/SO_4 concentrations control; (iii) improvements in analytic and thermodynamic data for Ca–Mg rock cation exchange and mineral chemical properties and (iv) the measurement of composition and stability constants of clay minerals actually present in the formation.

1. Introduction

A significant difference between the pore water in clay-rich rocks and conventional groundwater is the operation by which their chemistry is characterized. Ground-water samples are commonly available from wells and springs in volumes that are large enough for the performance of many field analyses and that permit collection of samples for a variety of laboratory analyses. Pore waters from clay-rich rocks, on the other hand, can rarely be sampled directly and then only in small volumes which have usually been affected by exposure to the sampling environment. Aqueous equilibrium modelling has long been applied to groundwaters to investigate mineral and other controls on their measured compositions and the extent to which they are in equilibrium with their environments. For clay–rock pore water, geochemical modelling is also applied to determine the chemistry of waters that cannot be sampled directly. While geochemical modelling is commonly

* Corresponding author.
E-mail address: fjpearson@gmail.com (F.J. Pearson).

0883-2927/$ - see front matter © 2011 Elsevier Ltd. All rights reserved.
doi:10.1016/j.apgeochem.2011.03.008

used to test the extent to which ground waters are in water–rock equilibrium, geochemical modelling of pore waters usually assumes that mineral–water reactions are in equilibrium.

One of the principal objectives of the research programme at the Mont Terri Underground Research Laboratory (URL) (http://www.mont-terri.ch/) was to develop techniques to characterize the chemistry of pore water in clay-rich, low-permeability rocks and, by applying these techniques, to characterize the pore-water chemistry of the Opalinus Clay at Mont Terri. A variety of techniques was anticipated. These included direct analyses of water seeping into boreholes drilled from the underground laboratory, of water ejected from core samples subjected to high-pressure squeezing, and of water expelled from core samples during high-pressure infiltration experiments. Indirect approaches included aqueous leaching of core samples to determine the soluble salt contents of the rocks and leaching with solutions that extracted exchangeable cations. Equilibrium modelling was used to evaluate the water analyses with respect to equilibria with formation minerals and cation exchange properties and for consistency between measured and calculated values of such properties as PCO_2.

The properties of the Opalinus Clay at the Mont Terri URL are such that pore water samples can be collected from boreholes drilled within the laboratory. These samples provide validation for calculations of pore-water chemistry based on measured properties of the Opalinus Clay itself. Such calculation methods, once validated, can be applied to other clay rock pore waters from which direct samples cannot be collected.

Studies are also in progress at a number of other clay sites many of which have recently been described by Mazurek et al. (2009). Clays at several sites including the Callovo-Oxfordian at the Site Meuse/Haute Marne (Bure), France, and the Boom Clay at Mol, Belgium, yield water to boreholes drilled from underground laboratories, as does the Opalinus Clay. The pore-water chemistry of these units can be determined directly. Clays at other sites are more indurated and do not yield water to boreholes drilled into unfractured, bulk rock. These include the Toarcian–Domerian at Tournemire, France, and two other clays not described by Mazurek et al. (2009), the Helvetic marls (Palfris marl) at Wellenberg, Switzerland, (Nagra, 1997) and the upper Ordovician Queenston and adjacent shales at the Bruce Site, Ontario (Jensen et al., 2010). To characterize the pore water from such indurated units will require calculations based on rock properties like those described here.

This paper discusses the state of equilibrium modelling of pore-water chemistry. The emphasis is on the experience gained from work at Mont Terri but similar modelling of other units is also referred to as it supports the Mont Terri work.

1.1. Chemistry of Opalinus Clay pore water

The geology and the layout of the Mont Terri URL are summarized by Wersin et al. (this issue). The pore-water chemistry and properties of the host rock that are relevant to the water chemistry are given by Pearson et al. (2003), Wersin et al. (2009) and Koroleva et al. (this issue). Degueldre et al. (2003) also discuss the water chemistry at Mont Terri based only on samples from boreholes in the Opalinus Clay and seeps in the adjacent limestones. Water chemical data are based on analyses and *in situ* measurements on water flowing from 4 boreholes drilled from the URL, from samples of drill core squeezed at high pressures and from aqueous leaching of core samples.

As shown in Fig. 2 of Wersin et al. (this issue), the Cl^- contents of pore water in the clay rocks at Mont Terri vary from about 13 g/L near the contact between the Opalinus Clay and the Lias to less than 1 g/L at the contacts of the clays with the limestone aquifers overlying and underlying the clay units. This pattern is considered to result from diffusion of solutes from initially saline pore water throughout the clay-rich units to fresh water in the adjacent aquifers. Such diffusion has been modelled by Mazurek et al. (2009, Sections 2.4 and 5.4) using transport parameters measured on samples from Mont Terri and seawater as the initial pore water. The measured profile could be matched by assuming that fresh water first invaded the upper aquifer at about 6.5 Ma and the lower aquifer at about 0.5 Ma. The different times for the initiation of diffusion are consistent with the geologic history of the region and account for the asymmetry of the Cl profile.

Of the several types of water samples available, those from the boreholes best represent *in situ* pore-water chemistry because they were collected with the least disturbance to parameters such as pH, redox state and gas compositions that are sensitive to sample handling. The boreholes are designated BWSA-3, which is located at a distance of about 40 m as shown on Fig. 2 of Wersin et al. (this issue), BWSA-2, at about 60 m, BWSA-1, at about 100 m, and PC-C, at about 110 m. Waters from these boreholes have Cl^- contents ranging from about 4.4 g/L in BWSA-3 to about 11.6 g/L in PC-C.

One of the major differences between laboratory-collected and borehole water samples was that SO_4^{2-} concentrations based on core leaching and squeezing were commonly higher than those in corresponding borehole samples. Fig. 1 shows the mole ratios of SO_4/Cl and of Br/Cl plotted against Cl^- concentrations. The dashed lines in this figure represent the ion ratios in normal seawater. The Br/Cl ratio of all samples is essentially that of seawater indicating that the dissolved salts in the pore water had a seawater origin and that the pore water has not been subject to salt dissolution nor to any physical processes that would fractionate Br^- and Cl^-. The lowest SO_4/Cl ratios are about that of seawater but there are also a number of samples with higher relative SO_4^{2-} contents. These occur in samples collected by core squeezing, in samples from the lower-Cl^- boreholes BWSA-2 and BWSA-3, and in samples with low Cl^- contents from seeps in the Mont Terri laboratory from units above and below the clay units (Wersin et al., this issue, Fig. 2).

The Opalinus Clay contains pyrite which is known to oxidize readily when clay rock containing it is exposed to the atmosphere (Baeyens et al., 1985b). The relatively higher SO_4^{2-} contents of the squeezed samples shown in Fig. 1 are attributed to the oxidation of pyrite during core preparation and squeezing. The relatively low SO_4^{2-} squeezed samples were prepared using a technique which protected the core from contact with the atmosphere during both preparation and squeezing. The agreement between the ratios in the protected, squeezed samples and the water samples collected from the boreholes indicates that pyrite oxidation did not contribute significantly to the SO_4^{2-} contents of either of these types of samples.

The diffusion model of Mazurek et al. (2009) is consistent with the seawater Br/Cl ratio of the pore water samples in that seawater was chosen as the composition of the initial water and the pore water should retain this Br/Cl ratio during diffusion because the diffusion properties of Cl^- and Br^- are closely similar.

The chemistry of the PC-C, BWSA-1 and BWSA-3 waters is given in Table 1. The average and one standard deviation values are those of samples taken from the PC-C borehole from 2004 through 2007 (Vinsot et al., 2008a, Table 2), and from the BWSA-1 and BWSA-3 boreholes from 1998 through 2000 (Pearson et al., 2003, Annex 1) and from 2003 through 2006 (Wersin et al., 2009, Tables 3.9 and 3.12). The BWSA-2 borehole yielded water of composition intermediate between those of BWSA-1 and BWSA-3 and is not included in Table 1. Analyses for samples from this borehole are given by (Pearson et al., 2003, Annex 1). The chemistry of all 3 BWSA boreholes is illustrated in Fig. 2.

The PC-C borehole was constructed to minimize possible oxidation and bacterial contamination, and was instrumented for *in situ* measurements (Vinsot et al., 2008a). Samples from this borehole

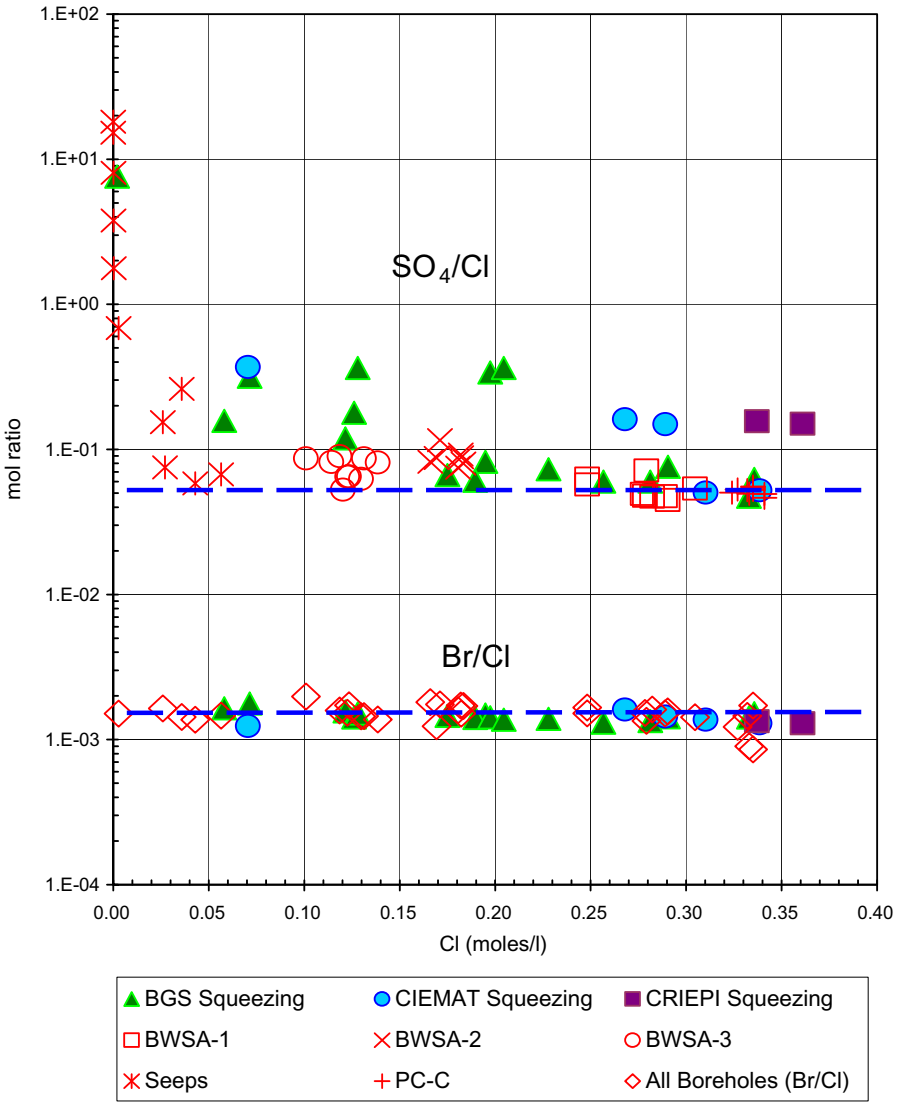

Fig. 1. Comparison of SO_4/Cl and Br/Cl ratios with Cl contents of borehole and squeezed water samples. Dashed lines represent the respective ratios in seawater. Data on borehole samples and water squeezed from core from various laboratories from June 1997 through February 2000 as reported by Pearson et al. (2003) and on PC-C borehole samples from Vinsot et al. (2008a).

Table 1
Composition of water samples from boreholes PC-C, BWSA-1 and BWSA-3 in Mont Terri URL. Averages and 1 standard deviation values are of analyses given by Vinsot et al. (2008a), Pearson et al. (2003) and Wersin et al. (2009).

pH value		PC-C			BWSA-1			BWSA-3		
		Mean		Std. dev.	Mean		Std. dev.	Mean		Std. dev.
		7.13	±	0.23	7.55	±	0.38	7.41	±	0.15
Na	(mol/L)	2.81 E−01	±	5.55E−03	2.32E−01	±	1.22E−02	1.22E−01	±	6.12E−03
K	(mol/L)	1.92E−03	±	7.24E−04	1.47E−03	±	1.94E−04	9.07E−04	±	2.07E−04
Mg	(mol/L)	2.20E−02	±	4.80E−04	1.66E−02	±	6.80E−04	5.93E−03	±	2.23E−04
Ca	(mol/L)	1.89E−02	±	5.48E−04	1.58E−02	±	7.23E−04	6.83E−03	±	3.85E−04
Sr	(mol/L)	4.59E−04	±	6.24E−05	4.63E−04	±	2.34E−05	3.51 E−04	±	2.30E−05
Cl	(mol/L)	3.27E−01	±	5.63E−03	2.76E−01	±	1.76E−02	1.24E−01	±	9.18E−03
Br	(mol/L)	5.54E−04	±	4.40E−04	4.63E−04	±	0.00E+00	1.94E−04	±	9.17E−06
S04	(mol/L)	1.68E−02	±	8.77E−04	1.26E−02	±	1.96E−03	7.79E−03	±	1.95E−03
Alkalinity	(eq/L)	4.00E−03	±	8.04E−04	1.22E−03	±	6.22E−04	3.35E−03	±	1.41E−03
Total CO2	(mol/L)	3.89E−03	±	5.60E−04	1.24E−03	±	6.61 E−04	4.47E−03	±	4.15E−03
Fe	(mol/L)	2.96E−05	±	1.19E−05	3.68E−06	±	6.03E−06	1.67E−06	±	6.36E−10
Al	(mol/L)		±		2.21E−06	±	2.74E−06	2.11E−07	±	2.26E−08
Si	(mol/L)	1.65E−04	±	4.91 E−05	5.74E−05	±	2.46E−05	1.69E−04	±	1.48E−04

are thought to be less subject to artefacts than those from the earlier boreholes which were constructed with fewer precautions. Therefore, the modelling in this paper has been tested against PC-C water chemistry. Modelling similar to that described here

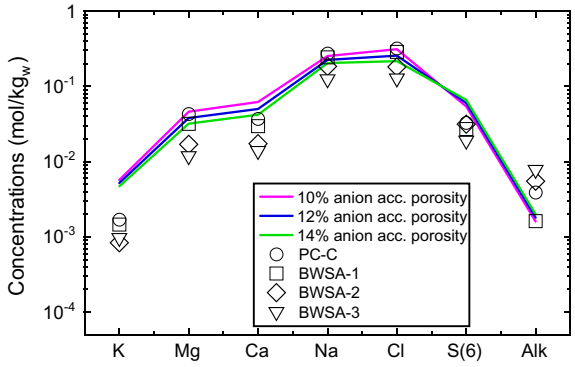

Fig. 2. Schoeller diagram comparing major ion compositions measured in samples from Mont Terri boreholes and shown in Table 1 with compositions calculated by Bradbury and Baeyens (1998) at 3 assumed values of anion-accessible porosities. Alkalinity (Alk) is given as HCO_3^-, S(6) represents SO_4.

has also been tested against the chemistry of BWSA-1 and -3 water as described in Chapter 3 of Wersin et al. (2009).

2. Equilibrium modelling of clay pore water

Calculations of clay–rock pore-water chemistry are based on equilibrium thermodynamic modelling of water–rock reactions which control the pore-water chemistry. Generations of studies of conventional ground waters have demonstrated equilibrium between the water and many aquifer minerals. Equilibrium between pore water and minerals in many clay rocks is even more likely than between ground waters and aquifer minerals because the residence times of pore waters in poorly-permeable clay rocks are typically considerably larger than those of ground waters. Furthermore, the grain size of reactive minerals in clay rocks is commonly smaller than that of typical aquifer rocks.

Gibbs' Phase Rule provides a convenient formal framework within which to discuss equilibrium modelling of clay pore water. It is written:

$$F = C + 2 - P \quad (1)$$

where F is the variance or the number of degrees of freedom of the system, C is the number of components, and P is the number of phases in equilibrium with each other. For a system at a fixed temperature and pressure in which all components are controlled by water–rock reactions, $P = C$, where P is the number of phases, including the solution.

Most ground waters and pore waters contain solutes such as Cl^- and Br^- that are commonly not controlled by water–rock reactions. In the absence of evaporite minerals, each of these solutes, which correspond to the "mobile" components of metamorphic petrology, adds a degree of freedom to the system (Thompson, 1955). To model equilibrium, the concentrations of free components must be fixed as must the system temperature and pressure.

Several types of reactions can be distinguished. One comprises homogeneous reactions in the solution phase such as ion-pairing, or solute speciation, and oxidation–reduction reactions. Two types of heterogeneous reactions are also considered. One includes mineral and gas dissolution and precipitation reactions which are also the dominant controls on ground waters. The other includes cation exchange reactions. While these also contribute to the properties of many ground waters, they are vital to understanding the behaviour of pore waters in clay rocks.

Calculations of mineral and gas equilibria with ground waters and of ion-pairing have been made for more than 40 a (e.g. Garrels and Christ, 1965; Garrels and Thompson, 1962). Reactions of these types are included in the aqueous computer modelling programs that are widely available and commonly used. Thermodynamic databases both for hand calculations and in formats compatible with aqueous modelling programs were developed to support the earliest calculations and are being continuously expanded and improved. Modelling techniques for these equilibria are so widely known as to require no additional discussion here.

Cation exchange reactions have long been recognized as important in controlling soil- and ground-water chemistry (e.g. Way, 1852; Foster, 1950; Pearson and White, 1967) but their inclusion in equilibrium computer models is more recent (Thorstenson et al., 1979; Appelo et al., 1989). Methods for modelling cation exchange reactions and for developing the often site-specific data needed are less well-known and will be discussed here.

2.1. Early modelling

2.1.1. Calculating water chemistry from core properties

The first modelling of pore water in the Opalinus Clay from Mont Terri was by Bradbury et al. (1997–1998) and Bradbury and Baeyens (1998). It was undertaken before water samples were available and was based on the properties of the rock itself. These authors assumed that the water would be in equilibrium with such reactive minerals as calcite, which are known to be in equilibrium with many ground waters. In addition, they expected the pore water to be in cation exchange equilibrium with the clay of the formation so that the exchangeable cation composition of the formation would be a "fingerprint" of the ratios of dissolved cations. Cation exchange equilibria had previously been considered in estimating the compositions of pore waters in the Boom Clay at the underground research laboratory operated by the Belgian Nuclear Research Centre (SCK·CEN) at Mol-Dessel, Belgium (Baeyens et al., 1985a) and in the Helvetic marls (Palfris formation) at Wellenberg, Switzerland (Baeyens and Bradbury, 1994).

The properties needed to support their modelling were the formation mineralogy and exchangeable cation populations, and the aqueous concentrations of "free" solutes such as Cl^-. These were measured on a sample from a core taken during the drilling of borehole BWSA-1 described above.

The mineralogy was based on microscopic and X-ray determinations. Bradbury and Baeyens (1998) determined the exchangeable cation contents by leaching with solutions of Ni-ethylenediamine (Ni-en) which displaces exchangeable cations. Leaching with pure water was also done at several rock-leachate ratios. "Mobile" solutes were identified as those with aqueous leachate concentrations that changed linearly with the rock-leachate ratio. When expressed per mass of rock leached, the concentrations of such solutes do not change with the rock-leachate ratio. These solutes were Cl^- and SO_4^{2-} which had concentrations of 12.3 ± 1.6 and 1.85 ± 0.2 mmol/kg rock, respectively, in the core sample examined. The apparent rock concentrations of other solutes varied with the rock-leachate ratio indicating reactions between the leachate and the rock.

To calculate the pore-water concentrations of Cl^- and SO_4^{2-} from their concentrations in the rock requires knowledge of the anion-bearing porosity of the rock as discussed by Pearson (1999) and Pearson et al. (2003, Annex 10). This information was not available to Bradbury and Baeyens (1998), so they assumed anion-bearing porosities from 10% to 14%. These led to pore-water concentrations from 0.216 to 0.394 mol/L (M) Cl^- and from 0.022 to 0.033 M SO_4^{2-} in their sample of core. It was necessary that the highest SO_4^{2-} concentrations, those corresponding to the lowest porosities, be adjusted downward during equilibrium modelling so that the calculated pore waters would not be oversaturated with respect to gypsum. Because gypsum is absent from undisturbed rock at Mont Terri, apparent gypsum saturation suggested that aqueous leaching overestimated the SO_4^{2-} content of *in situ* pore water.

Bradbury and Baeyens (1998) noted that although stringent precautions were taken to minimize contact of core material with the atmosphere, some oxidation of pyrite present in the Opalinus Clay could not be ruled out.

There are three sources for the cations contained in the Ni-en leachate solutions: cations displaced from exchange sites by the Ni-en, cations dissolved in the pore water in the sample, and cations resulting from mineral dissolution and precipitation reactions with the Ni-en leaching solution. Bradbury and Baeyens (1998) assumed that cation exchange reactions occurred more rapidly than dissolution/precipitation reactions. Thus, they calculated exchangeable cation occupancies from leachates made for the relatively short time of 7 days and corrected them for the solutes in the *in situ* pore water by assuming either that both Cl^- and SO_4^{2-} were balanced by Na or that Cl was balanced by Na and SO_4 by Ca. Although these assumptions led to different exchangeable cation populations and selectivity coefficients, their effects on the calculated water composition were within the range of those estimated from other laboratory uncertainties.

Cation exchange selectivity coefficients were found from the exchangeable cation populations and compositions of the aqueous leachate solutions. These were defined relative to Na and written:

$$K^{Na^+/K^+} = \frac{a_{Na^+}}{a_{K^+}} \times \frac{a_{KX}}{a_{NaX}} \quad \text{and} \quad K^{Na^+/M^{2+}} = \frac{a^2_{Na^+}}{a_{M^{2+}}} \times \frac{a_{MX_2}}{a^2_{NaX}} \tag{2}$$

In these equations, M^{2+} is any divalent cation, X represents a negatively charged exchange site and all quantities on the right are activities. Bradbury and Baeyens (1998) used the Gaines–Thomas convention in which activities of exchanged cations are assumed to equal their equivalent fractional occupancies (Gaines and Thomas, 1953). The selectivity coefficients were calculated using the solute activities in the aqueous leaching solutions that had reacted for 28 days. The corresponding exchangeable cation occupancies were derived from the inventory of exchangeable cations adjusted for the quantities of exchangeable cations extracted during the aqueous leaching. It was noted that the Ca/Mg activity ratio of the aqueous leachates decreased with leaching time until, by 28 days, it reached 1.35, the ratio for equilibrium between calcite and dolomite. From this ratio and the exchangeable Ca and Mg populations the Ca/Mg selectivity coefficient was calculated.

Ratios of dissolved cations were calculated from the selectivity coefficients and *in situ* exchangeable cation populations. The total cation content was calculated from the equation for solution electroneutrality:

$$m_{Na} + m_K + 2m_{Ca} + 2m_{Mg} = m_{Cl} + 2m_{Sulphate} \tag{3}$$

This equation is only approximate as it does not include minor species such as carbonate anions and minor metals.

In terms of Gibbs' Phase Rule, the system treated by Bradbury and Baeyens (1998) has 10 components: Cl, SO_4, CO_3, Na, K, Ca, Mg, F, Si and pH (H^+). Two of these, Cl and SO_4, were treated as free components and their concentrations were specified in the input. Seven reactive phases were considered: calcite equilibrium, the solution itself (corresponding to the electroneutrality constraint), exchangeable KX, exchangeable CaX_2, dolomite equilibrium, fluorite equilibrium, and quartz (chalcedony) equilibrium. One degree of freedom remained. This was accounted for by specifying the PCO_2.

The Cl and SO_4 concentrations were fixed at the values calculated from aqueous leaching of the core and the assumed porosity. The PCO_2 was fixed at 10^{-2} bars, a value chosen by expert judgment and supported by work of Hutcheon and Abercrombie (1990) and Coudrain-Ribstein and Gouze (1993). These authors proposed that the PCO_2 of waters in deep sedimentary basins could be explained by the reaction:

$$5\ \text{dolomite} + \text{kaolinite} + \text{quartz} + H_2O = \text{Mg-chlorite} + 5\ \text{calcite} + CO_2 \tag{4}$$

Using principally the thermodynamic data of Michard (1983), Coudrain-Ribstein and Gouze (1993) modelled this reaction at temperatures from 30 to 150 °C and compared the results with values measured on surface and borehole-sampled ground waters at temperatures from about 10 to 200 °C. At low temperatures (c. 10–30 °C) the modelled PCO_2 values were about 10^{-2} bars. With the PCO_2 fixed at this value the system as described by Bradbury and Baeyens (1998) was fully specified and could be modelled.

To reach their final water composition, Bradbury and Baeyens (1998) adjusted several parameters to optimize agreement between the modelled and measured exchangeable cation populations. Lowering the pH increased calcite and dolomite solubilities and so increased the dissolved and exchangeable Ca and Mg populations. The dissolved K concentration was chosen to match the measured exchangeable K population and Na was adjusted so that the full solution, now including carbonate species, silica, alumina and fluoride, would be charge balanced.

The compositions calculated by Bradbury and Baeyens (1998) at assumed anion-bearing porosities of 10%, 12% and 14% are illustrated in a Schoeller diagram in Fig. 2. The composition of water samples taken from boreholes discussed above are also shown. The PC-C and BWSA-1 boreholes have the highest Cl contents (0.33 and 0.28 mol/L (M), respectively) which correspond to Bradbury and Baeyens (1998) values calculated at an assumed porosity of about 10% (0.31 M Cl). There is general agreement between the composition derived by Bradbury and Baeyens (1998) and that of the high-salinity measured waters, which is as it should be considering that the core sample they characterized was from the BWSA-1 borehole. The modelled K is considerably higher than the measured value, as is the modelled SO_4. The modelled Ca/Mg ratio is greater than one while the ratio measured in water samples of similar salinity is less than one. The modelled alkalinity values agree with those of the BWSA-1 borehole but are lower than the values measured in the PC-C borehole of similar salinity and in the two lower-salinity samples.

2.1.2. Models calibrated against analysed pore-water chemistry

The modelling that followed the work of Bradbury and Baeyens (1998) was based on water samples collected from boreholes in the Mont Terri underground research laboratory and on exchangeable cation populations and selectivity coefficients measured on core samples across the entire section. The geochemical investigations at Mont Terri through 2001 are described in detail by Pearson et al. (2003, Annexes).

In the modelling of Pearson et al. (2003), Cl, Br and, in most cases, SO_4 were treated as free solutes in modelling the Mont Terri pore water. Chloride concentrations were fixed and the Br and SO_4 concentrations were chosen to correspond to their seawater ratios with the fixed Cl content. Because celestite ($SrSO_4$) appeared to be saturated in samples from the most saline boreholes (PC-C, BWSA-1), the effect of treating SO_4 as a solute controlled by celestite equilibrium was also examined.

The modelling performed on the borehole and squeezed samples collected during the first 4 years of Mont Terri underground research laboratory operation (1997–2001) is described in detail by Pearson et al. (2003, Chapter 5). The modelling attempted to reproduce the measured properties of the water samples using mineral equilibria and cation exchange reactions. This modelling will be described in the context of other models that have appeared in the literature for pore water in clay rocks.

Table 2
Correspondence between solution composition variables and constraints on their concentrations in various pore water equilibrium models.

	Coudrain-Ribstein and Gouze (1993), Tab 1 & Fig 5	Beaucaire *et al.* (2000)	Bradbury & Baeyens (1998)	Pearson *et al.* (2003), Table 5.8[d]	COX Reference model (Gaucher *et al.*, 2006, 2009)[a,b]	COX Alternate models (Gaucher *et al.*, 2006, 2009)[a,c]	PC-C pore-water calculation
	Dogger Aquifer, Paris Basin	Rupelian Aquifer and Boom Clay, Belgium	Opalinus Clay at Mont Terri, Switzerland	Opalinus Clay at Mont Terri, Switzerland	Callovo-Oxfordian (COx) at Bure, France	Callovo-Oxfordian (COx) at Bure, France	Opalinus Clay at Mont Terri, Switzerland
Source of thermodynamic data used	Michard (1983)	Principally Michard (1983)	Pearson and Berner (1991); Pearson *et al.* (1992)	Nagra/PSI Hummel *et al.* (2002)	THERMODDEM http://thermoddem.brgm.fr/index.asp?langue=GB	THERMODDEM http://thermoddem.brgm.fr/index.asp?langue=GB	THERMODDEM http://thermoddem.brgm.fr/index.asp?langue=GB
Element	*Constraint on element concentration*						
Cl^- Mobile element	Fixed at average value of water samples	Fixed	Calculated using bulk rock content from leaching and several estimated values of anion-accessible porosity	Fixed at average values measured in borehole samples	Calculated using bulk rock content from leaching and geochemical porosity evaluated from comparison of leachable Cl in clay-rich and carbonate-rich horizons	Calculated using bulk rock content from leaching and geochemical porosity evaluated from comparison of leachable Cl in clay-rich and carbonate-rich horizons	Fixed at average values measured in borehole samples
SO_4^{2-} Mobile or controlled element	Anhydrite saturation		Calculated using bulk rock content from leaching and several estimated values of anion-accessible porosity Decreased as necessary to avoid gypsum oversaturation	Fixed at SO_4/Cl ratio in seawater OR Calculated from celestite saturation and Na–Sr exchange (A3-C)	Calculated from leaching data, adjusted for consistency with celestite saturation and Na–Sr exchange	Calculated from leaching data, adjusted for consistency with celestite saturation and Na–Sr exchange	Fixed at SO_4/Cl ratio in seawater
Carbonate Mobile or controlled element	Dolomite saturation	Fixed at regional total carbonate	CO_3^{2-} from calcite saturation	pCO_2 fixed at values calculated from borehole sample data. OR CO_3^{2-} from dolomite saturation with Mg fixed by Na–Mg exchange (A3-E)	Calcite saturation	Calcite saturation	CO_3^{2-} from calcite saturation
pe (Electron)[e] Controlled element				SO_4^{2-}/S^{2-} couple at pyrite and siderite, goethite or $Fe(OH)_3$ (mic) saturation	SO_4^{2-}/S^{2-} couple at pyrite and daphnite (Fe-chlorite) saturation	SO_4^{2-}/S^{2-} couple at pyrite and daphnite (Fe-chlorite) saturation	SO_4^{2-}/S^{2-} couple at pyrite and siderite saturation
pH (H^+)[e] Controlled element	Solution electroneutrality	Solution electroneutrality	P_{CO2} fixed at generic value. Carbonate species and TIC calculated from CO_3^{2-}, P_{CO2}, and carbonate equilibria	Solution electroneutrality	Illite-Mg $K_{0.85}Mg_{0.25}Al_{2.35}Si_{3.4}O_{10}(OH)_2$,	Illite-Mg $K_{0.85}Mg_{0.25}Al_{2.35}Si_{3.4}O_{10}(OH)_2$, OR Illite_Imt-2 $(Na_{0.044}K_{0.762})(Si_{3.387}Al_{0.613})(Al_{1.427}Fe_{0.376}Mg_{0.241})O_{10}(OH)_2$,	Kaolinite, illite-Mg, Illite Imt-2Mg-montmorillionite Chlorite CCa-2 OR Daphnite saturation
Na^+ Controlled element	Albite saturation	Na feldspar saturation	Solution electroneutrality	Na–Ca exchange	Solution electroneutrality	Solution electroneutrality	Solution electroneutrality
K^+ Controlled element	K-feldspar saturation	K-feldspar saturation Feldspar properties chosen to match regional (Na)/(H) and (K)/(H)	Na–K exchange	Na–K exchange	Na–K exchange	Na–K exchange OR Illite-Mg saturation	Na–K exchange
Ca^{2+} Controlled element	Calcite saturation	Calcite saturation	Na–Ca exchange	Calcite saturation	Na–Ca exchange	Na–Ca exchange	Na–Ca exchange
Mg^{2+} Controlled element	Mg-chlorite saturation	Dolomite saturation	Dolomite saturation	Dolomite saturation AND (A3-E) OR (A3-D) Na–Mg exchange	Na–Mg exchange	Dolomite OR Illite-Mg, Illite_Imt-2 or Mg-montmorillonite saturation	Dolomite OR Na–Mg exchange
Sr^{2+} Controlled element				Na–Sr exchange	Na–Sr exchange ADJUSTED TO Celestite saturation	Na–Sr exchange ADJUSTED TO Celestite saturation	Celestite saturation
F^- Controlled element	Fluorite saturation		Fluorite saturation				
SiO_2 Controlled element	Chalcedony saturation	Chalcedony saturation	Chalcedony saturation	Quartz saturation	Quartz saturation	Quartz saturation	Quartz saturation
Al Controlled element	Kaolinite saturation	Kaolinite saturation		Kaolinite or halloysite saturation	Daphnite (Fe-chlorite) $Fe_5Al(AlSi_3)O_{10}(OH)_8$ saturation	Daphnite (Fe-chlorite) $Fe_5Al(AlSi_3)O_{10}(OH)_8$ OR Chlorite_Cca-2 $Mg_{2.97}Fe_{1.92}$, $Al_{2.49}$ $Ca_{0.01}Si_{2.63}O_{10}(OH)_8$ saturation	Kaolinite, illite-Mg, Illite-Imt2 Mg-montmorillionite

(*continued on next page*)

Table 2 (*continued*)

	Coudrain-Ribstein and Gouze (1993), Tab 1 & Fig 5	Beaucaire *et al.* (2000)	Bradbury & Baeyens (1998)	Pearson *et al.* (2003), Table 5.8[d]	COX Reference model (Gaucher *et al.*, 2006, 2009)[a,b]	COX Alternate models (Gaucher *et al.*, 2006, 2009)[a,c]	PC–C pore-water calculation
	Dogger Aquifer, Paris Basin	Rupelian Aquifer and Boom Clay, Belgium	Opalinus Clay at Mont Terri, Switzerland	Opalinus Clay at Mont Terri, Switzerland	Callovo-Oxfordian (COx) at Bure, France	Callovo-Oxfordian (COx) at Bure, France	Opalinus Clay at Mont Terri, Switzerland
Source of thermodynamic data used	Michard (1983)	Principally Michard (1983)	Pearson and Berner (1991); Pearson *et al.* (1992)	Nagra/PSI Hummel *et al.* (2002)	THERMODDEM http://thermoddem.brgm.fr/index.asp?langue=GB	THERMODDEM http://thermoddem.brgm.fr/index.asp?langue=GB	THERMODDEM http://thermoddem.brgm.fr/index.asp?langue=GB
							Chlorite CCa-2 OR daphnite saturation
Fe Controlled element				Siderite, goethite (A3-F) OR $Fe(OH)_3$ (mic) (A3-G) saturation	Na–Fe(II) exchange	Siderite saturation	Siderite saturation
Mn Controlled element				Rhodochrosite saturation			
U Controlled element				$UO_{2(s)}$ saturation			

[a] Minerals and properties modelled are those included in THERMODDEM (BRGM) database. See: Gaucher *et al.* (2009) Electronic Annex 1 or http://thermoddem.brgm.fr/index.asp?langue=GB.
[b] These associations are based on Electronic Annex 3 of Gaucher *et al.* (2009) and are consistent with Table 4 of that paper.
[c] These associations are based on Electronic Annex 4 of Gaucher *et al.* (2009) and are not entirely consistent with Table 4 of that paper.
[d] Designations in parentheses refer to modelling variations shown in Figs. 4 and 5 and discussed in Sections 2.1.3.2 and 2.1.3.3.
[e] Korzhinskii (1965) specifies H^+ and e^- as mobile components, but this is an *ad hoc* choice. His equations and those of Thompson (1955) show that any component can be mobile.

Table 2 illustrates the correspondence between pore-water chemical properties and constraints on them as represented in a number of pore water equilibrium models. The properties include the concentrations of all major and a few minor solutes as well as the pH and, in some cases, the redox potential of the solution. The constraints are mineral equilibria, cation exchange, fixed concentrations of free solutes and solution electroneutrality. In addition to models applied to Mont Terri waters, models described in the literature using different approaches to simulate pore waters in other systems are also included in Table 2.

2.1.2.1. Models including feldspars. Although the Bradbury and Baeyens (1998) and later models of Mont Terri pore waters include cation exchange, several models have been proposed for ground and pore waters from other locations in which feldspar equilibria were used instead of cation exchange. These are briefly discussed here because of their relevance to the broader question of the applicability of silicate mineral equilibria to the chemistry of low-temperature waters.

The first of these models is that used by Coudrain-Ribstein and Gouze (1993) to calculate PCO_2 values as functions of temperature in the Dogger of the Paris Basin. The PCO_2 value at 30 °C from this modelling was used in the calculations of Bradbury and Baeyens (1998). The PCO_2 was considered to be controlled by reaction (4), above, but in order to model this reaction, it was necessary to consider the full chemistry of the pore water. The first column of Table 2 illustrates the modelling scheme used. Chloride was considered a free anion and fixed at its average concentration in their ground-water samples. Sulphate concentrations were linked to equilibrium with anhydrite ($CaSO_4$), and Na, K, Ca and Mg to equilibrium with albite ($NaAlSi_3O_8$), K-feldspar or microcline ($KAlSi_3O_8$), calcite ($CaCO_3$), and Mg-chlorite ($Mg_3Al_2Si_3O_{10}(OH)_8$), respectively. Total carbonate was associated with dolomite ($CaMg(CO_3)_2$) and the pH with solution electroneutrality. The minor species SiO_2, F and Al were identified with fluorite (CaF_2), chalcedony (SiO_2) and kaolinite ($Al_2Si_2O_5(OH)_4$) equilibria. No redox calculations or concentrations of redox-sensitive elements were included in this modelling. The thermodynamic data used are shown in Table 2 of Coudrain-Ribstein and Gouze (1993) and were principally those of Michard (1983), with the dolomite equilibrium constant increased by 1.2 log units to represent disordered dolomite.

Calculations were made at temperatures from 30 to 180 °C and reasonably well reproduced the water chemistry and PCO_2 values measured in waters from the Dogger aquifer of the Paris Basin and PCO_2 values from other groundwater and geothermal systems (Coudrain-Ribstein and Gouze, 1993, Fig. 5). Modelling with two other sets of mineral constraints was also undertaken. With laumontite ($CaAl_2SiO_{12}{\cdot}4H_2O$) in place of Mg-chlorite, the calculated PCO_2 values were considerably below the measured values at all temperatures. With illite ($K_{0.6}Mg_{0.25}Al_{2.3}Si_{3.5}O_{10}(OH)_2$) replacing Mg-chlorite, PCO_2 values agreed with those from Paris Basin samples, all of which were between about 45 and 80 °C, but were far below values measured in higher-temperature waters.

The second model was developed by Beaucaire et al. (2000) to explore controls on the chemistry of pore water from the Boom Clay at the Mol URL and of a more Cl-rich water from the Rupelian aquifer, which underlies the Boom Clay. The second column in Table 2 describes the modelling scheme. The Cl and total CO_3 contents were fixed at values typical of those of water samples from the two formations. The cations modelled were Si, Al, Na, K, Ca and Mg. These were associated with the minerals chalcedony, kaolinite, albite, microcline, calcite and dolomite. The pH was associated with solution electroneutrality. With the fixed total carbonate and modelled pH values, the alkalinities could also be calculated for comparison with the measured values.

Beaucaire et al. (2000, Table 4) compare thermodynamic data on the minerals and selected aqueous species used in their model with values given in the data compilations of Michard (1983) and Bowers et al. (1984), and in the SUPCRT database (Johnson et al., 1992; http://geopig.asu.edu/) and the database for the aqueous modelling program MINTEQ. In their modelling, Beaucaire et al. (2000) principally use mineral data from Michard (1983) except for albite and microcline. Their values for the feldspars are different from those in any of the data sets. They were chosen so that they led to an a_{Na^+}/a_{K^+} ratio like those observed in pore waters and aquifer waters from the units being modelled.

Beaucaire et al. (2000) discuss the inclusion of Mg-chlorite in the models of Hutcheon and Abercrombie (1990) and of Coudrain-Ribstein and Gouze (1993) but point out that the stability constants for this mineral in the databases they considered range from −16.16 (Michard, 1983) to −22.57 (Bowers et al., 1984). PCO_2 values calculated using these values are −1.87 and −3.11 log bars, respectively. Although the former value is consistent with those of samples from the Rupelian aquifer, Beaucaire et al. (2000) choose not to include Mg-chlorite in their modelling but instead specified total CO_3 and associate Mg concentrations with dolomite equilibrium.

Beaucaire et al. (2000) also discuss the exclusion of clay minerals from their modelling despite the fact they make up more than 50% of the Boom Clay. They felt unable to include clay mineral equilibrium because it was not clear whether to treat clays as phases of defined compositions or as solid solutions. They also considered treating the clays as cation exchange substrates. In this case, if exchange selectivity coefficients and *in situ* cation populations were known, ratios of exchangeable cations in solution could have been calculated as was done by Bradbury and Baeyens (1998). Sufficient data were available for Beaucaire et al. (2000) to calculate Mg and Ca concentrations. These were within an order of magnitude of measured values, but did not agree nearly as well with them as those calculated using the equilibrium model described in Table 2. These authors also felt that because the cation exchange model is dependent on the quantities of solids present (i.e. the *in situ* populations of the exchangeable cations), it is not formally as well constrained a model for water chemistry as one based on equilibrium with pure phases like the feldspars.

Gaucher et al. (2009) consider feldspar equilibrium in discussing their model for COx pore-water chemistry. Their Fig. 6 shows that the exchangeable Na and K contents measured in COx samples are inconsistent with feldspar equilibrium in this formation. Fig. 3 compares $\log(a_{Na^+}/a_{K^+})$ values of samples from the Mont Terri boreholes BWSA-3, BWSA-1, and PC-C with values corresponding to equilibria with feldspars with the properties given in various thermodynamic databases and used by Beaucaire et al. (2000). This illustrates that feldspar equilibrium is inconsistent with the chemistry of Mont Terri pore water as it is with that of COx pore water.

It is of interest to explore why feldspar equilibrium does not prevail in Opalinus Clay and COx pore waters while it is apparently important in the waters modelled by Coudrain-Ribstein and Gouze (1993). A possible explanation can be found in the work of Stefánsson and Arnórsson (2000) who examined the saturation states of albite and microcline in a number of natural waters with temperatures ranging to over 300 °C. They found reasonable agreement between measured and calculated Na/K ratios for waters down to temperatures of about 50 °C. In lower temperature waters, though, the measured Na/K ratios, like those in Fig. 3, were lower than the calculated values (Stefánsson and Arnórsson, 2000, Fig. 6). They concluded that feldspar equilibrium was not common at temperatures below about 50 °C. Because the water temperature at Mont Terri is about 13 °C and that of the COx samples about 25 °C, below the lowest temperature at which Stefánsson and Arnórsson (2000) found feldspar equilibrium, the lack of feldspar equilibrium in samples from these sites is not surprising.

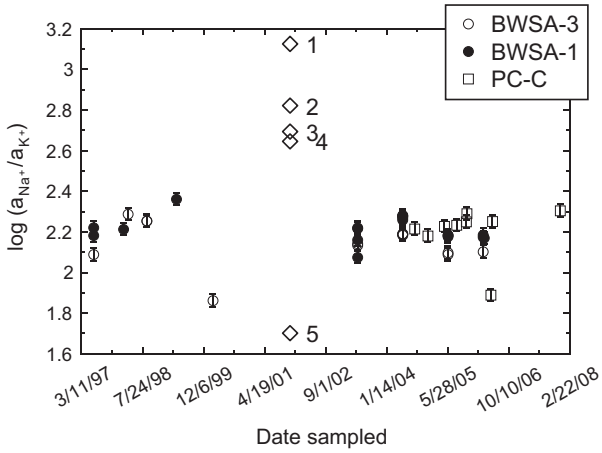

Fig. 3. Comparison of K/Na ratios measured in Mont Terri borehole waters (circles and squares) with ratios calculated using thermodynamic data for albite and K-feldspar from various compilations of thermodynamic data (diamonds). (1) Value from SUPCRT (from PHREEQC llnl.dat). (2) Value from Stefánsson and Arnórsson (2000, Table 2). (3) Value from THERMODDEM database. (4) Value from Coudrain-Ribstein and Gouze (1993, Table 2) and Michard (1983). (5) Value from Beaucaire et al. (2000, Table 4).

2.1.2.2. Modelling with cation exchange. The third column in Table 2 summarizes the modelling of Bradbury and Baeyens (1998) and of Bradbury et al. (1997–1998) described above. Note that in this model and those that follow in Table 2, cation exchange rather than feldspar equilibrium is used.

The fourth column summarizes the modelling undertaken by Pearson et al. (2003) as part of their compilation and interpretation of pore-water chemical data collected at Mont Terri through 2001. For several reasons this modelling could be considerably more extensive than previous modelling. First, analyses of additional pore-water solutes were available including trace elements and redox-sensitive species such as Fe, Mn and U. This made it possible to include redox reactions in the modelling. Second, field measurements were made of ephemeral properties of the borehole water such as its pH and Pt-electrode potentials. Finally, both laboratory and field measurements of the gas contents of pore water were also made which provided additional definition of the dissolved carbonate system.

Pearson et al. (2003, Section 5.4.1) describe the 2003 modelling approach in detail as it was applied to waters from the BWSA-1 and BWSA-3 boreholes. It was carried out using PHREEQC (Parkhurst and Appelo, 1999) with the Nagra/PSI thermodynamic database (Hummel et al., 2002) and can be exemplified by the modelling of the BWSA-3 borehole waters. The measured composition of the borehole waters is shown in Table 1 and Fig. 2. BWSA-3 water is also illustrated in Fig. 4 where it is compared with results of various models.

The average Cl content of the BWSA-3 borehole is 0.12 mol/kg_w. This corresponds to 23% of the Cl content of seawater. A water containing 23% of the solutes in sea water is shown in Fig. 4 and was the starting water for the modelling. The differences between the pore-water composition and seawater shown in that figure are as expected from diagenetic reactions. The aragonite and calcite originally precipitated from seawater contain a certain amount of Mg and Sr. Recrystallization of these early carbonates together with dolomitization increases the relative Sr content of the pore water and shifts the Ca/Mg ratio from its initially low value to a ratio slightly greater than one.

The nominal constraints on the 2003 modelling are those listed in column 4 of Table 2. These consisted of cation exchange for Na/Ca, Na/K and Na/Sr ratios and saturation with respect to calcite, dolomite, quartz and kaolinite. Solution electroneutrality was also

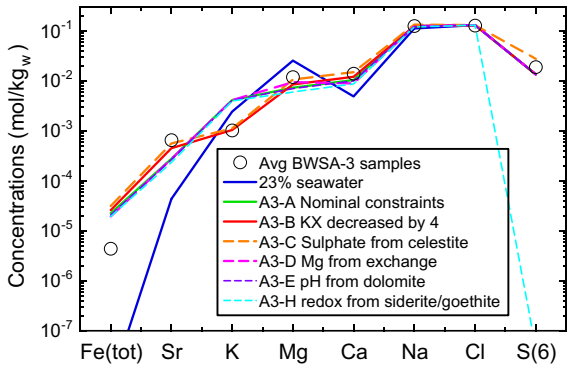

Fig. 4. Schoeller diagram comparing average measured BWSA-3 major solute compositions with results of models with different constraints. Designations of constraint sets refer to Table 5.10 of Pearson et al. (2003) and are given in the text.

a constraint and was associated with pH. The PCO_2 value establishes total carbonate content and alkalinity. PCO_2 was fixed at $10^{-2.2}$ bars which was an average of values calculated from pH and alkalinity measurements of the borehole samples. The nominal constraints on redox-sensitive solutes included control of the redox state of the solution by the S(VI)/S(-II) couple. S(VI) corresponds to the SO_4 concentration of the solution, and S(-II) is based on pyrite solubility. To calculate pyrite solubility requires an Fe concentration. In the nominal case, this was calculated by specifying saturation with siderite, a mineral present at about 2 weight% throughout the Opalinus Clay (Pearson et al., 2003, Annex 9).

Measured and modelled major solute compositions are shown in Fig. 4. The results of modelling with several sets of constraints are included, selected from a more extensive group shown in Table 5.10 of Pearson et al. (2003).

With a few exceptions, the nominal model (designated A3-A in Fig. 4 and Pearson et al., 2003) is generally consistent with the measured composition. The modelled K is considerably higher than that measured. Both Mg and Ca are somewhat lower than the measured values. The modelled Sr is lower than the measured value. The SO_4 and alkalinity are also lower than the measured values.

The effects of variations on some of the constraints on the nominal model are also shown in Fig. 4:

- Variation A3-B was an attempt to match the modelled K concentration to the measured values. Following Eq. (2) this could have been done by raising the selectivity coefficient or by lowering the exchangeable K content. The latter alternative was chosen and the exchangeable K population was arbitrarily reduced by a factor of 4 bringing the modelled K concentration into agreement with the measured value. As shown in Section 2.2.2, however, the wiser choice would have been to raise the selectivity coefficient.
- In all variations but A3-D, dolomite equilibrium is specified fixing the dissolved Mg concentration and, consequently, the exchangeable Mg population. In variation A3-D, dolomite saturation is not specified so the Mg concentration is established by the exchangeable Mg population which is specified in the input. The resulting dissolved Mg concentration is higher and is closer to the measured value than in the nominal case but the Ca/Mg ratio is less than one while that measured in BWSA-3 borehole water is greater than one.
- In variation A3-E, dolomite saturation is enforced and there is no initial PCO_2 constraint in the modelling so the total carbonate content is established by dolomite equilibrium. The resulting modelled Mg and Ca contents are nearly the same as in the nominal case but the alkalinity is considerably below both the measured value and those modelled in all other variations. The PCO_2 calculated in this variation is −3.8 log bars, considerably below the measured −2.2 log bars. The calculated pH is 8.2, well above the average measured value of 7.4
- In variation A3-C, the SO_4 concentration is established by celestite saturation rather than being fixed in the input. This produces a SO_4 concentration about 30% higher than the measured value and about 50% higher than the SO_4 concentration input to the other model variations, which corresponded to the SO_4/Cl ratio of seawater. The higher SO_4 requires higher cation concentrations to maintain solution electroneutrality. This raises the Mg, Ca and Sr concentrations to values closer to those of the pore water than in the nominal modelling scenario. The fact that the BWSA-3 pore water SO_4 is higher than that corresponding to a seawater SO_4/Cl ratio is also evident in Fig. 1. As discussed in Section 2.2.1, BWSA-3 borehole water is undersaturated with respect to celestite, assuming the solution concentrations and the activity corrections and celestite equilibrium constant in the database are correct. Thus, while variation A3-C reproduces the measured cation composition better than the nominal scenario or any of the other variations, it still does not completely represent formation controls on the pore-water chemistry.

2.1.2.3. Redox modelling. Fig. 5 compares the measured concentrations of the redox-sensitive elements U, Fe and Mn to those modelled with different sets of constraints. In all variations, U is established by uraninite (UO_2) saturation. Although this mineral has not been observed in Mont Terri rock, U concentrations in many ground waters are consistent with equilibrium with it. At U concentrations in the range of those measured, dissolved U is dominantly in an oxidized redox state, principally U(VI) (Langmuir, 1997). Thus, the different modelled U concentrations represent differences in the redox potentials produced by several redox-controlling reactions tested.

In all variations, Mn concentrations are associated with rhodochrosite ($MnCO_3$) saturation. No pure Mn minerals have been identified in the formation but Mn(II) is commonly present in carbonate minerals such as dolomite or ankerite (Deer et al., 1992). The fact that the Mn concentrations of all model variations are nearly the same indicates that Mn is present as Mn(II) over the entire range of redox conditions tested. The fact that the modelled and measured concentrations are similar suggests that Mn control by a carbonate mineral is a reasonable hypothesis.

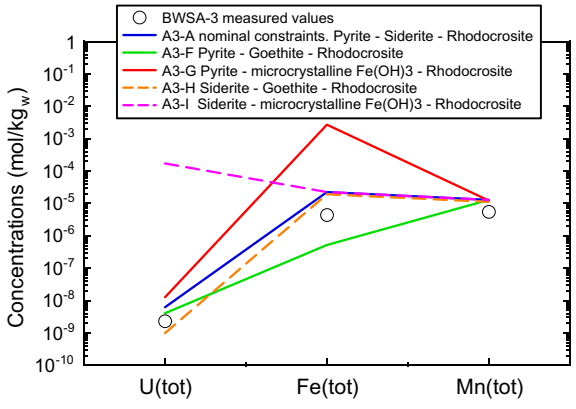

Fig. 5. Schoeller diagram comparing average measured BWSA-3 redox-sensitive solute concentrations with results of models with different constraints. Designations of constraint sets refer to Table 5.10 of Pearson et al. (2003) and are given in the text.

Three minerals were tested as controls on dissolved Fe concentrations: siderite ($FeCO_3$), goethite (FeOOH) and micro-crystalline ferric hydroxide ($Fe(OH)_3$). Siderite is present in the clays at Mont Terri. The ferric solids have not been specifically identified there but are common phases in Fe-bearing systems.

In the nominal scenario, A3-A, the redox state is specified by the SO_4/sulphide couple. Sulphate is fixed at the seawater SO_4/Cl ratio in the scenarios shown in Fig. 5, and sulphide by pyrite saturation. Three alternate scenarios differ in the equilibria controlling their dissolved Fe concentrations. Goethite control (A3-F) leads to the lowest Fe and so to the highest sulphide concentration at pyrite saturation. This, in turn, produces the lowest redox potential and, consequently, the lowest dissolved U concentration. Micro-crystalline $Fe(OH)_3$ control (A3-G) leads to the highest Fe and, consequently, to the lowest sulphide concentration and highest redox potential. This, in turn, produces the highest U concentration. In all other scenarios, siderite control is used leading to intermediate Fe concentrations.

In two of the scenarios, redox was established by the Fe(III)/Fe(II) couple with the Fe(II) concentration controlled by siderite. In variation A3-I, Fe(III) is controlled by micro-crystalline $Fe(OH)_3$ and in variation A3-H by goethite. The former leads to a relatively high Fe(III) which produces a high redox potential and a U concentration far above the measured value. The Fe(III) concentration in equilibrium with goethite is low, leading to a sulphide concentration at pyrite saturation high enough that sulphide rather than SO_4 is the dominant S species. This variation is also shown in Fig. 4 illustrating a modelled SO_4 concentration far below that measured. The fact that neither a goethite nor a micro-crystalline $Fe(OH)_3$ model leads to solute concentrations resembling those measured is consistent with the fact that neither phase has been observed in samples which have been preserved from oxidation.

2.1.3. Summary of shortcomings of early modelling

The 2003 modelling provided insights into the details of processes controlling the pore-water chemistry at Mont Terri and successfully reproduced many of the measured properties of the pore water. However, several questions remained including:

- While it is clear that the water is moderately reducing, with Mn(II), Fe(II), U(VI) and S(VI) the dominant redox states of the solute species of their respective elements, the specific minerals or solid solutions that control the concentrations of redox-sensitive species are not known;
- The relationship between Sr and SO_4 concentrations and celestite equilibrium in the less saline waters;
- The inability to model the dissolved K concentration with the cation exchange properties measured;
- The lack of consistency between measured Mg and Ca concentrations and ratios, and those modelled using Na/Mg exchange and dolomite saturation;
- An inability to reproduce the measured carbonate chemistry and pH of the pore water using mineral–water reactions alone. Successful modelling of carbonate and pH required that the PCO_2 or some other carbonate property such as total dissolved carbonate be specified in the model input.

To further clarify the reactions influencing the redox state will require additional petrographic and mineralogical study of the formation before the modelling can be improved. As this is not yet available, only the last 4 of these questions are addressed in the more recent modelling discussed here.

2.2. Recent advances

Advances in modelling have been made possible by improvements in the understanding of cation exchange processes, and by the availability of samples from the PC-C borehole and of additional samples from the BWSA series boreholes. A second set of samples from the BWSA series boreholes was taken roughly annually from May 2003 through March 2006. The analyses of these samples are given in the electronic annex of Wersin et al. (this issue) and are included in the averages in Table 1. Water samples and *in situ* measurements of pH and gas compositions were collected from the PC-C borehole from August 2004 through December 2007. These measurements are described and the water chemical data are given by Vinsot et al. (2008a) and the averages are included in Table 2. The recent modelling is described as it has been applied both at Mont Terri (Wersin et al., 2009) and to water from Callovo-Oxfordian (COx) sediments from the underground research laboratory operated by Andra at Bure (Gaucher et al., 2006, 2009).

The recent modelling has examined the controls on the Sr and SO_4 concentrations and on the dissolved K concentrations. It has also explored dependencies among Ca and Mg concentrations, carbonate mineral and cation exchange equilibria, and measured pH and PCO_2 values. While pH and PCO_2 are certainly related through equilibria in the carbonate system, their measurement on borehole water samples and on core samples are difficult and the results may not be consistent. Finally, the modelling addressed the extent to which pH and PCO_2 values could be modelled using silicate mineral equilibria like those proposed by Hutcheon and Abercrombie (1990) and used by Coudrain-Ribstein and Gouze (1993).

The modelling described by Pearson et al. (2003) was done using PHREEQC (Parkhurst and Appelo, 1999) and the Nagra/PSI thermochemical database (Hummel et al., 2002). The modelling discussed in the remainder of this paper was also done using PHREEQC but with the BRGM (THERMODDEM) database (Blanc et al., 2007). Results of modelling using the two databases are closely similar but the BRGM database includes a number of aluminosilicate minerals not present in the Nagra/PSI database.

2.2.1. Strontium and sulphate

In most of the 2003 modelling of samples from the BWSA series of boreholes, SO_4 was treated as a free solute with concentrations generally fixed at the SO_4/Cl ratio of normal seawater. Equilibrium with celestite was included in variation A3-C of the modelling, in which case SO_4 was a controlled solute (Table 2, Fig. 4).

Gaucher et al. (2009) concluded that water in the COx is saturated with celestite, which is present throughout the section studied. With Sr fixed by cation exchange, SO_4 concentrations are determined by celestite equilibrium.

Pore waters from the BWSA-1 and PC-C boreholes are saturated with respect to celestite, while those from the BWSA-2 and BWSA-3 are undersaturated (Pearson et al., 2003; Wersin et al., 2009). Celestite is reported in two core samples with pore-water Cl contents similar to that of the BWSA-1 borehole water (Pearson et al., 2003, Section A9.4). Celestite has not been reported from lower-Cl parts of the system, but no systematic search for it has been conducted so it could be present in small amounts. Celestite is also not reported from the PC borehole overcore, but again, no systematic search for it has been conducted (Koroleva et al., this issue). Wersin et al. (this issue, Section 3.5) point out that while the dissolved Sr concentrations of the borehole water remained relatively constant throughout the PC experiment, celestite became increasingly undersaturated as the dissolved SO_4 concentration decreased. This is consistent with the lack of evidence for celestite in the core.

No gypsum was observed in Mont Terri rocks except for small amounts on fracture surfaces of samples taken from or near the tunnel wall where partial desaturation and oxidation may well have occurred. The probable explanation for the gypsum oversaturation noted by Bradbury and Baeyens (1998) in their modelling is

that pyrite oxidation took place in the core before or during leaching producing higher SO_4 contents in aqueous leachates. Modelling to gypsum saturation would lead to the higher modelled-than-measured SO_4 contents evident in Fig. 2.

Fig. 1 shows that the SO_4/Cl ratios of the BWSA-2 and BWSA-3 waters are above that of seawater. These samples are undersaturated with celestite so the SO_4 they contain above that corresponding to the seawater SO_4/Cl ratio could have come from celestite dissolution. Modelling the BWSA-3 water at celestite saturation led to a dissolved SO_4 concentration above the measured value (Scenario A3-C, Fig. 4). If the SO_4 above that corresponding to the seawater ratio came from celestite dissolution, there could not have been sufficient celestite originally present to bring the waters to saturation and celestite should be absent from the formation where celestite-undersaturated waters are found.

As mentioned above, the distribution of pore-water salinity at Mont Terri can be explained as the result of diffusion of salts from an initial pore water of seawater composition to fresh-water bounding aquifers. Because of its size and charge, SO_4 diffuses more slowly than Cl (e.g. Appelo et al., 2008, Table 3). Thus, if the SO_4 concentration was determined only by diffusion, the SO_4/Cl ratios of the pore waters increase above that of seawater as the Cl content decreases. This is not the case for samples from the most saline boreholes (PC-C and BWSA-1), for which pyrite oxidation can be confidently ruled out, so some reaction must be occurring that decreases SO_4 relative to Cl. Waters from these boreholes are saturated with celestite so the most likely reaction is celestite precipitation. As diffusion proceeds and the salinity decreases, so will the Sr content which is controlled by cation exchange. At some point, Sr will drop below the level required for celestite precipitation and the SO_4/Cl ratio will increase as the Cl content decreases. Waters from the BWSA-1 and PC-C boreholes with highest Cl contents are saturated with respect to celestite. Water from the BWSA-1 and BWSA-3 boreholes have lower Cl contents, are undersaturated with respect to this mineral and have somewhat higher SO_4/Cl ratios.

If the Opalinus Clay was to be modelled based on rock properties alone, the presence of Sr as an exchanged cation and of celestite in at least a few core samples would indicate that SO_4 should be modelled as controlled by celestite saturation. Assuming correct Sr exchange properties, this would lead to correct SO_4 concentrations for high Cl waters (Table 5) and to SO_4 concentrations that are high by about 30% in waters with Cl contents as low as BWSA-3 (Fig. 5; Pearson et al., 2003, Table 5.10).

2.2.2. Potassium concentration control

In the early modelling of Bradbury and Baeyens (1998) and Pearson et al. (2003), K concentrations were based on Na/K exchange using measured, exchangeable K populations and Na/K selectivity coefficients measured on Mont Terri core samples or from the literature (Tables 3 and 4). The measured K concentrations were considerably below those calculated (Figs. 2 and 4) but could be reproduced by modelling with an exchangeable K concentration lower by a factor of 4 than the measured value (Fig. 4, model A3-B). This arbitrary correction was an unsatisfactory solution so laboratory work was undertaken to improve understanding of potassium and other cation exchange.

Selectivity coefficients measured on and used for modelling Mont Terri samples are shown in Table 4. In the earlier modelling, a single exchange site was considered with selectivity coefficients that were independent of the exchangeable cation populations. Laboratory studies on the clay-size fraction of a core sample from Mont Terri showed that the distribution of K could better be described by a model that included two exchange sites (Pearson et al., 2003, Section A3.6). However, these results were not taken into account in the modelling described in that report.

Multi-site exchange models proved to be very efficient in predicting the Cs sorption capacity of illite-containing materials by cation exchange reactions (Poinssot et al., 1999; Bradbury and Baeyens, 2000; Steefel et al., 2003). Such models include competition between K^+ and Cs^+ for sorption on the same sites. In particular, both K^+ and Cs^+ were shown to sorb on high and low affinity sites where the high affinity sites are less numerous than the low affinity sites. *In situ* fractional exchangeable K occupancies of Opalinus Clay samples measured by several laboratories ranged from 0.05 to 0.10 (Pearson et al., 2003, Table A3.12). Under these conditions, high affinity sites prevail over low affinity sites explaining why high selectivity coefficients are needed for Na/K exchange reaction. More recently, Tournassat et al. (2007, 2008, 2009) describe cation exchange on illite and on smectite and mixed-layer illite/smectite minerals based on their own and on literature data. For illite they tested two models, a two-site model with constant Gaines–Thomas selectivity coefficients, and a one-site model which included surface species activity coefficients. The latter led to selectivity coefficients that varied with the exchangeable cation population.

Fig. 6 compares Na/K selectivity coefficients measured on the <2 μm fraction of Opalinus Clay and on illite type Imt-2 from the Source Clay collection with values from the one-site Na/K model of Tournassat et al. (2009). Extrapolation of the curves in Fig. 6 to K occupancies from 0.05 to 0.1 indicates selectivity coefficients of about 0.9 or greater for Mont Terri samples and from about 1.1 to 1.2 for Imt-2. A more complete model that considers the effects of exchanged divalent cations on the Na/K selectivity coefficient has also been developed by Tournassat et al. (2009). Its application to an exchanger with the measured cation population shown in Table 3 led to a selectivity coefficient of 1.0. The model of Bradbury and Baeyens (2000) results in an even higher $\log K_{G-T}^{Na/K}$ value of 1.5 as the K occupancy becomes very small, but this model does not predict the decrease in the selectivity coefficient as the K occupancy exceeds about 0.6 (Fig. 6).

Fig. 3 shows $\log(a_{Na^+}/a_{K^+})$ for samples of the PC-C, BWSA-1, and BWSA-3 boreholes. Two samples have values below 2.0 due to exceptionally high reported K contents. It is assumed these are due to analytical artefacts and the samples are excluded from further consideration. The figure shows a pattern of increasing Na/K ratios for the BWSA-1 and BWSA-3 samples taken during the first two years and for all the PC-C samples. Ratios of BWSA-1 and BWSA-3 samples taken from 2003 to 2006 vary somewhat but there is no pattern of change with time and these ratios are all in the range of those of the earlier samples. The ratios of samples from all 3 boreholes overlap within one standard deviation. The mean and two standard deviation values of all but the two outlying $\log(a_{Na^+}/a_{K^+})$ values is 2.2 ± 0.2.

Eq. (2) for the Na/K selectivity coefficient can be written as:

$$\log K_{G-T}^{Na/K} = \log(a_{Na^+}/a_{K^+}) + \log E_{KX}/E_{NaX}) \quad (5)$$

where $\log(E_{KX}/E_{NaX})$ is the ratio of the exchanged ion population in equivalents and $\log K_{G-T}^{Na/K}$ is the log of the Gaines–Thomas selectivity coefficient.

Exchangeable Na and K populations measured on a number of samples from Mont Terri by several laboratories are given by Pearson et al. (2003, Tables 3.11 and 3.12) and are summarized in Table 3. From the measured values in this table the mean $\log(E_{KX}/E_{NaX})$ value is −0.89 ± 0.10. From Eq. (5), the $\log K_{G-T}^{Na/K}$ value corresponding to this $\log(E_{KX}/E_{NaX})$ and to the mean $\log(a_{Na^+}/a_{K^+})$ of 2.2 ± 0.2 from Fig. 3 is 1.3 ± 0.2.

Comparison with the values in Table 4 shows that this $\log K_{G-T}^{Na/K}$ value is considerably above the values measured on Mont Terri samples and those used for the 2003 modelling, but overlaps the values measured on and used for modelling COx samples. It also

Table 3
Exchangeable cation exchange populations measured on Opalinus Clay core samples from Mont Terri.

	Measured on core samples (Pearson et al., 2003, Table A3-11)		Used in modelling by Pearson et al. (2003)	Measured on PC core samples (Koroleva et al., this issue)	Used in PC-C modelling, Section 2.2.4.2
	Avg.	SD	BWSA-3 (Table 5.10)		
NaX	0.485	0.015	0.5	0.51	0.51
KX	0.062	0.005	0.08	0.09	0.09
MgX_2	0.182	0.008	0.17	0.19	0.19
CaX_2	0.274	0.019	0.24	0.21	0.21
SrX_2	0.010	0.001	0.01		
MgX_2/CaX_2	0.66		0.71	0.90	0.90
Log (E_{Mg}/E_{Ca})	−0.18		−0.15	−0.04	−0.04

Table 4
Cation exchange selectivity coefficients measured and used in modelling pore waters from the Opalinus Clay at Mont Terri and the COx at Bure.

	Pearson et al. (2003) Table 5.3					Used in PC-C modelling Section 2.2.4.2	Used for COx modelling in Gaucher et al. (2009), Table 3
	Measured on Opalinus Clay samples by:				Generic values given in PHREEQC database and used for 2003 modelling of BWSA-1 and BWSA-3		
	Unibern	CIEMAT	PSI	BRGM			
log Na/K	0.75	0.84	0.7	0.63	0.7	1.4	1.2
log Na/Mg	0.57	0.6	0.59	0.62	0.6	0.7	0.7
log Na/Ca	0.7	0.79	0.67	0.8	0.8	0.7	0.7
log Na/Sr	0.47	0.71			0.91	0.7	0.6
log Na/Fe					0.44	0.7	0.8

overlaps the range of selectivity coefficients calculated for illite Imt-2 but is slightly above those calculated for Mont Terri with the model of Tournassat et al. (2009) and slightly below those calculated with the model of Bradbury and Baeyens (2000) as shown in Fig. 6.

As Eq. (5) shows, the measured $\log(a_{Na^+}/a_{K^+})$ value would be consistent with the lower $\log K_{G-T}^{Na/K}$ values used in the earlier modelling and proposed by Tournassat et al. (2009) for illite from the Opalinus Clay if the exchangeable K content of the clay ($\log(E_{KX}/E_{NaX})$) was lower than the measured value used in the modelling. Scenario A3-B (Fig. 4) showed that lowering the exchangeable K population by a factor of 4 would give the measured, dissolved K concentration. It seems unlikely that the measurement of exchangeable cation populations would be this much in error. Thus, the incorrect K concentrations in the earlier modelling must be attributed to the use of an incorrectly low value for $\log K_{G-T}^{Na/K}$.

The recent work cited illustrates the improved understanding of Na/K exchange since the earlier modelling. This results principally from the realization that Na/K selectivity coefficients vary with the exchangeable K population and that the low K contents of the Mont Terri clays are associated with log K values of 1.0–1.4, higher than the values of around 0.7 found in the literature and used for the earlier modelling. The generic models developed by Tournassat et al. (2007, 2009) give an estimate for $\log K_{G-T}^{Na/K}$ values that reduces the difference between modelled and measured K concentrations. The agreement is, however, not perfect. Using a predicted log K value of 1 instead of a value of 1.3–1.4 (based on borehole pore water and core sample analyses) increases the calculated K concentration by a factor 2–3. This problem is inherent to a generic model that is calibrated on a wide range of data obtained on materials similar to but not identical with site material. The model of Bradbury and Baeyens (2000) gives approximately the expected $\log K_{G-T}^{Na/K}$ value but is not able to describe laboratory data at higher K occupancies. Even though neither of these two modelling approaches gives perfect results, they demonstrate that changes in cation exchange selectivities with exchanger composition (as well as with the nature of material and perhaps the nature of the counter-ions and salinity, Baeyens and Bradbury, 2004) must be taken into account

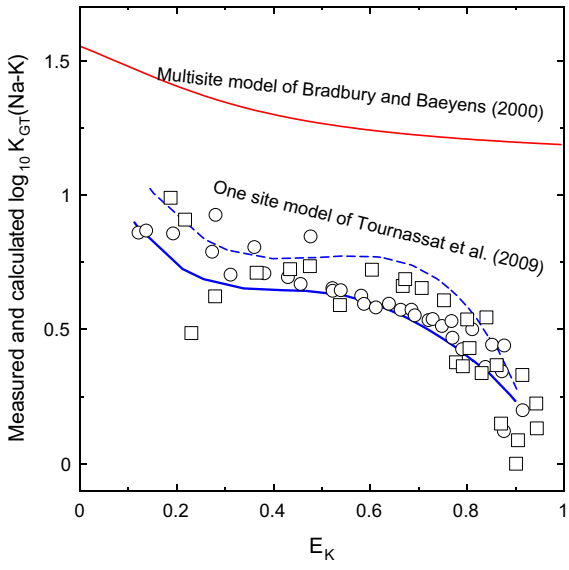

Fig. 6. Comparison of measured and calculated Na/K exchange selectivity coefficients as a function of K occupancy on Source Clay illite Imt-2 (square: data; dashed blue line: model from Tournassat et al., 2009) and <2 μm fraction of Opalinus Clay from Mont Terri (circles: data; plain blue line model from Tournassat et al., 2009) Modified from Fig. 15 in Tournassat et al., 2009. Prediction using the model from Bradbury and Baeyens (2000) is given for comparison (red plain line). (For interpretation of the references to colour in this figure legend, the reader is referred to the web version of this article.)

in predictive modelling. For this reason, a best independent measurement of selectivity coefficients value could be obtained by performing exchange experiments with an equilibrium solution having a composition similar to the pore-water composition instead of a binary solution (e.g. Na–K) at low ionic strength (low ionic strength conditions are usually necessary in these experiments to reduce the error bands on the determination of selectivity coefficient values, see Tournassat et al., 2009). Gaucher et al. (2009) performed such experiments on COx clay fraction and showed that selectivity coefficient values given by generic predictive models

were in quite good, although not perfect, agreement with values measured in these experiments (see Table 3 of this reference). For the present work, these experiments were not performed but selectivity coefficients can be calculated from borehole water and core sample exchanger composition analyses, resulting in a $\log K_{G-T}^{Na/K}$ value between 1.2 and 1.4. This last value is used in the following.

2.2.3. Carbonate mineral equilibria and calcium/magnesium exchange

Calcite is present in significant amounts (about 10–40%) throughout the Opalinus Clay (Pearson et al., 2003, Table A9.3; Koroleva et al., this issue). Ground waters in calcite-bearing aquifers are generally saturated with respect to this mineral. Thus, calcite saturation is included in all of the models of Table 2 associated with Ca or carbonate concentrations.

However, modelling the chemistry of a number of Mont Terri borehole water samples leads to calcite oversaturation (Pearson et al., 2003, Annex A; Vinsot et al., 2008a). This may be attributable to the loss of CO_2 from the samples before or during pH measurements, particularly those made in the laboratory (Pearson et al., 1978; Pearson, 1989), and so does not contradict the assumption of calcite equilibrium.

In most of the models of Table 2, dolomite equilibrium was assumed. Whether this assumption is correct in Opalinus Clay pore water requires further consideration.

Calcite and dolomite dissolution are described by the reactions:

$$CaCO_3 + H^+ \leftrightarrow Ca^{2+} + HCO_3^- \quad (6)$$

$$\text{and} \quad CaMg(CO_3) + 2H^+ \leftrightarrow Ca^{2+} + Mg^{2+} + 2HCO_3^-. \quad (7)$$

Combining the $\log K$ expressions for these reactions yields:

$$\log\left(a_{Ca^{2+}}/a_{Mg^{2+}}\right) = 2\log K_{calcite} - \log K_{dolomite} \quad (8)$$

Based on the $\log K(25)$ values of 1.85 for calcite and 3.53 for dolomite in the BRGM database, $\log\left(a_{Ca^{2+}}/a_{Mg^{2+}}\right)$ at equilibrium with both minerals should be 0.16 at 25 °C. At 13 °C, the typical *in situ* temperature in the Mont Terri laboratory, the value should be 0.06.

Fig. 7 shows $\log\left(a_{Ca^{2+}}/a_{Mg^{2+}}\right)$ values for Mont Terri borehole samples calculated at the temperatures at which they were collected. The range of values differs from borehole to borehole. The means and two standard deviations (SD) calculated for samples from the several boreholes are: BWSA-3 = 0.04 ± 0.04, BWSA-1 = −0.04 ± 0.03 and PC-C = −0.09 ± 0.02. These ranges of the BWSA-1 and PC-C boreholes overlap at the two SD level, but the range of the BWSA-3 does not overlap with either of the other boreholes.

The value that $\log\left(a_{Ca^{2+}}/a_{Mg^{2+}}\right)$ would have in water in equilibrium with both calcite and dolomite at 13 °C is also shown in Fig. 7. This value is within the range of values for BWSA-3 waters but differs by more than 2 SD from values for the other two boreholes. This suggests that although the measured ratios for BWSA-3 could be in equilibrium with dolomite, if the other boreholes are also in equilibrium with dolomite the mineral would have to have different thermodynamic properties to produce the pattern of $\log\left(a_{Ca^{2+}}/a_{Mg^{2+}}\right)$ values shown in Fig. 7. Such a variation of mineral properties seems unlikely within a single formation at distances of less than 100 m and casts doubt on the hypothesis that the water chemistry throughout the formation is in equilibrium with dolomite.

Calcium and Mg cation exchange is another possible control on pore-water chemistry. This exchange can be described by:

$$Mg^{2+} + CaX_2 \leftrightarrow Ca^{2+} + MgX_2 \quad (9)$$

The selectivity coefficient for this reaction is:

$$\log K_{G-T}^{Ca/Mg} = \log\left(a_{Ca^{2+}}/a_{Mg^{2+}}\right) + \log\left(E_{MgX_2}/E_{CaX_2}\right). \quad (10)$$

By combining Eq. (10) with Eq. (8), one can directly link the dolomite/calcite equilibrium to the Ca/Mg occupancy ratio in the exchanger. Using this relationship, Tournassat et al. (2008) showed that this occupancy ratio is rather constant in the Callovian–Oxfordian formation at Bure and concluded that calcite and dolomite are at equilibrium with pore-water composition in this formation. They could also conclude that, amongst the range of dolomite solubility products available in various databases (∼2.5, ∼3.5 or ∼4.1 as a function of crystallinity), the value of ∼3.5 derived from Hemingway and Robie (1994) was the most appropriate.

Measurements of the exchangeable cation populations of Mont Terri samples made by several laboratories are given in Pearson et al. (2003 Table A3.11) and summarized in Table 3. From the measured values in this table, the exchangeable Mg to Ca ratio is 0.63 ± 0.06 with a mean $\log\left(E_{MgX_2}/E_{CaX_2}\right)$ value of −0.20 ± 0.04.

Values of $\log K_{G-T}^{Ca/Mg}$ measured on various Mont Terri samples by several laboratories are shown in Table 4. They range from −0.08 to −0.19. A value of −0.20 was used in the 2003 modelling. The range of $\log\left(a_{Ca^{2+}}/a_{Mg^{2+}}\right)$ values calculated from these populations and selectivity coefficients using Eq. (10) is from −0.03 to 0.16.

As shown in Fig. 7, the $\log\left(a_{Ca^{2+}}/a_{Mg^{2+}}\right)$ values of samples from the PC-C, BWSA-1, and BWSA-3 boreholes range from about −0.11 to 0.07. This range broadly overlaps that calculated from the exchangeable cation populations and selectivity coefficients, and supports the use of cation exchange as a control on Mg concentrations in earlier modelling.

The question of why the measured ratios differ among the 3 boreholes is still present, however. One possibility is that the $\log K_{G-T}^{Ca/Mg}$ or $\log\left(E_{MgX_2}/E_{CaX_2}\right)$ values vary across the formation. Measured values for these properties are given in Tables A3.12 and A3.13 of Pearson et al. (2003). There is no pattern of either $\log K_{G-T}^{Ca/Mg}$ or $\log\left(E_{MgX_2}/E_{CaX_2}\right)$ values across the formation. The mean and two standard deviations of the $\log\left(a_{Ca^{2+}}/a_{Mg^{2+}}\right)$ values calculated from the measured data using Eq. (10) are 0.00 ± 0.24. This range encompasses all the $\log\left(a_{Ca^{2+}}/a_{Mg^{2+}}\right)$ values calculated from the water samples and shown in Fig. 7. This also suggests that there are no systematic variations in the cation exchange

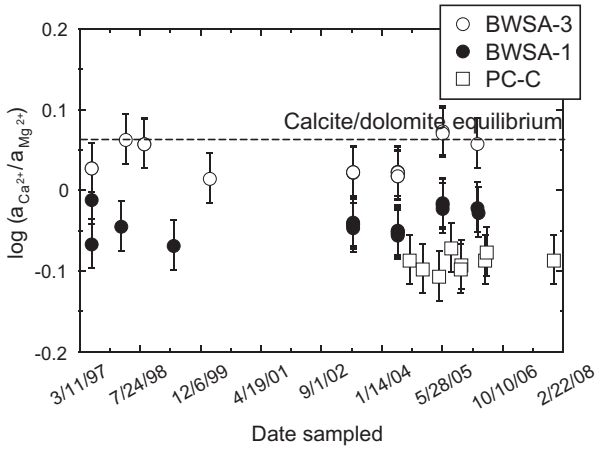

Fig. 7. Activity ratios of Ca^{2+} to Mg^{2+} calculated for samples from the PC-C, BWSA-1 and BWSA-3 boreholes using the THERMODDEM database (BRGM). Calculations were made at sample temperatures, which range from 10 to 13 °C. The value for $(2\log K_{calcite} - \log K_{dolomite})$ corresponds to 13 °C. The bars on the values represent 2 SD for 5% analytical error on Ca and Mg measurements.

properties of the formation that would lead to differences in the $\log\left(a_{Ca^{2+}}/a_{Mg^{2+}}\right)$ values of the samples from the various boreholes.

There is a correlation between the $\log\left(a_{Ca^{2+}}/a_{Mg^{2+}}\right)$ values and the Cl contents of the water samples ($R^2 = 0.995$). Several hypotheses can be advanced that would account for this.

First, it could be an artefact of the activity coefficient calculations. The BRGM database makes use of the ion-pairing model with individual ion activities calculated using the Helgeson B-dot form of the extended Debye–Hückel equation. The water analyses were also modelled with the Pitzer ion-interaction model by using database PITZER.DAT as supplied with the PHREEQC program (http://wwwbrr.cr.usgs.gov/projects/GWC_coupled/phreeqci/). The activities calculated by the two databases are virtually the same indicating that activity coefficients errors are unlikely to be a cause of the differences between the borehole values.

The second hypothesis is that the cation exchange model for divalent species may become less adequate as the solution Cl content increases. Underlying this hypothesis is the work of Charlet and Tournassat (2005) showing that there is preferential exchange of Cl-divalent ion pairs on clays in seawater and work of Ferrage et al. (2005) identifying Ca–Cl ion pairs in montmorillonite interlayers. If Cl ion pairs are important exchangeable entities, they could well lead to cation exchange behaviour that varies with the solution Cl content but that would not be reflected in the models so far applied to the Opalinus Clay. Vinsot et al. (2008b) published pore water solution composition data obtained from *in situ* borehole water sampling in the Callovian–Oxfordian formation. Chloride concentrations range from 28 to 50 mmol/L. Reported Ca and Mg concentrations lead to a mean $\log\left(a_{Ca^{2+}}/a_{Mg^{2+}}\right)$ of 0.05 ± 0.04 (2 SD on 6 values) in near agreement with the 0.16 value expected at 25 °C. This value is also similar to the value obtained in Mont Terri BWSA-3 borehole, with the least saline borehole solution composition (120 mmol/L).

This examination of the controls on Ca and Mg can be summarized as follows:

- The assumption that Ca and (or) carbonate concentrations are related to calcite equilibria is based on observations that ground waters in carbonate-bearing rocks are saturated with respect to this mineral.
- Dolomite equilibrium, although it can be associated with the Mg concentration of many ground waters, is not entirely consistent with the chemistry of pore water from all the Opalinus Clay boreholes sampled. The inconsistencies are relatively small and may be due to unreliable analytical data or thermodynamic properties. The minerals actually present in the Opalinus Clay may also not have the ideal composition of the database dolomite.
- The pore water Ca and Mg contents are consistent with control by cation exchange but there is considerable variation in the measured *in situ* exchangeable cation populations. Including these variations in the modelling would lead to large uncertainties in calculated water compositions.
- There is apparent correlation between $\log\left(a_{Ca^{2+}}/a_{Mg^{2+}}\right)$ values and Cl contents, for which there is as yet no explanation.
- To decide these questions about controls on Ca and Mg concentrations and to improve the ability to model clay pore water will require further, more detailed consideration of:
  - The reliability of the analytical data.
  - The precision of the cation exchange data.
  - The reliability of the thermodynamic data used.
  - The compositions of the minerals actually present in the formation and their effect on the thermodynamic properties of the minerals.
  - Whether any of these 4 types of data can be measured with sufficient precision to significantly improve the accuracy of pore-water compositions modelled from rock properties.

2.2.4. pH control: incorporation of silicate minerals in modelling

In the early models and in the models discussed by Pearson et al. (2003) the number of phases included was commonly insufficient to determine both the pH and the total carbonate content. As Table 2 shows, Beaucaire et al. (2000) specified total carbonate and associated pH with electroneutrality. Bradbury and Baeyens (1998) specified the PCO_2 which, with carbonate established by calcite equilibria, determined the pH. In most of the model variations described by Pearson et al. (2003), the PCO_2 was specified and pH was associated with solution electroneutrality. Exceptions were Scenario A3-E of the models of Pearson et al. (2003) (above, Section 2.1.2.2) and the modelling of Coudrain-Ribstein and Gouze (1993) (above, Section 2.1.2.2). In both cases, dolomite was associated with the total carbonate content because Mg was associated with another reaction. In the former case, Mg cation exchange was included; in the latter, equilibrium with Mg-chlorite was specified.

More recent modelling has explored equilibrium with the alumino-silicate minerals that make up much of the Opalinus Clay. As shown in Table A9.3 of Pearson et al. (2003) and in Wersin et al. (this issue), these minerals are quartz (6–32%), kaolinite (15–35%), illite (17–35%), mixed-layer illite/smectite (5–20%), and chlorite (7–20%). Quartz (or chalcedony) and kaolinite were included in a number of the early models, associated with dissolved SiO_2 and Al. The remainder of this section describes the inclusion of additional clay minerals in modelling Opalinus Clay pore water and in similar modelling of pore water from the COx at Bure.

2.2.4.1. THERMOAR modelling of Callovian–Oxfordian pore water. Gaucher et al. (2006, 2009) developed an approach called THERMOAR modelling to calculate the chemistry of pore water in the COx at Bure based on formation properties measured on core samples. This modelling includes silicate minerals, the presence of which avoids the need to specify pH, PCO_2 or total carbonate. The formal relationships between phases and solution components in the reference and alternate models are shown in the fifth and sixth columns of Table 2 and in Table 4 of Gaucher et al. (2009). Because of the complex chemistry of most of the silicates, defining these relationships is not straightforward. The modelling was done using PHREEQC and the THERMODDEM (BRGM) database. The PHREEQC input files and the thermodynamic database used are given in the electronic annexes to Gaucher et al. (2009).

The nominal or reference model of Gaucher et al. (2009) is similar to previous models in that Cl and SO_4 are specified in the input and the major cations are established by cation exchange and the electroneutrality constraint. Iron(II) in this model is also controlled by cation exchange. The modelling began by bringing a solution with Cl and SO_4 contents determined by core leaching to equilibrium with an exchanger with populations and selectivity coefficients equal to those measured on core samples. The charge balance of the solution was maintained by adjusting Na. This solution was initially oversaturated with celestite and gypsum indicating excess SO_4 in the leaching results. This was corrected by bringing the solution to equilibrium with celestite. This lowered both the dissolved SO_4 and Sr contents and the Sr content of the exchanger. Finally, the solution was also brought to equilibrium with calcite, pyrite, quartz, Fe-chlorite (daphnite-14A in the database) ($Fe_5Al_2Si_3O_{10}(OH)_8$) and illite (illite-Mg in the database) ($K_{0.85}Mg_{0.25}Al_{2.35}Si_{3.4}O_{10}(OH)_2$). Unlike the Opalinus Clay, the horizon of the COx examined by Gaucher et al. (2009) does not contain kaolinite.

Calcite equilibrium established the carbonate content of the solution. Dissolution of this mineral also added small amounts of Ca to the solution and to the exchanger. Quartz dissolution established the dissolved silica content. Iron-chlorite dissolution established the dissolved Al concentration and added a corresponding small amount of Fe(II) to the solution and to the exchanger. Pyrite established the S(II) concentration which, with the SO_4 (S(VI)) concentration, was used to calculate the redox potential of the solution. The final mineral, illite, specified the pH but its dissolution also influenced the dissolved and exchanged K and Mg. A final check insured that the influence of mineral dissolution was negligible relative to the uncertainties in the measurements of exchangeable cation populations.

Several alternative models were also examined using other plausible minerals. These included the silicates designated in the database as chlorite-CCa2 ($Mg_{2.97}Fe_{1.92}Al_{2.49}Ca_{0.01}Si_{2.63}O_{10}(OH)_8$) and Imt-2 illite ($Na_{0.044}K_{0.762}(Si_{3.387}Al_{0.613})(Al_{1.427}Fe_{0.376}Mg_{0.241})O_{10}(OH)_2$), and the carbonates siderite and dolomite. The structural formulae of chlorite-CCa2 and Imt-2-illite are more representative of the minerals present in the COx than the generic illite and daphnite used in the reference model and their solubilities have recently been determined calorimetrically (Gailhanou et al., 2007, 2009). As shown in Table 4 of Gaucher et al. (2009), the measured pH of COx water was 7.2 ± 0.2 and that of the reference model water was 7.1. The pH values modelled with combinations of other silicate minerals tested were from 7.0 to 7.4. All models led to major ion concentrations closely similar to each other and to the measured values.

The thermodynamic properties of minerals like those used in these models are generally not precisely known for specific formations because of the variable compositions of such minerals. However, as Gaucher et al. (2009) point out, pH values are relatively insensitive to uncertainties in the solubility products of silicates included in the THERMOAR modelling. For example, for the reference model, pH can be expressed as:

$$\mathrm{pH} = \frac{-0.85\mathrm{pK}^{+} + 5.875\mathrm{pFe}^{2+} - 0.25\mathrm{pMg}^{2+} - \log K_{\mathrm{illite}} + 1.175\log K_{\mathrm{chlorite}} - 0.125\log K_{\mathrm{quartz}}}{10.4} \quad (11)$$

in which, K, Fe(II) and Mg concentrations are associated with cation exchange. This equation indicates that an uncertainty of one log unit in the clay log *K* values gives rise to an uncertainty of only 0.1 pH units.

2.2.4.2. Modelling of Mont Terri PC-C borehole water including silicates. The THERMOAR methodology has also been applied to water from the PC-C borehole at Mont Terri. The Cl concentration specified was the average of the borehole samples, but a value based on core leaching could also have been used. The SO_4 content was based on the Cl content and the SO_4/Cl ratio of seawater, and was the same as the value measured in the borehole water (Fig. 1). The major cations, Na, K, Mg and Ca, were modelled with cation exchange using the populations shown in Table 3. These are based on values reported in Pearson et al. (2003) and values measured more recently on samples from the PC borehole. In the nominal case modelled and in all variations, saturation with calcite, celestite, siderite, quartz and pyrite was specified. These minerals were associated with total carbonate, Sr, Fe, silica and sulphide concentrations. The redox state was calculated from the SO_4/sulphide couple. Saturation with various pairs of the 4 clay minerals common to the Opalinus Clay was also specified. These minerals were associated with the Al concentration and the pH. Finally, the effects on the modelled Ca and Mg contents of specifying dolomite saturation was also examined. These associations are summarized in the last column of Table 2.

The specific minerals used for the modelling were Daphnite_14A, Chlorite CCa-2, Illite-Mg, Illite-Imt2, Kaolinite, and Mg-Montmorillonite-Na with compositions and properties given in the BRGM database.

The results of the calculations at 13 °C with and without dolomite and celestite are shown in Tables 5 and 6. The solute concentrations modelled without dolomite equilibrium agree well with the measured values except for Fe and alkalinity. Iron concentrations in ground waters may be difficult to measure because sample oxidation can lead to lowered Fe contents. An additional problem for modelling is that the solubility of the actual Fe carbonate mineral in the formation may differ from the value for siderite in the database, as mentioned in Section 2.2.3, above. The choice of clay minerals used in the modelling has a noticeable effect only on the solution pH, pe and alkalinity. The modelled pH ranges from 7.3 to 7.8 which overlaps the average measured value of 7.1 ± 0.4. The modelled alkalinity values range from 0.5 to 1.5 meq/kg H_2O, and all are below the measured value of 3.82 ± 0.68 meq/kg H_2O. All the measured samples are oversaturated with calcite at 20 °C (i.e. the measurement temperature, Vinsot et al., 2008a, Table 2). If modelled to calcite saturation, they would have had either lower pH or lower alkalinity values. The fact that the modelled alkalinity values vary by less than a factor of 4 in spite of the use of four different pairs of clay minerals supports the assumption that the pore water is in equilibrium with these clays and indicates that the thermodynamic data used for the modelling are not grossly inaccurate.

It would have been useful to compare modelled and measured Al concentrations but no Al data are available for the PC-C samples. Aluminium concentrations are available for the BWSA-1 and -3 waters as shown in Table 1. There is considerable variability in these concentrations, possibly because they are so low they would be affected by the presence of even very small quantities of contaminating solids in the samples. In spite of this, the calculated Al values in Table 5 are consistent with those measured for BWSA-1 samples, the salinity of which is close to that of PC-C water.

There is also good agreement between the modelled and measured exchangeable cation populations. The populations of all cations are virtually the same when modelled with various pairs of clay minerals. The modelled exchangeable Ca/Mg ratio is slightly higher than that measured but is well within the uncertainty in the measured values. Likewise, the modelled Ca and Mg contents of the water differ slightly from the measured values. This difference could be reduced by increasing the $\log K_{G-T}^{Na/9m}$ and/or decreasing slightly the $\log K_{G-T}^{Na/Mg}$ values while remaining within range of values measured for the Opalinus Clay fraction (see Table 4). Nearly perfect agreement between modelled and measured value is reached with $\log K_{G-T}^{Na/Ca} = 0.8$ and $\log K_{G-T}^{Na/Mg} = 0.6$ (in which case the calculated $\log\left(a_{Ca^{2+}}/a_{Mg}^{2+}\right)$ is −0.1, i.e. the measured value).

Tables 5 and 6 also show the same set of models with dolomite saturation included. Agreement between the measured and modelled values is similar to that in the models without dolomite even for Ca and Mg. This modelling result shows that predictive water composition calculations are not more accurate when considering only Ca–Mg cation exchange rather than dolomite–calcite equilibrium if cation exchange selectivity coefficients are not very accurately known.

Table 5
Comparison of measured solution composition in PC-C borehole with modelled pore-water composition using various mineralogical assemblages. Calculations were performed with BRGM THERMODDEM database.

	Solution composition mmol/L ± 2 standard deviations													
	pH[a]	pe	Alk	Na	K	Mg	Ca	Sr	Cl	S(6)	C(4)	Fe	Al	Si
PC-C borehole composition														
Vinsot et al. (2008a)	7.1 ± 0.4		3.9 ± 1.5	281 ± 11	1.7 ± 0.3[b]	22 ± 1	19 ± 1	0.46 ± 0.12	327 ± 11	16.8 ± 2	4.3 ± 1.7	0.03 ± −0.02		0.16 ± 0.1
Models at 13 °C without dolomite and with celestite														
Kaolinite/illite	7.83	−3.4	0.27	281	1.80	19.3	23.5	0.57	335	17.2	0.51	0.13	4.E−06	0.13
Kaolinite/Montmorillonite	7.74	−3.3	0.38	281	2.02	19.2	23.6	0.57	335	17.2	0.62	0.13	3.E−06	0.13
Kaolinite/daphnite	7.39	−2.9	1.11	281	2.02	19.4	23.7	0.57	335	17.2	1.42	0.13	1.E−06	0.12
Illite/daphnite	7.34	−2.9	1.28	281	2.12	19.4	23.7	0.57	335	17.2	1.61	0.13	2.E−06	0.12
Montmorillonite/daphnite	7.34	−2.9	1.27	281	2.02	19.5	23.7	0.57	335	17.2	1.59	0.13	2.E−06	0.12
Illite_IMt2/chlorite_CCa2	7.36	−2.9	1.18	281	2.16	18.9	24.2	0.57	335	17.2	1.50	0.13	1.E−05	0.12
Models at 13 °C with dolomite and with celestite														
Kaolinite/illite	7.83	−3.4	0.29	281	1.80	19.8	23.0	0.57	335	17.2	0.52	0.12	4.E−06	0.13
Kaolinite/montmorillonite	7.74	−3.3	0.41	281	2.02	19.8	23.0	0.57	335	17.2	0.64	0.12	3.E−06	0.13
Kaolinite/daphnite	7.39	−2.9	1.13	281	2.02	19.9	23.2	0.57	335	17.2	1.43	0.12	1.E−06	0.12
Illite/daphnite	7.34	−2.9	1.30	281	2.12	19.9	23.2	0.57	335	17.2	1.62	0.12	2.E−06	0.12
Montmorillonite/daphnite	7.35	−2.9	1.28	281	2.02	19.9	23.2	0.57	335	17.2	1.60	0.12	2.E−06	0.12
Illite_IMt2/chlorite_CCa2	7.35	−2.9	1.26	281	2.17	19.9	23.2	0.57	335	17.2	1.58	0.12	1.E−05	0.12
Models at 13 °C without dolomite and without celestite														
Kaolinite/illite	7.83	−3.4	0.27	281	1.80	19.3	23.5		335	16.6	0.51	0.13	4.E−06	0.13
Kaolinite/montmorillonite	7.74	−3.3	0.38	281	2.02	19.2	23.6		335	16.6	0.62	0.13	3.E−06	0.13
Kaolinite/daphnite	7.39	−2.9	1.11	281	2.02	19.4	23.7		335	16.6	1.42	0.13	1.E−06	0.12
Illite/daphnite	7.34	−2.9	1.28	281	2.11	19.4	23.7		335	16.6	1.61	0.13	2.E−06	0.12
Montmorillonite/daphnite	7.34	−2.9	1.26	281	2.02	19.5	23.6		335	16.6	1.59	0.13	2.E−06	0.12
Illite_IMt2/chlorite_CCa2	7.36	−2.9	1.17	281	2.16	18.9	24.2		335	16.6	1.50	0.13	1.E−05	0.12

[a] pH values of PC-C samples were measured at 20 °C in the lab.
[b] One high value neglected in the table from Vinsot et al. (2008a).

Table 6
Comparison of measured exchanger composition and saturation indices with those modelled using various mineralogical assemblages. Calculations were performed with BRGM THERMODDEM database.

	Exchanger composition					Saturation indices					
	E_{Ca}	E_{Mg}	E_{Sr}	E_{K}	E_{Na}	Calcite	Dolomite	Siderite	Celestite	Gypsum	Quartz
PC-C borehole composition											
	0.21	0.19		0.09	0.51	0.1 ± 0.5[a]	0.4 ± 1[a]	−0.6 ± 0.4	−0.1 ± 0.1	−0.46 ± 0.04	0.1 ± 0.3
Models at 13 °C without dolomite and with celestite											
Kaolinite/illite	0.22	0.19	0.005	0.08	0.51	0	−0.02	0	0	−0.36	0
Kaolinite/montmorillonite	0.22	0.18	0.005	0.09	0.50	0	−0.03	0	0	−0.36	0
Kaolinite/daphnite	0.22	0.19	0.005	0.09	0.50	0	−0.02	0	0	−0.36	0
Illite/daphnite	0.22	0.19	0.005	0.09	0.50	0	−0.02	0	0	−0.36	0
Montmorillonite/daphnite	0.22	0.19	0.005	0.09	0.50	0	−0.02	0	0	−0.36	0
Illite_IMt2/chlorite_CCa2	0.22	0.18	0.005	0.09	0.50	0	−0.04	0	0	−0.35	0
Models at 13 °C with dolomite and with celestite											
Kaolinite/illite	0.22	0.19	0.005	0.08	0.51	0	0	0	0	−0.37	0
Kaolinite/montmorillonite	0.21	0.19	0.005	0.09	0.50	0	0	0	0	−0.37	0
Kaolinite/daphnite	0.21	0.19	0.005	0.09	0.50	0	0	0	0	−0.37	0
Illite/daphnite	0.21	0.19	0.005	0.09	0.50	0	0	0	0	−0.37	0
Montmorillonite/daphnite	0.21	0.19	0.005	0.09	0.50	0	0	0	0	−0.37	0
Illite_IMt2/chlorite_CCa2	0.21	0.19	0.005	0.09	0.50	0	0	0	0	−0.37	0
Models at 13 °C without dolomite and without celestite											
Kaolinite/illite	0.22	0.19		0.08	0.51	0	−0.02	0		−0.37	0
Kaolinite/montmorillonite	0.22	0.19		0.09	0.51	0	−0.03	0		−0.37	0
Kaolinite/daphnite	0.22	0.19		0.09	0.51	0	−0.02	0		−0.37	0
Illite/daphnite	0.22	0.19		0.09	0.50	0	−0.02	0		−0.37	0
Montmorillonite/daphnite	0.22	0.19		0.09	0.51	0	−0.02	0		−0.37	0
Illite_IMt2/chlorite_CCa2	0.22	0.18		0.09	0.50	0	−0.04	0		−0.36	0

[a] For the five last sampling points, mean calcite saturation index is −0.02 ± 0.2 and mean dolomite saturation index is 0.1 ± 0.4.

2.2.5. Needs for improvement of recent models

While recent modelling of Opalinus Clay pore waters has overcome some of the shortcomings of earlier models, several still remain and recent modelling itself is not without uncertainties. The principal need to improve future modelling is additional or better data on rock properties. In particular:

- No attempt to improve the description of pore water redox conditions was made in the recent modelling. To improve these models will require more detailed identification of phases in the Opalinus Clay that include redox-sensitive elements. In addition, the compositions and corresponding thermodynamic properties of these phases must be available.
- The relationship between SO_4 and Sr concentrations and celestite saturation is not entirely clarified. An improved understanding of the distribution of celestite throughout the Opalinus Clay would provide insight to this question.
- At present, reactions affecting Mg concentrations and Ca/Mg ratios cannot be modelled precisely enough to be certain which is most important. Improvements in analytic and thermodynamic data and rock cation exchange and mineral chemical properties will be needed. It is uncertain whether the quality of such data can be improved sufficiently to decide the relative importance of possible reactions.
- The inclusion of clay mineral equilibria permits modelling of the pH without the need to specify PCO_2 or total carbonate concentrations, or dolomite saturation. For this to be most successful, the identity, composition, and stability constants of minerals actually present in the formation should be available. Use of generic stability constants was successful in the case described here but this may have been fortuitous.

3. Summary and conclusions

Pore waters in clay-rich rocks generally cannot be sampled directly. Instead, their chemistry must be found using the laboratory-measured properties of core samples and geochemical modelling. Many such measurements have been made on samples from the Opalinus Clay from the Mont Terri URL. Several boreholes in that URL yielded water samples against which pore water models have been calibrated.

Inputs to a pore water model must include a sufficient number of specified solute concentrations and equilibrium phases to satisfy Gibbs' Phase Rule. There are no mineral controls on Cl in Opalinus Clay pore water, so Cl concentrations must be specified in the model input. These can be determined from aqueous leaching data and anion-accessible porosities of core samples. Sulphate is present in Opalinus Clay pore water at virtually the same ratio to Cl as it is in seawater. Celestite is present but uncommon in the Opalinus Clay and the more saline pore waters appear to be saturated with respect to it. Sulphate concentrations are generally specified in the modelling but celestite saturation is included in some model variations.

The first Opalinus Clay modelling was done before pore water samples were available (Bradbury et al., 1997–1998; Bradbury and Baeyens, 1998). This modelling included saturation with calcite and dolomite, and cation exchange equilibria among Na, K andCa. The exchangeable cation populations and selectivity coefficients used for the cation exchange modelling were measured on Opalinus Clay samples. Chloride was specified and the solution electroneutrality constraint was included in the modelling. The PCO_2 of the water was also specified.

Similar modelling of ground waters and pore waters from other formations has been done specifying Na and K concentrations with feldspars, kaolinite and chalcedony saturation instead of with cation exchange. These models also included calcite and dolomite saturation. One of them (Coudrain-Ribstein and Gouze, 1993) included Mg-chlorite and anhydrite saturation. With these, the system was fully constrained and the pH, total carbonate, and PCO_2 of the water could be calculated. Another model (Beaucaire et al., 2000) specified total carbonate in the input and did not include SO_4. Feldspar equilibria are not included in Opalinus Clay modelling because feldspars are present only in very small quantities in the formation and because Na/K ratios measured in pore water samples are inconsistent with feldspar saturation.

Modelling supported by numerous measurements of core properties and many analyses of pore water samples was described by Pearson et al. (2003). This modelling was based on specified Cl, SO_4, and PCO_2 values, calcite, dolomite, kaolinite and quartz saturation, andNa, K, Ca and Sr cation exchange. In some model variations, Mg exchange replaced dolomite saturation and celestite saturation replaced Sr exchange. Redox was included based on the S(VI)/S(-II) couple with S(-II) established by pyrite and siderite saturation. Scenarios with goethite and micro-crystalline $Fe(OH)_3$ replacing siderite and with the Fe(III)/Fe(II) couple replacing S(VI)/S(-II) were also tested. Redox conditions established with the S(VI)/S(-II) couple and siderite equilibrium were most consistent with measured concentrations of the redox-sensitive elements Fe, Mn and U. The principal shortcomings of the 2003 modelling were: an inability to model the K concentrations correctly with the measured cation exchange properties; a lack of consistency between measured Mg and Ca concentrations and those modelled with Mg exchange, and calcite and dolomite saturation; and an inability to reproduce the measured carbonate chemistry and pH of the pore waters using mineral–water reactions alone.

These shortcomings have been largely overcome in recent modelling. It has been found (Tournassat et al., 2007, 2009) that selectivity coefficients for Na/K exchange used in the earlier modelling were too weak. Using stronger coefficients appropriate to the low exchangeable K population of the Opalinus Clay reproduces the measured pore water K concentrations.

Re-examination of the measured Ca/Mg activity ratios and consideration of the mineralogical composition of the Opalinus Clay suggested that Ca/Mg cation exchange rather than dolomite saturation may control the ratio of these ions in solution. This re-examination also suggests that the Ca/Mg ratio decreases with increasing pore-water salinity. Several possible reasons for this are proposed but not explored further in this paper.

Following the example of recent modelling of pore water from the Callovo-Oxfordian at Bure (Gaucher et al., 2006, 2009), saturation with clay minerals has been included in recent Opalinus Clay modelling. These additional minerals eliminate the need to specify pH or total carbonate in the model input. The clay minerals present in the Opalinus Clay are kaolinite, chlorite, and illite/smectite. Water from the PC-C borehole was modelled with six scenarios, each with one of the possible pairs of these minerals. When dolomite saturation is not included, modelled solute concentrations and exchangeable cation contents agree with the measured values, and the modelled pH ranges from 7.3 to 7.8 at 13 °C, comparing well with the measured value of 7.1 ± 0.4.

Acknowledgments

This work was undertaken in close co-operation with, and with the financial support of the Mont-Terri Consortium, ANDRA and Nagra. We appreciate fruitful discussions with Agnes Vinsot, Paul Wersin, Olivier Leupin, Suzanne Mettler, Tres Thoenen and Scott Altmann, during the Porewater Chemistry and the Geochemical Data Experiments. Many thanks also to the Mont Terri team, including Christophe Nussbaum and Paul Bossart (Swisstopo), for their continuous support of the project. We also appreciate the comments of two anonymous referees for the journal.

References

Appelo, C.A.J., Ponten, J., Beekman, H.E., 1989. Natural ion-chromatography during fresh-/sea water displacements in aquifers: a hydrogeochemical model of the past. In: Miles, D.L. (Ed.), Water–Rock Interaction WRI-6: Proc. 6th Internat. Sympos. Water–Rock Interaction. A.A. Balkema, Rotterdam, pp. 23–28.

Appelo, C.A.J., Vinsot, A., Mettler, S., Wechner, S., 2008. Obtaining the porewater composition of a clay rock by modeling the in- and out-diffusion of anions and cations from an in-situ experiment. J. Contam. Hydrol. 101, 67–76.

Baeyens, B., Bradbury, M.H., 1994. Phyisco-Chemical Characterisation and Calculated In Situ Porewater Chemistries for a Low Permeability Palfris Marl Sample from Wellenberg: Wettingen, Switzerland, Nagra Technical Report 94-22.

Baeyens, B., Bradbury, M., 2004. Cation exchange capacity measurements on illite using the sodium and cesium isotope dilution technique: effects of the index cation, electrolyte concentration and competition: modeling. Clays Clay. Miner. 52, 421–431.

Baeyens, B., Maes, A., Cremers, A., Henrion, P.N., 1985a. In situ physico-chemical characterization of boom clay. Radioact. Waste Manage. Nucl. Fuel Cycle 6, 391–408.

Baeyens, B., Maes, A., Cremers, A., Henrion, P.N., 1985b. Aging effects in boom clay. Radioact. Waste Manage. Nucl. Fuel Cycle 6, 409–423.

Beaucaire, C., Pitsch, H., Toulhoat, P., Motellier, S., Louvat, D., 2000. Regional fluid characterisation and modelling of water–rock equilibria in the boom clay formation and in the Rupelian aquifer at Mol, Belgium. Appl. Geochem. 15, 667–686.

Blanc, P., Lassin, A., Piantone P., 2007. THERMODDEM A Database Devoted to Waste Materials, BRGM, Orleans, France. http://thermoddem.brgm.fr.

Bowers, T.S., Jackson, K.J., Helgeson, H.C., 1984. Equilibrium Activity Diagrams for Coexisting Mineral and Aqueous Solutions at Pressures and Temperatures to 5 kb and 600 °C. Springer-Verlag, Berlin.

Bradbury, M.H., Baeyens, B., 1998. A physiochemical characterisation and geochemical modelling approach for determining porewater chemistries in argillaceous rocks. Geochim. Cosmochim. Acta 62, 783–795.

Bradbury, M.H., Baeyens, B., 2000. A generalised sorption model for the concentration dependent uptake of caesium by argillaceous rocks. J. Contam. Hydrol. 42, 141–163.

Bradbury, M.H., Baeyens, B., Pearson, F.J., Berner, U., 1997–1998. Derivation of In Situ Opalinus Clay Porewater Compositions from Experimental and Geochemical Modelling Studies with Addendum. Wettingen, Switzerland, Nagra, Technical Report 97-07.

Charlet, L., Tournassat, C., 2005. Fe(II)–Na(I)–Ca(II) cation exchange on montmorillonite in chloride medium: evidence for preferential clay adsorption of chloride-metal ion pairs in seawater. Aquat. Geochem. 11, 115–137.

Coudrain-Ribstein, A., Gouze, P., 1993. Quantitative study of geochemical processes in the Dogger aquifer, Paris Basin, France. Appl. Geochem. 8, 495–506.

Deer, W.A., Howie, R.A., Zussman, J., 1992. An Introduction to the Rock-Forming Minerals, second ed. Longman Scientific & Technical, Harlow, England.

Degueldre, C., Scholtis, A., Laube, A., Turrero, M.J., Thomas, B., 2003. Study of the pore water chemistry through an argillaceous formation: a paleohydrochemical approach. Appl. Geochem. 18, 53–73.

Ferrage, E., Tournassat, C., Rinnert, E., Charlet, L., Lanson, B., 2005. Experimental evidence for Ca-chloride ion pairs in the interlayer of montmorillonite. An XRD profile modeling approach. Clays Clay Miner. 53, 348–360.

Foster, M.D., 1950. The origin of high sodium bicarbonate waters in the Atlantic and Gulf Coastal Plains. Geochim. Cosmochim. Acta 1, 33–48.

Gailhanou, H., Rogez, J., van Miltenberg, J.C., van Genderen, A.C.G., Greneche, J.M., Gilles, C., Jalabert, D., Michau, N., Gaucher, E.H., Blanc, P., 2009. Thermodynamic properties of chlorite CCa-2. Heat capacities, heat contents and entropies. Geochim. Cosmochim. Acta 73, 4738–4749.

Gailhanou, H., van Miltenberg, J.C., Rogez, J., Olives, J., Amouric, M., Gaucher, E.H., Blanc, P., 2007. Thermodynamic properties of anhydrous smectite MX-80, illite IMt-2 and mixed-layer illite-smectite ISCz-1 as determined by calorimetric methods. Part I: heat capacities, heat contents and entropies. Geochim. Cosmochim. Acta 71, 5463–5473.

Gaines Jr., G.L., Thomas, H.C., 1953. Adsorption studies on clay minerals. II. A formulation of the thermodynamics of exchange adsorption. J. Chem. Phys. 21, 714–718.

Garrels, R.M., Christ, C.L., 1965. Solutions, Minerals, and Equilibria. Harper & Row, New York.

Garrels, R.M., Thompson, M.E., 1962. A chemical model for sea water at 25 °C and one atmosphere total pressure. Am. J. Sci. 260, 57–66.

Gaucher, É.C., Blanc, P., Bardot, F., Braibant, G., Buschaert, S., Crouzet, C., Gautier, A., Girard, J.-P., Jacquot, E., Lassin, A., Negrel, G., Tournassat, C., Vinsot, A., Altmann, S., 2006. Modelling the porewater chemistry of the Callovian–Oxfordian formation at a regional scale. C. R. Geosci. 338, 917–930.

Gaucher, E.C., Tournassat, C., Pearson, F.J., Blanc, P., Crouzet, C., Lerouge, C., Altmann, S., 2009. A robust model for pore-water chemistry of clayrock. Geochim. Cosmochim. Acta 73, 6470–6487.

Hemingway, B.S., Robie, R.A., 1994. Enthalpy and Gibbs Energy of Formation of Dolomite, CaMg(CO3)2, at 298.15 K from HCl Solution Calorimetry. US Geol.l Surv. Open-file Rep. 94-575.

Hummel, W., Berner, U., Curti, E., Pearson, F.J., Thoenen, T., 2002. Nagra/PSI Chemical Thermodynamic Data Base 01/01. Parkland, Florida, Universal Publishers/uPublish.com. (Also Published as Wettingen, Switzereland, Nagra Technical Report NTB 02-16).

Hutcheon, I., Abercrombie, H., 1990. Carbon dioxide in clastic rocks and silicate hydrolysis. Geology 18, 541–544.

Jensen, M., Lam, T., Luhowy, D., McLay, J., Semec, B., Frizzell, R., 2010. Ontario Power Generation's Proposed L & ILW Deep Geologic Repository: An Overview of Geoscientific Studies. GeoHalifax'2009: 62nd Canadian Geotechnical Conf. and 10th Joint CGS/ IAH-CNC Groundwater Specialty Conf., 20–24 September 2009, Halifax, Nova Scotia, pp. 1339–1347.

Johnson, J.W., Oelkers, E.H., Helgeson, H.C., 1992. SUPCRT92 – a software package for calculating the standard molal thermodynamic properties of minerals, gases, aqueous species, and reactions from 1-bar to 5000-bar and 0 to 1000-degrees-C. Comput. Geosci. 18, 899–947.

Koroleva, M., Lerouge, C., Mäder, U., Claret, F., Gaucher, E., 2011. Biogeochemical processes in a clay formation *in situ* experiment: part B – insights and data from the overcoring and evidence of strong buffering by the rock formation. Appl. Geochem. 26, 954–966.

Korzhinskii, D.S., 1965. The theory of systems with perfectly mobile components and processes of mineral formation. Am. J. Sci. 263, 193–205.

Langmuir, D., 1997. Aqueous Environmental Chemistry. Prentice Hall, Upper Saddle River, New Jersey.

Mazurek, M., Alt-Epping, P., Bath, A., Gimmi, T., Waber, H.N., 2009. Natural Tracer Profiles across Argillaceous Formations. The CLAYTRAC Project: Paris, Nuclear Energy Agency, OECD NEA No. 6253.

Michard, G., 1983. Recueil des donées thermodynamiques concernant les équilibres eaux-minéaux dans les réservoirs hydrothermaux. CCE EUR 8590 FR.

Nagra, 1997. Geosynthese Wellenberg 1996, Ergebnisse der Untersuchungsphasen I und II. Wettingen, Switzerland, Nagra, Technischer Bericht 96-01, 2 vols.

Parkhurst, D.L., Appelo, C.A.J., 1999. User's Guide to PHREEQC (Version 2) – A Computer Program for Speciation, Batch-reaction, One-dimensional Transport, and Inverse Geochemical Calculations. US Geol. Surv. Water-Resour. Invest. Rep. 99-4259.

Pearson, F.J., 1999. What is the porosity of a mudrock? In: Aplin, A.C., Fleet, A.J., Macquaker, J.H.S. (Eds.), Muds and Mudstones: Physical and Fluid Flow Properties. Geol. Soc. London Spec. Pub. 158, pp. 9–21.

Pearson Jr., F.J., Berner, U., 1991. Nagra Thermochemical Data Base I. Core Data, Wettingen, Switzerland, Nagra Technical Report NTB 91-17.

Pearson Jr., F.J., White, D.E., 1967. Carbon 14 ages and flow rates of water in Carrizo Sand, Atascosa County, Texas. Water Resour. Res. 3, 251–261.

Pearson, F.J., Arcos, D., Bath, A., Boisson, J.-Y., Fernández, A.M., Gäbler, H.-E., Gaucher, E., Gautschi, A., Griffault, L., Hernán, P., Waber, H.N., 2003. Mont Terri Project – Geochemistry of Water in the Opalinus Clay Formation at the Mont Terri Rock Laboratory: Bern, Switzerland, Federal Office for Water and Geology (FOWG). Geology Series 5.

Pearson F.J., Berner U., Hummel W., 1992. Nagra Thermochemical Data Base II. Supplemental Data 05/92. Wettingen, Switzerland, Nagra Technical Report NTB 91-18.

Pearson Jr., F.J., Fisher, D.W., Plummer, L.N., 1978. Correction of ground-water chemistry and carbon isotopic composition for effects of CO_2 outgassing. Geochim. Cosmochim. Acta 42, 1799–1807.

Pearson Jr., F.J., Lolcama, J.L., Scholtis, A., 1989. Chemistry of Waters in the Böttstein, Weiach, Riniken, Schafisheim, Kaisten and Leuggern Boreholes: A Hydrochemically Consistent Data Set. Baden, Switzerland, Nagra, Technical Report 86-19.

Poinssot, C., Baeyens, B., Bradbury, M.H., 1999. Experimental and modelling studies of caesium sorption on illite. Geochim. Cosmochim. Acta 63, 3217–3227.

Steefel, C.I., Carroll, S., Zhao, P., Roberts, S., 2003. Cesium migration in Hanford sediment: a multisite cation exchange model based on laboratory transport experiments. J. Contam. Hydrol. 67, 219–246.

Stefánsson, A., Arnórsson, S., 2000. Feldspar saturation state in natural waters. Geochim. Cosmochim. Acta 64, 2567–2584.

Thompson Jr., J.B., 1955. The thermodynamic basis for the mineral facies concept. Am. J. Sci. 253, 65–103.

Thorstenson, D.C., Fisher, D.W., Croft, M.G., 1979. The geochemistry of the Fox Hills-Basal Hell Creek aquifer in southwestern North Dakota and northwestern South Dakota. Water Resour. Res. 15, 1479–1498.

Tournassat, C., Gailhanou, H., Crouzet, C., Braibant, G., Gautier, A., Gaucher, E.C., 2009. Cation exchange selectivity coefficient values on smectite and mixed-layer illite/smectite minerals. Soil Sci. Soc. Am. J. 73, 928–942.

Tournassat, C., Gailhanou, H., Crouzet, C., Braibant, G., Gautier, A., Lassin, A., Blanc, P., Gaucher, E.C., 2007. Two cation exchange models for direct and inverse modelling of solution major cation composition in equilibrium with illite surfaces. Geochim. Cosmochim. Acta 71, 1098–1114.

Tournassat, C., Lerouge, C., Blanc, P., Brendlé, J., Greneche, J.-M., Touzelet, S., Gaucher, E.C., 2008. Cation exchanged Fe(II) and Sr compared to other divalent cations (Ca, Mg) in the bure Callovian–Oxfordian formation: implications for porewater composition modelling. Appl. Geochem. 23, 641–654.

Vinsot, A., Appelo, C.A.J., Cailteau, C., Wechner, S., Pironon, J., De Donato, P., De Cannière, P., Mettler, S., Wersin, P., Gäbler, H.-E., 2008a. CO_2 data on gas and pore water sampled *in situ* in the Opalinus Clay at the Mont Terri rock laboratory. In: Proc. Internat. Meeting Clay in Natural and Engineered Barriers for Radioactive Waste Confinement, Lille, 2007. Phys. Chem. Earth 33, pp. S54–S60.

Vinsot, A., Mettler, S., Wechner, S., 2008b. In situ characterization of the Callovo-Oxfordian pore water composition. Phys. Chem. Earth 33, S75–S86.

Way, T.J., 1852. On the power of soils to absorb manure. J. Roy. Agric. Soc. England 13, 123–143.

Wersin, P., Gaucher, E., Gimmi, Th., Leupin, O., Mäder, U., Pearson, F.J., Thoenen, T., Tournassat, C., 2009. Geochemistry of Pore Waters in Opalinus Clay at Mont Terri: Experimental Data and Modelling. St-Ursanne, Switzerland, Mont Terri Project, Technical Report 2008-06.

Wersin, P., Leupin, O.X., Mettler, S., Gaucher, E., Mäder, U., De Cannière, P., Vinsot, A., Gabler, H.E., Kunimaro, T., Kiho, K., Eichinger, L., 2011. Biogeochemical processes in a clay formation *in situ* experiment: part A – overview, experimental design and water data of an experiment in the Opalinus Clay at the Mont Terri underground research laboratory, Switzerland. Appl. Geochem. 26, 931–953.

Applied Geochemistry 26 (2011) 1009–1022

Contents lists available at ScienceDirect

Applied Geochemistry

journal homepage: www.elsevier.com/locate/apgeochem

Biogeochemical processes in a clay formation *in situ* experiment: Part F – Reactive transport modelling

Christophe Tournassat [a,*], Peter Alt-Epping [b], Eric C. Gaucher [a], Thomas Gimmi [b,c], Olivier X. Leupin [d], Paul Wersin [e]

[a] BRGM, French Geological Survey, Orléans, France
[b] Rock–Water Interaction Group, Institute of Geological Sciences, University of Bern, Switzerland
[c] Laboratory for Waste Management, Paul Scherrer Institut, Villigen, Switzerland
[d] NAGRA, CH-5430 Wettingen, Switzerland
[e] Gruner Ltd., CH-4020 Basel, Switzerland

ARTICLE INFO

Article history:
Available online 17 March 2011

ABSTRACT

Reactive transport modelling was used to simulate solute transport, thermodynamic reactions, ion exchange and biodegradation in the Porewater Chemistry (PC) experiment at the Mont Terri Rock Laboratory. Simulations show that the most important chemical processes controlling the fluid composition within the borehole and the surrounding formation during the experiment are ion exchange, biodegradation and dissolution/precipitation reactions involving pyrite and carbonate minerals. In contrast, thermodynamic mineral dissolution/precipitation reactions involving alumo-silicate minerals have little impact on the fluid composition on the time-scale of the experiment. With the accurate description of the initial chemical condition in the formation in combination with kinetic formulations describing the different stages of bacterial activities, it has been possible to reproduce the evolution of important system parameters, such as the pH, redox potential, total organic C, dissolved inorganic C and SO_4 concentration. Leaching of glycerol from the pH-electrode may be the primary source of organic material that initiated bacterial growth, which caused the chemical perturbation in the borehole. Results from these simulations are consistent with data from the over-coring and demonstrate that the Opalinus Clay has a high buffering capacity in terms of chemical perturbations caused by bacterial activity. This buffering capacity can be attributed to the carbonate system as well as to the reactivity of clay surfaces.

1. Introduction

Over the past two decades, reactive transport models have evolved as valuable diagnostic and prognostic tools and have made a significant contribution to elucidating the inherently complex dynamics of natural and engineered environments (Appelo, 1994; Steefel et al., 2003, 2005; Gaucher and Blanc, 2006; Appelo et al., 2008; Gaus et al., 2008; Han et al., 2010). These models provide the theoretical framework for simulating coupled thermal–hydraulic–chemical–biological processes within earth systems. As such, these models constitute a basis for testing concepts and hypotheses and for integrating new experimental, observational and theoretical knowledge about geochemical, biological and transport processes (e.g. Steefel and Lichtner, 1994; Lichtner et al., 1996; Appelo et al., 1998; Maher et al., 2009).

The Porewater Chemistry (PC) experiment in the Mont Terri Laboratory was designed to improve understanding of the compositional characteristics and the buffering mechanisms of the porewater in the Opalinus Clay. For that purpose, a vertical borehole of 52 mm diameter was drilled to a depth of 10.10 m. The bedding dips at an angle of about 45° to the SE. The first 5 m of the borehole were drilled with air. For the remaining 5.1 m, N_2 was used in order to minimise ingress of O_2 and hence oxidation of pyrite and organic matter around the borehole wall. Immediately after drilling, the borehole was filled with Ar. The downhole equipment including the 4.5 m long screen made of porous (40 μm mesh size) low pressure polyethylene with a porosity of 0.3 and a 0.33 m long hydraulic mechanical packer was emplaced into the borehole. The remaining part of the borehole was filled with epoxy resin (Sikadur 52).

The borehole was filled with synthetic porewater (2.8 L) which had been previously saturated with an Ar/CO_2 gas mixture corresponding to a P_{CO_2} of $10^{-3.5}$ bar, as in air. This synthetic porewater was traced to keep track of transport-controlled exchange of solutes between the borehole and the surrounding formation. More details

* Corresponding author. Address: BRGM, Environment and Process Division (EPI/MIS), 3 Avenue Claude Guillemin, 45060 Orléans Cedex 2, France. Tel.: +33 (0)2 38 64 47 44; fax: +33 (0)2 38 64 30 62.
E-mail address: c.tournassat@brgm.fr (C. Tournassat).

0883-2927/$ - see front matter © 2011 Elsevier Ltd. All rights reserved.
doi:10.1016/j.apgeochem.2011.03.009

about the design and results of the experiment are summarized in Wersin et al. (2011). The original focus of this experiment was to obtain high-quality data on the porewater composition and thus to reduce uncertainties in pH/P_{CO_2} and Eh. However, unexpected microbial activity in the borehole observed after about 9 months led to a revised research program with the following objectives:

i. to identify biogeochemical processes occurring in the borehole and describe these quantitatively,
ii. to obtain diffusion parameters of injected conservative tracers,
iii. to identify the source of organic C for microbial degradation,
iv. to draw conclusions on the findings with regard to conditions of the clay host rock around a nuclear waste repository.

To understand the complexity of processes and to identify and/or quantify crucial system parameters of the PC experiment, modelling efforts were initiated by different groups involved in the project. These efforts were only loosely coordinated and different groups were allowed to use a software package of their choice and were free to decide on how to approach the task. Consequently, it was never expected that the different groups would produce exactly the same results. A summary of these modelling efforts can, therefore, only touch on some of the aspects that had to be taken into account by the groups during the design of their model (e.g. model dimensions and geometry, initial and boundary conditions, choice of parameters, choice of relevance) and the reasons for differences in the model outputs.

The following Section 2 aims at giving an overview of the reactive transport simulations performed over the course of the PC experiment. This overview serves as an introduction to a model, discussed in detail in Section 3 of the paper, that is almost fully capable of reproducing the evolution of the borehole fluid during the 5a of the experiment, as well as the observations made on the over-core samples. The geochemical and transport properties of the Opalinus clay formation are then discussed in the light of modelling results.

2. Overview of previous reactive transport simulations of the PC experiment

Over the course of the PC experiment, reactive transport models that couple diffusive transport with chemical reactions were designed and simulations were carried out in a collective effort by different groups involved in the PC experiment. The aim was to develop models that reproduce not only the time series of tracer concentrations but also time series of reactive species and the evolution of the redox state and the pH of the borehole fluid. A model that successfully represents the measured time series of borehole fluid compositions can then be used to identify critical processes and to quantify system parameters and properties within the borehole as well as in the surrounding rock. Furthermore, a working model can be used to make predictions about the system's behaviour in the future and/or to test 'what-if' scenarios that assess the system's response to different physical or chemical conditions (ANDRA, 2005).

Common to all reactive transport models was the incorporation of the processes that were thought to control the chemical evolution of the system: diffusive transport, ion exchange, biodegradation and mineral precipitation/dissolution reactions. Even though these were considered the processes driving the chemical evolution of the system, relatively little was known about the relative importance of each of these processes and if and how these processes interact. One aim of coupled modelling was to elucidate some of these issues.

Integrating transport and chemistry into a model entails a much larger number of system parameters that need to be constrained than in a model that considers non-reactive transport alone. Because few constraints were available for conditions in the surrounding rock, values for critical parameters regarding conditions outside the borehole could only be based on "educated guesses" and were, therefore, associated with a large degree of uncertainty (see discussion in Gaucher and Blanc, 2006). Owing to this uncertainty and other factors, which include among many others: (1) the use of different software packages and geochemical datasets, (2) the choice of parameters and the degree of detail, (3) the choice and the mathematical implementation of processes and the couplings between them, (4) the choice of initial and boundary conditions, (5) species dependent or independent diffusion, (6) uniform or species dependent accessible porosities, it was expected that the results from different modelling efforts could show substantial differences but should agree at least qualitatively and in some aspects quantitatively.

The earliest simulations that couple diffusive transport with chemical reactions were carried out by Arcos (2003). Reactive transport was modelled in one dimension with the PHREEQC (Parkhurst and Appelo, 1999) code. These simulations already included the most important processes that were thought to control the chemistry of the porewater: the degradation of organic matter via SO_4 reduction, ion exchange reactions and mineral precipitation/dissolution reactions. Of these processes, the degradation of organic matter was thought to be that which dominates the behaviour of the system in agreement with preliminary microbiological analyses (Stroes-Gascoyne et al., 2011). Biodegradation was formulated as:

$$2CH_2O + SO_4^{2-} = H_2S + 2HCO_3^- \quad \text{(Reaction1)}$$

and incorporated into the model via a Monod-type rate equation.

Overall, the model was able to reproduce on-line measurements of critical parameters such as the pH and Eh reasonably well and confirmed the significance of biodegradation as the most prominent process in controlling the redox evolution of the system. Discrepancies between measured and modelled data, in particular those related to SO_4 and inorganic C, were attributed to the oversimplification of the formulation for organic matter degradation, the selection of the type of dissolved organic matter and the choice of kinetic parameters used in the degradation reactions.

Tournassat and Gaucher (2004) used the PHAST code (Parkhurst et al., 2004) to simulate, in 1D, the evolution of the borehole fluid composition by using constraints from isotopic data (e.g. $\delta^{13}C$), dissolved CH_4, the SO_4^{2-} concentration, the pH and the alkalinity. They concluded that methanogenic and SO_4-reducing bacteria in the borehole led to a redox zonation that causes methanogenesis and CH_4 oxidation to occur simultaneously. The redox state of the system is controlled by the S(−2)/S(+6) couple, whereby the S(−2) and S(+6) activities are buffered by pyrite (FeS_2) and a Fe-carbonate-phase ($FeCO_3$). The authors suggested that the system is in a redox disequilibrium that is used by SO_4-reducing bacteria to produce CH_4, acetate and various organic acids.

Grandia et al. (2006) used PHREEQC to implement a kinetic formulation for the degradation of acetone through a carboxylation process:

$$CH_3COCH_3 + HCO_3^- = 2CH_3COO^- + H^+ \quad \text{(Reaction2)}$$

and a Monod-type rate equation for the subsequent degradation of acetate to carbonate ions via SO_4 reduction:

$$CH_3COO^- + SO_4^{2-} = 2HCO_3^- + HS^- \quad \text{(Reaction3)}$$

The production of HS^- leads to the precipitation of an amorphous FeS-phase, which controls the Fe concentration in the borehole.

All rate parameters in the biodegradation process were adjusted to match the measured data from the PC experiment and the simulations were able to reproduce many aspects of the evolving system.

Alt-Epping et al. (2006) used FLOTRAN (Lichtner, 2007) to run simulations of a cylindrical model with radial coordinates, which accounted for the oblique angle between the borehole and the bedding. These simulations were fully coupled, which implies that these simulations also considered the feedback between porosity changes following mineral dissolution/precipitation reactions and diffusive transport. This study incorporated many parameters and built on results from previous studies: the formulation and selectivity coefficients for ion exchange were taken from Tournassat and Gaucher (2004) and biodegradation was formulated in an analogous manner to that of Grandia et al. (2006). Simulations included a sensitivity analysis that compared different model outcomes as a function of the initial borehole fluid composition.

To elucidate the importance of individual reaction processes (ion exchange, biodegradation, mineral dissolution/precipitation), different model scenarios included a successive increase in model complexity, from the implementation of a single process only to the implementation of all reaction processes and a full coupling between them. The results from the simulations showed that the different initial compositions of the borehole fluid (Scenarios 1–3) have relatively little impact on the evolution of the system. Without ion exchange or biodegradation, the reactivity of the system is low, which is consistent with very small volumes of calcite, dolomite and siderite precipitation (Fig. 1). Species concentrations in the borehole either increase or decrease monotonously, which indicates that these changes are primarily controlled by diffusive exchange with the surrounding rock (Fig. 2).

In contrast, after implementing biodegradation and ion exchange, the evolution of the fluid composition in and around the borehole becomes more complex and the system has not attained steady state after 1426 days. The system is more reactive, which is reflected in a larger amount of precipitated carbonate minerals. The implementation of biodegradation reproduces one of the key characteristics of the borehole fluid, which is the decrease in S over time (Fig. 2). In the borehole, organic matter reduces SO_4 to sulfide, which subsequently diffuses outward into the formation where it precipitates as pyrite (Fig. 1). The uptake of sulfide into pyrite outside the borehole steepens the total S concentration profiles, thus enhancing outward diffusion and causing a decrease in the total S concentration in the borehole fluid (Fig. 2).

These results demonstrate the buffering capacity of the system, which is due primarily to ion exchange and the buffering by carbonate phases. Biodegradation exerts the strongest impact on the evolving fluid composition and causes the precipitation of pyrite. These simulations were successful in describing qualitatively the processes occurring in the borehole and the surrounding formation. The simulations also suggest that by selecting only those constituents and processes that are relevant to the chemical evolution of the system, it is possible to design a "minimal" model that is simple yet fully capable of reproducing quantitatively the evolution of the borehole fluid over the 5a of this experiment. This model is presented in the following sections.

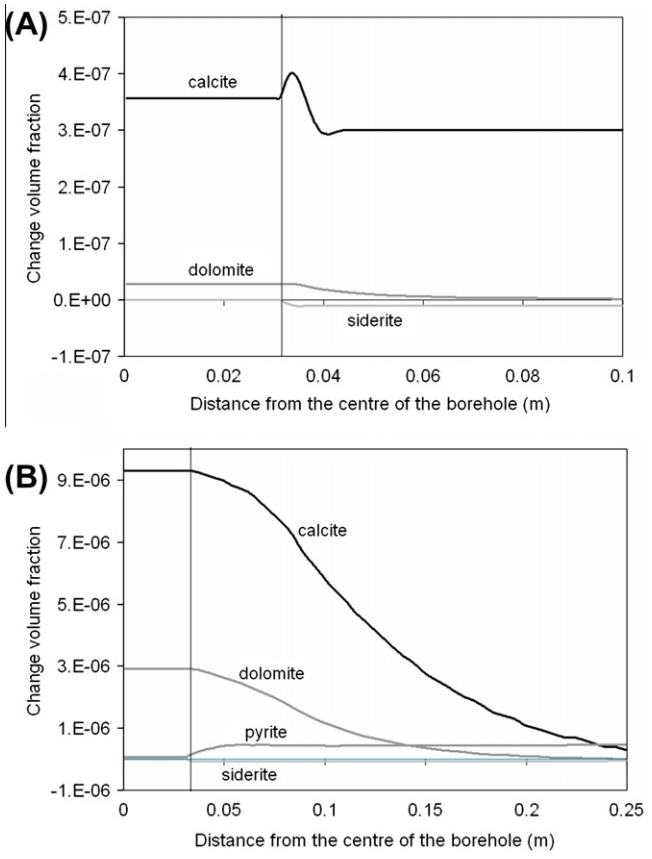

Fig. 1. Profiles of mineral volume changes over a period of 1426 days, without (A) and with ion exchange and biodegradation (B) from Alt-Epping et al. (2006). The vertical line represents the borehole/rock interface. The precipitation of carbonate phases, calcite, dolomite and siderite along with ion exchange with clay surfaces act as buffers for the fluid composition. Increasing chemical complexity leads to a larger volume fraction of carbonate minerals. Sulphate reduction through biodegradation causes pyrite to precipitate.

3. A simplified reactive transport model

3.1. Overview of the proposed reactive transport model

As stated above, the aim of this modelling exercise was to develop a "minimal" model capable of reproducing the chemical evolution of the PC experiment, i.e. the chemical evolution of compounds that are coupled with each other through the simultaneous occurrence of biological transformation of solute or solid compounds, in-diffusion and out-diffusion of solute species and precipitation/dissolution of minerals (in the borehole and in the formation).

This section aims at giving an overview of the concepts and parameters used in the model. Each of these parameters, including their calibration, are then discussed in the following Section 4.

Mainly because biological activities are highly non linear, processes occurring in the experimental borehole could not be modelled using a purely mechanistic approach without fitting parameters. Thus, it is not within the scope of this paper to try to present a biological mechanistic model.

Different events during the course of the experiment (e.g. water sampling, leakage and others) caused changing boundary conditions. As discussed elsewhere in this series of papers, the major changes in the water chemistry during the PC experiment included decreasing concentrations of Br^-, ^2H and SO_4^{2-} and increases in the organic C and total dissolved carbonate contents. The changes in the Br^- and ^2H contents were expected because the test water was spiked with both of them to act as tracers. The measured concentrations of these tracers in the borehole are shown in Part A, Fig. 7 (Wersin et al., 2011). They differ considerably from those expected in that the concentrations in samples taken late in the experiment, instead of continuing to decreasing asymptotically to the low concentrations in the formation water, began to increase toward those of the initial test water. This behaviour could be linked to the experimental needs, where the chemical composition of the water in the borehole was changed through dilution of the

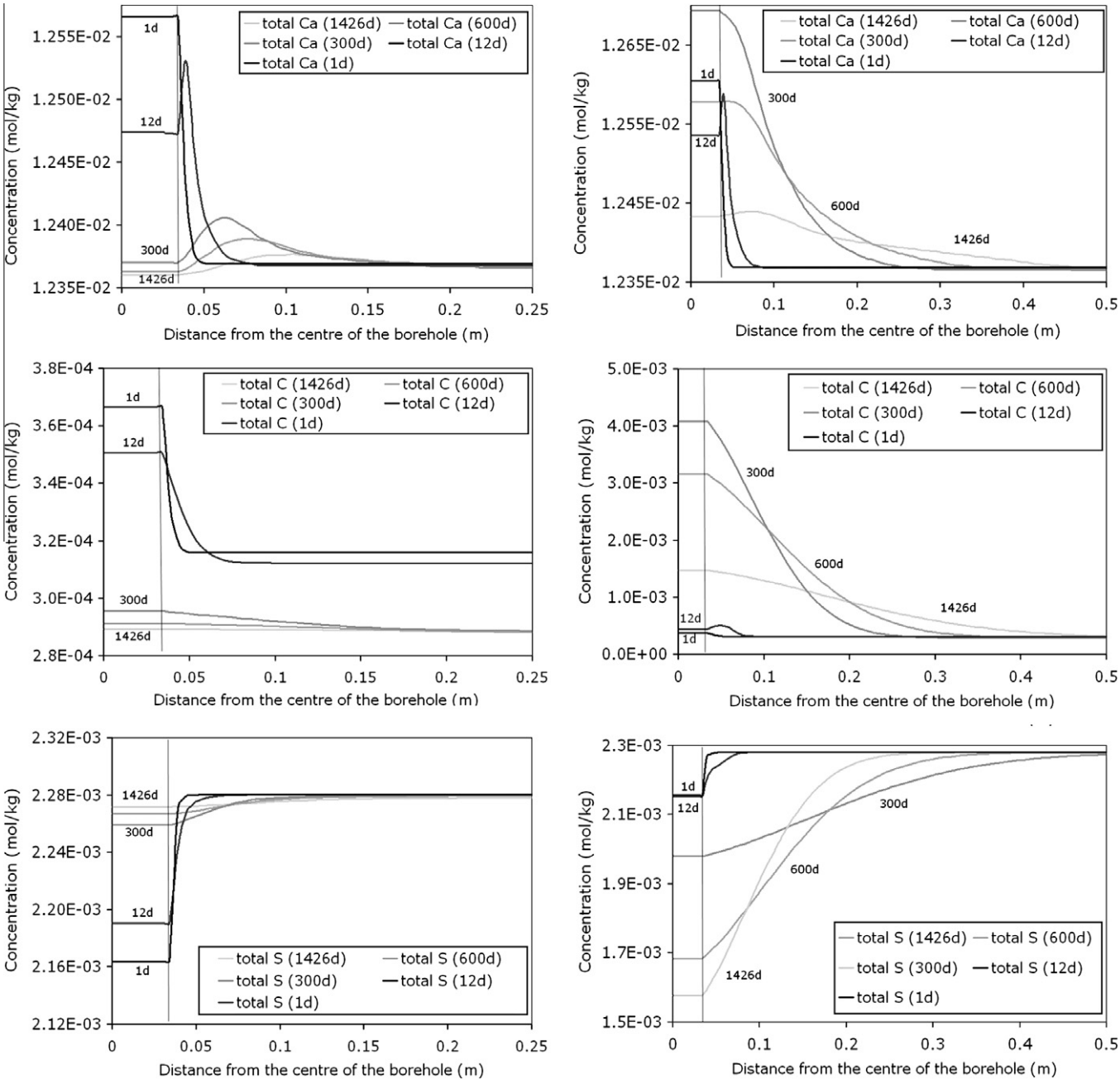

Fig. 2. Spatial profiles of selected species concentrations at different times during the simulation from Alt-Epping et al. (2006). The left and right panels are model scenarios without and with ion exchange and biodegradation, respectively. The interface between borehole and surrounding rock is marked by a vertical line. The profiles show that a greater complexity of system processes entails a non-monotonous evolution of species concentration in the borehole.

borehole water with volumes of synthetic water (high concentration of Br^-, but also zero concentration of sulfides, etc.) introduced into the system to compensate the losses due to sampling or leakages. As a second consequence, these events led also to changes in the concentration gradients between the borehole and the surrounding formation, hence having an effect on the solute diffusion in/from the formation. It was then necessary to take these events into account in the reactive transport calculation to achieve good mass balance. This was achieved by building a model with several restarts after having changed the conditions in the borehole through mixing of the borehole water with synthetic porewater.

Changing boundary conditions as a function of time had to be considered also for bacterial activity. Biological analyses (Stroes-Gascoyne et al., 2011) showed that different bacterial strains with different sources of energy (e.g. SO_4 reduction vs. methanogenesis) were active in the borehole. Four different periods of bacterial activity can be discerned in Fig. 3. Phase 1 is characterized by almost no release of organic matter into the system. As a consequence, a low bacterial activity is expected. A significant release of organic matter different from acetate is observed in phase 2, while in phase 3 there is a release of organic matter and a concomitant transformation into acetate. In phase 4, the organic matter concentration in the borehole decreases due to degradation into inorganic C and diffusion into the surrounding formation, providing that the organic matter release in the borehole stopped or decreased drastically. Fig. 4 also shows that phase 4 must itself be subdivided into two periods for the description of a bloom of methanogenesis before it slows down. This event has been recorded in

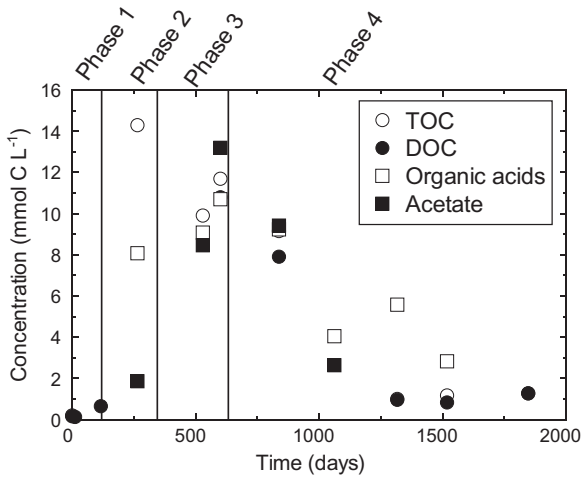

Fig. 3. Measurement of organic compounds as a function of time (TOC = total organic C, DOC = dissolved organic C).

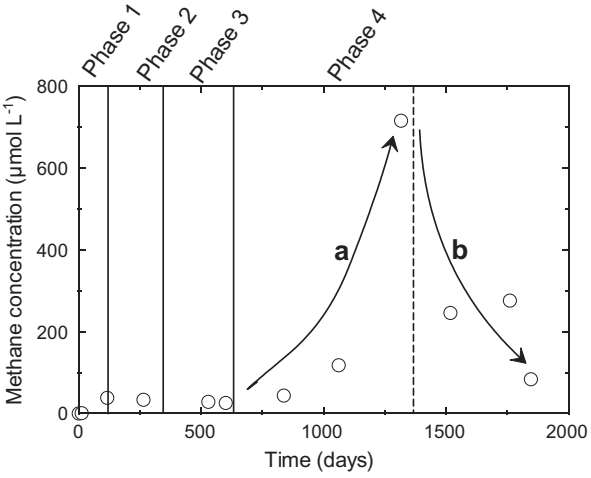

Fig. 4. Measurements of CH_4 concentrations as a function of time. a: bloom of methanogenic activity. b: decrease in methanogenic activity.

biological analysis through the presence of active methanogenic bacteria at the end of the experiment.

Fig. 3 clearly shows that acetate was not the primary source of organic C in the system because acetate concentration is well below total or dissolved organic C concentration before phase 3. Acetate must, therefore, be considered as a secondary product of the bacterial activity. This secondary product can itself be degraded into inorganic C, as will be shown later. The nature of the primary source organic matter that was released into the borehole and then transformed into acetate was the subject of much controversy over the course of the experiment: among the possible candidates, acetone (CH_3–CO–CH_3), which was used for cleaning the filters before the experiment, was long preferred until modern C measurements on dissolved organic C revealed that the C source was a modern one (De Cannière et al., 2011). After thoroughly scrutinizing the potential sources of modern C in the system, De Cannière et al. (2011) came to the conclusion that glycerol ($C_3H_8O_3$), originating from the gel pH-electrode, was the most probable candidate as the primary source of organic C in the system.

The two samples during phase 3 exhibited acetate concentration of the same level as total organic matter. Moreover, these concentrations increased during phase 3. This observation can only be explained by considering that the primary source of organic C, once released into the borehole water, is immediately converted into acetate. From a modelling conceptual point of view, this behaviour is equivalent to the presence of a "solid" source of C that is not released into solution but is directly degraded into acetate. If it is considered that glycerol from the electrode is indeed the primary source of C, this could be explained by the presence of an intense bacterial activity in the vicinity of the electrode degrading glycerol into acetate. On the contrary, during phase 2, total organic C concentration is much higher than acetate concentration, evidencing a release from the electrode that is faster than the consumption by surrounding bacteria, possibly because the initial population of active bacteria was very small. As a consequence, organic matter releases in the system were modelled by three distinct kinetic rates accounting for these three situations: (i) a rate for glycerol (or another organic compound) release into solution, (ii) a rate for its degradation into acetate and (iii) a rate for direct release of acetate into solution accounting for the rapid conversion of glycerol (or another organic compound) into acetate at the source term.

These rates were arbitrarily changed as a function of time in order to accurately reproduce the data shown in Fig. 3. This approach must be seen as a purely fitting approach that is justified because the interest of the modelling was to understand the response of the system to the bacterial activity.

3.2. Numerical modelling methods

3.2.1. Geometry and transport

In the modelling approach that follows, the experimental borehole was considered to be a perfect cylinder. Diffusion taking place at the bottom and the top ends of the cylinder was neglected in comparison to radial diffusion owing to the low value of their surface area as compared to radial surfaces. Anisotropy of diffusion due to the bedding of the rock (Arcos et al., 2004; Van Loon et al., 2004a,b) was not taken explicitly into account. With this approximation, the system turned into a 1D radial model. This type of geometry can be implemented in PHREEQC using the "-stagnant_cells" option (Parkhurst and Appelo, 1999; Appelo and Wersin, 2007). Transport by diffusion is solved at each time step by mixing iteratively adjacent cells (n and $n+1$) following the relationship:

$$mix\, f_{n,n+1} = \varepsilon \times D_p \times \Delta t \times \frac{A_{n,n+1}}{h_{n,n+1} \times V_n} \times f_{bc} \quad (1)$$

where $\varepsilon \times D_p$ is the harmonic mean of the effective diffusion coefficient, i.e.:

$$\varepsilon \times D_p = 2\frac{\varepsilon_n \times D_{p,n} \times \varepsilon_{n+1} \times D_{p,n+1}}{\varepsilon_n \times D_{p,n} + \varepsilon_{n+1} \times D_{p,n+1}} \quad (2)$$

where Δt is the time step (s), $A_{n,n+1}$ is the shared surface area among cells n and $n+1$ (m^2), $h_{n,n+1}$ is the distance between midpoints of the cells n and $n+1$ (m), V_n is the water volume in cell n for which the concentration change is calculated (m^3), and f_{bc} is a correction factor that equals 2 for constant concentration (end cell of the system) and 1 otherwise (inner cell of the system with closed boundary). ε_n (–) is the porosity of cell n. $D_{p,n}$ is the pore diffusion coefficient of cell n ($m^2\ s^{-1}$). If no surface diffusion (in the electrostatic double layer at charged mineral surfaces) is considered, the pore diffusion coefficient is related to the effective diffusion coefficient (D_e) by the relationship:

$$D_{e,n} = \varepsilon_n \times D_{p,n} \quad (3)$$

The borehole was modelled using only one numerical cell representative of the ring volume containing the test water (the inner part of the borehole was filled with instrumental devices). Surface to volume ratios between adjacent cells were calculated according

to the diameter of the borehole (0.052 m) and the size of each numerical cell. The Opalinus Clay formation was represented by 33 cells extending 1.5 m into the clay formation. Grid size was refined when approaching the borehole/formation interface: cell sizes ranged from 0.002 m at the interface up to 0.2 m in the clay formation. Considering the total length of the borehole (4.63 m), this corresponds to a porous rock volume of 0.0016 m^3 for the cell at the interface and 8.3 m^3 for the last cell in the clay formation. Transport parameters were fitted according to the Br and ^2H diffusion profiles using the multi-component diffusion option of PHREEQC (different D_p values can be attributed to different solutes in the system). All dilution events (sampling and leakages reported in Wersin et al., 2011) were taken into account.

3.2.2. Chemistry database

The BRGM Thermoddem database (http://thermoddem.brgm.fr/index.asp? langue=GB) was used for chemical species and minerals solubility given the need for reliable thermodynamic data of clay minerals. Preliminary simulation runs made it possible to simplify calculations by removing unnecessary solute species. The database used for the simulation is given in Electronic Annex 1.

3.3. Boundary conditions

3.3.1. Anion concentration and accessible porosity

Because of the out-diffusion of Cl at the Lias and Dogger boundaries, porewaters of the Opalinus Clay at Mont Terri show a distinct diffusion profile through the formation (see Fig. 2 in Wersin et al., 2011). The stability of the Cl + Br concentration profile due to diffusion of Br from the borehole in the formation and Cl from the formation in the borehole confirmed that porewater Cl concentration was about 0.3 mol/L (Fig. 5). Sulphate concentration was adjusted to match the Cl/SO_4 seawater ratio in agreement with porewater modelling results (Pearson et al., 2011).

Total water loss at 105 °C (7.42—8.4 kg_{water} kg_{rock}^{-1}) together with rock bulk density determination (2.38–2.4 kg dm^{-3}) enabled Koroleva et al. (2011) to determine a mean total porosity of 0.19. This value is also in agreement with reported grain density of 2.7 kg dm^{-3} (Pearson et al., 2003, Table A9.12). This porosity value is high when compared to previously reported values measured with the same method (Pearson et al., 2003, Table A9.12). However, it is still in agreement with porosity values obtained from HTO diffusion experiments: for instance Van Loon et al. (2003) reported values up to 0.2. According to (i) this porosity value, (ii) the total Cl content that can be leached from the sample and (iii) the Cl concentration in the porewater (as given by the final concentration of the test water), Koroleva et al. (2011) also calculated that anion accessible porosity represents ~75% of total porosity. This value is higher than the usually reported mean value of ~50–60%, but still in reasonable agreement with the range of variation reported in the literature (40–70%, Van Loon et al., 2003, 2004a, 2007). As a consequence, it was decided to consider this measured value in the modelling exercise. In the following, an anion accessible porosity of 0.14 corresponding to 0.06 kg_w/kg_r will be used and the remaining 0.02 kg_w/kg_r must be considered as "surface water" (Appelo and Wersin, 2007; Appelo et al., 2008).

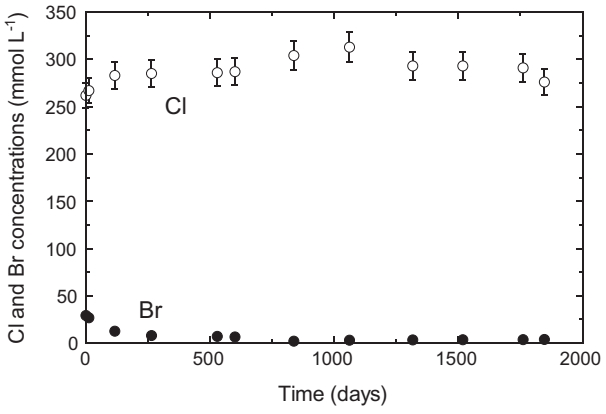

Fig. 5. Cl (open circles) and Br (closed circles) concentrations as a function of time.

3.3.2. Major cations (Na, K, Ca, Mg, Sr) and cation exchange

A cation exchange reaction can be represented by the following reaction equation, in the case of a Na^+/Me^{z+} binary system (Me = K, Ca, Mg or Sr):

$$z\ NaX + Me^{z+} \Longleftrightarrow MeX_z + z\ Na^+ \qquad \text{(Reaction4)}$$

where X^- represents a negatively charged surface site. The selectivity coefficient of this reaction is $K_{GT}^{Na/Me}$:

$$K_{GT}^{Na/Me} = \frac{\{Na^+\}^z}{\{Me^{z+}\}} \times \frac{E_{Me}}{E_{Na}^z} \qquad (4)$$

where E values are charge fractions on the exchanger.

The over-coring analysis showed that cation exchanger composition is very constant as a function of borehole distance (Koroleva et al., 2011). In these conditions, Eq. (4) implies that the $\frac{\{Na^+\}^z}{\{Me^{z+}\}}$ is also constant. This can be verified in Fig. 6.

The exchange selectivity coefficient of Na/Me exchange reactions can then be calculated from exchanger population analysis and borehole sample data (Table 1). These values can be compared to those predicted by the illite and smectite exchanger models given by Tournassat et al. (2007, 2009). The present exchange

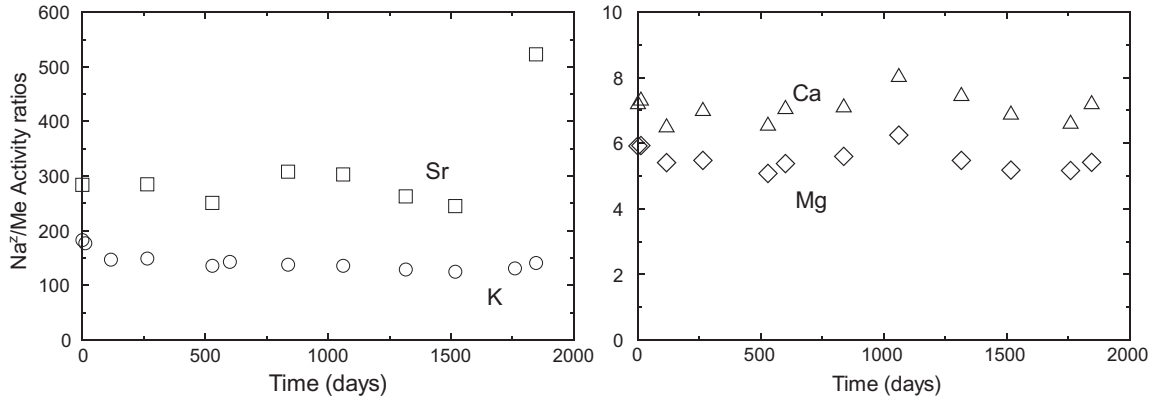

Fig. 6. $\frac{\{Na^+\}^z}{\{Me^{z+}\}}$ solute activity ratio as a function of time in the PC experiments (Me = K, Ca, Mg and Sr).

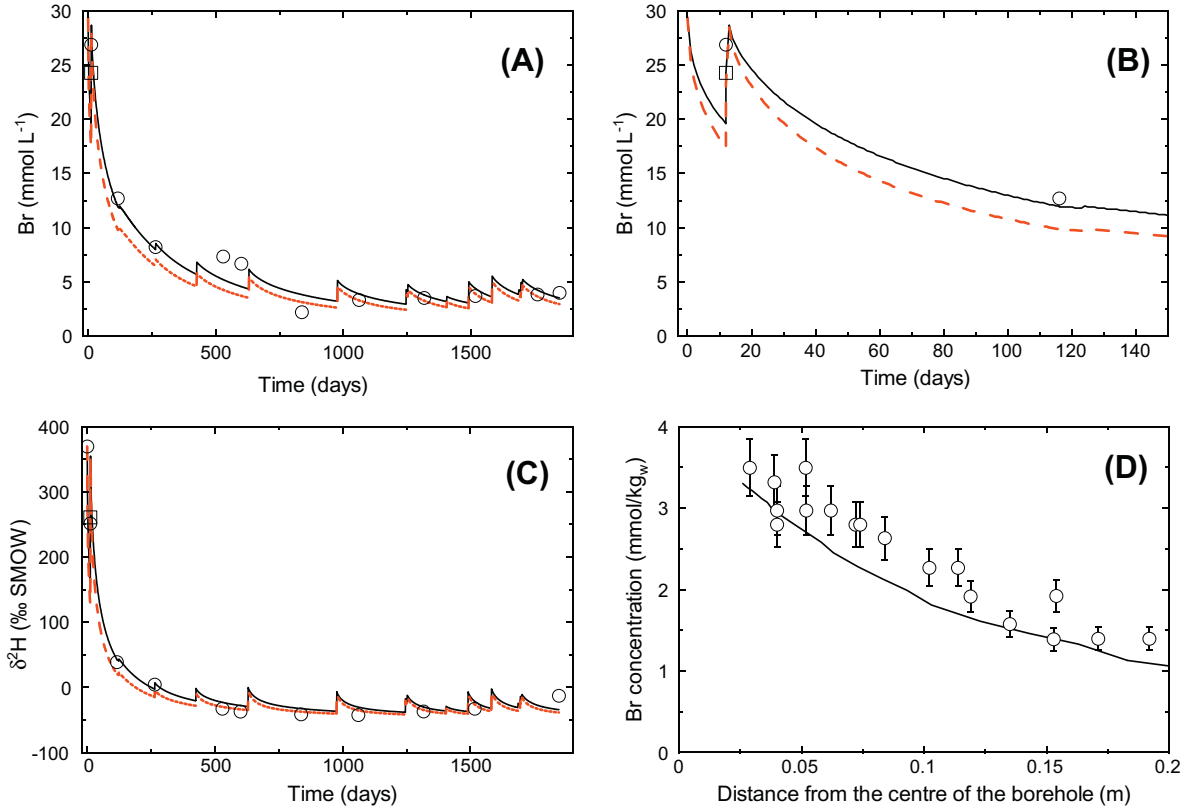

Fig. 7. Comparison between measurements (circles and red dashed line) and Br and HDO modelled diffusion profiles. Plain and dashed curves are representative of calculations using porosities of 75% or 100% of the measured total water content. Squares are representative of the sample taken at day twelve while refilling the borehole. The pore diffusion coefficient (D_p) remained unchanged at 0.9 and 2.4 $\times$ 10^{-11} m^2 s^{-1} for anions and HDO respectively. Upper left figure: Br concentration in the borehole as a function of time. Upper right figure: focus on the initial stage of the experiment. Bottom left figure: HDO concentrations in the borehole as a function of time. Bottom right figure: Br concentration ratio profile in the rock at the end of the experiment. The distance is expressed in the bedding plane geometry (see Koroleva et al., 2011). (For interpretation of the references to colour in this figure legend, the reader is referred to the web version of this article.)

Table 1
Calculated and predicted selectivity coefficient for Na/Me exchange on Opalinus Clay.

Exchange reaction	Calculated $\log_{10}K_{GT}$ from borehole and core sample analysis	Predicted $\log_{10}K_{GT}$ for illite surfaces (from [a])	Predicted $\log_{10}K_{GT}$ for smectite surfaces (from [b])	Calculated $\log_{10}K_{GT}$ for BWS-A1 samples water (from [c])	Calculated $\log_{10}K_{GT}$ for BWS-A3 samples water (from [c])
Na → K	1.40 ± 0.05	0.96	0.96	1.32	1.26
Na → Ca	0.78 ± 0.06	0.41	0.99	0.83	0.63
Na → Mg	0.62 ± 0.05	0.71	0.75	0.61	0.48
Na → Sr	1.14 ± 0.22	–	1.17	0.97	0.51

[a] Tournassat et al. (2007).
[b] Tournassat et al. (2009), including effects of cation-chloride ion pairs.
[c] Pearson et al. (2011).

selectivity coefficients can be explained by a combination of illite and smectite surfaces: modelled Na/K selectivity coefficients are lower than the measured selectivity coefficient for illite/smectite mixed layer minerals (I/S). This observation is in agreement with the recommendation of Tournassat et al. (2009) to increase the Na/K coefficient by 0.2–0.4 $\log_{10}$ unit for I/S surfaces. Exchange selectivity coefficients are also in agreement with those calculated at another location with the same chlorinity (BWS-A1), while they are slightly different for a location with lower chlorinity (BWS-A3) (Pearson et al., 2011).

In the following, the $\log_{10}K_{GT}$ value calculated from borehole and core samples (first column of Table 1) will be used to run the simulations.

3.3.3. Porewater chemistry

Initial porewater chemistry was calculated at 25 °C with the model presented in Pearson et al. (2011) and with the parameters given above. The minerals considered at equilibrium with the formation porewater were: quartz, calcite, siderite, chlorite (Chlorite-CCa-2), illite (Illite_IMt2) and pyrite. Chosen chlorite and illite data were originally obtained from calorimetric measurements (Gailhanou et al., 2007, 2009). Porewater modelling results are given in Table 2.

3.3.4. HDO and Br^- diffusion

Diffusion parallel to the bedding of Opalinus Clay from Mont Terri has already been studied at the laboratory scale (Van Loon et al., 2004a) as well as in *in situ* experiments (Van Loon et al., 2004b). Van Loon et al., 2004b report a diffusion coefficient (D_p) of 1.1 $\times$ 10^{-10} and 2.7 $\times$ 10^{-10} m^2 s^{-1} for I^- and HTO respectively. Together with the measured accessible porosity Koroleva et al. (2011), these values were used in the calculations and then slightly adjusted to better match the data. A good fit was obtained with D_p

Table 2
Modelled initial porewater composition.

	Modelled initial porewater composition	Analysed test water composition (mean of initial and final)
pH	7.01	7.74
pe	−2.74	
Elements	Concentration (mmol/kg$_w$)	
Cl	300	262
Br[a]	0.6	29.0
S(6)	15.0	14.8
TIC	3.16	1.3
Na	257	256
K	1.96	1.45
Ca	16.7	15.8
Mg	19.9	18.0
Sr	0.43	0.33
Fe	0.14	
Si	0.18	
Al	21.4×10^{-6}	
Acetic acid[b]	0.2	
Methane[c]	0.035	

[a] From Pearson et al. (2003).
[b] From Courdouan et al. (2007).
[c] Taken at the value of the first plateau of CH_4 concentration from day 116 to day 529.

of 0.9×10^{-10} and 2.4×10^{-10} m^2 s^{-1} for Br^- and HDO, respectively (Fig. 7).

Koroleva et al. (2011) report spatial profiles of Br and Cl concentrations in the immediate vicinity (first 17 cm) of the borehole. Even though the data, in particular the data for Cl^-, are associated with a relatively large degree of uncertainty, there appears to be a discrepancy between the computed (with diffusivities estimated from time-series of tracer concentrations in the borehole fluid) and measured spatial profiles (Fig. 7, lower right panel). It is not easy to decide whether this shift is significant or not. If significant, this shift would suggest the presence of a disturbed zone surrounding the borehole having enhanced diffusion properties (Cartalade et al., 2007). Considering the overall good agreement of the model and the measured data and their associated uncertainty, the possibility of a disturbed zone is not discussed further.

In the following models, a porosity corresponding to the volume of 75% of the total water content (i.e. volumetric porosity = 0.14) was assumed for the entire rock formation. In the proposed reactive transport model, this porosity applies not only to anions but also to positively charged and neutral species for simplicity and calculation time saving reasons. Incidentally, considering the total porosity instead of the reduced porosity for HDO transport has little effect on the calculated HDO concentrations as a function of time in the borehole (Fig. 7). It is possible to consider different D_p for different solute species using the multi-component diffusion option of PHREEQC (Appelo and Wersin, 2007). Differences in D_p originate from differences in the diffusion coefficient in pure water (D_0) and tortuosity (τ) for different solute species. For each species i, the relationship $D_p = \tau D_0$ applies. In the present studies, D_0 values from the Phreeqd.dat database were considered together with a tortuosity factor calculated from experimental D_p for Br and HTO: the tortuosity (τ) for anions and neutral species were set as $\tau_{anions} = D_p(\mathrm{Br})/D_0(\mathrm{Br})$ and $\tau_{neutral} = D_p(\mathrm{HDO})/D_0(\mathrm{HDO})$. D_0 for OH^- and H^+ were set to the value of HDO for calculation time saving reasons. As a further simplification of the system, it was considered that the same tortuosities τ_{anions} applied to all of the anions, independently of their charge and $\tau_{neutral}$ to both neutral species and cations. Cations are expected to have lower tortuosities than neutral species (Appelo and Wersin, 2007) but this effect was neglected.

3.4. Borehole conditions

3.4.1. Biological activity kinetic parameters

Once the solute species diffusion properties were fixed, six kinetic parameters for material degradation and bacterial activity could be fitted: 3 of them account for the release of the primary organic matter and its transformation into acetate (see Section 2); two others are for SO_4 reduction/acetate oxidation and the last one is for methanogenesis. Each of these parameters was constrained by measured data:

- The release rate of primary organic C source in solution can be computed through the difference between TOC (total organic C) and acetate concentrations.
- The degradation rate of this organic C together with the degradation rate of a "solid" C source into acetate was fitted with the acetate concentrations as a function of time.
- The SO_4 reduction rate (through acetate oxidation) was constrained by SO_4 concentration as a function of time.
- The rate of CH_4 production from acetate degradation was given by the CH_4 concentration profile as a function of time.

As stated in the introduction, it was not within the scope of this work to describe the system with all of the intermediate degradation products and no attempt has been made to find them in the literature. Measurable initial and final products solely were considered, as well as zero-order kinetic reactions. Bacteria are considered here only as catalysts for thermodynamically possible reactions.

Glycerol (described as $C_3H_8O_3$) transformation into acetate was described with:

$$2/7C_3H_8O_3 + 1/7HCO_3^- \Rightarrow 1/2CH_3COO^- + 5/14H^+ + 2/7H_2O \quad \text{(Reaction5)}$$

Even though it is now clear that the source of C in the system was glycerol that leached from the electrode (De Cannière et al., 2011), the question regarding the nature of this source was also addressed through this reactive transport model exercise by considering two other potential sources of C. One of these potential sources was acetone that could have entered the system after the filter cleaning procedure (De Cannière et al., 2011):

$$1/4CH_3{-}CO{-}CH_3 + 1/4HCO_3^- \Rightarrow 1/2CH_3COO^- + 1/4H^+ \quad \text{(Reaction6)}$$

The other potential source was natural organic matter present in the formation, taken here as a generic CH_2O formula:

$$CH_2O \Rightarrow 1/2CH_3COO^- + 1/2H^+ \quad \text{(Reaction7)}$$

The sensitivity of the modelling result to the considered source of C could then be tested. Acetate degradation during SO_4 reduction was described with

$$CH_3COO^- + SO_4^{2-} \Rightarrow 2HCO_3^- + HS^- \quad \text{(Reaction8)}$$

and methanogenesis with:

$$CH_3COO^- + H_2O \Rightarrow HCO_3^- + CH_4 \quad \text{(Reaction9)}$$

Table 1 in Electronic Annex 2 gives the fitted parameters for all of these reactions. Reaction (5)–(9) were normalized to ½ acetate (corresponding to 1 organic C atom). Changes in kinetic rates were defined at each experimental event.

Fig. 8 shows the good agreement (because fitted) between modelled concentrations in the borehole as a function of time for organic compounds, SO_4 and CH_4.

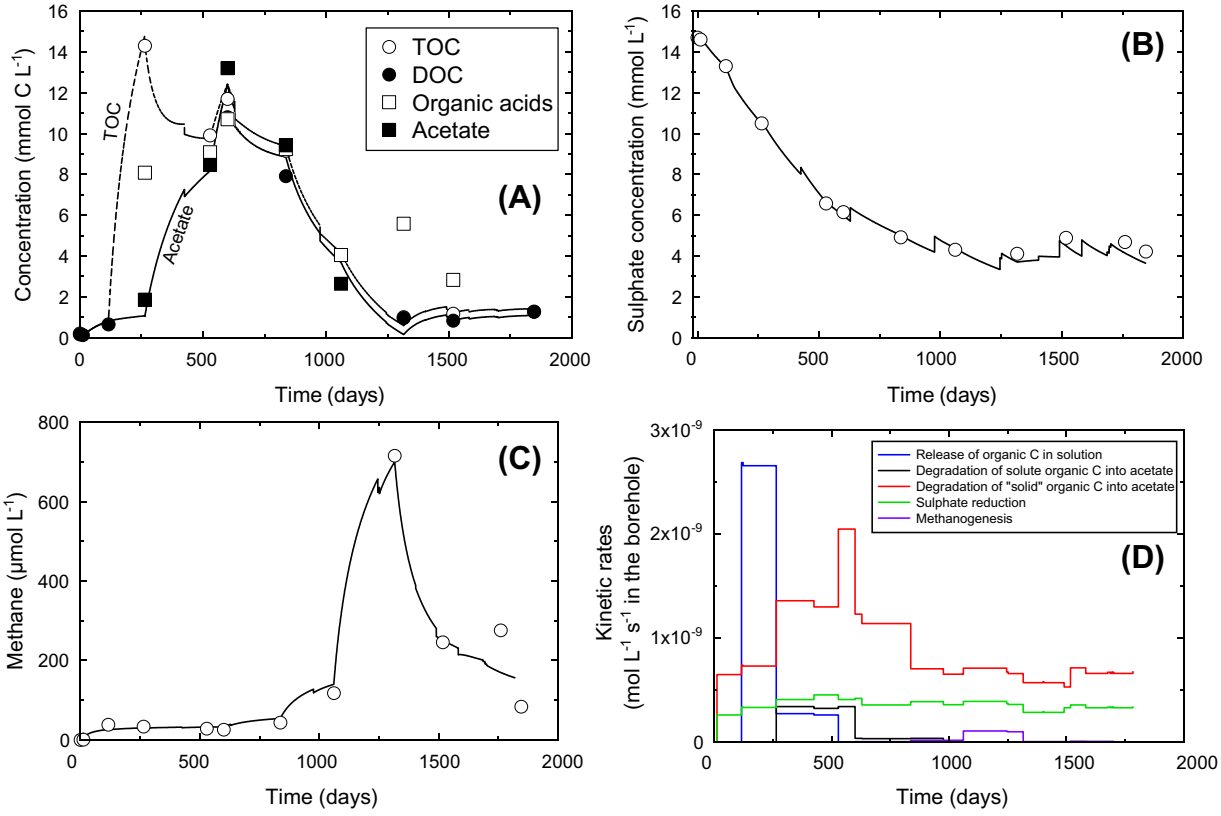

Fig. 8. Comparison of experimental results and model using glycerol as the organic C source. Top left figure: organic matter. Plain line = acetate; dashed line = TOC (=acetate + solute organic source). Top right figure: SO_4 concentration. Bottom left figure: CH_4 concentration. Bottom right figure: evolution of kinetic rates as a function of time.

3.4.2. Mineral precipitation/dissolution

Due to the intense bacterial activity, a large amount of sulfide has been produced that has precipitated as FeS compounds and pyrite (Koroleva et al., 2011). According to speciation calculations using experimental data (pH, Fe(II) and sulfide concentration when available), pyrite was oversaturated. As a consequence, pyrite could not be considered at equilibrium in the simulation. According to the fast kinetic of precipitation for FeS in the experimental conditions (Rickard, 1995) with regards to the simulation time-step, it was decided to consider equilibrium for a FeS compound:

$$FeS + H^+ \Rightarrow Fe^{2+} + HS^- \qquad \text{(Reaction10)}$$

The solubility K_{FeS} of the compound was fixed at the mackinawite solubility tabulated in the database ($\log_{10} K_{FeS} = -3.54$). Pyrite precipitation was considered as a kinetic process linked to the abundance of FeS (Rickard and Luther, 2007). The rate of pyrite precipitation had little influence on the outcome of the simulation with regards to simulated Fe and sulfide concentrations in the borehole. The only effect is on the FeS/pyrite ratio of precipitated minerals. Unfortunately, no quantitative data is available for this parameter.

Calcite was found to precipitate in the borehole as well (Koroleva et al., 2011), in agreement with its saturation index calculated from alkalinity, pH and Ca concentration (Fig. 9). Calcite was oversaturated during the whole of the experiment due to (i) kinetic limitation for its precipitation and/or (ii) measurement uncertainties and/or (iii) uncertainties in the database regarding the solute complex of Ca. These effects were taken into account by considering that calcite precipitated in the borehole at thermodynamic equilibrium but with a saturation index of 0.2 instead of 0.

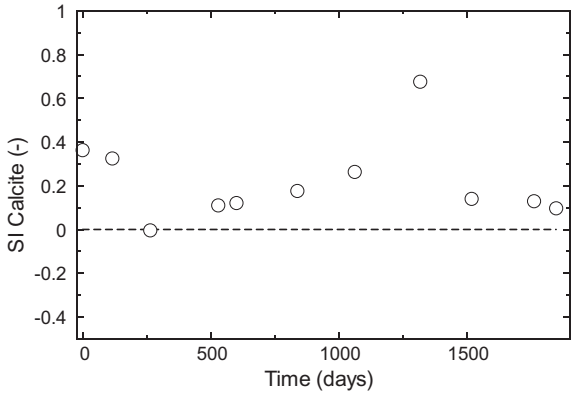

Fig. 9. Saturation index of calcite as a function of time.

3.4.3. pH buffer effect of clay mineral surfaces

The pH buffer effect of clay minerals was taken into account by considering the clay 2-pK non electrostatic model of Bradbury and Baeyens (1997). The amounts of sites were recalculated from the measured amount of illite + illite/smectite in the rock (~38%, Koroleva et al., 2011). It was considered that illite and smectite sites have nearly the same buffer properties (Bradbury and Baeyens, 2009a,b). In addition, it was considered that H^+ could undergo cation exchange reaction with the same affinity for the surface as Na^+ (Laudelout et al., 1968; Ferrage et al., 2005). The effect of compaction on site accessibility in the intact rock material was not taken into account.

4. Results and discussion

4.1. Influence of the nature of the organic matter on modelling results

Once organic matter production and degradation rates have been determined, the effect of these reactions can be assessed on key parameters such as pH and alkalinity. However, these parameters are potentially highly buffered by the surrounding formation. In a first attempt, the pH buffer of the clay surfaces was considered as described above together with the equilibrium of the formation with its calcite and siderite constituents. No other mineral in the formation was introduced into the model. Fig. 9 shows that the consideration of CH_2O, glycerol or acetone as the primary source of C has a significant effect on the result. Modelled alkalinity increases in the order acetone < glycerol < CH_2O. Conversely, pH decreases in the order acetone > glycerol > CH_2O. These relationships can be easily appreciated through the consideration of combinations of reactions (11)–(13) that all concern organic matter degradation via SO_4 reduction:

$$4/7C_3H_8O_3 + SO_4^{2-} \Rightarrow CH_3COO^- + 5/7H^+ + 4/7H_2O + 12/7HCO_3^- + HS^- \quad \text{(Reaction11)}$$

$$2CH_2O + SO_4^{2-} \Rightarrow 2HCO_3^- + H^+ + HS^- \quad \text{(Reaction12)}$$

$$1/2CH_3{-}CO{-}CH_3 + SO_4^{2-} \Rightarrow 3/2HCO_3^- + 1/2H^+ + HS^- \quad \text{(Reaction13)}$$

For each SO_4 mole that is transformed into sulfide in these reactions, glycerol produces 1.7 mol of HCO_3, CH_2O, 2 mol and acetone, 1.5 mol. The evolution is similar for pH: the acetone case, with 0.5 H^+ produced per mole of SO_4, exhibits logically the highest pH while the CH_2O case led to the most acidic result with 1 H^+ per SO_4 molecule. Glycerol produces 0.7 H^+ per SO_4 and leads to an intermediate result between CH_2O and acetone.

Whereas, in all cases, pH predicted by the simulation is in general agreement with measured pH, TIC and alkalinity are best reproduced with the glycerol model (Fig. 10). This result is in agreement with the results of De Cannière et al. (2011), who demonstrate that glycerol is the best candidate for the organic source in the system.

4.2. Influence of the pH buffer from the formation

The test-case without clay surface pH buffering in the formation revealed that this buffer has an important effect on the outcome of the simulation: without this buffering effect, total inorganic C concentration increases too much while the pH is too low (Fig. 11). The results, however, remain in good agreement with the measurements. Increasing the buffering capacity by a factor of 3 has little effect on the results (Fig. 11): as a consequence, the present experiment cannot be used to finely determine this buffering capacity although it confirms its existence. With regard to the boundary conditions, the pH of the porewater is a parameter whose uncertainty must be addressed: measured and modelled pH values up to 7.5 have been reported (Pearson et al., 2011). An additional simulation was run with an initial pH of 7.4 in the porewater of the formation. The alkalinity value was adjusted accordingly to achieve equilibrium with calcite without changing the Ca concentration. This change has a marked effect on the modelling result (Fig. 11) with inorganic C concentration being too low and pH too high: as a consequence, at the location of the experiment, the pH of the porewater is at a value of 7 rather than 7.5. The outcome of this sensitivity analysis is summarized in Table 3.

4.3. Iron and sulfide controls

Iron and sulfide concentrations are not well reproduced by the model as a function of time (Fig. 12). It should be noted that the maximum concentration of sulfide at day 600 in the system is in agreement with the solubility of mackinawite, representative here of an "amorphous" FeS compound (note that, at that time, the predicted Fe concentration is not too much in error). It was, however, neither possible to reproduce the decrease in sulfide after day 600, nor the strong increase in Fe concentration at day 1061. The Fe and sulfide systems are highly oscillatory and it is thus difficult to describe them with an equilibrium approach. In particular, the peak of sulfide concentration is fully correlated with the peak in acetate concentration, although the precipitated FeS in the borehole should have buffered its concentration as shown by the model. Potential degassing (loss of H_2S) and introduction of atmospheric O_2 during the leakage events were not taken into account in the simulations and could have played a role in the control of the sulfide concentration.

Regarding Fe, the presence of organic chelates in solution, originating from bacterial activity, could be an explanation for its measured concentration being too high compared to the model.

4.4. Concentrations of major cations

Major cations (Na, Ca, Mg, K, Sr) are adequately described by the model (Fig. 13). This result was fully expected since the porewater composition was calculated in agreement with their concentrations that remained almost constant in the borehole during the

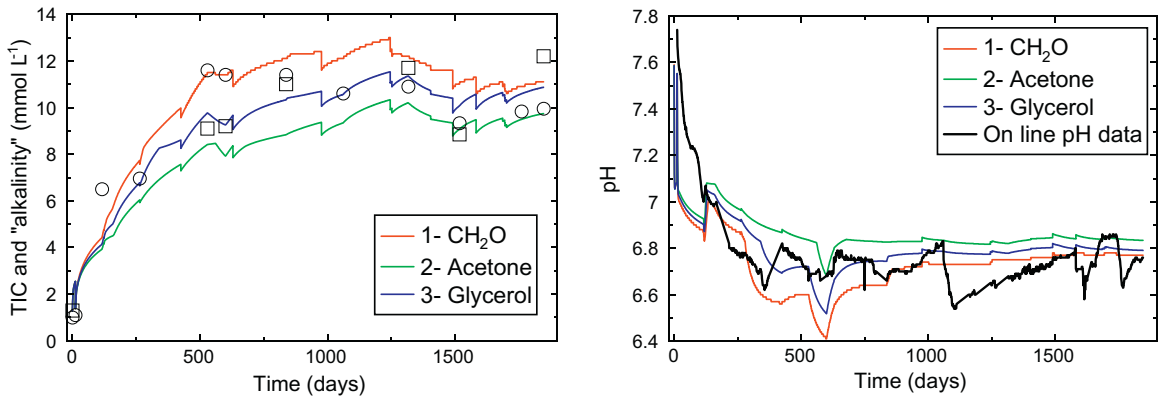

Fig. 10. Left: total inorganic C (squares) and alkalinity (circles) as a function of time. Right: pH (solid black line) as a function of time. Lines are indicative of modelled total inorganic C and pH according to the following scenario (organic C release in solution/solid source of C): 1 – CH_2O/CH_2O; 2 – Acetone/Acetone; 3 – Glycerol/glycerol.

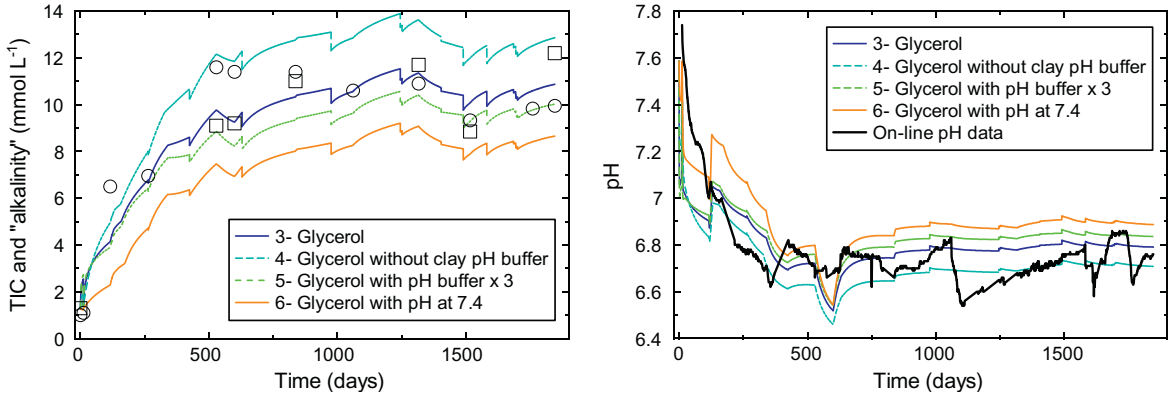

Fig. 11. Left: total inorganic C (squares) and alkalinity (circles) as a function of time. Right: pH (solid black line) as a function of time. Lines are indicative of modelled total inorganic C and pH according to the following scenario (organic C release in solution/solid source of C): 4 – Glycerol/Glycerol without pH buffer of clay surfaces; 5 – buffering capacity × 3; 6 – porewater pH at 7.4 instead of 7.

Table 3
Outcome of sensitivity analysis on organic matter source and clay pH buffer effect.

	Organic matter	Clay pH buffer	Comment
Simulation 1	CH_2O	Yes	High alkalinity, low pH
Simulation 2	Acetone	Yes	Low alkalinity, high pH
Simulation 3 = reference simulation	Glycerol	Yes	
Simulation 4	Glycerol	No	High alkalinity, low pH
Simulation 5	Glycerol	Yes × 3	Almost no effect
Simulation 6	Glycerol	Yes and initial pH = 7.4	Low alkalinity, high pH

experiment. It may be noted that the modelled Ca concentration decreases with time in the borehole and with an evolution parallel to the measured concentration. A slight increase in the Ca concentration in the porewater (corresponding to a small decrease in the exchange selectivity coefficient for Ca) together with an increase in the saturation index of calcite would make it possible to reproduce the data almost perfectly (not shown).

4.5. Comparisons with over-coring data

Mineralogical and chemical data obtained from over-coring sampling did not show significant changes in the composition of the clayrock material directly surrounding the experiment in spite of the dramatic changes of concentration of some components in the borehole (e.g. SO_4, S, pH and total inorganic C). Conversely, the analysis of mineralogical phases having precipitated inside the borehole revealed the high reactivity of the system. This type of contrasting information between clay–rock and borehole is direct proof of the high buffering capacity of the rock with regard to chemical perturbations and it can be further ascertained from the analysis of reactive transport modelling outcomes.

The precipitation of "amorphous" sulfide mineral in the borehole together with a kinetically controlled precipitation of pyrite was an input condition for the modelling. The important information obtained from the modelling work is that (i) sulfide minerals can effectively precipitate (from the thermodynamic and kinetic points of view) and (ii) that more than 99.9% of amorphous sulfide mineral precipitated at the interface. Fig. 14 illustrates the presence of a zone enriched in precipitates at the borehole/clay formation interface (the *y*-axis is in log scale). Detachment of minerals from this zone due to water circulation causing erosion of the borehole wall could explain the massive presence of sulfide minerals at the bottom of the borehole and in the circulation tubes at the end of the experiment. This simulation result also explains why it was not possible to detect precipitation of such phases inside the clayrock formation.

While calcite precipitation has been observed in the borehole, it was not possible to detect any newly precipitated calcite in the first centimetres of the formation. The simulations are also in agreement with this observation, since only the borehole shows

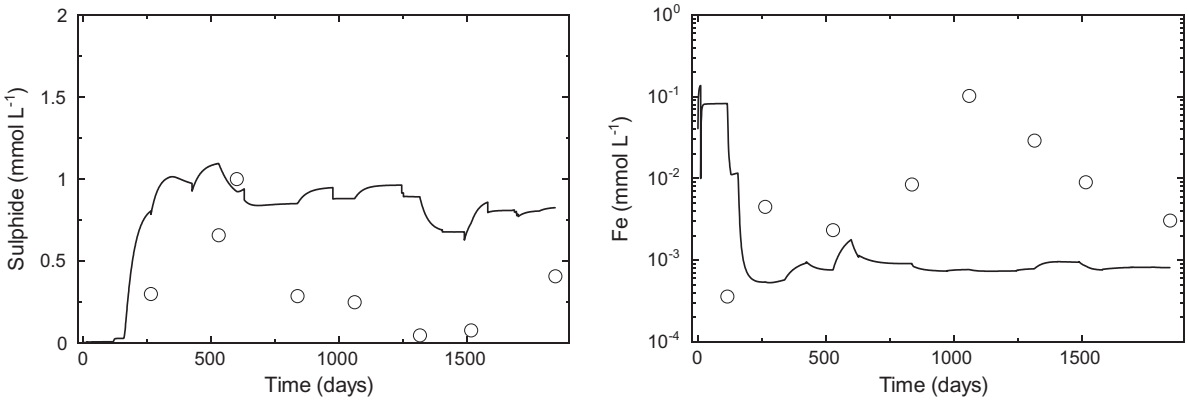

Fig. 12. Left: sulfide concentration as a function of time. Right: Fe concentration as a function of time (note that the concentration is in log scale). Lines are indicative of modelled concentrations (Scenario 3 with glycerol).

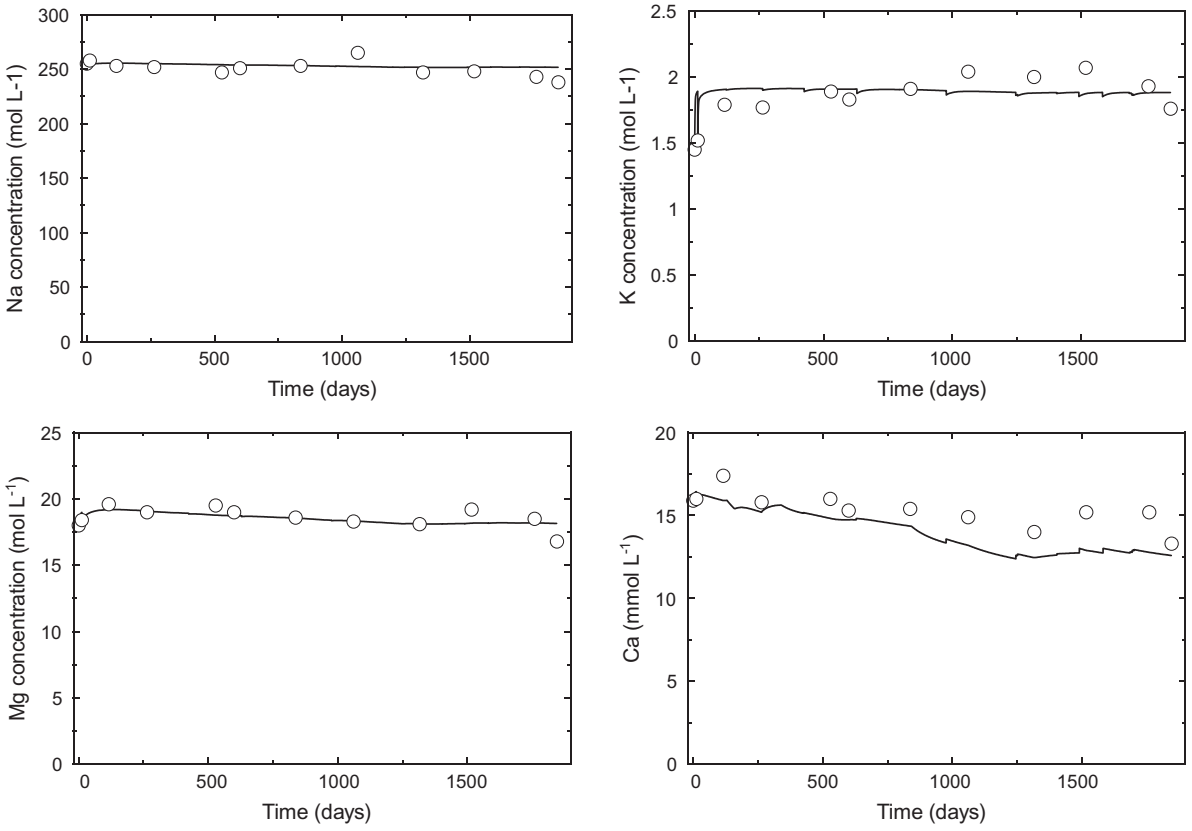

Fig. 13. Concentrations of major cations as a function of time. Circles: measurements. Lines: model (Scenario 3 with glycerol).

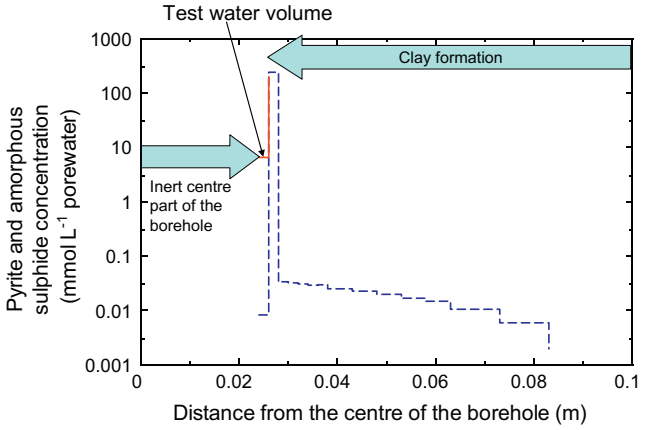

Fig. 14. Modelled pyrite (red) and amorphous sulfide (blue) solid concentration profile (in mmol L^{-1} porewater) after 1846 days of perturbation (Glycerol simulation case). (For interpretation of the references to colour in this figure legend, the reader is referred to the web version of this article.)

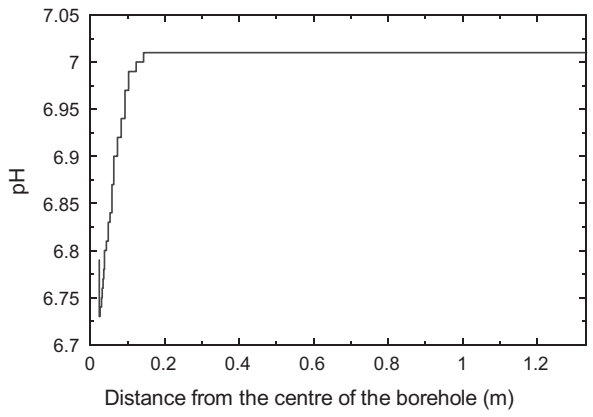

Fig. 15. pH profile after 1846 days of perturbation (Glycerol simulation case).

significant change in its calcite content (8.85 mmol L^{-1} were precipitated in the borehole according to simulation results). The maximum relative increase in calcite content is at the interface and accounts for only 0.3% of the initial amount of calcite. Accordingly, the change of pH in the formation is rapidly buffered as shown in Fig. 15.

5. Conclusions

Reactive transport modelling simulation of the porewater chemistry experiment at Mont Terri proved to be efficient in reproducing a complex set of chemical analyses as a function of time. The good agreement between the model and the measurements performed in the borehole water and also in samples from overcoring enables the following conclusions to be drawn:

(i) The Opalinus Clay rock formation has a high buffering capacity with regard to chemical perturbation due to bacterial activity: S production as well as pH decrease or alkalinity increase was buffered within a few centimetres of the borehole. This buffering capacity is attributed to the carbonate system as well as to the clay surface reactivity.

(ii) The chemical controls of pH and major cations and anions in Opalinus Clay porewater chemistry are now well constrained (Pearson et al., 2011), enabling realistic simulations of a perturbed system thanks to an accurate description of the initial unperturbed system.

(iii) Reactive transport models proved to be useful in discriminating between hypotheses with regard to different reactive pathways (e.g. different sources of organic C for bacteria in this experiment).

Of course, it is not possible to prove that the proposed model is the unique solution to the system regarding the numerous parameters that are (or could be) included. The present work only shows that it is possible to reproduce all the main outcomes of a chemical perturbation in a clay host-rock with a model that takes into account the state of the art on chemical controls in these rocks. Potential applications of this model are discussed in the next synthesis paper (Wersin et al., 2011).

Acknowledgements

This work was undertaken in close co-operation with, and with the financial support of, the Mont Terri Consortium. We appreciate fruitful discussions with Agnes Vinsot, Suzanne Mettler, Pierre De Cannière, David Arcos, Urs Mader, Nick Waber and Sim Stroes-Gascoyne during the Porewater Chemistry experiment. Many thanks also to the Mont Terri team, including Christophe Nussbaum and Paul Bossart (Swisstopo), for their continuous support to the project.

Appendix A. Supplementary material

Supplementary data associated with this article can be found, in the online version, at doi:10.1016/j.apgeochem.2011.03.009.

References

Alt-Epping, P., Gimmi, T., Waber, H.N., 2006. Porewater Chemistry (PC) Experiment at Mt. Terri, Switzerland: Reactive Transport Simulations. NAGRA Technical Note, TN 2006-66.

ANDRA, 2005. Référentiel du comportement des radionucléides et des toxiques chimiques d'un stockage dans le Callovo-Oxfordien jusqu'à l'Homme. Dossier 2005 Argile. Agence Nationale pour la gestion des déchets radioactifs, Châtenay-Malabry, France.

Appelo, C.A.J., 1994. Some calculations on multicomponent transport with cation-exchange in aquifers. Ground Water 32, 968–975.

Appelo, C.A.J., Wersin, P., 2007. Multicomponent diffusion modeling in clay systems with application to the diffusion of tritium, iodide, and sodium in Opalinus clay. Environ. Sci. Technol. 41, 5002–5007.

Appelo, C.A.J., Verweij, E., Schäfer, H., 1998. A hydrogeochemical transport model for an oxidation experiment with pyrite/calcite/exchangers/organic matter containing sand. Appl. Geochem. 13, 257–268.

Appelo, C.A.J., Vinsot, A., Mettler, S., Wechner, S., 2008. Obtaining the porewater composition of a clay rock by modeling the in- and out-diffusion of anions and cations from an in-situ experiment. J. Contam. Hydrol. 101, 67–76.

Arcos, D., 2003. Porewater chemistry (PC) experiment: results of the geochemical modelling. Mont Terri Project TN 2003, 18.

Arcos, D., Duro, L., Gimmi, T., Waber, H.N., 2004. Modeling of tracer behaviour and dominant reactions during the Pore Water Chemistry (PC) experiment in the Opalinus Clay, Switzerland. In: Wanty, R.B., Seal II, R.R. (Eds.), Water Rock Interaction. Proc, 11th Int. Symp. Water–Rock Interaction, WRI 11, Saratoga Springs. A.A. Balkema, pp. 337–341.

Bradbury, M.H., Baeyens, B., 1997. A mechanistic description of Ni and Zn sorption on Na-montmorillonite. Part II: modeling. J. Contam. Hydrol. 27, 223–248.

Bradbury, M.H., Baeyens, B., 2009a. Sorption modelling on illite Part I: titration measurements and the sorption of Ni, Co, Eu and Sn. Geochim. Cosmochim. Acta 73, 990–1003.

Bradbury, M.H., Baeyens, B., 2009b. Sorption modelling on illite. Part II: actinide sorption and linear free energy relationships. Geochim. Cosmochim. Acta 73, 1004–1013.

Cartalade, A., Montarnal, P., Filippi, M., Mugler, C., Lamoureux, M., Martinez, J.M., Clement, F., Wileveau, Y., Coelho, D., Tevissen, E., 2007. Application of inverse modeling methods to thermal and diffusion experiments at Mont Terri Rock laboratory. Phys. Chem. Earth 32, 491–506.

Courdouan, A., Christl, I., Meylan, S., Wersin, P., Kretzschmar, R., 2007. Characterization of dissolved organic matter in anoxic rock extracts and in situ pore water of the Opalinus Clay. Appl. Geochem. 22, 2926–2939.

De Cannière, P., Schwarzbauer, J., Höhener, P., Lorenz, G., Salah, S., Leupin, O.X., Wersin P., 2011. Biogeochemical processes in a clay formation in situ experiment: part C – organic contamination and leaching data. Appl. Geochem. 26, 967–979.

Ferrage, E., Tournassat, C., Rinnert, E., Lanson, B., 2005. Influence of pH on the interlayer cationic composition and hydration state of Ca-montmorillonite: analytical chemistry, chemical modelling and XRD profile modelling study. Geochim. Cosmochim. Acta 69, 2797–2812.

Gailhanou, H., van Miltenburg, J.C., Rogez, J., Olives, J., Amouric, M., Gaucher, E.C., Blanc, P., 2007. Thermodynamic properties of anhydrous smectite MX-80, illite IMt-2 and mixed-layer illite–smectite ISCz-1 as determined by calorimetric methods. Part I: heat capacities, heat contents and entropies. Geochim. Cosmochim. Acta 71, 5463–5473.

Gailhanou, H., van Miltenburg, J.C., van Genderen, A., Rogez, J., Greneche, J.M., Gilles, C., Gaucher, E.C., Blanc, P., 2009. Thermodynamic properties of ripidolite CCa-2. Part I. Heat capacities, heat contents and entropies. Geochim. Cosmochim. Acta 73, 4738–4749.

Gaucher, E.C., Blanc, P., 2006. Cement/clay interactions – a review: experiments, natural analogues, and modeling. Waste Manage. 26, 776–788.

Gaus, I., Audigane, P., Andre, L., Lions, J., Jacquemet, N., Dutst, P., Czernichowski-Lauriol, I., Azaroual, M., 2008. Geochemical and solute transport modelling for CO_2 storage, what to expect from it? Int. J. Greenhouse Gas Control 2, 605–625.

Grandia, F., Domènech, C., Arcos, D., 2006. Pore water chemistry (PC) experiment: results of the geochemical modelling. ENVIROS Report, R-2225.1.

Han, W.S., McPherson, B.J., Lichtner, P.C., Wang, F.P., 2010. Evaluation of trapping mechanisms in geologic CO_2 sequestration: case study of sacroc northern platform, a 35-year CO_2 injection site. Am. J. Sci. 310, 282–324.

Koroleva, M., Lerouge, C., Mäder, U., Claret, F., Gaucher, E., 2011. Biogeochemical processes in a clay formation in situ experiment: part B – results from overcoring and evidence of strong buffering by the rock formation. Appl. Geochem. 26, 954–966.

Laudelout, H., Van Bladel, R., Bolt, G.H., Page, A.L., 1968. Thermodynamics of heterovalent cation exchange reactions in a montmorillonite clay. Trans. Faraday Soc. 64, 1477–1488.

Lichtner, P.C., 2007. FLOTRAN Users Manual: Two-phase Non-isothermal Coupled Thermal–hydrologic–chemical (THC) Reactive Flow and Transport Code, Version 2. Los Alamos National Laboratory, Los Alamos, New Mexico.

Lichtner, P.C., Steefel, C.I., Oelkers, E.H. (Eds.), 1996. Reactive Transport in Porous Media. Reviews in Mineralogy, vol. 34. Mineralogical Society of America.

Maher, K., Steefel, C.I., White, A.F., Stonestrom, D.A., 2009. The role of reaction affinity and secondary minerals in regulating chemical weathering rates at the Santa Cruz Soil Chronosequence, California. Geochim. Cosmochim. Acta 73, 2804–2831.

Parkhurst, D.L., Appelo, C.A.J., 1999. User's guide to PHREEQC (Version 2) – a computer program for speciation, batch-reaction, one-dimensional transport, and inverse geochemical calculations. US Geol. Surv. Water-Resour. Invest. Rep. 99-4259.

Parkhurst, D.L., Kipp, K.L., Engesgaard, P., Charlton, S.R., 2004. PHAST – a program for simulating ground-water flow, solute transport, and multicomponent geochemical reactions. US Geol. Survey Techniques and Methods 6-A8.

Pearson, F.J., Arcos, D., Bath, A., Boisson, J.-Y., Fernández, A.M, Gäbler, H.-E., Gaucher, E., Gautschi, A., Griffault, L., Hernán, P., Waber, H.N., 2003. Mont Terri Project – Geochemistry of Water in the Opalinus Clay Formation at the Mont Terri Rock Laboratory. Bern, Switzerland, Federal Office for Water and Geology (FOWG). Geology Series 5.

Pearson, F.J., Tournassat, C., Gaucher, E., 2011. Biogeochemical processes in a clay formation in situ experiment: part E – equilibrium controls on chemistry of pore water from the Opalinus Clay, Mont Terri Underground Laboratory, Switzerland. Appl. Geochem. 26, 990–1008.

Rickard, D., 1995. Kinetics of FeS precipitation: part 1. Competing reaction mechanisms. Geochim. Cosmochim. Acta 59, 4367–4379.

Rickard, D., Luther III, G.W., 2007. Chemistry of iron sulfides. Chem. Rev. 107, 514–562.

Steefel, C.I., Lichtner, P.C., 1994. Diffusion and reaction in rock matrix bordering a hyperalkaline fluid-filled fracture. Geochim. Cosmochim. Acta 58, 3595–3612.

Steefel, C.I., Carroll, S., Zhao, P., Roberts, S., 2003. Cesium migration in Hanford sediment: a multisite cation exchange model based on laboratory transport experiments. J. Contam. Hydrol. 67, 219–246.

Steefel, C.I., DePaolo, D.J., Lichtner, P.C., 2005. Reactive transport modeling: an essential tool and a new research approach for the Earth sciences. Earth Planet. Sci. Lett. 240, 539–558.

Stroes-Gascoyne, S., Sergeant, C. Schippers, A., Hamon, C.J., Neble, S., Vesvres, M.-H., Barsotti, V., Poulain, S., Le Marrec, C., 2011. Biogeochemical processes in a clay formation in situ experiment: part D – microbial analyses – synthesis of results. Appl. Geochem. 26, 980–989.

Tournassat, C., Gaucher, E., 2004. Progress in modelling PC-experiment results including thermodynamics, kinetics, micro-organism activity and isotopic fractionation considerations. BRGM/RP-53395-FR, NAGRA/TN 2004-72.

Tournassat, C., Gailhanou, H., Crouzet, C., Braibant, G., Gautier, A., Gaucher, E.C., 2009. Cation exchange selectivity coefficient values on smectite and mixed-layer illite/smectite minerals. Soil Sci. Soc. Am. J. 73, 928–942.

Tournassat, C., Gailhanou, H., Crouzet, C., Braibant, G., Gautier, A., Lassin, A., Blanc, P., Gaucher, E.C., 2007. Two cation exchange models for direct and inverse modelling of solution major cation composition in equilibrium with illite surfaces. Geochim. Cosmochim. Acta 71, 1098–1114.

Van Loon, L.R., Glaus, M.A., Müller, W., 2007. Anion exclusion effects in compacted bentonites: towards a better understanding of anion diffusion. Appl. Geochem. 22, 2536–2552.

Van Loon, L.R., Soler, J.M., Jakob, A., Bradbury, M.H., 2003. Effect of confining pressure on the diffusion of HTO, $^{36}Cl^-$ and $^{125}I^-$ in a layered argillaceous rock (Opalinus Clay): diffusion perpendicular to the fabric. Appl. Geochem. 18, 1653–1662.

Van Loon, L.R., Soler, J.M., Muller, W., Bradbury, M.H., 2004a. Anisotropic diffusion in layered argillaceous rocks: a case study with Opalinus Clay. Environ. Sci. Technol. 38, 5721–5728.

Van Loon, L.R., Wersin, P., Soler, J.M., Eikenberg, J., Gimmi, T., Hernan, P., Dewonck, S., Savoye, S., 2004b. In-situ diffusion of HTO, $^{22}Na^{+}$, Cs^{+} and I^{-} in Opalinus Clay at the Mont Terri underground rock laboratory. Radiochim. Acta 92, 757–763.

Wersin, P., Leupin, O.X., Mettler, S., Gaucher, E., Mäder, U., De Cannière, P., Vinsot, A., Gabler, H.E., Kunimaro, T., Kiho, K., Eichinger, L., 2011. Biogeochemical processes in a clay formation in situ experiment: part A – overview, experimental design and water data of an experiment in the Opalinus Clay at the Mont Terri underground research laboratory, Switzerland. Appl. Geochem. 26, 931–953.

Wersin, P., Stroes-Gascoyne, S., Pearson, F.J., Tournassat, C., Leupin, O.X., Schwyn, B., 2011. Biogeochemical processes in a clay formation in situ experiment; part G – key interpretations and conclusions. Implications for repository safety.. Appl. Geochem. 26, 1023–1034.

Applied Geochemistry 26 (2011) 1023–1034

Contents lists available at ScienceDirect

Applied Geochemistry

journal homepage: www.elsevier.com/locate/apgeochem

Biogeochemical processes in a clay formation *in situ* experiment: Part G – Key interpretations and conclusions. Implications for repository safety

P. Wersin [a,e,*], S. Stroes-Gascoyne [b], F.J. Pearson [c], C. Tournassat [d], O.X. Leupin [a], B. Schwyn [a]

[a] NAGRA, Hardstrasse 73, 5430 Wettingen, Switzerland
[b] Atomic Energy of Canada Limited (AECL), Whiteshell Laboratories, Pinawa, Manitoba, Canada R0E 1L0
[c] Ground-Water Geochemistry, 5108 Trent Woods Drive, New Bern, NC 28562, USA
[d] BRGM, French Geological Survey, 3 Avenue Claude Guillemin, B.P. 36009, 45060 Orléans Cedex 2, France
[e] Gruner Ltd., Gellertstrasse 55, 4020 Basel, Switzerland

ARTICLE INFO

Article history:
Available online 17 March 2011

ABSTRACT

The *in situ* porewater chemistry (PC) experiment carried out in the Opalinus Clay formation at the Mont Terri Rock Laboratory, Switzerland for a period of 5 a allowed the identification and quantification of the biogeochemical processes resulting from and affected by an anaerobic microbial disturbance. The unintentional release of degradable organic compounds (mainly glycerol) induced microbially-mediated SO_4 reduction in the borehole with concomitant significant geochemical changes in the circulating water and the adjacent porewater. These changes included a decrease in SO_4^{2-} concentration and pH and an increase in pCO_2 and alkalinity relative to the non-affected formation water. However, the cation composition of the water and the mineralogy of the clay close to the borehole wall showed very little change. This is explained by (1) the strong chemical buffering processes in the clay and (2) by the diffusion-limited flux of solutes.

With the aid of a reactive transport model with a minimum set of kinetic parameters for the hypothesised degradation reactions, the evolution of solutes in the borehole could be modelled adequately. The model was also applied to the prediction of restoration times upon depletion of the C source and results indicated restoration times to undisturbed conditions of about 15 a, but also highlighted the rather large uncertainties inherent in the geochemical model. Nevertheless, the simulations provided additional evidence of the high pH buffer capacity of the Opalinus Clay.

The results from the microbiological investigations do not allow unambiguous identification of the origin of the microbial population in the borehole. Possible sources were the drilling procedure, the artificial porewater, and perhaps some revival of indigenous dormant strains. Regardless of the origin of the microbes, the results from the PC experiment underlined the importance of anaerobic microbial activity in the "disturbed" Opalinus Clay, facilitated by the introduction of space, water and organic material, in rapidly establishing very reducing conditions.

The PC experiment also yielded valuable insight with regard to the safety of a high-level radioactive waste repository emplaced in Opalinus Clay. Anaerobic microbial perturbations in the clay host rock may occur from the construction and excavation procedures and emplaced organic by-products. The resulting effects on porewater chemistry, i.e., especially on pH and Eh, may affect the mobility of radionuclides eventually released from the waste. However, the overall results of the PC experiment suggest that such effects are temporary and spatially limited because of the large buffering capacity and diffusive properties of the clay formation. Nevertheless, the results also indicate that the amounts of organic materials in a high-level waste repository should be kept small in order to achieve background conditions within a short time period after repository closure. A further conclusion from the PC experiment is that commonly used equipment materials may not display commonly assumed inert behaviour. This particularly holds for the gel-type "robust" reference electrodes, which may release substantial amounts of glycerol.

1. Introduction

Argillaceous formations are foreseen as host rocks for nuclear waste repositories in an increasing number of countries, such as France, Belgium, Canada and Switzerland. Suitable indurated clay

* Corresponding author at: Gruner Ltd., Gellertstrasse 55, 4020 Basel, Switzerland. Tel.: +41 61 317 64 15; fax: +41 61 271 79 48.
E-mail address: paul.wersin@gruner.ch (P. Wersin).

0883-2927/$ - see front matter © 2011 Elsevier Ltd. All rights reserved.
doi:10.1016/j.apgeochem.2011.03.010

formations, such as for example the Opalinus Clay in Switzerland, display favourable hydraulic and mechanical properties, which include low permeability and the capacity of self-sealing (Nagra, 2002). Moreover, such formations are characterised by their remarkable geochemical stability (Beaucaire et al., 2004). This point is addressed in more detail below. The transport of radionuclides, which may eventually enter the geosphere once the canister containment is breached and the waste form is dissolving, is limited by diffusion and retardation processes (e.g. Nagra, 2002; ANDRA, 2005). These processes are affected by the porewater chemistry and, therefore, it is important to know the solute composition and the underlying processes which regulate it.

An *in situ* experiment, termed the porewater chemistry (PC) experiment, designed to obtain better knowledge of porewater composition in the Opalinus Clay, was carried out in the Mont Terri Rock Laboratory for a period of 5 a. As described in a companion paper (Wersin et al., 2011) the scope of this experiment was reformulated after observing unexpected microbiological activity in the packed-off borehole: it was recognised that it was important to understand the biogeochemical processes occurring in a "disturbed" clay formation and to interpret these also from a repository safety point of view, i.e. evaluate the possible consequences on the safety case (discussed later in this paper). Hence, an extensive experimental and modelling program was conducted during and after the *in situ* PC test. The procedures and results of this work are presented in companion papers in this special issue: In Wersin et al. (2011), the experimental procedures for the *in situ* test are outlined and the results from the evolving water composition in the borehole are presented and interpreted qualitatively. Koroleva et al. (2011) gives the procedures of the overcoring and presents analytical results of the rock samples close to the borehole/rock interface. The experimental study related to the identification of the source(s) of degrading organic C is presented in De Cannière et al. (2011). The microbiological results from a variety of analyses are outlined and interpreted in Stroes-Gascoyne et al. (2011). Equilibrium constraints on porewater chemistry are discussed in Pearson et al. (2011). The quantitative interpretation of the biogeochemical processes, using reactive transport modelling, is given in Tournassat et al. (2011).

The objectives of this contribution are twofold: First, the results from the PC experiment are summarised and the main conclusions formulated. Second, the results are discussed in the light of their relevance for the long-term safety of a repository embedded in a clay host rock. The main question in the latter is: How relevant is the observed microbial perturbation for the safety functions of the safety barriers, i.e., the host rock and the engineered components (e.g. the waste canisters)?

2. Summary of procedures, analyses and modelling efforts

As noted, the detailed procedures of the *in situ* PC test and the accompanying laboratory and modelling work are presented in the different companion papers in this issue. Here only a brief summary is presented.

2.1. In situ test

The *in situ* PC experiment, which was carried out at the Mont Terri Rock Laboratory in the Liassic Opalinus Clay formation (Fig. 1), was based on the concept of diffusive equilibration. Traced synthetic water with a composition similar to that expected in the surrounding formation porewater was circulated in a packed-off vertical borehole (BPC-1). The contact between the synthetic water and the clay formation occurred via a 4.5 m polyethylene (PE) porous filter (previously washed with acetone to remove traces of grease). All materials in contact with the circulation water were made of chemically "inert" plastic materials (PE, polyamide, PEEK, polyurethane). The solution was monitored continuously online for pressure, temperature, pH, Eh and EC. The pH and Eh electrodes contained gel-filled (polymer) reference electrodes and the initial EC electrode was of a graphite type. The pH electrode displayed non-linear drift and needed to be replaced at irregular intervals because of leakage of K and glycerol from the gel, as well as from the reaction of Ag in the electrode with sulphide in the water. The graphite-type EC electrode was replaced by a more reliable Pt-type electrode because it showed anomalous behaviour. The Eh electrode displayed only small drift and was replaced only once within the 5 a of experimental duration.

2.2. Analyses

The water was sampled at regular time intervals using Teflon-coated cylinders placed in the circuit. The analytical program included major chemistry components (Na, Ca, Mg, K, Sr, Cl, SO_4, HCO_3) and added tracers (HDO, Br, ^{13}C-DIC), but was extended significantly after the discovery of microbial processes (after 6 months). Thus, various organic (TOC/DOC and its components: carboyxlic and other organic acids, alkanes) and inorganic species (Fe, Mn, NH_4, Si, Al, S species) and isotopic ratios (^{13}C-DOC, ^{14}C-DIC, ^{14}C-DOC, ^{18}O-H_2O, ^{34}S-SO_4, ^{34}S-H_2S) were also determined, in the later course of the experiment. Microbiological analysis of the PC borehole water started once it was apparent that there was a significant disturbance of the geochemistry from microbial activity. The PC water was analysed for microbial characteristics in 2003, 2004, 2005 (twice) and 2006. At the termination of the PC experiment, both water and clay overcore samples were shipped by courier to three independent laboratories for much more extensive microbial analysis, which included both traditional culture-based and modern molecular methods.

The circulation system was protected with a cabinet filled with Ar to ensure anoxic conditions in the borehole. These conditions were disturbed during short intervals of electrode replacement and also by a few experimental difficulties during the 5-a period. The associated increase in Eh was quickly re-established to reducing conditions (within 1–2 days), as recorded from Eh measurements.

After a period of 5 a, the experiment was dismantled and the test interval section was overcored with a core diameter of 284 mm. The focus of this overcoring exercise was to obtain mineralogical, geochemical and microbiological data of the rock, possibly disturbed by the biochemical processes in the borehole, and also of the potentially affected equipment material. Thus, rock samples were taken as a function of distance to the borehole and analysed for standard parameters (water content, density), mineralogical composition (XRD, SEM-EDX), cation exchange properties, aqueous leachates and stable isotopes.

2.3. Laboratory and modelling studies

CO_2 gas measurements on two core samples from BPC-1 were carried out by gas extraction under controlled atmosphere after an equilibration period of 40 days. Furthermore, the isotopic compositions ($\delta^{13}C$, $\delta^{18}O$) of the extracted CO_2 as well of CO_2 extracted from carbonate minerals (calcite, siderite, dolomite) were measured.

Undisturbed formation porewater was extracted from a core sample taken from a neighbouring borehole (BPC-A1). The extraction was performed by advective displacement in a pressure vessel where a high confining He pressure is applied (Mäder, 2004). Extracted water samples were analysed for major constituents and pH. Only the pH data are reported in this special issue (Wersin et al., 2011).

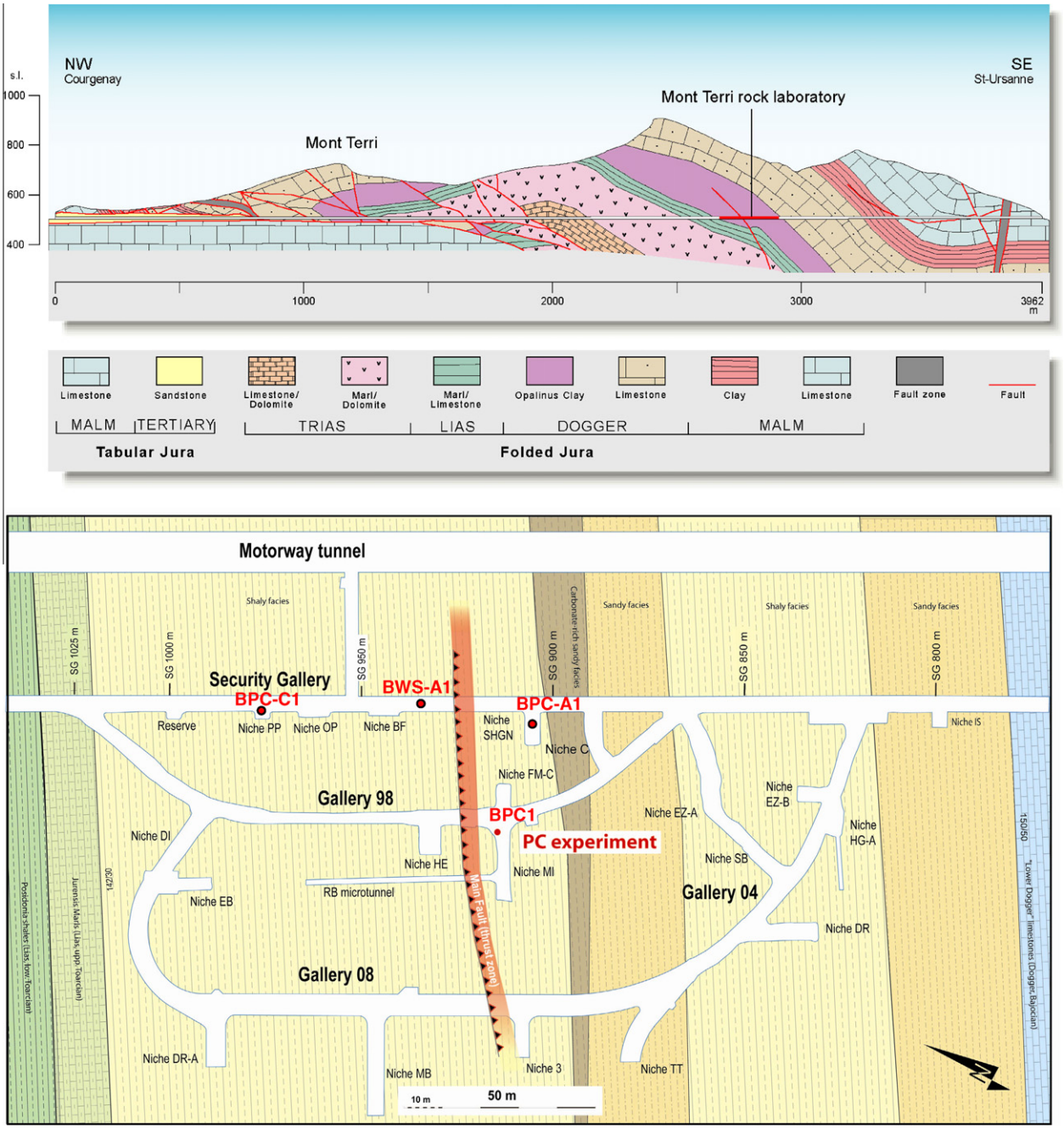

Fig. 1. Sketch of the geological profile and the Mont Terri Rock URL (upper) and location of the PC experiment (lower). Location of boreholes cited in text also shown.

The leaching behaviour of samples from plastic equipment materials (PE, polyurethane, polyamide) was investigated to shed light on the C source fuelling the observed microbial activity in the borehole. In addition, soaking tests with PE immersed with acetone, under conditions similar to those used to wash the porous PE filter prior to installation, were carried out. A further potential C source is the polymer-filling of the pH and Eh electrodes, which contains hydrophilic compounds (glycerol, polyethylene glycol and polyacrylate derivatives). Leaching tests with this gel-material were also conducted and the leachates analysed.

The microbiological study of the PC experiment was necessarily limited to PC borehole water samples while the experiment was ongoing. Analyses during the period 2003–2006 were limited mainly to determining the total and active number of cells in the PC water (using a number of dyes and specific probes). At the termination of the PC experiment, carefully taken PC water- and clay overcore samples were shipped by courier to three independent laboratories for much more extensive microbial analyses, including: total and active cell counts, quantitative and enrichment culturing for a number of physiological groups, while molecular methods included phospholipid fatty acid (PLFA) analysis, quantitative polymerase chain reaction (QPCR); and DNA extraction followed by amplification, separation, sequencing and identification.

The modelling effort focused on the development of a "minimum" model that could reproduce the chemical evolution of the water composition (in the borehole and in the formation) during the experiment. The following items were necessary pre-requisites for the construction of this "minimum" model:

(i) Knowledge of the transport properties of the rock. These properties (i.e., diffusion coefficients and porosity) could be obtained from the tracer (HDO, Br) concentrations in the

borehole water as a function of the time. Through the overcoring the analyses this could be refined by taking into account the tracers' profiles in the rock and by providing direct measurements of the total and anion accessible porosity values, through water content analysis and anion leaching experiments. The transport properties are of premium importance because the flux of dissolved species from the borehole water to the formation and vice versa is governed by these parameters. For instance, the flux of SO_4^{2-} from the formation to the borehole counter-balanced its transformation into sulphide in the borehole and a correct mass balance calculation could be achieved only by considering this diffusive flux.

(ii) Knowledge of the undisturbed porewater composition. This composition was established by modelling work using data obtained from other boreholes. This composition represents the initial and the boundary condition of the system to which all of the perturbation is scaled.

(iii) A scenario or set of scenarios describing the bacterial activity as a function of time in the borehole. This scenario must be represented as a sum of different reactions (governed by kinetics) in order to be implemented in the calculation code.

With respect to point (iii), it was not within the scope of this study to try and develop a mechanistic biological model because the biological processes identified were highly non-linear, due to different phases of bacterial growth and activity as a function of time. For this reason, only the main reaction pathways identified (e.g., acetate production, SO_4 reduction and methanogenesis), were introduced in the model without consideration of intermediate reactions. Similarly, it was not possible to attribute one given chemical reaction to one given bacterial strain and to relate it to its abundance as a function of time. The main interest of the modelling exercise was to reproduce the effects (i.e., concentration changes, precipitation or dissolution of minerals) induced by the bacterial activities but not the bacterial activity itself.

3. Main conclusions from the PC experiment

3.1. Evidence and quantification of diffusion processes

The behaviour of the conservative tracers HDO and Br observed in the circulation water and the rock shows that their transport is controlled by diffusion in the clay formation. The derived pore diffusion coefficients from 1D radial diffusion modelling parallel to the bedding planes are about 1 and 4×10^{-11} m^2/s for Br and HDO respectively, which is consistent with diffusion data for Opalinus Clay (Van Loon et al., 2004a,b; Wersin et al., 2008). Modelled diffusion porosities (Tournassat et al., 2011) were consistent with water content and leaching data (Koroleva et al., 2011) which indicated water loss porosities of ~0.18 (volume fraction) and anion porosities ("geochemical" porosity according to Pearson, 1999) of about 75% of this value. This is considerably higher than determined on core samples from other Mont Terri boreholes, in which 50–60% of the total porosity was accessible to anions (Pearson et al., 2003). The fact that anion accessible porosity is less than total porosity is attributed to anion exclusion from the negatively charged clay surface. This difference, as well as the slightly increased total porosity at the borehole rim, suggests a slight disturbance of the micro-fabric around the PC borehole. But, as outlined below, no other changes in the rock were noted.

Diffusion posed a severe constraint for the microbially-mediated redox reactions occurring in the borehole, as indicated also from accompanying modelling study of Tournassat et al. (2011).

3.2. Qualitative and quantitative description of microbial perturbation

Table 1 illustrates the difference between expected and observed water compositions. The first two compositions correspond to seepage waters from the nearby boreholes BWS-A1 and BPC-C1 where disturbances are much lower than in BPC-1. The log pCO_2 values in the seepage waters are lower than −2, which is consistent with CO_2 gas measurements from cores and the porewater extraction laboratory study (Wersin et al., 2011). The waters in the PC experiment displayed high pCO_2 values of −1.4 to −1.5 which is the result of microbial CO_2 production from the degradation of an organic C source.

The main "driver" for this degradation process is fermentation and SO_4 reduction, which schematically can be represented as:

$$2C + SO_4^{2-} + 2H_2O \rightarrow HS^- + 2HCO_3^- + H^+$$

The decrease in SO_4 and the concurrent increase in sulphide and alkalinity (Fig. 2) are manifested in the chemistry of the PC waters, which also reveal a decrease in pH related to the degradation process. The actual reaction pathway turned out to be complex, involving changing DOC concentrations, intermediate organic species and bacterial strains (or physiological groups of bacteria)

Table 1
Selected Water compositions in PC experiment and comparison with seepage water from nearby boreholes.

Borehole number	BPC-1	BPC-1	BPC-1	BWS-A1	BPC-C1
Sample number	PC-0	PC-6	PC-12	A1-85	#185378
Sample description	Initial synthetic water before experiment start	Porewater composition at peak DOC conc., 600 days after start	Porewater composition at end, 1846 days after start	Porewater composition	
(seepage water)					
28 April 99 (seepage water)	Porewater composition				
pH	7.7	6.7	6.8	7.5	7.2
Eh_{SHE} (mV)		−227	−250		–
log(pCO_2)[a]	−2.6	−1.36	1.48	−2.56	−2.08
Alk (mM)	1.0	11.4	10.4	2.5	3.3
DOC (mM)	0.2	10.6	1.3	1.1[b]	4.8
$SO_{4\ tot}$ (mM)	14.7	6.2	4.3	14.1	17.0
HS_{tot} (mM)		1.0	0.4		
Cl & Br (mM)	291	294	285	292	330
Na (mM)	255	251	243	246	281
Ca (mM)	15.9	15.3	13.5	15.0	19.3
Mg (mM)	18.0	19.0	17.1	16.9	22.3
C_{13}-DIC (‰)	−29.1	−16.6	−11.5	−13.1[b]	−7.3

[a] Calculated from Alkalinity & pH measurement.
[b] Sample taken on February 18, 1998.

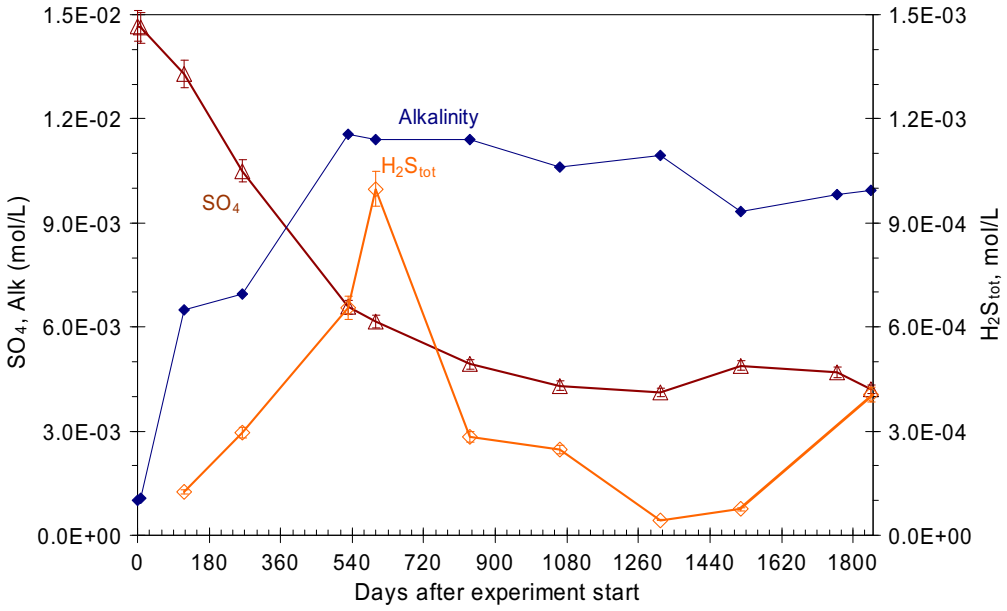

Fig. 2. Evolution of the dissolved SO_4, alkalinity and sulphide concentrations in borehole of PC experiment as function of time.

during the experiment. With the aid of the analysed data and reactive transport modelling (Tournassat et al., 2011), the degradation process can be represented by a pathway consisting of 4 distinct phases of microbial activity (Fig. 3).

During phase 1, only small amounts of organic C were released into the borehole water and little bacterial activity and SO_4 reduction occurred (lag phase). In phase 2 (which lasted until about 300 days after the start of the experiment) significant amounts of dissolved organic C (DOC) appeared in solution. This DOC consisted of various organic acids and other unknown compounds, but contained relatively little acetate at this point. In phase 3 (which lasted until 600 days), the DOC decreased and virtually all of it was transformed to acetate, as shown schematically:

$$4C + SO_4^{2-} + 4H_2O \rightarrow CH_3COOH^- + HS^- + 2HCO_3^- + H^+$$

The reaction pathway then changed in phase 4, which resulted in a strong decrease in DOC (still composed primarily of acetate) with continuing SO_4 reduction. During this last period (phase 4) a strong increase in CH_4 occurred, followed by a slight decrease in CH_4 towards the end of the experiment, suggesting the rising influence of a methanogenic degradation pathway in this stage.

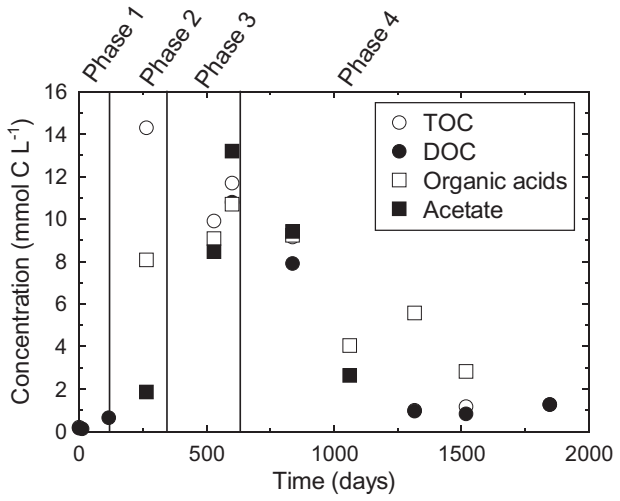

Fig. 3. Measurement of organic compounds as a function of time (TOC = total organic C, DOC = dissolved organic C) and suggested phases of microbial degradation (see text).

The low solubility of Fe-sulphide induced precipitation of X-ray amorphous FeS and subsequent formation of pyrite (observed):

$$Fe^{2+}_{rock} + HS^- \rightarrow FeS + H^+$$

$$FeS + HS^- + H^+ \rightarrow FeS_2 + H_2$$

The organic degradation process was accompanied by other abiotic side-reactions including release of Fe(II) from the rock, calcite precipitation and cation and proton exchange reactions at the clay surfaces as deduced from the reaction modelling. These reactions contributed to buffering of the chemical conditions in the PC experiment, in particular with regard to pH and Eh. The relatively stable concentrations of the major cations Na^+, Ca^{2+} and Mg^{2+} during the biodegradation process highlights the impact of cation exchange and carbonate dissolution/precipitation processes.

All the geochemically relevant reactions were accounted for in the reactive transport modelling exercise (Tournassat et al., 2011) on the basis of the conceptual geochemical understanding of the Opalinus Clay (Pearson et al., 2003; Vinsot et al., 2008) and of the geochemically similar Callovo-Oxfordian formation (Gaucher et al., 2009). The main challenge was to simulate the complex kinetic degradation reactions affected by a variable microbial community. This was achieved by assuming simple zero-order reactions (e.g. acetate production, acetate degradation) with fitted reaction rate constants over different time intervals (e.g. acetate production, acetate degradation, methanogenesis), and by testing possible C sources (e.g. acetone, glycerol) and their release rates. The observed evolution in general was well-matched by the simulations, especially when glycerol was assumed as the source of the organics (see section below). According to the modelling results (Tournassat et al., 2011), a total amount of about 5 g of FeS (and 5 g of pyrite) precipitated in the borehole (whose volume is about 3 L), the majority of which formed in the borehole water and at the water–clay interface. This is in line with observations of significant amounts of black sulphides (and gold flecks of pyrite) in the PEEK circulation tubes and at the bottom of the borehole, whereas no such products were observed inside the rock. The

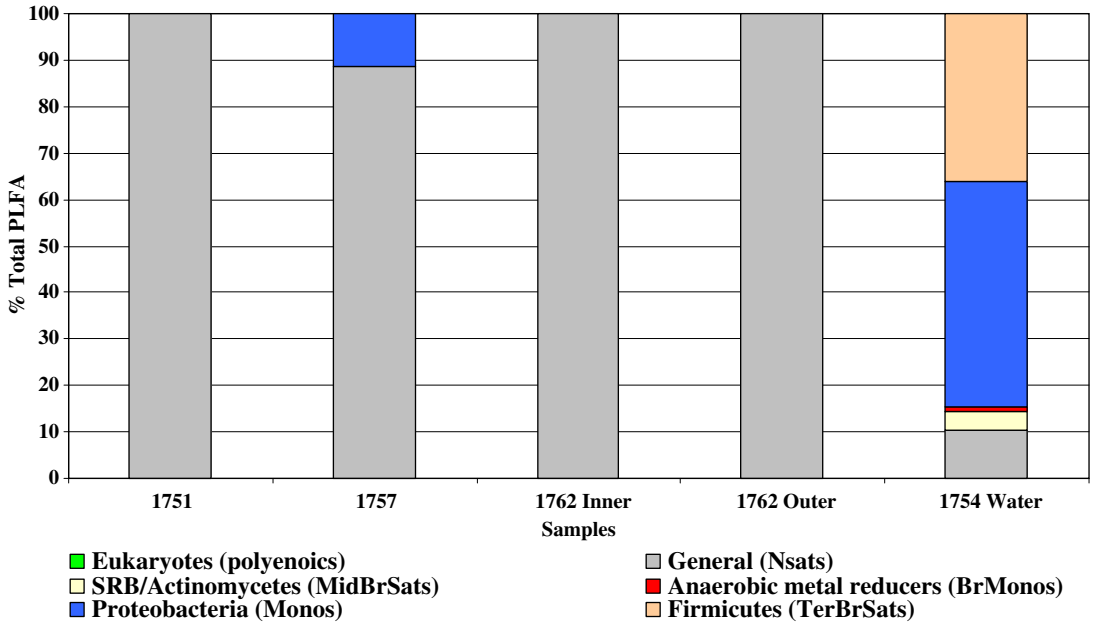

Fig. 4. Relative percentage of Total PLFA structural groups in Opalinus cores drilled with N_2 (1751 and 1757), in the PC clay overcore (near the borehole (1762 Inner) and further away from the borehole (1762 outer) and in the PC borehole water after termination (1754). Structural groups are assigned according to PLFA chemical structure, which is related to fatty acid biosynthesis.

amount of degrading C necessary to produce this sulphide mass depends on the source assumed and, according to modelling results, corresponds to about 11 g of acetone or 17 g of glycerol leached in the whole volume of the borehole in the course of the experiment (see discussion below). Modelling results indicate that even at its peak, the CH_4 produced represented less than 1% of the total organic C that was degraded during the experiment. Providing that the modelling hypotheses were correct with regard to CH_4 concentration in the formation, this result indicates that CH_4 had very little influence on the C mass balance during the experiment.

The results of the microbial analyses of the PC water indicated the presence of a substantial microbial population, with total cell numbers of between 2×10^8 and 7×10^8 cells/mL, while the active bacterial population was of the order of 6×10^7 cells/mL and the active Archaeal population of the order of 3×10^6 cells/mL. The actually active bacterial population was, therefore, about 10–30% of the total bacterial population, much higher than usually seen in oligotrophic groundwaters. The culturable heterotrophic aerobic population ranged from about 3×10^5 to 7×10^6 colony-forming units (CFU) per mL, while the culturable heterotrophic anaerobic population ranged from 2×10^5 to 9×10^5 CFU/mL. The culturable population size for NO_3-, Fe-, and SO_4-reducing bacteria ranged from 5×10^2 to 10^4 MPN (most probable number) per mL. These populations are higher than generally found in oligotrophic deep groundwaters, and orders of magnitude higher and more diverse than in undisturbed Opalinus Clay. Fig. 4 shows the microbial diversity in the PC borehole water at the end of the experiment compared to the diversity in Opalinus Clay cores, based on PLFA analysis. Three of the four clay core samples analysed showed only the presence of normal saturated PLFA, which is present in all organisms. Its presence in high proportions often indicates a less diverse (and likely stressed) population. The PC water in contact with the Opalinus Clay showed a much more diverse population with a much smaller percentage of normal saturated PLFA.

Microbial species identified (with similarity indices between 97% and 100%) in the pore water (from direct DNA extraction) included *Pseudomonas stutzeri*, *Bacillus licheniformis*, *Desulfosporosinus sp.* and *Hyphomonas*. Species identified from DNA extractions after enrichment cultures from the overcore samples included *Pseudomonas stutzeri*, three species of *Trichococcus*, *Caldanaerocella colombiensis*, *Geosporobacter subterrenus* and *Desulfosporosinus sp.* (Stroes-Gascoyne et al., 2011). The origin of these (mostly facultative or anaerobic) microbial species cannot be determined with certainty from the data as discussed by Stroes-Gascoyne et al. (2011). Some species likely resulted from contamination during drilling and some likely from the artificial porewater (not sterilised) that was added to the borehole. Unfortunately, this water was not analysed for microbial content prior to addition to the PC borehole. However, subsequent batches of artificial water prepared with identical composition showed the presence of a considerable population of heterotrophic microbes (Stroes-Gascoyne and Hamon, 2008; unpublished results). While this does not prove that the artificial porewater added to the PC experiment contained microbes, it supports the suggestion that it likely did. Other species could possibly be revived species indigenous to the Opalinus Clay, although the very old age of the formation (170 Ma) may exclude that (as discussed in Stroes-Gascoyne et al. (2007, 2011).

Regardless of the origin of the microbes, the experience with the PC experiment illustrates that it is very difficult to keep even an *in situ* microbiologically almost inactive environment, such as the Opalinus Clay formation (Stroes-Gascoyne et al., 2007), from becoming locally active as a result of disturbances. If indigenous dormant organisms are present, some of these can probably be revived if the original formation is disturbed, because such disturbances would provide space, water and nutrients, as could be the case during repository excavation and construction, which almost certainly also will introduce non-indigenous species.

3.3. Geochemical buffering by rock

Contrary to observations in the borehole water, virtually no chemical or mineralogical changes in the adjacent rock were detected. This is explained by the strong buffering effect of the rock and is entirely consistent with results from reactive transport modelling. The rock thus effectively buffers microbially-induced anaerobic redox reactions leading to increased CO_2 and alkalinity

by carbonate dissolution/precipitation and proton exchange reactions at the clay surfaces. According to the modelling results, a total of about 3 g of calcite precipitated in the borehole volume or in the surrounding rock resulting from the degradation process, which if distributed across the rock interface, amounts to merely 0.3% of the initial calcite concentration of the rock at the interface. This supports mineralogical data indicating no changes in calcite content at the interface. Furthermore, the simulations indicate that pH changes (ranging from 6.7 to 7.0) in the porewater are limited to a zone of about 20 cm within the rock.

The rock also acts as an effective redox buffer and its redox-active species such as siderite, pyrite, Fe(II) from the clay exchanger, organic matter and to some extent Fe-rich silicates endow it with a large reducing and oxidising capacity. The main effect of the degradation process on these species was the release of Fe(II) in the rock and the concomitant precipitation of FeS. The latter process led to a general increase in reducing capacity of the rock close to the water-clay interface.

3.4. Source(s) of organic carbon

The identification of the degrading C source(s) was one of the main and most challenging issues in the interpretation of the results of the PC experiment, as discussed in detail in De Cannière et al. (2011). The results from a laboratory study on materials used in the *in situ* experiment that could potentially have degraded during the experiment, combined with the ^{14}C data shed light on this issue and also evaluated the (in)adequacy of the various materials for use in future *in situ* tests. The interpretation was aided further by the reactive transport modelling study presented in detail in Tournassat et al. (2011). The conclusions from this combined set of information are:

- The PE screen and the Teflon-type materials (e.g. PEEK) were shown to be inert and released (almost) no water-soluble compounds.
- The polyamide tubing and polyurethane material used in the packer system released significant amounts of soluble, degradable compounds which, however, were not sufficient to explain the degradation process in the borehole. This was also true for the graphite material released by the EC electrode placed initially.
- Acetone that may have remained in the pores of the PE screen after the cleaning process may have contributed to the fuelling of bacterial activity. The modern signal of the ^{14}C of the DOC and DIC in the water, however, is not consistent with acetone or other material from the packer system as principal degrading agents. Moreover, the modelling exercise showed that a source with the C valence of glycerol is the most likely candidate. Also, the amount of acetone residue estimated to remain in the PE screen after cleaning was substantially lower (max. 5 g of acetone) than the amount required (~11 g of acetone) to reduce the mass of SO_4 lost during the experimental period.
- Glycerol, which is highly soluble and degradable, was released from the gel-filling of the reference electrodes immersed in the circulation water. The amount of glycerol in the gel has been determined to be 19.5% of the polymer-filling, i.e. about 1.6 g of glycerol per electrode (De Cannière et al., 2011). Carbon-14 data and modelling results were in line with glycerol being the main C source fuelling microbial activity. The amount required to reduce all of the SO_4 in borehole according to modelling results (~17 g) appears rather high, but is in line with the amount of this compound involved as pH and Eh electrodes (the pH electrode was replaced 12 times and Eh electrode once, leading to a total of 15 gel-filled electrodes emplaced in the circuit, yielding a total of ~24 g of glycerol). The other amide-type compounds in the gel display much lower water solubility and degradability relative to glycerol.
- Rock-derived CH_4 is also a potential C source, which may fuel SRB in the absence of other organic sources. Indeed, modelling attempts using CH_4 as one contributor to the C budget were carried out early in the project. However, CH_4 together with natural organic matter in the rock is very unlikely to be the C source in view of the ^{14}C results. Moreover, the natural organic matter is known to exhibit low reactivity and degradability (Courdouan et al., 2007).

To conclude, glycerol is the most likely candidate to have fuelled SO_4 reduction. Possibly, other sources, such as acetone residues in the PE screen also may have contributed to a lesser extent (<5%) to the degradation process.

3.5. Longer-term effects

One aspect of particular interest for the safety case of a repository (next section) is the impact of degradable organic material that may be emplaced during the disposal process, on the safety functions of the clay host rock. In this respect, the PC experiment has provided valuable insight on the response of the rock to the effects of microbial degradation of a continuous organic C source. The analytical data together with the reactive transport modelling results have highlighted the effective geochemical buffering capacity of the rock, which limits the induced changes to a narrow zone around the degrading source.

One question of interest is the time frame required for restoring initial (or "undisturbed") conditions once the C source is depleted. For this purpose, the reactive transport model calibrated with the data obtained from the extensive PC analysis was applied under the assumption that no more C (i.e., glycerol) was released after the 5-a experiment. The main results of this modelling exercise are illustrated in Fig. 5. The model predicts that 10 a after the end of bacterial perturbation, the system is not completely restored. In particular, redox conditions are still significantly affected ($\Delta pe > 0.2$) at distances >1 m from the borehole. This is due to the diffusion of remaining S(-II) species (H_2S and HS^-) from the production location (the borehole) into the rock. However, there is large uncertainty relative to this aspect because the kinetics of pyrite precipitation in the formation were not considered for these simulations. Precipitation of pyrite would drastically lower the S(-II) concentrations to levels comparable with the concentration in the undisturbed porewater. Sulphate concentration, pH and alkalinity values have been almost restored after 15 a due to out-diffusion of H_2CO_3, HCO_3^- and in-diffusion of Ca, leading to a calcite precipitation front at the borehole/formation interface. This calcite precipitation should lead to decrease of pH in the borehole but is buffered by the dissolution of calcite in the formation, just behind the interface (see Fig. 5, bottom right).

These simulations together with observations of overcore samples are convincing evidence and confirmation of the high pH buffer capacity of the Opalinus Clay formation.

3.6. Remaining uncertainties

The details of the complex biodegradation process involving temporally and probably also spatially variable reaction pathways and microbial populations in the PC experiment could be unravelled only partially. Moreover, the redox conditions in the borehole were affected by the sampling procedures and several experimental disturbances. Hence, for the reactive transport model, simplified empirical kinetic reaction rates, with rate constants fitted to

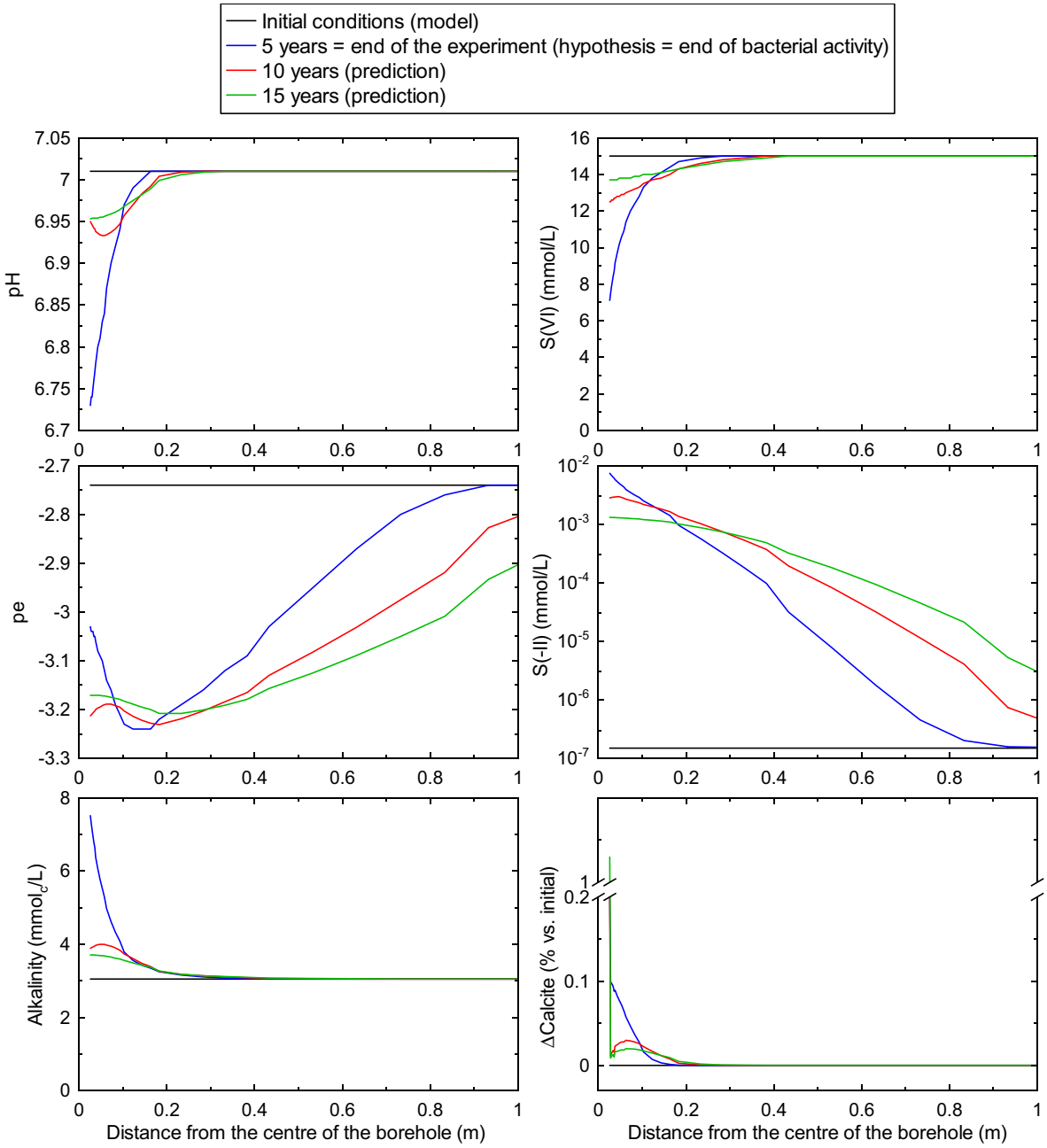

Fig. 5. Results of predictions from reactive transport model. This model was used to predict the biogeochemical evolution in the borehole and the adjacent rock of the PC experiment with glycerol as carbon source (Tournassat et al., this issue). Five years: simulation results at the end of experiment with degrading glycerol. Ten, 15 years: prediction results under assumption that no more bacterial activity occurs. The borehole with the circulating fluid is still in contact with the rock and in and out-diffusion from the borehole occurs. Only the formation is represented here.

the data, were formulated. There is thus considerable conceptual uncertainty underlying the modelling results. Further uncertainty arises from the model assumptions about mineral reactants in the clay, such as the source for released Fe, which ended up in the Fe-sulphide. The precipitation process of this Fe-sulphide is another major uncertainty. In particular, the kinetics of pyrite precipitation in the clay, which affected the influence zone of the perturbation according to modelling data.

As indicated by the modelling results, the main reactions buffering the porewater pH were carbonate dissolution/precipitation and proton exchange reactions at the clay surfaces. There is uncertainty with regard to the reactivity of silicate phases in response to microbial perturbation because of uncertainty in the thermodynamic and kinetic data associated with these phases. However, because solubility and reaction rates are low under the near-neutral pH conditions encountered (pH ranging from 6.7 to about 7.5), dissolution of silicates probably contributed less to pH buffering than the carbonate and proton reactions.

While the origin of the organic C source was resolved, the origin of the microbes found in the PC experiment could not be determined with certainty (Stroes-Gascoyne et al., 2011). Contamination during drilling and especially from the artificial porewater cannot be ruled out and is in fact likely (Section 3.2). Indigenous organisms are also a possibility. An extensive study was carried out to investigate the occurrence of indigenous microbes and their community size and structure in Opalinus Clay cores drilled with

aseptic techniques (Mauclaire et al., 2007; Stroes-Gascoyne et al., 2007; Poulain et al., 2008). The results from this study provided limited evidence that a small, viable but most likely largely dormant, microbial community is present in Opalinus Clay, which was corroborated by a second, much more limited set of analyses (Stroes-Gascoyne et al., 2008), on large diameter Opalinus Clay cores, drilled using air-cooling. The microbial characterisation of Opalinus Clay suggested that unperturbed Opalinus Clay contains

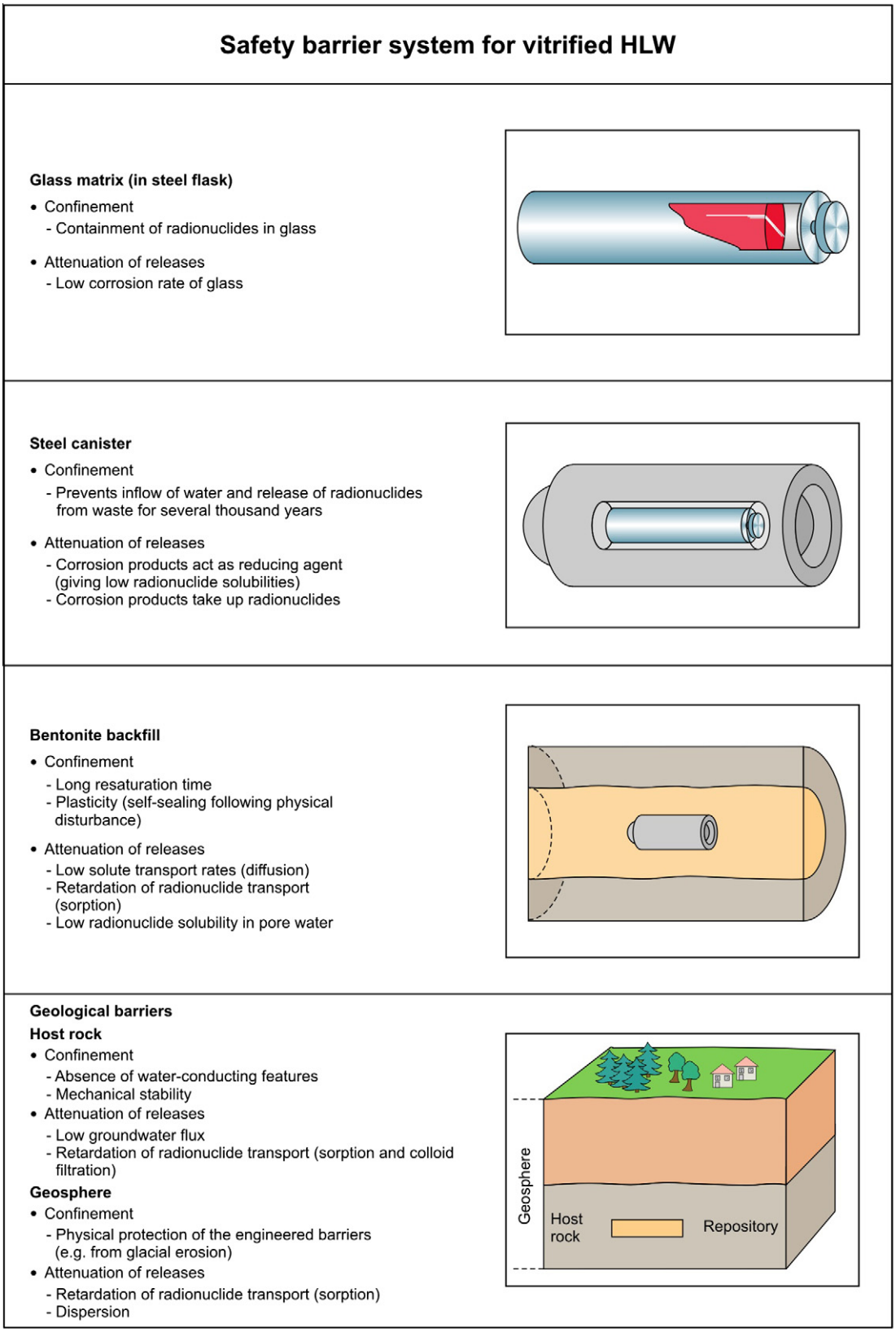

Fig. 6. Components and their safety functions of a repository in the Swiss concept for vitrified high-level radioactive waste disposal (Nagra, 2002).

only a small viable microbial community, which is probably metabolically (almost) inactive (i.e., dormant cells and spores), due to water, space and nutrient restrictions. It is not possible to determine how old such surviving species might be. The Opalinus Clay formation is 170 Ma old, but survival of microbes (in spore or dormant form) beyond 0.6–3 Ma, in ancient geological formations, is currently being disputed. Another possible source of indigenous microbes, therefore, could be a recent (<3 Ma) intrusion of water into the Opalinus Clay formation, although this appears unlikely. Stroes-Gascoyne et al. (2011) discuss these possibilities in more detail.

4. Implications for repository safety

4.1. The multi-barrier concept and assessment of long-term safety

Deep geological disposal relies on effective isolation of the high-level nuclear waste (HLW) from the human environment for very long time periods (i.e. 10^5–10^6 a). This long time period is required for the radiotoxicity of the waste to reach acceptable levels resulting from radioactive decay (e.g. ANDRA, 2005). The geological disposal of HLW is based on the multi-barrier concept, acknowledging the difficulty of assuring complete isolation of the waste for such long timescales. Thus, the disposal system is designed to retard and to attenuate the releases of decaying radionuclides through various barriers in the engineered system (i.e., low-solubility waste matrix, corrosion-resistant metal waste containers, low-permeability backfilling material) and hydrologically isolating the surrounding natural system (host rock). A simplified sketch of the main safety barriers in the Swiss HLW disposal concept is illustrated in Fig. 6. The geological claystone barrier, i.e. the 50 m thick layer of Opalinus Clay below and above the HLW repository, plays a central role in this disposal concept, as outlined more in detail below.

The implementation of a HLW waste repository is a complex and lengthy process necessitating, apart from the delicate political decisions and societal efforts, a staged approach with an advanced scientific and technical programme. A key aspect in this programme is long-term safety, which needs to be addressed in a thorough, transparent and traceable manner. In view of the extensive experience with this issue gained in the various international nuclear waste management programmes, procedures for evaluating long-term safety have been established. Thus, rather than presenting a set of radionuclide transport- and resulting dose-calculations, as was often the strategy 20–30 a ago, a comprehensive safety case is presented. According to the Nuclear Energy Agency of OECD (NEA, 2004), "A safety case is the synthesis of evidence, analyses and arguments that quantify and substantiate a claim that the repository will be safe after closure and beyond the time when active control of the facility can be relied on". Important elements of the safety case are: the safety concept (e.g. description of disposal system components and their safety functions), the assessment basis (e.g. methods, models, scientific and technical data for different repository components and geosphere), evidence, analyses and arguments (e.g. quantitative analyses, such as radionuclide transport calculations and qualitative safety arguments), and a synthesis (overall interpretation of all safety-relevant considerations).

The safety case strategy generally can be applied to different geological disposal concepts, but the relevance of the different repository components to safety is of course site- and concept-specific. Hence, the safety functions need to be defined and evaluated for each safety barrier within a given disposal system, also taking into account possible interactions between the different system components and perturbation scenarios. A common procedure for this is to systematically consider all possible factors which could affect the safety functions of a safety barrier with the aid of a so-called FEP (features, events and processes) catalogue (NEA, 2000).

4.2. The role of the claystone barrier in the safety case

As noted above, the argillaceous host rock is a central part of the safety concept for a number of current HLW disposal systems. Its main safety functions are (e.g. Nagra, 2002) (1) to confine the waste and to protect the engineered barriers by its low permeability, mechanical stability and favourable geochemical properties and (2) to attenuate releases of radionuclides by retardation and slow diffusion processes. The FEPs, which may affect the safety functions of the clay host rock, have been evaluated by an international working group of NEA and reported in Mazurek et al. (2003). These FEPs are compiled in a hierarchically structured list, a simplified and adapted version of which is presented in Table 2. In the first order structuring, FEPs are separated for the "undisturbed" clay system and for the clay system "perturbed" by repository-induced or external (not shown in Table 2) effects (such as glaciations for instance).

In the PC experiment, FEPs from both the undisturbed and perturbed clay system have been addressed as well as the linked processes between these. The FEPs addressed for the PC experiment are given in Table 2, and the most relevant ones highlighted in bold.

4.3. Concept of geochemical stability in clay host rocks

Geochemical stability is one of the principal characteristics of argillaceous rocks, and initially attracted interest in them as possible host rock formations. One property that gives rise to this

Table 2
List of features, processes and events (FEPs) for clay host rocks according to the FEPCAT list (Mazurek et al., 2003) and FEPs relevant with regard to the PC experiment, most relevant FEPs addressed by PC in bold.

Structured FEPs classification	FEPs relevant to PC
Undisturbed system	
Transport mechanisms	
• Advection/dispersion	
• **Diffusion**	×
• Colloid formation, transport and filtration	
Retardation mechanisms	
• Matrix diffusion	
• Sorption (broad definition)	
• **Mineralogy of rocks**	×
• Natural organics/complexation	×
• **Porewater composition (e.g. pH, pCO_2, Eh)**	×
• **Dissolution/precipitation**	×
• **Ion exchange/surface complexation**	×
System understanding	
• Paleo-hydrogeology of host rock and embedding formations	
• **Evolution of pore-fluid chemistry**	×
• Water residence times in host formation	
Repository-induced perturbations	
Chemical and microbiological perturbations	
• **Oxidation/reduction of the host rock**	×
• **Redox buffer capacity of host rock**	×
• **Changes in pCO_2 and pH**	×
• **pH buffer capacity of host rock**	×
Thermal perturbations	
Geomechanical perturbations	
Hydraulic perturbations	
Perturbation from coupled processes	

stability is a diffusion-only transport regime, which limits the flux of materials from the interior of such formations to their boundaries. A second attractive property is that the dominant amounts of reactive and others solutes are associated with the reactive solids in the formation itself rather than with the pore waters. The formation solids buffer the pore water chemical composition including such properties as pH and redox potential.

The slow response of systems in which diffusion dominates can be demonstrated by two studies at Mont Terri. The first considered the regional distribution of porewater Cl concentrations (illustrated in Fig. 2 of Wersin et al. (2011)). This pattern can be simulated by modelling diffusion from the Opalinus and adjacent Liassic clays into overlying and underlying aquifers. A detailed analysis of this profile was provided by Mazurek et al. (2009). The basis of the conceptual model is that the clays and surrounding units initially had a uniform Cl content throughout. As fresh-water began to flow in adjacent aquifers, out-diffusion from the clay began. The times at which this fresh-water flow began could be fitted to the measured Cl profiles. The asymmetric shape of the profile indicated that fresh-water had been present in the overlying Malm aquifer longer than in the underlying Keuper aquifer. Adjusting the times in the modelling for a best fit indicated opening of the Malm aquifer at about 6.5 Ma and of the Keuper at 0.5 Ma, if an initial concentration of 19 g Cl/L was present, i.e., that of seawater. If an initial concentration of 15 g Cl/L was assumed, slightly above 13.9 g Cl/L, the highest measured value, the corresponding times for the opening of the aquifers were similar, i.e., 4.4 Ma and 0.4 Ma. These times correspond very well with the times at which the upper and lower aquifers were first breached during erosion of the Jura Mountains, so that fresh-water circulation could begin.

The PC experiment itself supports the slow response of the Clay system, although on a much smaller spatial and much shorter time scale than the regional studies by Mazurek et al. (2009).

The second aspect that confirms geochemical stability is the high buffering capacity of clay rocks. As Pearson et al. (2011) and Tournassat et al. (2011) showed, the water chemistry was controlled by such water–rock reactions as cation exchange and mineral equilibria. Chloride and Br are present only in the pore water. Sulphate is found sporadically in the Opalinus Clay as celestite in veins but it is not clear whether the pore water is in equilibrium with this mineral (Pearson et al., 2011). All other solutes can be related to cation exchange or mineral equilibria and 99% or more of the total mass of each of these elements is present in the solid phase as minerals or bound to mineral surfaces rather than in the pore water, except for Na of which about 88% is in the rock. Thus, the capacity of the rock to buffer changes in bulk water chemistry is very high.

In modelling porewater pH values, several reactions have been used including carbonate and silicate reactions and pH buffering by clay surfaces. As discussed in Pearson et al. (2011), reactions among carbonate species CO_3^{2-}, HCO_3^- and $CO_{2(aq)}$ can be associated with solution electroneutrality and so establish the pH. Reactions among silicate minerals such as kaolinite chlorite and illite can also buffer pH. Large amounts of carbonate and silicate minerals are present within the Opalinus Clay. Moreover, the clay surfaces display a large proton exchange capacity, i.e. protonation and deprotonation reactions at the variably charged surfaces, depending on pH conditions contribute substantially to the overall pH buffering capacity and pH buffering is included in the reaction modelling in Tournassat et al. (2011) as an influence on the chemistry of water in the borehole.

4.4. Microbiological perturbations and their effects on safety functions

The need to consider the effects of microbial metabolism on geochemical conditions in the deep subsurface in relation to a future repository for HLW is a relatively new concept, stemming from the mid 1980s (e.g., West and McKinley, 1984; West et al., 1985). It has been an element of investigations made to assess the safety of potential repositories since that time. Microbial activity in a HLW repository is of concern for a number of reasons (e.g., Stroes-Gascoyne and West, 1996), one of which is their effect on Eh and pH. Specifically, the likely scenario in the PC experiment contained the following elements: Microbial organotrophic metabolism (fed by glycerol) caused the production of CO_2 (and H_2O), which increased the pCO_2 in a system, leading to a drop in pH and a potential increase in the mobility of radionuclides, because most radionuclides are least soluble at neutral pH values. The continued microbial breakdown of organic matter rapidly depleted any O_2 in the system, after which the microbial metabolism switched to fermentation, which then produced the low-C fatty acids that are required for heterotrophic SO_4-reducing bacteria activity. The products of the SO_4 reduction are observed reduced S species including sulphide, which is a well-known corrosion agent for both Cu and steel waste containers.

However, the intense effects of the microbial disturbances seen in the PC experiment were of relatively short duration. In a repository setting, the time frame of possible disturbances would largely depend on the size and duration of the disturbance, i.e., how much organic material, water and space were introduced and where. Once introduction stops and nutrients have been used up, the system can only be fed through nutrients that are present in the formation itself. *In situ* metabolism would then be limited by the diffusion kinetics of such nutrients to places where microbial activity is possible (i.e., where adequate porespace and water are present, either in localities naturally existing in the clay formation or induced by excavation processes such as for instance the excavation damage zone (EDZ)). Microbial metabolism not enhanced by disturbances is likely very limited and slow in the tight undisturbed Opalinus Clay formation, leaving most microbes in a dormant state, which can only be activated through such disturbances as evident in the PC experiment. The actual occurrence of a very low level metabolism in pristine undisturbed Opalinus Clay is at present a hypothesis only and has, thus far, not been confirmed or measured.

4.5. Discussion and outlook

The unintentional placement of a degradable organic C source, which resulted in anaerobic microbial perturbation of the PC experiment, has contributed significantly to the understanding of potential biogeochemical processes in Opalinus Clay. In particular, similar perturbations could occur in zones disturbed by excavation (EDZ) where porosities are increased and microbial activity could take place. The results of the PC experiment highlighted the significant potential for SRB activity in Opalinus Clay that could be realised as a result of disturbance of the system. Sulphate reduction is accompanied by an increase in pCO_2 and alkalinity, and a decrease in pH and Eh relative to the undisturbed porewater. Biodegradation moreover produces low molecular weight organic acids with concentrations that may be highly variable and are presumably affected by methanogenic reactions. The reaction pathways are complex and dependent on many site-specific parameters, and are not yet understood in detail. The origin of the bacteria fuelling degradation is not clear, but for safety considerations, this is not a relevant issue because the same processes by which bacteria could have been introduced into the PC borehole would be expected to occur during repository construction and operation. Furthermore, the large amount of participating dissolved and solid reactants from the clay complicates the quantitative description of the biogeochemical processes. Consequently, uncertainties from

quantitative modelling of biodegradation are still rather large, especially with regard to the predictive use of the model.

In summary, the results from the PC experiment are a valuable contribution with respect to the safety case. Any geochemical changes induced by anaerobic microbial perturbation, should they occur, would affect the solubility and sorption behaviour of radionuclides eventually released from the engineered system. Also, the production of reduced S species, such as sulphide may adversely affect corrosion of the metal waste overpacks. This emphasises that the amount of organic compounds emplaced in a HLW repository should be limited as much as possible to avoid such effects. Nevertheless, it should be noted that many of the large solute changes observed in the PC experiment were of a transient nature (e.g. elevated HS^- or DOC levels) and decreased again rather rapidly (on a repository time scale). The changes in pH and Eh conditions were quite significant, but not dramatic with regard to repository safety. The large buffering capacity of the clay as well as its diffusive properties are effective in limiting geochemical gradients in the porewater and also the geochemical and mineralogical changes induced by the microbial disturbance. As suggested also by modelling, restoration times to achieve natural or background conditions are expected to be rather short once the degradable sources have been depleted.

The experiment also highlighted the fact that equipment materials commonly used in *in situ* tests do not always display the commonly assumed inert behaviour. This particularly holds for gel-type "robust" reference electrodes, which may release substantial amounts of glycerol. The assessment of potential experimental artefacts should always be a part of the overall analysis of the results of large *in situ* tests.

Acknowledgements

This work was carried out within the Mont Terri Project in close co-operation with the Mont Terri Consortium. We especially appreciate the support of Thomas Fierz (Solexperts), Pierre De Cannière and Hugo Moers (SCK-CEN), Urs Mäder (Univ. Bern), Bernd Frieg (Nagra), Paul Bossart, Christophe Nussbaum, Heinz Steiger, Olivier Meier (Geotechnical Institute/Swisstopo) and the COREIS and Schützeichel teams for the field work. The support of Lorenz Eichinger (Hydroisotop) for the analytical work is acknowledged. The manuscript has benefited from many fruitful discussions with scientists within and outside the team of the PC experiment. S. Stroes-Gascoyne thanks the Nuclear Waste Management Organisation in Canada for funding her contribution to this work.

References

ANDRA, 2005. Référentiel du comportement des radionucléides et des toxiques chimiques d'un stockage dans le Callovo-Oxfordien jusqu'à l'Homme. Dossier 2005 Argile. Agence Nationale pour la gestion des déchets radioactifs, Châtenay-Malabry, France.

Beaucaire, C., Pearson, F.J., Gautschi, A., 2004. Chemical buffering capacity of clay rock. In: Stability and Buffering Capacity of the Geosphere for Long-term Isolation of Radioactive Waste. "Clay Club" Workshop Proc., Braunschweig, Germany, 9–11 December 2003. OECD 2004. NEA No. 5503, pp. 147–154.

Courdouan, A., Christl, I., Meylan, S., Wersin, P., Kretzschmar, R., 2007. Characterization of dissolved organic matter in anoxic rock extracts and *in situ* pore water of the Opalinus Clay. Appl. Geochem. 22, 2926–2939.

De Cannière, P., Schwarzbauer, J., Höhener, P., Lorenz, G., Salah, S., Leupin O.X., Wersin P., 2011. Biogeochemical processes in a clay formation *in situ* experiment: part C – organic contamination and leaching data. Appl. Geochem.

Gaucher, E.C., Tournassat, C., Pearson, F.J., Blanc, P., Crouzet, C., Lerouge, C., Altmann, S., 2009. A robust model for pore-water chemistry of clayrock. Geochim. Cosmochim. Acta 73, 6470–6487.

Koroleva, M., Lerouge, C., Mäder, U., Claret, F., Gaucher, E., 2011. Biogeochemical processes in a clay formation *in situ* experiment: part B – results from overcoring and evidence of strong buffering by the rock formation. Appl. Geochem.

Mäder, U., 2004. Porewater Chemistry (PC) Experiment: A New Method of Porewater Extraction from Opalinus Clay with Results for a Sample from Borehole BPC-A1. Mont Terri Project Technical Note TN2002-25.

Mauclaire, L., McKenzie, J.A., Schwyn, B., Bossart, P., 2007. Detection and cultivation of indigenous microorganisms in Mesozoic claystone core samples from the Opalinus Clay Formation (Mont Terri Rock Laboratory). Phys. Chem. Earth 32, 232–240.

Mazurek, M., Pearson, F.J., Volkaert, G., Bock, H., 2003. Features, Events and Processes Evaluation Catalogue for Argillaceous Media. OECD/NEA, Paris.

Mazurek, M., Alt-Epping, P., Bath, A., Gimmi, T., Waber, H.N., 2009. Natural Tracer Profiles across Argillaceous Formations: The CLAYTRAC Project. Nuclear Energy Agency, OECD, Paris.

Nagra, 2002. Project Opalinus Clay, Demonstration of Disposal Feasibility for Spent Fuel, Vitrified High-level Waste and Long-lived Intermediate-level Waste, Safety Report. NTB Technical Report 02-05. Wettingen, Switzerland.

NEA, 2000. Features, Events and Processes (FEPs) for Disposal of Radioactive Waste – An International Database. OECD/NEA, Paris.

NEA, 2004. Post-closure Safety Case for Geological Repositories, Nature and Purpose. OECD/NEA, Paris.

Pearson, F.J., 1999. What is the porosity of a mudrock? In: Aplin, A.C., Fleet, A.J., Macquaker, J.H.S. (Eds.), Muds and Mudstones: Physical and Fluid Flow Properties. Geol. Soc. London, Spec. Publ. 158, 9–21.

Pearson, F.J., Arcos, D., Bath, A., Boisson, J.Y., Fernández, A.M., Gäbler, H.-E., Gaucher, E., Gautschi, A., Griffault, L., Hernán, P., Waber, H.N., 2003. Mont Terri Project – Geochemistry of Water in the Opalinus Clay Formation at the Mont Terri Rock Laboratory. Bern Switzerland, Federal Office for Water and Geology (FOWG). Geology Series No. 5.

Pearson, F.J., Tournassat, C., Gaucher, E., 2011. Biogeochemical processes in a clay formation *in situ* experiment: part E – equilibrium controls on chemistry of pore water from the Opalinus Clay, Mont Terri Underground Laboratory, Switzerland. Appl. Geochem.

Poulain, S., Sergeant, C., Simonoff, M., Le Marrec, C., Altmann, S., 2008. Microbial investigation of Opalinus Clay, an argillaceous formation under evaluation as a potential host rock for a radioactive waste repository. Geomicrobiol. J. 25, 240–249.

Stroes-Gascoyne, S., West, J.M., 1996. An overview of microbial research related to high-level nuclear waste disposal with emphasis on the Canadian concept for the disposal of nuclear fuel waste. Can. J. Microbiol. 42, 349–366.

Stroes-Gascoyne, S., Schippers, A., Schwyn, B., Poulain, S., Sergeant, C., Le Marrec, C., Simonoff, M., Altmann, S., Nagaoka, T., Mauclaire, L., McKenzie, J., Daumas, S., Vinsot, A., Beaucaire, C., Matray, J.M., 2007. Microbial community analysis of Opalinus Clay drill core samples from the Mont Terri Underground Research Laboratory, Switzerland. Geomicrobiology 24, 1–17.

Stroes-Gascoyne, S., Sergeant, C., Schippers, A., Hamon, C.J., Nèble, S., Vesvres, M.-H., Poulain, S., Le Marrec., C., 2008. Microbial Analyses of PC Water and Overcore Samples: Synthesis of Results. Mont Terri Project Technical Note TN2006-69, Bern (CH).

Stroes-Gascoyne, S., Sergeant, C., Schippers, A., Hamon, C.J., Neble, S., Vesvres, M.-H., Barsotti, V., Poulain, S., Le Marrec. C., 2011. Biogeochemical processes in a clay formation *in situ* experiment: part D – microbial analyses – synthesis of results. Appl. Geochem.

Tournassat, C., Alt-Epping, P., Gaucher, E.C., Gimmi, T., Leupin, O.X., Wersin, P., 2011. Biogeochemical processes in a clay formation *in-situ* experiment: part F – reactive transport modelling. Appl. Geochem. 26, 1009–1022.

Van Loon, L.R., Soler, J.M., Müller, W., Bradbury, M.H., 2004a. Anisotropic diffusion in layered argillaceous rocks: a case study with Opalinus Clay. Environ. Sci. Technol. 38, 5721–5728.

Van Loon, L.R., Wersin, P., Soler, J.M., Eikenberg, J., Gimmi, Th., Hernán, P., Dewonck, S., Matray, J.-M., 2004b. *In-situ* diffusion of HTO, $^{22}Na^+$, Cs^+ and I^- in Opalinus Clay at the Mont Terri Underground Rock Laboratory. Radiochim. Acta 92, 757–763.

Vinsot, A., Appelo, C.A.J., Cailteau, C., Wechner, S., Pironon, J., De Donato, P., De Cannière, P., Mettler, S., Wersin, P., Gäbler, H.-E., 2008. CO_2 data on gas and porewater sampled *in situ* in the Opalinus Clay at the Mont Terri Rock Laboratory. Phys. Chem. Earth 33, S54–S60.

Wersin, P., Soler, J.M., Van Loon, L., Eikenberg, J., Baeyens, B., Grolimund, D., Gimmi, T., Dewonck, S., 2008. Diffusion of HTO, Br^-, I^-, Cs^+, $^{85}Sr^{2+}$ and $^{60}Co^{2+}$ in a clay formation: Results and modelling from an *in situ* experiment in Opalinus Clay. Appl. Geochem. 23, 678–691.

Wersin, P., Leupin, O.X., Mettler, S., Gaucher, E., Mäder, U., De Cannière, P., Vinsot, A., Gabler, H.E., Kunimaro, T., Kiho, K., Eichinger, L., 2011. Biogeochemical processes in a clay formation *in situ* experiment: part A – overview, experimental design and water data of an experiment in the Opalinus Clay at the Mont Terri Underground Research Laboratory, Switzerland. Appl. Geochem.

West, J.M., McKinley, I.G., 1984. The geomicrobiology of nuclear waste disposal. In: Mater. Res. Soc. Symp. Proc. 26, Scientific Basis for Nuclear Waste Management, vol. VII, pp. 487–494.

West, J.M., Christofi, N., McKinley, I.G., 1985. An overview of recent microbiological research relevant to the geological disposal of nuclear waste. Rad. Waste Manage. Nucl. Fuel Cycle 6, 79–95.